Charles University in Prague
2nd Faculty of Medicine

Human Physiology and Pathophysiology

Markéta Bačáková, MSc.

The Growth of Vascular and Skin Cells on Polymer Materials for Tissue Engineering

Růst cévních a kožních buněk na polymerních nosičích pro tkáňové inženýrství

PhD Thesis

Supervisor: Lucie Bačáková, MD, PhD, Assoc. Prof.

Prague 2016

Prohlášení:

Prohlašuji, že jsem závěrečnou práci zpracovala samostatně a že jsem řádně uvedla a citovala všechny použité prameny a literaturu. Současně prohlašuji, že práce nebyla využita k získání jiného nebo stejného titulu.

Souhlasím s trvalým uložením elektronické verze mé práce v databázi systému meziuniverzitního projektu Theses.cz za účelem soustavné kontroly podobnosti kvalifikačních prací.

V Praze, 27. 6. 2016

Ing. Markéta Bačáková

Podpis

Identifikační záznam:

BAČÁKOVÁ, Markéta. *Růst cévních a kožních buněk na polymerních nosičích pro tkáňové inženýrství. [Growth of Vascular and Skin Cells on Polymer Materials for Tissue Engineering]*. Praha, 2016. 79 s, 5 příloh. Disertační práce (Ph.D.). Univerzita Karlova v Praze, 2. lékařská fakulta, Oddělení biomateriálů a tkáňového inženýrství, Fyziologický ústav Akademie věd České Republiky. Vedoucí práce Bačáková, Lucie.

Abstract

The ideal vascular or skin substitute is able to simulate the functions of original vascular or skin tissue. To reach this goal, the tissue substitute should be based on a biomaterial scaffold of an appropriate structure and desirable physical and chemical properties. These properties strongly influence successful implantation of the substitute to the patient's organism, substitute durability in the organism, and the desired colonization of the scaffolds with cells. These properties have a great impact on the adhesion, proliferation, differentiation, and desired phenotypic maturation of cells. Most of the biomaterials used for constructing clinically used tissue substitutes do not have appropriate properties for sufficient cell colonization, and thus their surface modification is needed. This thesis focuses on the improvement of biomaterial surface properties for successful cell colonization by plasma treatment, or by grafting and coating biomaterials with bioactive substances and extracellular matrix proteins.

The modification of polyethylene (PE) foils by Ar^+ plasma discharge showed a positive effect on the spreading, proliferation, and phenotypic maturation of vascular smooth muscle cells (VSMC). Subsequent grafting of the plasma-activated surface with bioactive substances further influenced cell behavior. Grafting with Gly or polyethylene glycol (PEG) predominantly promoted cell spreading and the formation of focal adhesion plaques. PE grafted with bovine serum albumin (BSA) or BSA with carbon nanoparticles (BSA+C) enhanced the growth and desired phenotypic maturation of VSMC, manifested by a higher concentration of contractile protein α-actin and SM1 and SM2 myosin. However, BSA grafted on polymer surface hampered cell proliferation in the cell culture medium without a serum supplement.

In order to improve the attractiveness of nanofibrous membranes for skin cells, the membranes were treated by oxygen plasma or coated with extracellular proteins (collagen, fibronectin, or fibrin). The plasma-treated membranes enabled better attachment, spreading and proliferation of human HaCaT keratinocytes. Fibrin nanocoating on nanofibrous membranes improved the adhesion and proliferation of human dermal fibroblasts, whereas collagen nanocoating positively impacted the behavior of human HaCaT keratinocytes. In addition, the fibrin combined with ascorbic acid added into the cell culture medium stimulated fibroblasts to synthetize and deposit collagen I in the form of a fibrous extracellular matrix. Fibronectin attached on the fibrin or collagen nanocoating further enhanced cell adhesion.

Key words: tissue engineering, vascular prosthesis, skin substitute, plasma discharge, nanotechnology, nanomedicine, electrospinning, fibrin, collagen, smooth muscle cells, fibroblasts, keratinocytes

Abstrakt

Cílem tkáňového inženýrství je vytvořit náhradu cévy nebo kůže, která by byla schopna co nejlépe simulovat funkce původní tkáně. Základem tkáňové náhrady je biomateriál o vhodné struktuře, fyzikálních a chemických vlastnostech, které zajistí úspěšnou implantaci náhrady do organismu a její kolonizaci buňkami. Vlastnosti biomateriálu významně ovlivňují adhezi, růst, diferenciaci a fenotypickou maturaci buněk. Většina biomateriálů užívaných pro konstrukci tkáňových náhrad nemá vhodné vlastnosti pro jejich úspěšnou kolonizaci buňkami. Tato dizertační práce se zaměřuje na modifikace biomateriálů s potenciálním využitím v tkáňovém inženýrství cévní a kožní tkáně. Cílem je zlepšit povrchové vlastnosti materiálů, a tím podpořit adhesi a růst buněk.

Jednou z modifikací, která byla použita pro úpravu povrchových vlastností polyethylenu, byla modifikace v argonovém plasmatu. Na povrch polyethylenu ozářený plasmatem byly následně roubovány bioaktivní molekuly. Modifikace v plasmatu výrazně zlepšila rozprostření, proliferaci a fenotypickou maturaci hladkých svalových buněk cévní stěny. Gly a polyethylenglykol (PEG), naroubované na ozářený povrch materiálu, dále podpořily především rozprostření buněk a formování fokálních adhezních plaků, zatímco bovinní sérový albumin (BSA) a BSA s uhlíkovými nanočásticemi (BSA+C) podporovaly spíše růst a fenotypickou maturaci hladkých svalových buněk, projevující se zvýšenou syntézou kontraktilního proteinu α-aktinu a SM1 a SM2 isoformy myosinu. Bylo však zjištěno, že v bezsérovém médiu BSA nepodporuje adhesi a následný růst buněk.

Za účelem zvýšení atraktivity nanovlákenných membrán pro adhesi a růst kožních buněk byly membrány modifikovány v kyslíkovém plasmatu nebo potaženy proteiny extracelulární matrix (kolagenem, fibronektinem nebo fibrinem). Modifikace v plasmatu zlepšila uchycení, rozprostření a růst lidských keratinocytů linie HaCaT. Fibrinová síť na nanovlákenných membránách výrazně podpořila adhesi a růst lidských dermálních fibroblastů, kdežto lidské keratinocyty linie HaCaT adherovaly přednostně na membrány modifikované kolagenem. Fibrin navíc stimuloval dermální fibroblasty k produkci kolagenu I a jeho ukládání v podobě extracelulárních vláken na povrch membrány. Síť z fibronektinu vytvořená na povrchu fibrinové nebo kolagenové vrstvy dále podpořila adhesi a rozprostření kožních buněk.

Klíčová slova: tkáňové inženýrství, cévní protéza, kožní náhrada, modifikace plasmou, nanotechnologie, nanomedicina, elektrostatické zvlákňování, fibrin, kolagen, cévní hladké svalové buňky, fibroblasty, keratinocyty

Acknowledgements

First of all, I would like to gratefully thank my supervisor Lucie Bačáková, M.D., Ph.D., Assoc. Prof. for giving me the opportunity to work in her lab and for her thorough guidance during my work and study. Much gratitude is also owed to all colleagues of our research team for their useful help and kind assistance during experiments.

The external co-workers are acknowledged for their great cooperation and professional support while performing experiments. Thanks are especially owed to the research group led by Vaclav Svorcik, MSc., Ph.D., Prof. (University of Chemistry and Technology in Prague, Czech Republic) and the research group led by Eduard Brynda, MSc., Ph.D. (Institute of Macromolecular Chemistry, Czech Academy of Sciences of the Czech Republic).

Important thanks have to be expressed to my close friends and family for their patience and understanding during my study and to my small pet – a female rabbit for keeping me optimistic and enthusiastic by her unforgettable enjoyment of life.

Finally, this research was supported by the Grant Agency of the Charles University in Prague (Grant No. 38214), the Grant Agency of the Czech Republic (Grant No. P108/12/G108 and P108/12/1168), and by the project ‘‘BIOCEV – Biotechnology and Biomedicine Centre of the Academy of Sciences and Charles University’’ (CZ.1.05/1.1.00/02.0109).

Abbreviations

AA	2-phospho-L-ascorbic acid trisodium salt
AFM	atomic force microscopy
BSA	bovine serum albumin
C	colloidal carbon nanoparticles
DMEM	Dulbecco's Modified Eagle's Medium
ECM	extracellular matrix
EGF	epidermal growth factor
ELAM-1	endothelial-leukocyte adhesion molecule-1
ELISA	Enzyme-Linked Immunosorbent Assay
FBS	fetal bovine serum
FGF	fibroblast growth factor
Fn	fibronectin
GAGs	glycosaminoglycans
GAPDH	glyceraldehyde 3-phosphate dehydrogenase
Gly	glycine
HaCaT	spontaneously transformed keratinocyte cell line from adult skin
HDPE	high-density polyethylene
ICAM-1	intracellular adhesion molecule-1
IL	interleukins
INF	interferon
KGF	keratinocyte growth factor
LDPE	low-density polyethylene
MMP	metalloproteases
PBS	phosphate-buffered saline
PCR	polymerase chain reaction
PDGF	platelet derived-growth factor
PDLLA	poly-D,L-lactide
PE	polyethylene
PEG	polyethylene glycol
PET	polyethylene terephthalate

PEO	polyethyleneoxide
PLA	polylactide
PLGA	poly(lactide-*co*-glycolide)
PS	polystyrene cell culture dish
PTFE	polytetrafluorethylene
RBS	Rutherford Backscattering Spectroscopy
TGF	transforming growth factor
TNF	tumor necrosis factor
UV	ultraviolet light
VCAM-1	vascular adhesion molecule-1
VEGF	vascular growth factor
VSMC	vascular smooth muscle cells
XPS	X-ray photoelectron spectroscopy

Table of Contents

1. Introduction

The contemporary lifestyle is often the cause of many health problems. Widespread diseases in our population include cardiovascular diseases, such as atherosclerosis or hypertension, diabetes, cancer, or skin damage, such as burns or bedsores. These problems strongly influence the length and quality of life. Modern medicine has been developing new drugs that help to reduce the symptoms and consequences of these diseases. However, in some cases, the tissue is irreversibly damaged and must be replaced.

In clinical practice, grafts derived from the same patient or transplants derived from human or animal donors are still widely applied for the replacement of damaged tissue. However, this approach brings a number of problems. Patient tissue is available in a limited quantity and its transplantation could lead to further damage to the tissue itself, along with infection and prolonged rehabilitation. Grafts from human or animal donors can cause disease transmission and severe immune responses leading to transplant rejection. Consequently, new approaches are needed to overcome these limitations.

A promising strategy is the construction of artificial substitutes with appropriate properties for replacing damaged tissue. This task is dealt with a new developing interdisciplinary field - tissue engineering. The strategy is to develop a suitable material scaffold seeded by patient's cells and to implant whole construct into the patient's body. However, the clinically applied vascular and skin substitutes do not meet all the requirements of ideal substitutes. The vascular prostheses are fabricated from porous polymers polyethylene terephthalate (PET, Dacron®) and expanded polytetrafluoroethylene (ePTFE, Teflon®, Gore-Tex®). These commercially available vascular prostheses are steady, safe, and able to resist the stress generated by the bloodstream. However, they are less attractive for cell colonization due to the relatively high hydrophobicity of the polymer surface. This high hydrophobicity does not allow the reconstruction of a continuous non-thrombogenic layer of endothelial cells which is the best prevention of graft occlusion and failure due to the adhesion of thrombocytes, immunocompetent cells, and other blood components.

The skin substitutes currently used in clinical practice mostly serve as temporary wound coverages (dressings) or carriers of skin cells due to their final rejection by the organism. This transplant rejection is mainly caused by using non-resorbable materials

or allogenic cells which are the subjects of inflammatory reactions. The advanced substitutes should be made from materials of appropriate physical and chemical properties that support the cell colonization of materials. A promising approach could be developing biodegradable carriers with cells which would be slowly resorbed by the organism and finally replaced by a newly formed (regenerated) tissue.

This work is focused on the modifications of planar or nanofibrous polymer materials and its interaction with vascular and skin cells. The aim of the modifications is to enhance the cell colonization of materials for the purpose of potentially applying these materials to vascular and skin substitute construction.

1.1 Vascular anatomy and physiology

Blood vessels (arteries and veins) are composed of three main concentrically organized layers, namely the *tunica intima*, *tunica media* and *tunica adventitia* (Fig. 1).

The *tunica intima* is the inner layer of the blood vessels. It contains a monolayer of endothelial cells, supported by the internal elastic lamina. In healthy blood vessels, the endothelial cell layer is continuous and semipermeable, and the endothelial cells are phenotypically mature, i.e. non-proliferating, non-thrombogenic, non-immunogenic, and produce factors, which help to maintain the vascular smooth muscle cells (VSMC) of the *tunica media* in mature contractile phenotypes. These factors include e.g. sulfated glycosaminoglycans, heparin-like molecules, nitric oxide etc. (Glukhova and Koteliansky 1995).

The *tunica media* is the middle layer of the blood vessel wall. It contains VSMC arranged into layers disposed circularly around the vessel. Very large vessels, such as the aorta, also contain layers of longitudinally arranged VSMC in the outer part of the media. An important feature of VSMC in a healthy adult blood vessel is that these cells are in a mature, quiescent (i.e. non-proliferative and non-migratory) phenotype, referred to as a contractile (because of the abundance of contractile filaments), and exert their contractile function (for a review, see Bacakova et al. 2004; Bacakova and Svorcik 2008; Bacakova et al. 2011).

The *tunica adventitia* is the outer layer of the blood vessel. It is composed of fibroblasts, and particularly small blood vessels (referred to as "*vasa vasorum*") and nerves, which provide blood supply and innervation to the cells in the vessel wall. Other functions of the *tunica adventitia* is to anchor the blood vessel to the surrounding tissue

(Shin et al. 2003), and also to provide a source of stem and progenitor cells for the physiological renewal of the blood vessel or for its regeneration in case of its damage (Stenmark et al. 2006).

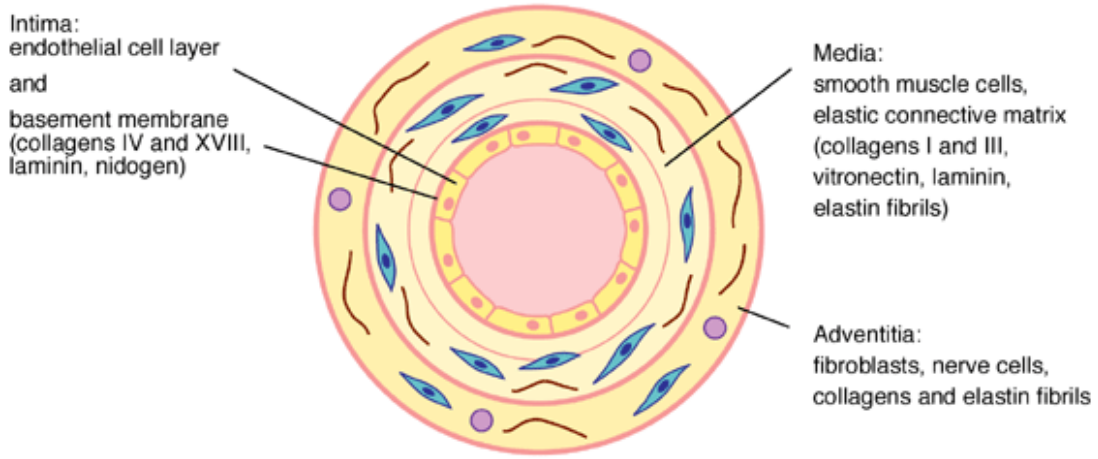

Fig. 1: The structure of the arterial wall in cross section (Adams 2002)

1.2 Blood vessel damage

Blood vessel damage is most often associated with atherosclerosis and hypertension. Vessel injury is initiated through mechanical or biochemical damage to the endothelial cell lining. Mechanical damage is especially induced by pathologically high blood pressure (hypertension). Biochemical injury can be caused by increased levels of glucose or cholesterol, or the presence of free radicals or nicotine (for a review, see (Parizek et al. 2011). Damage to the endothelial cell lining is manifested by increasing its permeability for molecules that normally do not occur inside the vessel wall. In a healthy adult organism, vascular smooth cells (VSMC), forming the *tunica media* of vessels, are in the quiescent non-proliferative state and have a mature differentiated contractile phenotype (Stiebellehner et al. 2003). The molecules which penetrate from an ambient environment to the vessel wall stimulate the VSMC to abnormal migration and proliferation. These molecules include particularly platelet derived-growth factor (PDGF) and other growth factors, e.g. fibroblasts growth factor (FGF) or epidermal growth factor (EGF). Other blood proteins, such as albumin, fibronectin, vitronectin, globulins, and lipoproteins, penetrate through the endothelial cell lining and change the composition of the ECM of the vessel wall. This process initiates the immune activation of endothelial cells and VSMC (Rudijanto 2007). The

cells synthesize the immunoglobulin and selectin adhesion molecules, e.g. intracellular adhesion molecule-1 (ICAM-1), vascular adhesion molecule-1 (VCAM-1), and endothelial-leukocyte adhesion molecule-1 (ELAM-1), exposed on their surface. These adhesion molecules on the cell membrane bind immune cells, such as leukocytes, lymphocytes, monocytes, macrophages, and mast cells (Glaser et al. 2011). The inflammatory cells migrate inside the vessel wall, produce cytokines, e.g. interleukins and tumor necrosis factor (TNF), and proteolytic enzymes, e.g. tryptase, chymase, and metalloproteases (MMP) (Sprague and Khalil 2009), which degrade the ECM of the vessel wall and activate the VSMC to migrate and proliferate (Stiebellehner et al. 2003).

All these mechanisms stimulate the VSMC to phenotypic modulation, i.e. the cells change their phenotype from contractile to synthetic (Stiebellehner et al. 2003; Orr et al. 2010). This change is manifested by the loss of contractile proteins, such as alpha-actin and the isoforms SM1 and SM2 of myosin (Sung et al. 2005), and an increase in the number of cell organelles involved in proteosynthesis (endoplasmatic reticulum, ribosomes, Golgi complex) (Fager et al. 1989). The phenotypically-modulated VSMC increase the production of ECM proteins, which support cell migration from the *tunica media* into the *tunica intima*, and their subsequent proliferation. The migration and proliferation of VSMC lead to a thickening of the vascular wall, the formation of atherosclerotic plaques, and a reduction of the vascular lumen diameter (Stiebellehner et al. 2003; Parizek et al. 2011).

Atherosclerosis is usually treated with a specific low fat diet and medicine use. However, in some cases, the vessel is seriously and irreversibly damaged and must be replaced with an autologous or artificial substitute (Chlupac et al. 2009).

1.3 Skin anatomy and physiology

Skin is the largest organ of the human body serving as a protective barrier against environmental influences. It plays a crucial role in thermoregulation and nutrition. Skin protects the organism against mechanical insults and the penetration of potentially harmful chemical and microbiological agents into the internal organs (Pereira et al. 2013).

The skin is composed of three main layers – the epidermis, dermis and hypodermis (Fig. 2A). The epidermis, the outermost layer, consists mainly of keratinocytes (more than 90 % of all cell types), but it also contains subpopulations of

melanocytes, Langerhans cells and Merkel cells. The epidermal cells form five sublayers: *stratum basale*, *stratum spinosum*, *stratum granulosum*, *stratum lucidum* and *stratum corneum* (Fig. 2B). These sublayers are bound together by complexes of cell adhesion proteins referred as to desmosomes. Desmosomes attach (link) the cell surface adhesion proteins to intracellular keratin filaments and enable cell-cell interactions. The cell adhesion proteins of desmosomes important in keratinocyte-keratinocyte bonding are cadherins, desmogleins and desmocollins. New epidermal cells are created in the deepest basal layer as stem cells, and then they differentiate and mature in adult keratinocytes and move towards the skin surface. The basal cells are the most mitotically active, thus the defects in the homeostasis of this layer have a critical impact on the maintenance of an intact and viable epidermis. As keratinocytes mature and ascend towards the epidermal layers, their shape becomes flattened, and these cells synthetize the structural protein keratin. The outermost keratinized layer is created by dead keratinocytes rich in the protein keratin. The importance of keratinization is to create a barrier to prevent fluid loss and the unwanted entry of potentially harmful molecules and microorganisms. The keratinocytes also produce many important molecules - growth factor and protective immunogenic molecules. These molecules include interleukins (IL), transforming growth factors (TGF-α, TGF-β), PDGF, FGF, TNF-α, and interferons (IFN-α, IFN-β). The melanocytes produce the pigment melanin that protects the skin against the harmful effect of sunlight. The Langerhans cells, i.e. a type of leucocytes, are responsible for immune activation. The function of Merkel cells is not yet clearly elucidated, but they probably occasionally participate in the formation of the synaptic junction with peripheral nerves, and in lower vertebrates, they participate in slow-adapting touch perception (Nguyen et al. 2009; Imahara and Klein 2009)

The dermis, situated below the epidermis, is responsible for the elasticity and mechanical integrity of the skin, cutaneous nutrition, immunosurveillance, sensory perception and temperature regulation. The dermis contains fibers of ECM - collagen and elastin that run throughout this layer in all directions. Collagen is a major structural protein of the dermis. It comprises approximately 70 % of its weight and occurs in the majority as type I and the rest is type III. The dermis also contains glycosaminoglycans (GAGs, e.g. hyaluronic acid, heparin-like molecules). The major function of these components is to bind water and cationic molecules, to serve as a cofactor for multiple enzyme pathways and to participate in cell adhesion and growth. Collagen and GAGs

are commonly utilized molecules for creating the bioactive scaffolds used to induce skin regeneration (Nguyen et al. 2009; Imahara and Klein 2009). The main cellular types of dermis are the fibroblasts which are responsible for the synthesis and degradation of dermal proteins. The other cells included in the dermis are endothelial cells, smooth muscle cells, and immune cells (dendritic cells, monocytes, lymphocytes). The dermis also contains nerves, vessels, sweat glands and hair follicles (Imahara and Klein 2009).

Hypodermis, the undermost layer, is mainly composed of adipose tissue and collagen and acts as a fat storage, an energy source, and enables the anchorage of the skin to bone or muscle (Imahara and Klein 2009).

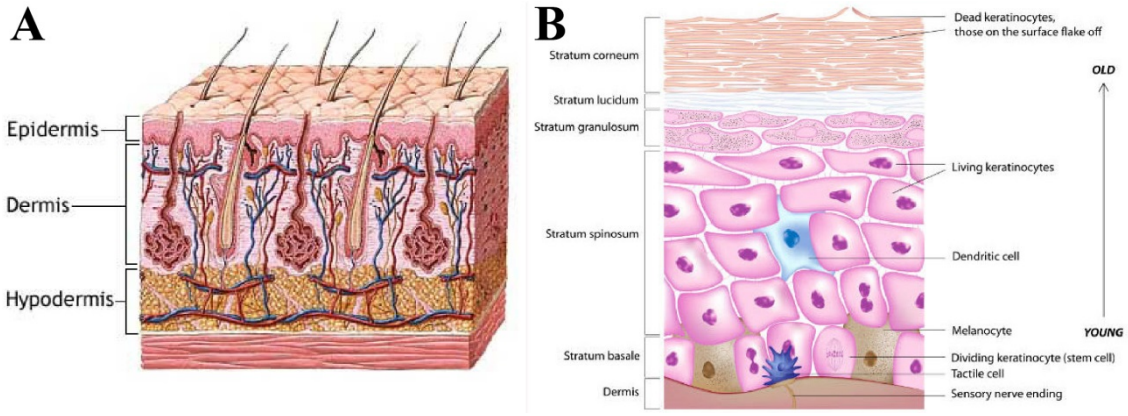

Fig. 2: The anatomy of skin layers (A) and the structure of the epidermis (B)

1.4 Skin damage and wound healing

Skin damage is especially caused by burns, acute trauma, skin diseases, chronic wounds (venous, pressure, leg ulcers), tumors, and surgical interventions (Groeber et al. 2011; Pereira et al. 2013). Skin defects can be divided according to their depth as epidermal, superficial partial-thickness, deep partial-thickness, and full-partial thickness defects. Wound size is a critical factor in the process of epithelialization. A wound regenerates by the skin´s self-healing ability, i.e. the initiation of fibroblasts and keratinocyte migration from the wound edge or from hair follicles and sweat glands in the surrounding undamaged skin tissue. However, full-thickness wounds often result in extensive scar formation. To prevent scar formation, skin grafting is needed (Groeber et al. 2011).

At the moment of the injury, a complex cascade of highly integrated and overlapping reactions is activated. The process of wound healing can be divided into four phases: hemostasis, inflammation, proliferation, and remodeling (Nguyen et al.

2009; Pereira et al. 2013). The first process is responsible for preventing the extension of a hemorrhage. This is attained by platelet aggregation and by the activation of a hemostasis cascade. Blood platelets are activated and form a platelet plug, which is the primary hemostasis process that stops bleeding from the wound. Activation of the coagulation cascade results in the conversion of soluble fibrinogen by thrombin to a network of insoluble fibrin fibers. The network of fibrin fibers stabilizes the platelet plug. This primarily formed plug, referred to as a scab, together with the ECM protein fibronectin, serves as a provisional matrix for wound healing (Mutsaers et al. 1997; Laurens et al. 2006). Activated platelets initiate inflammation by releasing a number of growth factors, including PDGF and TGF-β. PDGF initiate the chemotaxis of immune cells (neutrophils and macrophages), fibroblasts, and endothelial cells. TGF-β enables infiltration of the wound site by macrophages (Nguyen et al. 2009). Macrophages provide a continuous source of cytokines and growth factors such as FGF, interleukins, TNF-α, and also PDGF. These factors promote the migration, proliferation, and differentiation of fibroblasts and endothelial cells, and thus they play an important role in stimulating fibroplasia and angiogenesis, the process of forming new blood vessels (Mutsaers et al. 1997; Nguyen et al. 2009).

During the angiogenesis process, the endothelial cells migrate to the wound, promote the degradation of the fibrin clot by plasmin, and proliferate and form new capillary-like tubes. The proliferation of endothelial cells and tubular sprouting is activated by the vascular growth factor (VEGF) (Nguyen et al. 2009). Blood vessels play an important role in supplying the newly formed tissue by oxygen and nutrients (Laurens et al. 2006). Simultaneously with angiogenesis, i.e. two or three days after injury, fibroblasts migrate to the wound site and produce new molecules of the ECM, predominantly collagen of type I and III, which increase the tensile strength of the wound. At first, type III collagen is deposited, and during the remodeling phase, it is replaced by a stronger collagen of type I (Mutsaers et al. 1997).

Within several hours after a skin injury, the process of reepithelialization begins. The main cells responsible for epithelialization are keratinocytes from the basal layer of wound edges, and also the cells from hair follicles and sweat glands. The epidermal cells change their phenotype, become longer and flatter, dissolve their desmosomes and start migrating to the wound. The migration of epidermal cells is promoted by ECM molecules such as collagen, fibrin, or fibronectin. The cells produce a plasminogen

activator that activates the plasminogen to convert into plasmin that dissolves the scab. Migration and proliferation of the epidermal cells continues until all layers of the epidermis are restored. The proliferation of keratinocytes are regulated in the early stage of reepithelialization by the EGF and TGF-α (secreted by macrophages and epidermal cells), and by the PDGF and keratinocyte growth factor (KGF) secreted by fibroblasts in the middle and late stage of reepithelialization (Nguyen et al. 2009).

During wound healing, the ECM proteins, mainly collagen, are rapidly synthetized by fibroblasts and subsequently degraded (Mutsaers et al. 1997). When the deposition of collagen is in abundance, the remodeling of the ECM begins. This remodeling of the ECM results in scar tissue that contains mostly collagen of type I. The excess collagen is removed, and the remaining collagen fibrils are reorganized and stabilized by crosslinking to provide a more suitable environment for cellular function. This process can last between weeks and months, depending on the size of the wound, but occasionally it can last for years (Nguyen et al. 2009). The degradation of collagen is controlled by collagenase and other proteolytic enzymes such as matrix metalloproteinases. These enzymes are secreted by granulocytes, macrophages, epidermal cells, and fibroblasts. The scar tissue is gradually degraded by altering its texture over a period of many months. Pathological increase in metalloproteinases can lead to excess degradation of collagen resulting in the development of chronic wounds (Mutsaers et al. 1997; Nguyen et al. 2009).

1.5 Tissue engineering and biomaterials

In 1993, Langer and Vacanti defined tissue engineering as an interdisciplinary field that applies the principles of engineering and the life sciences toward the development of biological substitutes that restore, maintain, or improve tissue function (Langer and Vacanti 1993). Tissue engineering designs new material scaffolds, which can be purely biological (ECM) or bioartificial and artificial, and serve as carriers for cells in order to substitute the damaged tissues and organs.

Currently, the autologous grafts, i.e. grafts derived from the same patient, or allogenous and xenogenous grafts, i.e. transplants derived from human or animal donors, are still widely applied for the replacement of damaged tissue. However, both approaches bring a number of problems. Autologous tissue is available in a limited quantity, and its harvesting could lead to additional damage to a patient's tissue, along

with infection and prolonged rehabilitation. Allogeneic or xenogenous grafts can cause transmission of diseases and severe immune responses leading to transplant rejection. Consequently, new approaches are being generated to overcome these limitations. A promising strategy is the construction of biocompatible artificial substitutes with appropriate properties for replacing the damaged tissue. The crucial property of artificial materials designed for tissue substitutes is their biocompatibility. The biocompatibility of the material is its ability to simulate the mechanical and other properties of the original tissue without any toxic, immunogenic, or mutagenic effects on cells or tissues (Bacakova and Svorcik 2008).

Biomaterials can be designed as bioinert or bioactive. Bioinert materials do not allow the adsorption of proteins important for cell adhesion. These types of materials are used in applications in which it is necessary to prevent the activation of the immune system, blood coagulation, thrombosis, extracellular matrix deposition, or other interactions between the material and surrounding environment. These materials have been applied for constructing intraocular lenses, heads, and cups of joint prostheses, heart valves, vascular prostheses (Chlupac et al. 2009), catheters for haemodialysis, or vehicles for therapeutic drug delivery (Bacakova et al. 2004). Bioactive materials are not passively tolerated by cells. They promote the colonization of material with cells, i.e. they actively regulate the adhesion, migration, proliferation, and differentiation of cells, the secretion of various molecules by cells, and also the viability and programmed death of cells. Thus bioactive materials can mimic the functions of original tissue and act as analogs of a natural ECM in controlling cell behavior (Bacakova and Svorcik 2008). Bioactive carriers for cells have been constructed in a two-dimensional way, i.e. as surfaces colonized by cells. Two-dimensional materials have been used for heart valves and vascular prostheses colonized by endothelial cells, bone implants (Bacakova et al. 2004), or skin substitutes containing a carrier with a feeder of fibroblasts covered by keratinocytes (Auxenfans et al. 2009). However, a more advanced approach is the construction of three-dimensional scaffolds for substitutes of vessels, bones, cartilage tissue, or whole organs, such as the liver, kidney, intestines etc. Ideally, the artificial substitute should serve as a temporary support for cell colonization, and it should be gradually resorbed in the organism and replaced by the newly formed ECM and cells (Bacakova et al. 2004).

The bioactivity of materials strongly depends on their physical and chemical properties, mainly the surface polarity and wettability, electrical charge and

conductivity, surface roughness and topography, and the rigidity and deformability of the material. These properties control the adsorption of the cell adhesion-mediating ECM molecules on the material surface in an appropriate concentration and spatial conformation (Bacakova et al. 2011).

1.6 Mechanism of cell-material interaction

The cells adhere to artificial materials through ECM molecules spontaneously adsorbed from the serum supplement of the culture medium under *in vitro* conditions and from the blood and other body fluids under *in vivo* conditions. In addition, these molecules are also synthetized and deposited on the material surface by cells. The most important ECM molecules playing a role in cell anchorage to the material surface are collagen, laminin, elastin, fibrinogen, fibrin, fibronectin, and vitronectin. These ECM proteins mediate cell-material adhesion, but also markedly influence subsequent cell behavior, such as cell spreading, migration, proliferation, viability, metabolic activity, and differentiation. The adhesion-mediating molecules are bound to the material surface through weak chemical bonds such as hydrogen bonds, Van der Waals forces, or electrostatic interactions (Bacakova et al. 2004; Bacakova and Svorcik 2008).

After the adsorption of the cell adhesion-mediating molecules, the cells bind the specific amino acid sequences (oligopeptide ligands) of these molecules by cell adhesion receptors (Fig. 3). These amino acid sequences are typical for certain ECM proteins or they are preferred by specific cell types. Commonly used sequences are RGD and REDV which are typical for fibronectin, KQAGDV for vitronectin, DGEA for collagen, YIGSR and IKVAV for laminin, and VAPG for elastin. Vascular smooth muscle cells preferentially bind KQAGDV and VAPG amino acid sequences (Gobin and West 2003). The REDV amino acid sequence is recognized preferentially by endothelial cells (Wang et al. 2014), KRSR by osteoblasts (Balasundaram and Webster 2007), and YIGSR and IKVAV by neurons. RGD and DGEA amino acid sequences have no significant preference for a specific cell type (Bacakova et al. 2004).

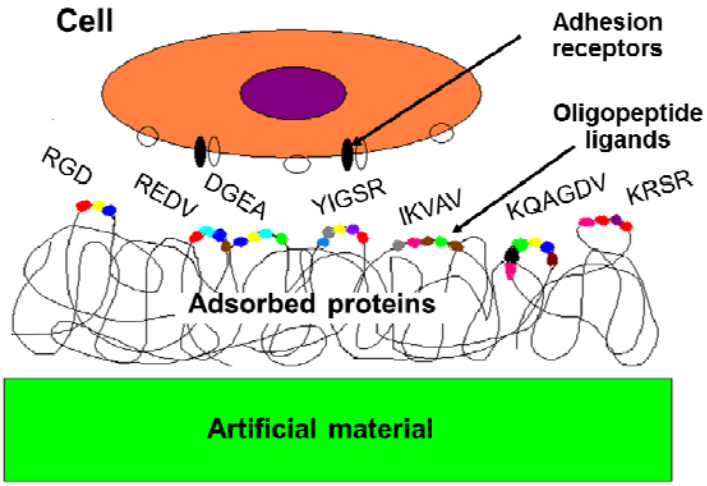

Fig. 3: The mechanism of cell-material interaction (Bacakova and Svorcik 2008)

For successful cell adhesion, the cell adhesion-mediating molecules have to be adsorbed not only in a sufficient amount and homogeneity, but also in an appropriate geometrical conformation. This conformation enables good accessibility of active sites on these molecules by adhesion receptors on the cell membrane (Shin et al. 2003; Bacakova and Svorcik 2008; Bacakova et al. 2011). The geometrical conformation of the ECM proteins is strongly influenced by the physical and chemical surface properties of the material which is discussed in section 1.7 *"Physical and chemical properties of the material surface"*.

The cells bind the ECM proteins adsorbed on the material surface by adhesion receptors located on the cell membrane. The most known and best-described receptors are integrins. Integrins are heterodimeric transmembrane glycoproteins composed of one alpha and one beta chain. Various combinations of alpha and beta chains result in many types of integrin receptors that have preferential affinity to specific amino sequences of the ECM proteins, and are also located preferentially on certain types of cells. For example, the amino acid sequence RGD typical for fibronectin is bound by the $\alpha_v\beta_3$ receptor. Cell adhesion on the material can also be mediated by non-integrin receptors, e.g. proteoglycan-based receptors. These receptors bind the amino acid sequences of the ECM proteins but also the saccharide-based parts of the ECM molecules (Shin et al. 2003; Bacakova and Svorcik 2008). For example, dermal keratinocytes adhere through this way. One group of non-integrin keratinocyte receptors is galectins, a member of the lectin family that binds galactosides (Reno et al. 2008).

After binding the ligands, the integrin adhesion receptors associate into specific sites on the cell membrane, referred to as focal adhesion plaques. In these sites, the integrins communicate with various structural and signaling molecules such as paxillin, talin, vinculin, and focal adhesion kinase. These proteins further communicate with the cytoplasmic actin cytoskeleton, which crosses the entire cell structure and is associated with the nuclear membrane and membranes of cellular organelles. This signaling pathway influences gene expression and proteosynthesis in cells resulting in specific cell behavior, such as spreading, migration, viability or death. It also affects the decision between proliferation and differentiation, along with the transport and secretion of various molecules (Bacakova and Svorcik 2008).

1.7 Physical and chemical properties of material surface

Cell behavior strongly depends on the physical and chemical properties of the material surface. These properties determine the concentration, spatial conformation, and stability of cell adhesion ECM mediating molecules adsorbed on the material surface from the culture media, blood, and other body fluids. These factors influence cell adhesion, spreading, proliferation, migration, and differentiation. The most important physical and chemical properties of a material surface are surface polarity and wettability, electrical charge and conductivity, surface roughness and topography, material rigidity and deformability, and the presence of a specific chemical group on the material surface (e.g. oxygen groups, amino groups, carbon etc.) (Shin et al. 2003; Bacakova et al. 2011).

1.7.1 Surface wettability, rigidity, and deformability

It has been repeatedly shown that hydrophilic surfaces enable the adsorption of ECM molecules in appropriate geometrical conformations which are well-accessible for cell adhesion receptors. In addition, on wettable surfaces, the proteins are adsorbed in a flexible form and can be actively reorganized by cells to reach appropriate spatial conformation. However, on hydrophobic surfaces, cell adhesion-mediating molecules are adsorbed in a denatured and rigid form. The geometrical conformation of these molecules is inappropriate for binding to cells and cells adhere insufficiently (Bacakova and Svorcik 2008; Bacakova et al. 2011). For example, in previous studies, the modification of hydrophobic polyterafluorethylene (PTFE) or polyethylene (PE) by UV

light irradiation or plasma discharge increased the hydrophilicity of the polymer surface and promoted cell adhesion and growth (Heitz et al. 2003; Rimpelova et al. 2013).

However, the material surface has to be moderately hydrophilic for optimal cell adhesion. On highly hydrophilic surfaces, the cell adhesion-mediating molecules either cannot be adsorbed or are relatively weakly bound and cannot resist the traction forces generated by the adhered cells. As a result, the cells cannot primarily adhere to the material surface or they are detached mainly at later culture intervals, when the ECM molecules are not able to bind a larger number of cells (Bacakova et al. 2011). For example, in our earlier studies, a highly hydrophilic substrate composed of copolymer poly-D,L-lactide (PDLLA) and polyethylene oxide (PEO) inhibited the adhesion and spreading of rat aortic smooth muscle cells. Moreover, PEO chains were highly mobile which further disabled the stable adsorption of cell adhesion-mediating molecules and led to poor cell adhesion (Bacakova et al. 2007).

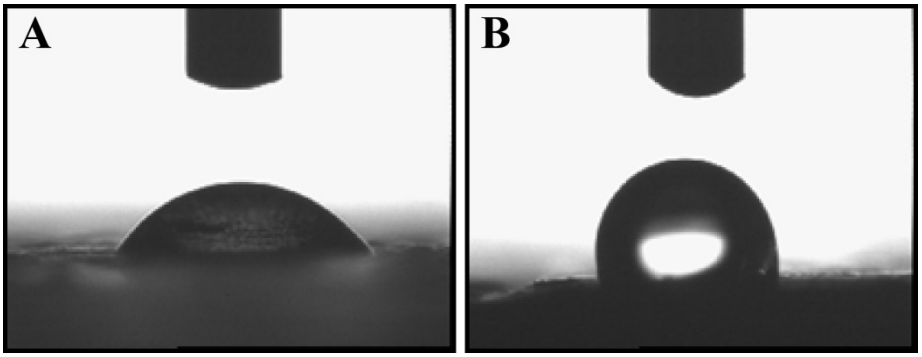

Fig. 4: A water drop on hydrophilic (A) and hydrophobic substrate (B)

A similar situation is found on highly flexible and elastic and deformable materials, e.g. gels. Although these materials allow the adsorption of cell adhesion-mediating molecules, even in an appropriate geometrical conformation, the whole material surface collapses under the traction forces of adhering cells. The cell adhesion receptors can bind specific ligands adsorbed on these materials (e.g. on a non-crosslinked collagen gel or on polyacrylamide gel covalently bound with collagen), but these receptors cannot cluster into focal adhesion plaques and cannot associate with the structural and signaling molecules within these plaques. The actin cytoskeleton cannot be assembled, and the specific signal for further cell proliferation and other cell functions cannot be delivered into the cells (Engler et al. 2004; Bacakova et al. 2011). For this reason, appropriate stiffness and rigidity of the material are required.

1.7.2 Electrical charge and conductivity

The electrical charge and conductivity of the material are other important factors for its colonization with cells. It has been often reported that the positively charged surfaces enable better cell adhesion than negatively charged surfaces. The reason is that the cell adhesion-mediating molecules are negatively charged; thus they are preferentially adsorbed to the positively charged surfaces. In addition, on positively charged substrates, the EMC molecules are adsorbed in more favorable spatial conformations (Bacakova et al. 2011). Iwai *et al*. prepared polyionic nanoparticles mixing positively charged polymer poly(N,N-dimethylaminoethyl methacrylate) with negatively charged plasmid DNA. The substrate was prepared with various charge ratios. The adipose-derived stromal progenitor cells seeded to the substrate preferentially adhered to the positively charged surface. Moreover, on the positively charged substrate, the cells produced a significantly higher amount of VEGF and formed a capillary like network (Iwai et al. 2013). Liu *et al*. showed different effects of the self-assembled monolayers of alkanethiols terminated with the positively charged amino ($-NH_2$) group and negatively charged carboxy (-COOH) groups on the adhesion and spreading of endothelial cells. The cells preferentially adhered and were more pervasively spread on the positively – NH_2 charged surface due to a more appropriate conformation of the ECM protein osteopontin for cell adhesion receptors (Liu et al. 2005).

On the other hand, negatively charged oxygen groups (carboxyl, aldehyde, ketone groups) increase substrate wettability and enable the grafting of various adhesion biomolecules which support cell adhesion and growth (Bacakova et al. 2011). Dadsetan *et. al*. reported that the negatively charged oligo(poly(ethylene glycol) fumarate hydrogel stimulated chondrocyte to produce collagen II and glycosaminoglycans (Dadsetan et al. 2011). Recent studies of our group have shown that the negatively charged groups formed on titanium during thermal oxidation supported the osteogenic differentiation of human osteoblast-like Saos-2 or MG-63 cells, while positively charged groups on thermally oxidized TiNb were associated with the increased proliferation activity of these cells (Jirka et al. 2013; Vandrovcova et al. 2014).

The electrical conductivity of various materials also enhanced the adhesion, growth, and differentiation of various cell types (Jeong et al. 2008; Reznickova et al. 2013). This enhancement was apparent even without the active stimulation of cells with

an electrical current running through the material, e.g. in human osteoblast-like MG-63 cells in cultures on nanocrystalline diamond films doped with boron (Kromka et al. 2010; Grausova et al. 2011).

1.7.3 Surface roughness and topography

Material surface roughness and topography also play a crucial role in cell adhesion and growth, with key factors being the size, shape, and distance of irregularities. Surface roughness can be distinguished according to the size of the irregularities such as macroroughness (irregularities 100 μm to 1mm in size), microroughness (1μm to 100 μm), submicron-scale roughness (100 nm to 1 μm), and nanoroughness (less than 100 nm) (Bacakova et al. 2011).

Macroscale surface roughness is usually not felt by cells, because the irregularities are sufficiently large to allow cell adhesion on these formations, e.g. in hollows or on the sidewalls of prominences on the material surface. In addition, macroscale irregularities often help to anchor the implant in the surrounding tissue, e.g. in the bone.

However, microroughness seems to be less appropriate for the adhesion and spreading of cells. The size of the irregularities is similar to the spreading area of the cells, thus the cells cannot adhere to the material surface by whole area. The result is that the cells adhere in a way which is enabled by the surface irregularities. The cells try to bridge the irregularities or squeeze between them, which leads to the deformation of the cell spreading area (Bacakova and Svorcik 2008; Bacakova et al. 2011).

An advanced approach is constructing surfaces with nanoscale roughness. The nanostructure of materials can better mimic the structure and mechanical properties of the fibrous component of the natural ECM. Nanostructured surfaces enable the adsorption of cell adhesion-mediating ECM molecules in appropriate geometrical conformations; thus the cell adhesion receptors can easily bind the specific amino acid sequences of these molecules (Sun et al. 2012). From this point of view, the surface nanoroughness has a similar effect to surface wettability. The surface nanoroughness can even compensate for the low wettability of a material. For example, the addition of carbon nanotubes to a highly hydrophobic terpolymer of polytetrafluoroethylene, polypropylene, and polyvinyldifluoride provided nanoscale surface roughness on this terpolymer and markedly enhanced the adhesion and growth of human osteoblast-like cells, although the surface hydrophobicity of the material did not change significantly

(Bacakova et al. 2011). In addition, nanofibrous membranes are advantageous for constructing a bilayer of skin cells – fibroblasts and keratinocytes. These membranes will separate the two cell types, but due to the porous structure of the material, they will ensure the physical and humoral communication of the cells. The layer of fibroblasts can therefore serve as a nutrient feeder for keratinocytes, similar to the native skin. Nanofibrous or nanoporous materials can also be advantageous for constructing tubular three-dimensional vascular substitutes. The wall is designed for the ingrowth of vascular smooth cells, which would form a contractile multilayer. The inner surface of the vascular substitute would be colonized with endothelial cells (Parizek et al. 2011).

1.8 Polymer modification for constructing vascular and skin substitutes

The modification of a polymer surface leads to a change in its physical and chemical properties, such as polarity, wettability, chemical composition (presence of oxygen-containing groups etc.), surface roughness and topography, and electrical charge and conductivity. As mentioned above, these characteristics strongly influence the adsorption of cell adhesion-mediating ECM molecules to a sufficient amount and appropriate geometrical conformation, which is important for cell adhesion, spreading, and growth. Modification of the material surface is needed if the substrate does not meet the requirements for sufficient cell colonization. A range of physical or chemical modifications are available for creating a bioactive surface for cell colonization. For example, physical modification can be induced by exposure of the polymer surface to high-energy particles (ions, electrons, radicals etc.). Chemical modification means altering the chemical composition of the material surface after its reaction with chemical solutions, e.g. acids or bases, or after direct grafting various chemical groups or molecules onto the material surface (Bacakova and Svorcik 2008; Bacakova et al. 2011).

1.8.1 Physical Modification

Physical modifications, based on the exposition of the polymer surface to a beam of particles with high energy, are ultraviolet (UV) light irradiation, ion irradiation, and plasma discharge (Bacakova and Svorcik 2008). A common feature of these techniques is splitting the bonds in the macromolecule chains of a polymer, which results in the creation of free radicals, double bonds, and new functional groups (mainly oxygen-

containing groups) on the polymer surface. Oxidized groups increase surface wettability which enables the adsorption of cell adhesion-mediating molecules in an appropriate geometrical conformation for cell adhesion receptors. Free radicals and unsaturated bonds can be subsequently used for functionalizing the material surface with various biomolecules, e.g. amino acids, oligopeptides, or proteins, which can further influence the colonization of the material with cells. Conjugated unsaturated double bonds increase the electrical conductivity of the material surface, and as mentioned above, electrical conductivity improves cell behavior (Bacakova and Svorcik 2008; Bacakova et al. 2011).

Modification of the material surface by UV irradiation is especially used for synthetic polymers, such as polytetrafluorethylene (PTFE) and polyethylene terephthalate (PET). These polymers have been applied for the construction of clinically used vascular prostheses (Chlupac et al. 2009), but in their pristine state, they are relatively highly hydrophobic. The positive effect of UV irradiation on cell adhesion can be further enhanced by irradiation in a reactive atmosphere, e.g. an ammonia atmosphere, which enriched the polymer surface with amine groups (Heitz et al. 2003), or an acetylene atmosphere, which induced the formation of a carbon film on the polymer surface (Kubova et al. 2007). Ion irradiation is based on the interactions of energetic ions with the polymer matrix. Ions are generated in the ion implanter and accelerated by the electrical field. Plasma discharge is performed in a vacuum chamber (Bacakova and Svorcik 2008) where the applied gas can be inert or reactive. Argon, helium, or neon can be used as inert gases, while frequently used reactive gases are oxygen, nitrogen, fluorine, hydrogen, or organic components such as tetrafluoromethane. The electrical discharge accelerates the free electrons which ionize, cleave, and excite the gas molecule. The result is highly reactive gas products which react with the exposed polymer surface and cleave bonds in macromolecules. As mentioned before, the cleavage of bonds leads to the generation of free radicals and unsaturated double bonds. The products of the macromolecule cleavage also react with the oxygen present in the ambient atmosphere and create oxidized groups on the polymer surface, e.g. carboxyl, carbonyl, and ester groups (Bacakova and Svorcik 2008; Svorcik et al. 2009). The resulting surface properties of the modified polymer are dependent on several physical factors of the plasma modification process, especially the type of gas used, plasma power, and exposure time (van Kooten et al. 2004; Svorcik et al. 2006). After plasma modification, the polarity and wettability of the polymer surface

increase with the exposure time due to a higher concentration of oxidized groups on the material surface. Oxidized groups, occurring on the polymer surface after plasma discharge, are reoriented from the surface to the inside of the polymer. This is the aging period of the polymer after plasma exposition. This rearrangement of the surface structure causes a decrease in the polarity and wettability of the modified polymer, but in most cases, the surface wettability still remains higher than in the non-treated polymer. The rearrangement of the oxidized groups during the aging period is influenced by the degree of crosslinking of the polymer structure and by the plasma exposure time. A less crosslinked structure and a longer exposure time lead to a greater mobility of these groups and a stronger decrease in the surface wettability of the modified polymer (Svorcik et al. 2006; Kotal et al. 2007).

1.8.2 Chemical modification

Advanced chemical modifications of materials for tissue engineering are based particularly on grafting bioactive molecules and nanoparticles on the material surface, which further affects the attractiveness of the material for cells. These biomolecules and nanoparticles include e.g. amino acids (e.g. glycine, alanine, leucine) (Svorcik 2004), oligopeptidic ligands for cell adhesion receptors, e.g. RGD (Rockova-Hlavackova et al. 2004), carbon particles (Parizek et al. 2013), or gold particles (Svorcik et al. 2009).

The grafting of biomolecules can be enhanced by UV irradiation, ion irradiation, or plasma discharge (Fig. 5). Free radical, double groups, and various chemical functional groups newly formed on the material surface easily create bonds with various bioactive molecules (Bacakova et al. 2011). In previous studies, polyethylene (PE) of low density (LDPE) was treated by plasma discharge and subsequently grafted with glycine, polyethylene glycol (PEG), bovine serum albumin, and colloidal carbon nanoparticles. This grafting further promoted the adhesion, spreading, and growth of smooth muscle cells (VSMC) (Parizek et al. 2013). In another study, the PE was grafted with the bovine serum albumin and cell adhesion-mediating molecule fibronectin after plasma treatment. The VSMC cultivated in a serum-free medium did not adhere to the PE grafted with the bovine serum albumin, i.e. a cell non-adhesive protein, whereas on PE grafted with fibronectin, cell adhesion was better than on non-grafted PE (Novotna et al. 2013). The grafting of gold (Au) nanoparticles on an Ar^+ plasma-activated surface

further enhanced the cell adhesion and proliferation of mouse embryonic 3T3 fibroblasts and VSMC (Svorcik et al. 2009).

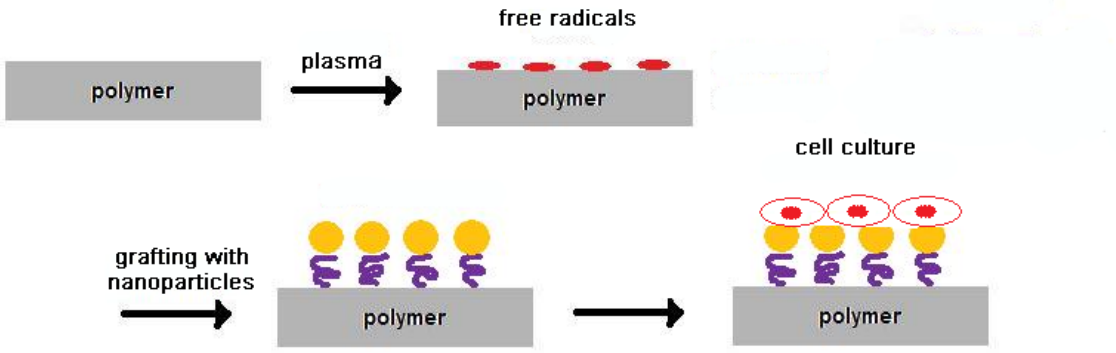

Fig. 5: The principle of grafting nanoparticles on a plasma-activated surface (Svorcik et al. 2010)

The bioactivity of biomaterials can also be enhanced by coating with durable or degradable layers. For the fabrication of skin and vascular substitutes, mainly soft degradable layers are applied. These degradable layers are represented by the various ECM molecules, e.g. collagen, laminin, fibronectin, or fibrin, which are normally present in native tissues or participating in tissue regeneration and wound healing (Filova et al. 2014; Chlupac et al. 2014). These molecules represent a natural source of ligands for cell adhesion receptors and enhance the physiological behavior of cells. In addition, the bioactive layers on the material surface can contain growth factors or drugs which can be released by a controllable manner. These ligands can be suitable for modifying the inner surface of clinically used PET vascular prostheses in order to enhance their endothelialization (Chlupac et al. 2014). For the fabrication of a skin substitute, natural biomolecules, such as collagen I, hyaluronic acid, fibronectin, or fibrin, could be applied for coating suitable carriers of skin cells. Skin cell carriers could be constructed as porous or nanostructured scaffolds from biodegradable materials. Collagen I and hyaluronic acid are normally present in natural skin, and fibrin - as a provisional matrix molecule - plays an important role in skin regeneration (Imahara and Klein 2009; Nguyen et al. 2009). Previous studies proved that a fibrin scaffold supported the proliferation of fibroblasts and keratinocytes, collagen I and III production by dermal fibroblasts, and keratinocyte differentiation (Mazlyzam et al. 2007; Seet et al. 2012). In addition, collagen, fibrin, and hyaluronic acid are often the main components of current clinically used skin substitutes.

The most advanced approach to tissue engineering is binding not all of the ECM molecules, but their active sites, i.e. oligopeptidic ligands for cell adhesion receptors on the material surface. The oligopeptidic ligands are tethered to the material surface through flexible polymeric chains, i.e. PEO or PEG, in defined concentrations, spacing, and distribution in order to precisely control the extent and strength of cell adhesion, the size of the cell spreading area, and the subsequent cell growth. Flexible PEO or PEG chains ensure appropriate spatial conformation of the ligands and good accessibility of the ligands to cell adhesion receptors. In addition, these chains provide a bioinert and protein-repulsive background preventing unwanted protein adsorption and aberrant uncontrolled cell adhesion to these surfaces. Another benefit is that direct functionalization with adhesion oligopeptides enables the binding of specific ligands for a specific cell type. Moreover, the oligopeptide ligands are not species-specific, and thus they are not immunogenic like whole ECM molecules (Bacakova et al. 2004; Bacakova et al. 2007; Bacakova and Svorcik 2008).

1.9 Vascular substitutes

Autologous native vessels are still considered as vascular substitutes of the highest quality. The most important advantage is that natural vessels consist of a phenotypically mature endothelial cell layer which is considered as the best prevention against the adhesion and activation of immunocompetent cells and thrombocytes on a vascular graft, as well as against the abnormal migration and proliferation of VSMC (Chlupac et al. 2009). In addition, autologous vascular substitutes do not cause an immune response leading to graft rejection or the transmission of diseases like allogenous or xenogenous grafts. However, this approach also has several limitations. Healthy autologous vascular substitutes are available in a limited quantity mainly due to the patient's older age. The other limits are the burden to the patient due to additional surgery and damage of the donor site (Parizek et al. 2011). In addition, typical artery replacements are carried out as a bypass created from vein grafts (e.g. aortocoronary bypass) (Chlupac et al. 2009). After implantation, the venous grafts are exposed to higher blood pressure leading to damage of the endothelial cell layer, activation of VSMC migration and proliferation, thrombosis, and immune activation. This failure to adapt causes restenosis of the venous grafts and failure of the autologous vessel

substitute (Parizek et al. 2011). From this point of view, the new approach tries to overcome these limitations by constructing synthetic vascular substitutes.

The ideal vascular substitute should be composed of all three parts as in the natural vessel: the *tunica intima*, *tunica media,* and *tunica adventitia* (Shin et al. 2003). The vascular substitute can be constructed either purely from biological material (i.e., without any synthetic material), i.e. from ECM molecules and endothelial cells and VSMC, or it can be based on a synthetic scaffold seeded with cells (Chlupac et al. 2009). The synthetic scaffolds should be constructed as three-dimensional porous or fibrous tubular structures. The wall of these structures is adapted for ingrowth of VSMC, which can form a contractile multilayer, while the wall of the scaffold should also enable ingrowth of nourishing capillaries and nerves. The lumen of the synthetic vascular substitute is constructed for colonization by the endothelial cells and these cells should form a confluent layer of phenotypically mature cells, which is non-immunnogenic and non-trombogenic (Parizek et al. 2011).

The scaffolds used for the fabrication of advanced bioartificial vascular prostheses should mimic the function of the natural ECM, i.e. they should regulate the extent of cell adhesion, proliferation, differentiation, and maturation to the desired phenotype. The most promising scaffolds could be made from degradable materials, such as polylactide, polyglycolide, polycaprolactone, or their copolymers and polyurethane derivatives. The goal is that a degradable vascular substitute can serve as a temporary supportive structure for cells stimulating the regeneration of a damaged vessel. The degradable materials can be slowly resorbed in the living organisms and replaced by cells and a newly formed natural ECM. However, studies have revealed that the degradation rate of the degradable substitute is faster than the regeneration of new vascular tissue. In addition, synthetic degradable polymers have often insufficient mechanical properties (Ravi et al. 2009; Ravi and Chaikof 2010). These drawbacks can lead to the formation of an aneurysm on the vascular substitute or a rupture of the vascular prosthesis. Therefore, there has been resurgence in the use of biostable non-degradable polymers, namely PET and PTFE, in vascular wall regeneration or they are combined with degradable materials (Chlupac et al. 2009).

Clinically used vascular prostheses made from non-degradable PET and PTFE polymers are fabricated as porous structures. These polymers have appropriate mechanical properties resistant to stress from the bloodstream. However, these polymers are less attractive for the adhesion and growth of vascular cells mainly due to

the high hydrophobicity of the material surface. This high hydrophobicity does not allow the reconstruction of a continuous layer of endothelial cells. As mentioned above, a phenotypically mature endothelial cell layer is the best anti-thrombogenic surface. A missing endothelial cell layer may lead to a high risk of failure in the vascular substitute, due to the adhesion of thrombocytes, immunocompetent cells and other blood components (Chan-Park et al. 2009; Chlupac et al. 2009; Ravi and Chaikof 2010). This negative effect predominantly occurs in blood vessel substitutes of small diameter (less than 6 mm) due to the relatively slow blood flow. The slow blood flow allows the accumulation of thrombocytes and immune cells, leading to stenosis of the vascular prosthesis. In vascular substitutes of a larger diameter (more than 6 mm), the fast blood flow prevents the adhesion of undesirable blood components. From this point of view, the mature continuous layer of anti-thrombogenic endothelial cells should be specifically reconstructed on a vascular substitute of small diameter (Chan-Park et al. 2009). The attractiveness of the polymer surface for cell colonization can be enhanced by the many forms of physical and chemical modifications mentioned above in section 1.8 *"Polymer modification for constructing vascular and skin substitutes"*.

Many studies deal with the reconstruction of the functional mature endothelial cell layer on vascular prostheses. In addition, the endothelization of vascular prostheses has already been applied in clinical practice, although this procedure is not yet currently used in the surgical treatment of vascular diseases. However, in clinical practice, reconstruction of *the tunica media*, consisting of layers of VSMC, is still omitted in vascular substitutes due to the risk of excessive migration and proliferation of the VSMC and subsequent restenosis of the prosthesis. The construction of the contractile VSMC multilayer remains on a theoretical level and it is applied in experiments *in vitro* or on laboratory animals (Parizek et al. 2011). The contractile phenotype of VSMC can be maintained by the appropriate structure and chemical composition of the scaffolds. Previous studies showed that a three-dimensional structure contributed to maintaining cells in a contractile phenotype (Hu et al. 2010). In addition, some molecules of the ECM, such as laminin, collagen IV, elastin, and sulfated and heparin-like glykosaminoglycans maintain a differentiated contractile phenotype of cells (Moiseeva 2001; Chan-Park et al. 2009). From this point of view, the surface of the vascular substitute can be constructed from these ECM molecules or can be modified by the oligopeptidic ligands derived from ECM molecules, e.g. the amino acid sequence Val-Ala-Pro-Gly (VAPG) derived from elastin, which maintains VSMC in a contractile

phenotype (Andukuri et al. 2010). In addition, the desired VSMC phenotype can be reached by stimulation using the specific growth factors released from the scaffolds or present in the cultivation media (Thyberg 1996; Ucuzian et al. 2010), and particularly by the appropriate mechanical stimulation of cells, e.g. uniaxial cyclic strain stress (Li et al. 2011) or pulsatile flow of the culture medium (Wang et al. 2010) in dynamic bioreactors.

1.10 Skin substitutes

Using autologous tissue (i.e., autografts) is still preferred in the treatment of skin injuries because it enables effective wound healing without immune reactions and decreases the risk of subsequent infection. However, in many cases, autografts are available in a limited quantity for grafting or the patient's conditions do not permit using it. Allografts and xenografts provide only temporary coverage of wounds due to their immune rejection, and also bring problems with potential disease transfer, availability, as well as cultural and ethical problems (Murphy and Evans 2012). For these reasons, a promising approach is the development of bioengineered skin substitutes that would be available in any quantity needed, inexpensive, not the subject of immune rejection, mimicking the physiology and mechanical properties of normal skin, and highly effective in the acceleration of tissue regeneration. Unfortunately, the current clinically applied skin substitutes have not yet achieved all of these expectations (Eisenbud et al. 2004). They often consist of allogeneic cells or xenogeneic materials; thus, they cannot provide permanent coverage. Another common problem of skin substitutes is their high cost.

Most models of skin replacements consist of artificial or biological material serving as a carrier for the anchorage of fibroblasts and subsequently for the cultivation of keratinocytes. Many previous studies have reported that cultivating keratinocytes without a feeder of fibroblasts is often unsuccessful because the dermis with the main fibroblast cellular type plays a crucial nutritional role for keratinocytes (Auxenfans et al. 2009). Nevertheless, clinically used skin substitutes without fibroblasts exist. For example, the skin substitute Laserskin (Fidia Advances Biopolymers, Italy) is a biodegradable matrix composed of benzyl-esterified hyaluronic acid derivate. Autologous keratinocytes are directly cultured on the matrix.

Many synthetic and natural polymers have been used for constructing scaffolds suitable for treating skin injuries. They have different structures (planar, porous or fibrous materials) and chemical compositions. A synthetic skin replacement could be constructed from nylon (Malin et al. 2013), polybutylene terephthalate (El-Ghalbzouri et al. 2004), polyHEMA (Dvorankova et al. 1996), hydroxybutyrate (Peschel et al. 2008), polylactic acid (Selig et al. 2013), polyglycolic acid, polycaprolactone (Dai et al. 2004), or their copolymers (Chen et al. 2005; Selig et al. 2013). The most widely applied natural materials are collagen (Morimoto et al. 2001), chitosan (Pajoum Shariati et al. 2009), hyaluronic acid (Harris et al. 1999; Liu et al. 2004), chondroitin sulfate (Lacroix et al. 2007) etc.

Clinically used skin substitutes are mainly applied for burns, non-healing wounds, chronic ulcers such as venous leg ulcers and diabetic foot ulcers (Eisenbud et al. 2004). They can be divided into three groups: epidermal, dermal, and combined epidermal/dermal substitutes. Epidermal substitutes are composed of autologous keratinocytes, which are cultivated on the biomaterial matrix, or autologous keratinocytes cultivated on mitotically-inactivated mouse fibroblasts. Substitutes, consisting of matrix, are for example MySkin (CellTran Ltd., UK), a silicone support layer; Laserskin (Fidia Advances Biopolymers, Italy), a laser-microperforated matrix of hyaluronic acid derivate (Groeber et al. 2011); or Bioseed-S (BioTissue TechnologieGmBH, Germany), a fibrin sealant (Vanscheidt et al. 2007). An epidermal substitute, consisting of no matrix but inactivated fibroblasts, could for example be Epicel (Genzyme Biosurgery, USA) (Eisenbud et al. 2004).

For treating full-thickness burns, dermal substitutes are applied. These substitutes enable the replacement of both the epidermal and dermal layers of the skin. Some of these substitutes are based on the allogeneic human acellular dermis without the cultivation of the cells (e.g. AlloDerm, LifeCell Corporation, USA). However, most of these substitutes consist of synthetic or biological carriers designed for the subsequent cultivation of skin cells (Groeber et al. 2011). For example, Integra (LifeSciences, USA) is composed of a porous biodegradable matrix of cross-linked bovine collagen with chondroitin sulfate and a semi-permeable silicone layer which prevents water loss (Winfrey et al. 1999). Dermagraft (Advanced Tissue Sciences, USA) consists of human foreskin fibroblasts cultured on a biodegradable polyglactin (PGA/PLA) mesh. As the fibroblasts proliferate across the mesh, they secrete ECM proteins, growth factors, and cytokines (Marston et al. 2003). Hyalograft 3D (Fidia Advanced Biopolymers, Italy) is

based on an hyaluronic acid-derived matrix seeded with autologous fibroblasts (Shevchenko et al. 2010).

The most advanced and sophisticated products available for clinical applications are epidermal/dermal substitutes which mimic both the epidermal as well as dermal layers. These substitutes consist of autologous or allogeneic keratinocytes and fibroblasts incorporated into a biomaterial scaffold. Epidermal/dermal skin substitutes provide growth factors, cytokines, and ECM molecules for effective wound healing. However, they only serve as temporary skin replacements due to tissue rejection (Shevchenko et al. 2010). The other disadvantage is the high manufacturing cost (Groeber et al. 2011). A more durable product has been developed by Fidia Advanced Biopolymers (Italy), which combines two products, i.e. Hyalograft (a dermal substitute) and Laserskin (an epidermal substitute) (Monami et al. 2011). This substitute is based on a microperforated hyaluronic acid membrane seeded with autologous fibroblasts and keratinocytes (Shevchenko et al. 2010). Other epidermal/dermal substitutes are for example Apligraf (Organogenesis Inc., USA), which consists of allogeneic neonatal fibroblasts cultivated on a bovine type I collagen matrix integrated with allogeneic neonatal keratinocytes (Eaglstein and Falanga 1997) or OrCell (Ortec International, USA), which is composed of allogeneic fibroblasts seeded into a bovine type I non-porous collagen sponge. Keratinocytes obtained from the same source are cultivated on the top of the construct (Shevchenko et al. 2010).

Recently, many efforts have been expended to develop full-thickness skin replacements including not only fibroblasts and keratinocytes, but also endothelial cells which form capillary-like structures and melanocytes to induce skin pigmentation (Auxenfans et al. 2009). The angiogenesis in transplanted grafts has been stimulated by applying growth factors such as VEGF using drug delivery systems (Groeber et al. 2011) or integrating endothelial cells directly into the graft (Auxenfans et al. 2009). The most advanced skin substitute development focuses on all three layers of skin, including the hypodermis (Auxenfans et al. 2009) and skin appendages like hair follicles, sweat glands, and sebaceous glands (Groeber et al. 2011). Another promising approach could be the use of stem and progenitor cells.

2. Objectives of the work

The main objective of the work was to study cell behavior on surface-modified biomaterials. The proposed modifications of biomaterials were expected to enhance the cell colonization of materials and would enable successful integration of the implant into the patient´s body.

The objectives of this work can be summarized as follows:

2.1 The first objective of the study was to observe the adhesion, proliferation, and phenotypic maturation of VSMC on polymers treated with plasma and subsequently grafted with bioactive molecules. The hypothesis was that a plasma-activated surface enables the grafting of various bioactive molecules. These biomolecules significantly influence cell behavior on the material. Thus, by grafting specific bioactive molecules on the material surface, it can be possible to modulate the adhesion, proliferation, and phenotypic maturation of VSMC (Novotna et al. 2013; Parizek et al. 2013).

2.2 The next objective of the study was to observe the adhesion and growth of skin cells on PLA nanofibrous membranes modified by plasma treatment. The hypothesis was that plasma discharge alters the physical and chemical properties of the material surface, mainly the surface wettability, morphology, roughness, electrical discharge, conductivity, and presence of chemical groups on the material surface. These alterations of material properties influence cell behavior. The main goal was to modify the nanofibrous membrane by plasma discharge in order to enhance its colonization by keratinocytes (Bacakova et al. 2015).

2.3 The last aim of the study was to modify the nanofibrous membrane from degradable polymers (PLA and PLGA) using the ECM molecules normally present in natural skin (collagen, fibronectin) or occurring during wound healing (fibrin). The study was based on the hypothesis that the nanostructure positively influences cell behavior, because it simulates the structure of the natural extracellular matrix and enables the adsorption of cell adhesion-mediating molecules in an appropriate spatial conformation accessible for cell adhesion receptors. Moreover, coating materials with appropriate ECM molecules is expected to enhance the cell colonization of materials and to promote desired cell behavior. The main goal was to construct nanofibrous carriers with ECM coatings for

skin cells with potential application in skin tissue engineering (Bacakova et al. 2016; Bacakova et al. submitted).

3. Materials and methods

This interdisciplinary work is based on the collaboration of material engineers, physicists, chemists, and biologists. The experiments include the chemical preparation of samples, evaluating the physical and chemical properties of samples, and *in vitro* tests evaluating the cell-material interactions. In this section, a brief description of the materials and methods used is provided. The detailed parameters and conditions of performing the experiments are described in the Appendix (section 10).

3.1 Preparation of polymer foils and degradable nanofibrous membranes

The high-density (HDPE) and low-density polyethylene (LDPE) foils were purchased from Granitol A. S., Moravsky Beroun, Czech Republic.

Nanofibrous membranes made of poly(L-lactide) (PLA; Ingeo™ Biopolymer 4032D, NatureWorks, USA) and poly(L-lactide-*co*-glycolide) copolymer (PLGA; ratio 85:15, Purasorb PLG 8531, Purac Biomaterials, Germany) were prepared using the novel Nanospider needleless electrospinning technology in external collaboration with Elmarco Ltd. (Liberec, Czech Republic) and with InStar Technologies, Joint-Stock Co. (Liberec, Czech Republic). A detailed description of the polymer solvent preparation and electrospinning process conditions is published in Bacakova et al. 2016 and Bacakova et al., submitted.

3.2 Plasma modification

The plasma modification of the HDPE and LDPE polymer foils' surface was carried out in external collaboration with Prof. Václav Švorčík, PhD and his colleagues at the Department of Solid State Engineering (Faculty of Chemical Technology, University of Chemistry and Technology in Prague, Czech Republic). The plasma modification of the PLA nanofibrous membranes were carried out in external collaboration with the Institute of Physics (Czech Academy of Sciences, Czech Republic).

The HDPE and LDPE foils were modified with Ar^+ plasma discharge. The samples were treated for different times (50, 100 or 300 s). The detailed parameters and conditions of the plasma treatment are described in Parizek et al. 2013 and Novotna et al. 2013.

PLA nanofibrous membranes were treated with oxygen plasma discharge. The membranes were treated with different discharge powers (from 25 W to 100 W) and exposure times (from 10 s to 120 s). The detailed parameters and conditions of the plasma treatment are described in Bacakova et al. 2015.

3.3 Grafting of biomolecules to the plasma-activated polymer surface

The HDPE and LDPE polymer foils were grafted with various biomolecules after Ar^+ plasma treatment. The experiments were carried out in external collaboration with the Department of Solid State Engineering (Faculty of Chemical Technology, University of Chemistry and Technology in Prague, Czech Republic). Immediately after the plasma treatment, the samples were immersed in a solution of bovine serum albumin (BSA), fibronectin (Fn), glycine (Gly), polyethylene glycol (PEG), or into a suspension of colloidal carbon particles (C). The samples were incubated for 12 - 24 h at room temperature in order to allow grafting of the biomolecules to the plasma-activated polymer surface. The samples were then rinsed in distilled water, air-dried at room temperature, and stored in an air atmosphere for three weeks in order to reorganize and stabilize their surface structure, particularly the orientation of the oxidized structures on the material surface (the so-called aging period) (Parizek et al. 2013; Novotna et al. 2013).

3.4 Preparation of ECM protein nanocoatings on nanofibrous membranes

The fibrin nanocoating on the PLA or PLGA nanofibrous membranes was prepared by enzymatic activation of human fibrinogen with human thrombin (Riedel et al. 2009). For the creation of the 2D nanostructured fibrin layer, antitrombin III was added. The antitrombin III blocked the unreacted thrombin in the solution.

Collagen nanocoating was prepared from a collagen solution by a change of pH (from acid to basic pH) in the ammonia vapor.

Fibronectin, the cell-adhesion mediating protein, was attached to the fibrin or collagen nanocoating in order to further enhance cell adhesion and spreading.

Detailed conditions of the protein nanocoating preparation are described in Bacakova et al. 2016 and Bacakova et al., submitted.

3.5 Characterization of the physical and chemical properties of the materials

The structure, morphology, and physical and chemical compositions of the materials, along with changes in their properties after the modifications, were observed by using a variety of physical and analytic methods. These measurements were carried out in external collaboration with the Faculty of Chemical Technology (University of Chemistry and Technology in Prague, Czech Republic), the Institute of Physics (Czech Academy of Sciences, Czech Republic), the Institute of Rock Structure and Mechanics (Czech Academy of Sciences, Czech Republic) and with the Department of Anatomy and Biomechanics (Faculty of Physical Education and Sport, Charles University, Czech Republic).

The surface wettability was determined by measuring the contact angle using the static water drop method (Parizek et al. 2013; Novotna et al. 2013). The chemical composition (e.g. the concentration of oxygen and oxygen-containing groups) of the polymer surface was determined by X-ray photoelectron spectroscopy (XPS) (Novotna et al. 2013) or by Rutherford Backscattering Spectroscopy (RBS) (Parizek et al. 2013). The changes in surface morphology and roughness were observed by atomic force microscopy (AFM) (Parizek et al. 2013; Novotna et al. 2013).

The morphology of the nanofibrous membrane was observed by scanning electron microscopy (SEM) (Bacakova et al. 2015; Bacakova et al. 2016; Bacakova et al. submitted). The alteration of the nanofibrous membranes' mechanical properties after plasma treatment was evaluated using a uniaxial tensile test which determined the Young modulus, ultimate tensile strength, and maximal membrane deformation (Bacakova et al. 2015).

3.6 Cells and cell culture conditions

The HDPE and LDPE foils were seeded with vascular smooth muscle cells (VSMC) isolated from a rat aorta using the explantation method (Bacakova et al. 1997) and cultivated in serum-supplemented modified Eagle's Medium (DMEM) with 10 % of fetal bovine serum and 40 μg/mL of gentamicin, or in serum-free medium SmGM®-2 Smooth Muscle Growth Medium-2 supplemented with epithelial growth factor (EGF), basic fibroblast growth factor-B (bFGF), and insulin according to the manufacturer's protocol. The serum-free medium was used in order to enhance the effects of the chemical functional groups and biomolecules grafted onto the material surface on cell

adhesion and growth. This influence can be masked, at least partly, by secondary adsorption of various biomolecules from the serum supplement of the culture medium on the polymer surface. The culture conditions of the VSMC on polymeric foils are described in detail in Parizek et al. 2013 and Novotna et al. 2013.

The plasma-treated or protein-coated PLA or PLGA nanofibrous membranes were seeded with human HaCaT keratinocytes, spontaneously transformed keratinocyte cell line from adult skin, purchased from CLS Cell Lines Service (Germany) (Boukamp et al. 1988), or with neonatal human dermal fibroblasts purchased from Lonza (Basel, Switzerland). Both cell types were cultivated in DMEM with 10% of fetal bovine serum and 40 μg/ml of gentamicin. For experiments focused on collagen synthesis and its deposition on a substrate as ECM, 50 μg/ml 2-phospho-L-ascorbic acid trisodium salt (AA) was added into the cell culture medium to stimulate the dermal fibroblasts to produce collagen. The culture conditions of HaCaT keratinocytes and dermal fibroblasts on polymeric foils are described in detail in Bacakova et al. 2015, Bacakova et al. 2016 and Bacakova et al., submitted.

All types of cells were cultivated in a cell incubator at 37°C and in a humidified atmosphere with 5% of CO_2 in the air.

3.7 Cell number, mitochondrial activity, morphology, and cell spreading area

The spreading and morphology of the cells on the samples were visualized by staining of the cells with a combination of fluorescent dyes diluted in PBS. The cell cytoplasm was stained with Texas Red C_2-maleimide. F-actin, an important molecule of the cell cytoskeleton, was stained with phalloidin conjugated with TRITC, and the cell nucleus was stained with Hoechst #33258. Before the staining, the cells were fixed with -20 °C cold 70 % ethanol. Images of the cell morphology were taken using an epifluorescence microscope or scanned in confocal microscope. At early cell culture intervals (i.e., days 1 or 2 after seeding) the size of the spreading area of individual cells or cell clusters (in HaCaT keratinocytes) was measured on the images of the cells taken under a fluorescence microscope using Atlas software (Tescan Ltd., Brno, Czech Republic).

At earlier cell culture intervals (less than 7 days after seeding), the cell number was estimated by counting the cells on microphotographs taken in 10 randomly chosen fields homogenously distributed on the material surface. The cells were stained by a

combination of fluorescent dyes as described above. The counting of the cells on the microphotographs was not applicable at later culture intervals (7 days and more) because the cells on some samples reached confluence and started to overlap each another. In this case, the cells were detached from the material surface by a trypsin/EDTA solution, and the cells were counted using an automatic counter Vi-CELL XR Analyser (Beckman Coulter, Brea, CA, USA). The cell numbers obtained at various time intervals were expressed as cells per cm^2 and were used for constructing growth curves (Parizek et al. 2013; Novotna et al. 2013).

The cell population density in some studies (Bacakova et al. 2015; Bacakova et al. 2016) was also estimated by the amount of cellular DNA using the Picogreen dsDNA assay kit (Invitrogen®). The assay is based on measurements of Picogreen fluorescence, a nucleic acid stain for quantifying the double-stranded DNA in a solution.

The cell mitochondrial activity was used as an indirect marker of cell proliferation activity, because it usually increases with increasing cell numbers. This parameter was measured by the XTT Cell Proliferation Kit or by the MTS assay. The principle of these assays is the cleavage of yellow tetrazolium salt XTT or MTS and the formation of water-soluble brown formazan salt by the activity of the mitochondrial enzymes in cells. Formazan dye is then quantified by measuring the absorbance using a spectrophotometer (ELISA reader) (Bacakova et al. 2015; Bacakova et al. 2016).

Cell viability was determined using the LIVE/DEAD Viability/Cytotoxicity Kit (Molecular Probes, Life Technologies). This assay is based on the different penetration abilities of two fluorescent dyes through the cell membrane of live and dead cells. Calcein AM penetrates into the live cells and is converted by esterases to a calcein emitting green fluorescence. Ethidium homodimer-1(EthD-1) penetrates through the membrane of the dead cells and stains them with red fluorescence (Bacakova et al. submitted).

3.8 Characterization of markers of cell adhesion, phenotypic maturation, and ECM synthesis

The relative mRNA expression of cellular markers of adhesion and ECM synthesis (collagen I) was measured by a real-time Polymerase Chain Reaction (real-time PCR) (Bacakova et al. 2016). The concentration of adhesion and differentiation molecules in the cells was determined by the Enzyme-Linked Immunosorbent Assay

(ELISA) (Parizek et al. 2013). The total amount of collagen produced by the cells (dermal fibroblasts), i.e. intracellular collagen and collagen deposited on the material as ECM, was measured by the Sircol soluble collagen assay. The Sircol dye binds the acid- and pepsin-soluble collagen synthesized by cells and deposited onto the surface as ECM. The Sircol reagent binds to the [Gly-X-Y] helical structure, as found in all types of collagen (Bacakova et al. 2016).

Immunofluorescence staining was used for the qualitative evaluation of important cell markers and the morphology of protein nanocoating on nanofibrous membranes. The samples were incubated with primary antibodies against specific molecular markers. Subsequently, a secondary antibody conjugated with Alexa Fluor® 488 (Molecular Probes, Invitrogen, USA) was applied to the samples. Before the application of antibodies, the cells were fixed with -20 °C cold 70% ethanol and treated with 1% bovine serum albumin (Sigma-Aldrich, USA) and 1% Tween 20 (Sigma-Aldrich, USA) to block nonspecific binding sites. Images of the cells were taken using an epifluorescence microscope or scanned on a confocal microscope.

3.9 Statistical analysis

The quantitative data are presented as a mean ± standard deviation (SD) or mean ± standard error of mean (S.E.M.) usually from three or four independent samples for each experimental group and time interval. Statistical significance was evaluated using the analysis of variance and Student–Newman–Keuls method. Values of $P \leq 0.05$ were considered significant.

4. Results

The results describe the impact of the biomaterial properties and their modifications on cell behavior. The results are summarized in four impacted publications (sections 4.1 – 4.3) and one manuscript submitted for publication (section 4.5). Detailed results including figures are given in the Appendix (section 10).

4.1 Vascular smooth muscle cells on plasma-treated and biofunctionalized polymer foils surface

Parizek M., Slepickova Kasalkova N., Bacakova L., Svindrych Z., Slepicka P., Bacakova M., Lisa V., Svorcik V. **Adhesion, growth, and maturation of vascular smooth muscle cells on low-density polyethylene grafted with bioactive substances**. *BioMed Research International,* 2013, 371430.

Novotna K.*, Bacakova M.*, Kasalkova N., Slepicka P., Lisa V., Svorcik V., Bacakova L. **Adhesion and Growth of Vascular Smooth Muscle Cells on Nanostructured and Biofunctionalized Polyethylene**. *Materials,* 2013, 6 (5): 1632-1655.

(*These authors contributed equally to this work.)

Both studies focus on the evaluation of the adhesion, growth, and phenotypic maturation of VSMC with plasma-treated and biomolecule-grafted polyethylene (PE) foils. The aim of the studies was to alter the physical and chemical surface properties in order to enhance the cell colonization of PE. These modifications of the polymer surface could be potentially applied in the construction of artificial vascular prostheses.

In the first study, the LDPE foils were treated by Ar^+ plasma discharge and then grafted with biologically active substances, such as glycine (Gly), polyethylene glycol (PEG), bovine serum albumin (BSA), colloidal carbon nanoparticles (C) and BSA with C nanoparticles (BSA+C). The plasma treatment and grafting with bioactive substances significantly improved the colonization of material with VSMC. Grafting with Gly and PEG had a positive effect on cell spreading and the development of focal adhesion plaques containing the proteins talin and vinculin. Grafting of the LDPE with BSA and BSA+C predominantly promoted cell growth, the formation of a confluent layer of cells, and the phenotypic maturation of the VSMC as demonstrated by higher concentrations of α-actin and SM1 and SM2 myosin. The modification of the LDPE

also led to changes in its physical and chemical properties. All modifications increased the oxygen content and surface wettability compared to non-modified LDPE. These changes were the most pronounced on LDPE grafted with Gly and PEG. The grafting of LDPE with C and BSA+C created nanoscale and submicron-scale irregularities of various shapes on the material surface.

In the second study, the HDPE and LDPE foils were treated by Ar^+ plasma discharge for different exposure times (50 – 300 s) and subsequently grafted with fibronectin (Fn) or bovine serum albumin (BSA), i.e. with two important components of the serum supplement of cell culture medium. The samples were then seeded with VSMC and incubated in two types of cell culture media. The first type was a standard cell culture medium supplemented with fetal bovine serum (serum-supplemented medium). The second type was medium without serum (serum-free medium). It is known that the serum supplement of cell culture medium contains ECM molecules, such as fibronectin, vitronectin etc., which are spontaneously adsorbed on the material surface and support cell adhesion and spreading. For this reason, serum-free medium was used in order to enhance the effects of the grafted biomolecules (BSA and Fn) on cell adhesion and growth. In the serum-supplemented medium, all modifications improved the adhesion, spreading, and growth of the VSMC compared to non-modified samples. The cells reached on average higher final population densities on LDPE than on HDPE. On the contrary, in the serum-free medium, the cell non-adhesive properties of BSA were manifested, and BSA did not support cell colonization. Cell population density was even lower and the cell spreading area was smaller than on non-modified samples. The effects of the grafted fibronectin were controversial. We expected the high adhesion and growth of cells on these samples, due to specific adhesion-mediating receptors for Fn on the cell membrane. However, the cell densities in general on all Fn-grafted samples were similar to the values on the plasma-irradiated surfaces (Fig. 6). Similarly, as in the first study, the plasma treatment and grafting with biomolecules increased surface wettability, nanoscale surface roughness (mainly manifested on HDPE), and the formation of oxidized groups on the polymer surface.

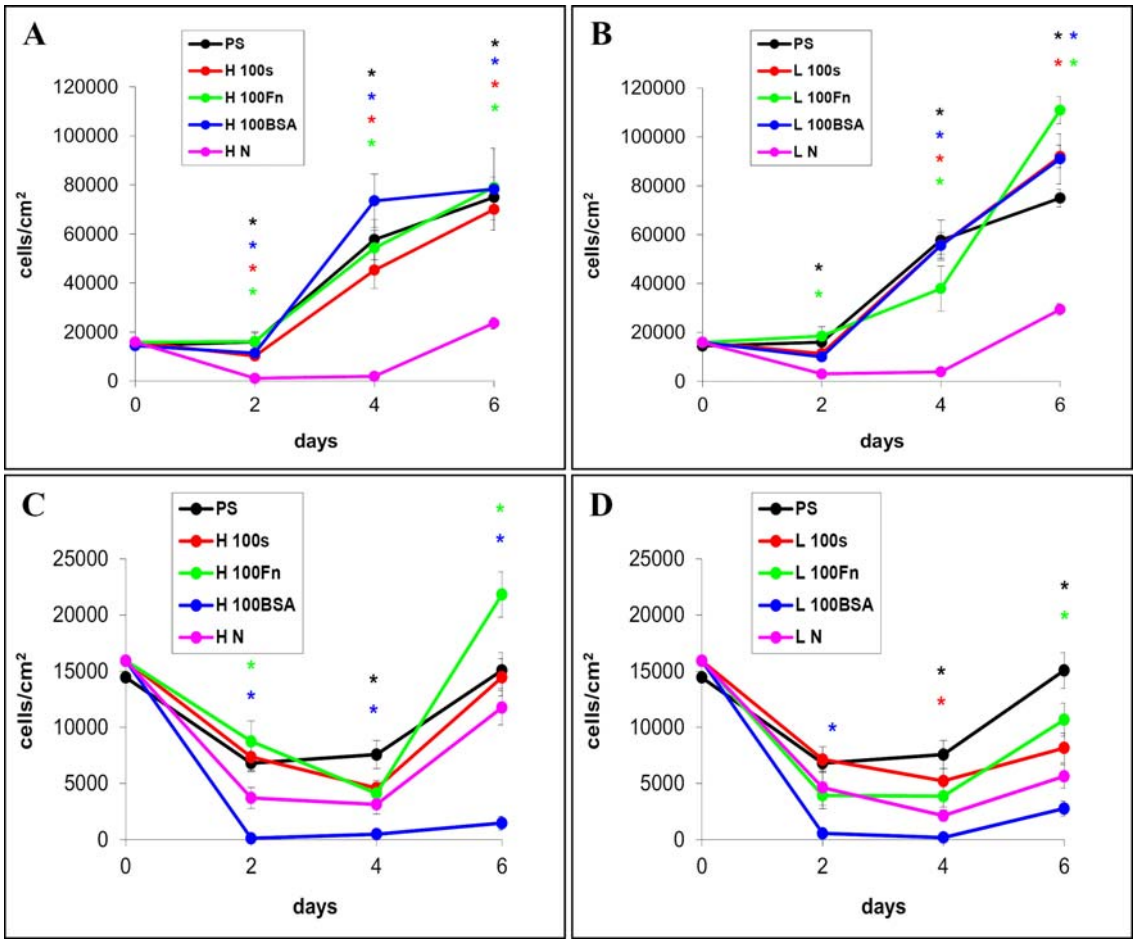

*Fig. 6: Growth curves of rat aortic smooth muscle cells cultured in a serum-supplemented medium (A, B) and in a serum-free medium (C, D) on HDPE (**H**) (A, C) or on LDPE (**L**) (B, D) in a non-treated form (**N**)* or *treated with plasma for **100 s** and subsequently grafted with fibronectin (**Fn**) and bovine serum albumin (**BSA**). A standard cell culture polystyrene dish (**PS**) was used as a reference material. Mean ± S.E.M. ANOVA, Student–Newman–Keuls Method. Statistical significance: * $p \leq 0.05$ compared to the non-modified HDPE or LDPE.*

4.2 Interaction of HaCaT keratinocytes with plasma-treated biodegradable nanofibrous membranes

Bacakova M., Lopot F., Hadraba D., Varga M., Zaloudkova M., Stranska D., Suchy T., Bacakova L. **Effects of fiber density and plasma modification of nanofibrous membranes on the adhesion and growth of HaCaT keratinocytes**. *Journal of Biomaterials Applications,* 2015, 29 (6): 837-853.

The study is focused on evaluating the behavior of human HaCaT kratinocytes on a polylactide (PLA) nanofibrous membrane treated by oxygen plasma. The biodegradable nanofibrous membrane is a promising carrier of skin cells for the

construction of skin replacements. However, the synthetic polymers often do not favor cellular adhesion, growth, and ECM deposition in their pristine state. In this case, the polymers can be physically or chemically modified in order to improve their cell colonization. In this study, we modified the nanofibrous membranes of various fiber densities (5, 9, 16 and 30 g/m^2) with a range of plasma power and exposure times.

We revealed that the cell colonization of biodegradable nanofibrous membranes could be regulated by the treatment and density of the fibers. The plasma treatment strongly altered the morphology and mechanical properties of the nanofibers. The intensity of the fiber alteration and degradation increased with the plasma power and exposure time (Fig. 7). The exposure time seemed to have a more significant effect than the plasma power on fiber alteration. In addition, the fibers in the membranes of higher fiber densities seemed to be more degraded than the fibers in the membranes of lower fiber densities. Plasma treatment increased the membrane stiffness. However, the membranes became more brittle. The modification by plasma slightly increased the concentration of oxygen containing groups on the membrane surface.

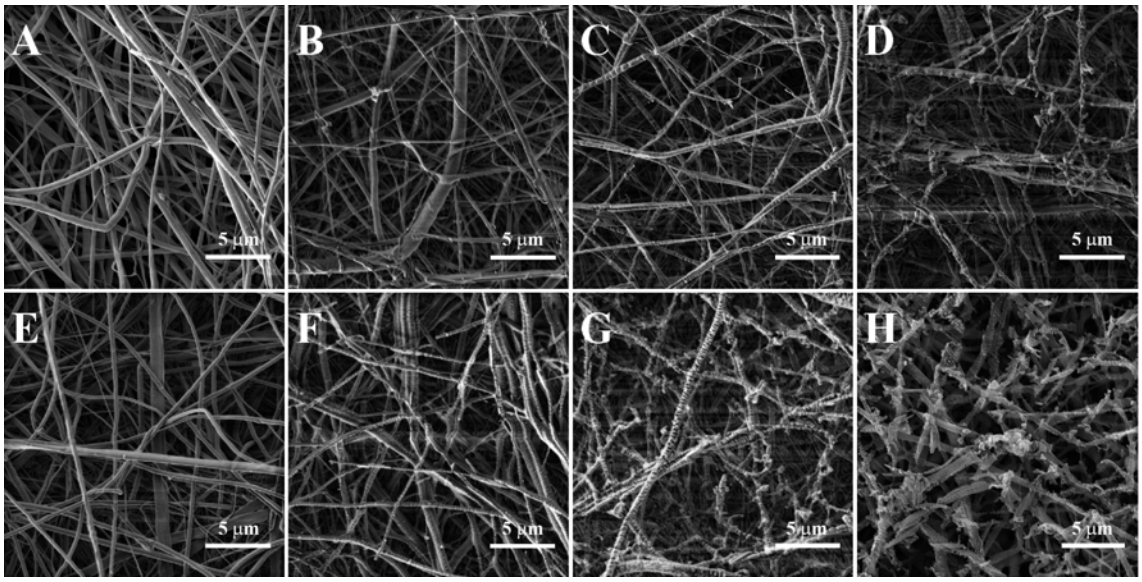

Fig. 7: SEM images of PLA membranes of a fiber density of 16 g/m^2 before (A) and after plasma treatment with various power and exposure times: (B) 50W 30 s, (C) 50W 60 s, (D) 50W 120 s, (E) 75W 30 s, (F) 100W 30 s, (G) 100W 60 s, (H) 100W 120 s. FE-SEM Tescan MIRA3, objective magnification 10 000x.

The treatment of nanofibrous membranes by oxygen plasma has positive effects on their colonization by HaCaT keratinocytes. However, we did not reveal a clear dependence of the cell behavior on specific plasma conditions (i.e., plasma power and

exposure time). Higher plasma power and, in particular, longer exposure times resulted in a more pronounced improvement of the cell adhesion and growth. The fiber density (mainly of the plasma-treated membranes) had a significant effect on cell adhesion and growth (Fig. 8). The cells preferentially adhered with larger cell cluster areas and in higher cell densities to plasma-treated membranes of lower fiber densities (5 or 9 g/m^2) than to plasma-treated membranes of higher fiber densities (16 or 30 g/m^2).

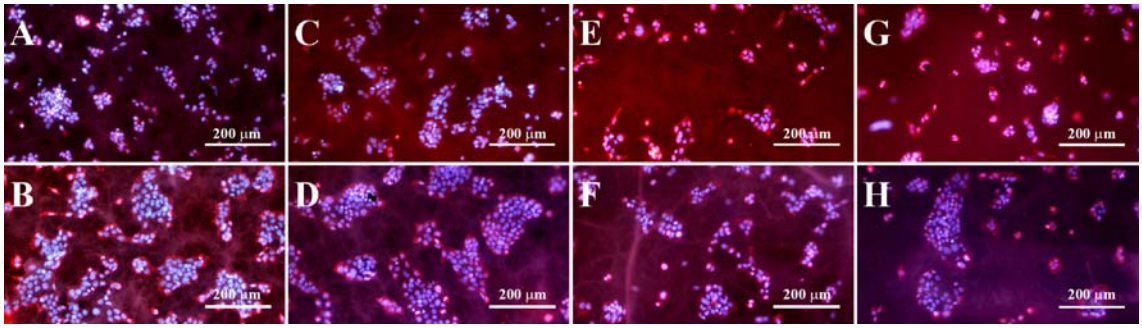

Fig. 8: The morphology of human HaCaT keratinocytes after a three-day cultivation on non-treated (A, C, E, G) and plasma-treated (power 75W, exposure time 30 s; B, D, F, H) PLA membranes of various fiber densities (A, B: 5 g/m^2; C, D: 9 g/m^2; E, F: 16 g/m^2, G, H: 30g/m^2). Cells stained with Texas Red C_2-Maleimide (red) and Hoechst #33342 (blue). Olympus IX 51 microscope, DP 70 digital camera, obj. 10x.

4.3 Dermal fibroblasts and HaCaT keratinocytes on protein-coated biodegradable nanofibrous membranes

Bacakova M., Musilkova J., Riedel T., Stranska D., Brynda E., Zaloudkova M., Bacakova L. **The potential applications of fibrin-coated electrospun polylactide nanofibers in skin tissue engineering**. *International Journal of Nanomedicine*, 2016, 11: 771-789.

Bacakova M., Pajorova J., Stranska D., Riedel T., Brynda E., Zaloudkova M., Bacakova L. **Protein nanocoatings on synthetic polymeric nanofibrous membranes as carriers for skin cells.** Submitted to PLoS ONE.

In both studies we observed the behavior of skin cells, human dermal fibroblasts, and HaCaT keratinocytes on biodegradable nanofibrous membranes modified with cell-degradable protein nanocoating (fibrin, fibronectin or fibrin nanocoating). These molecules are naturally presented in skin (collagen and fibronectin) or occur during

wound healing (fibrin). The combination of a degradable nanofibrous scaffold with these proteins could be promising in constructing skin replacements.

In the first study, we prepared electrospun nanofibrous membranes made of PLA modified with fibrin nanocoating. We seeded them with human dermal fibroblasts and evaluated the cell adhesion and growth. We further investigated the synthesis of collagen by fibroblasts, which is the main component of ECM in skin dermis. For this purpose we added ascorbic acid (AA) into the cell culture medium. It is known that AA plays an important role in the synthesis of hydroxyproline and hydroxylysine, i.e. important molecules forming stable mature collagen with a triple-helical structure. The absence of hydroxyproline and hydroxylysine results in non-stable collagen, which cannot be secreted from the cells at a normal rate (Tajima and Pinnell 1996; Chan-Park et al. 2009).

Fibrin promoted the adhesion and spreading of fibroblasts, manifested by well-developed focal adhesion containing β_1-integrins, and by a higher expression of mRNA for these adhesion receptors. Cell proliferation was also higher on fibrin-coated membranes than on non-coated membranes. This cell performance was further improved by the addition of AA into the cell culture medium. Fibrin nanocoating increased the expression and synthesis of collagen I in dermal fibroblasts. This effect was further enhanced by AA, which promoted the deposition of collagen I in the form of a fibrous ECM on the PLA membrane surface (Fig. 9).

We also evaluated fibrin morphology, stability, and durability. We further investigated fibrin nanocoating degradation and reorganization by cells. Fibrin surrounded the individual fibers in the membrane, and also formed a thin fibrous mesh on several places on the membrane surface. The cell-free fibrin nanocoating remained stable in the cell culture medium for 14 days, and did not change its morphology. On membranes populated with human dermal fibroblasts, the rate of fibrin degradation correlated with the degree of cell proliferation. Fibroblasts penetrated into the fibrin mesh and gradually degraded the fibrin nanocoating. Nevertheless, on day 14, some fibrin-coated fibers and the rest of the thin fibrin nanofibrous mesh were still apparent.

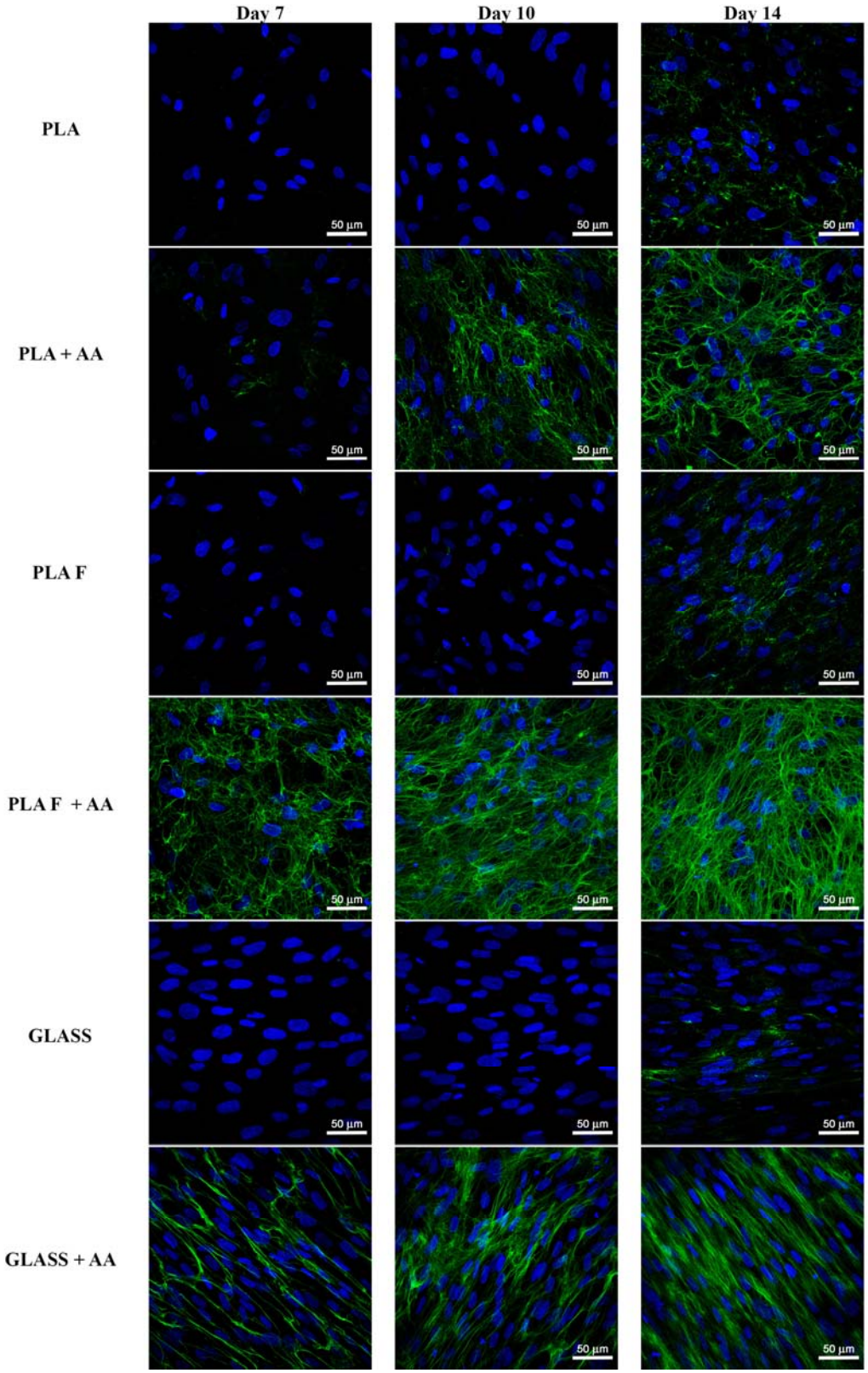

Fig. 9: Immunofluorescence staining of extracellular collagen I fibers (green) produced by human dermal fibroblasts on day 7, 10, and 14 after seeding on non-modified PLA membranes, or on PLA membranes with a fibrin nanocoating (F). The cells were cultivated in a standard cell culture medium or in a medium supplemented with AA. Microscopic glass coverslips

(GLASS) served as a control. Cell nuclei were stained with Hoechst #33258 (blue). Leica TCS SPE DM2500 confocal microscope, obj. 40x/1.15 NA oil.

In the second study, we modified PLGA and PLA electrospun nanofibrous membranes with fibrin and collagen. Moreover, we attached fibronectin (an important cell-adhesion mediating protein) on the fibrin and collagen nanocoating in order to further enhance cell adhesion. We evaluated the adhesion, spreading, and growth of human dermal fibroblasts and HaCaT keratinocytes on these protein-coated membranes.

In the first part of the study we evaluated the morphology, stability, and durability of the protein nanocoatings (Fig. 10). We further investigated the protein degradation and reorganization by these two types of cells. Fibrin morphology, stability, and degradation by dermal fibroblasts have already been described above (in the first study). Collagen coated most of the fibers in the membranes but not regularly. Moreover, collagen randomly created soft gel on the membrane surface. Fibronectin predominantly adsorbed on the thin fibrin mesh or collagen gel and created a thin nanofibrous structure. The durability of the protein nanocoating on nanofibrous membranes was tested over 7 days under the same conditions used for cell cultivation. The results show that fibrin, collagen, or fibronectin nanocoatings on polymer membranes were stable and their morphology was almost unchanged after one week (Fig. 10).

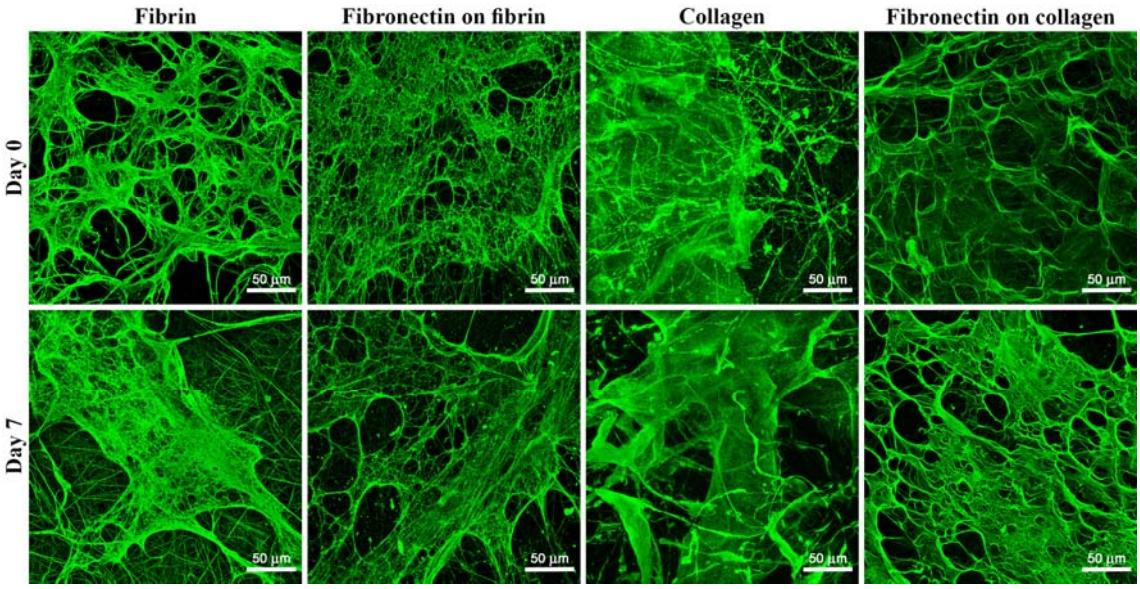

Fig. 10: The morphology of fibrin, collagen, and fibronectin nanocoating on PLGA membranes in a fresh state (Day 0) and after 7 days of incubation in DMEM at 37 °C and in air with 5% CO_2 (Day 7). Protein nanocoatings were stained by immunofluorescence using relevant primary

and secondary antibodies (green). Leica TCS SPE DM2500 confocal microscope, obj. 40x/1.15 NA oil.

The method and time of the degradation and reorganization of protein nanocoating by the cells differed between the fibroblasts and keratinocytes (Fig. 11). The fibroblasts penetrated inside the nanofibrous membranes, mainly in the fibrin-coated membranes, and gradually degraded the protein nanocoating. HaCaT keratinocytes adhered to the membrane surface and did not ingrow into the membranes. These cells bound to the protein nanocoatings and tended to pull down the thin fibrous mesh of fibrin. The fibronectin attached to the fibrin was also completely degraded by keratinocytes together with the fibrin mesh. The collagen gel was capable of resisting the traction forces of the keratinocytes, and was only slightly altered.

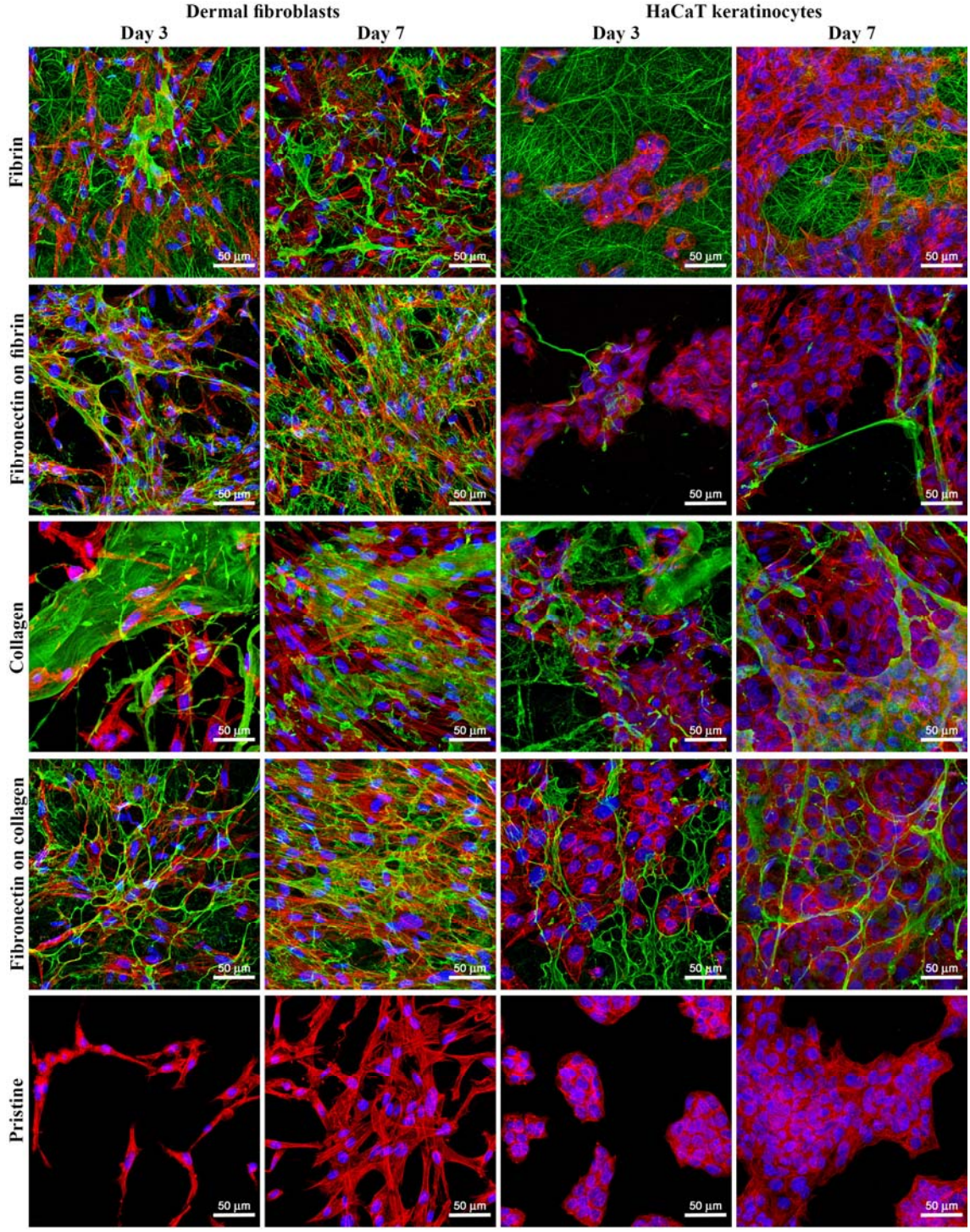

Fig. 11: The morphology of fibrin, collagen, and fibronectin nanocoating on PLGA membranes 3 and 7 days after seeding with human dermal fibroblasts and HaCaT keratinocytes. Pristine: the cells on non-coated PLGA membranes. Protein nanocoatings were stained by immunofluorescence using relevant primary antibodies and secondary antibodies conjugated with Alexa 488 (green). Cells were stained with Phalloidin-TRITC (red) and Hoechst #33258 (blue). Leica TCS SPE DM2500 confocal microscope, obj. 40x/1.15 NA oil.

In the second part of the study we evaluated the adhesion, spreading, morphology, and growth of dermal fibroblasts and HaCaT keratinocytes. The proteins on the membranes significantly improved cell adhesion and growth. The fibroblasts preferentially adhered to the fibrin-coated membranes. The fibrin nanocoating notably improved the fibroblast attachment and spreading, and increased cell mitochondrial activity, i.e. an indirect marker of cell proliferation. Moreover, the fibrin stimulated the fibroblasts to produce fibronectin and deposit it in the cell surroundings as the ECM. In comparison with the dermal fibroblasts, the keratinocytes preferentially adhered on the membranes coated with collagen. The cells were well-spread and formed larger cell islands than on membranes coated with fibrin or on non-coated membranes. The collagen nanocoating also improved keratinocyte proliferation. On the membranes coated with collagen, cell mitochondrial activity was significantly higher than on non-coated membranes and membranes coated with fibrin. Fibronectin attached to fibrin or collagen coating further enhanced the adhesion, spreading, and proliferation of both cell types. No significant differences in the adhesion and growth of cells on protein-coated PLGA and PLA membranes were noticed.

5. Discussion

Advanced tissue substitutes should mimic the physiology, morphology, composition, and functions of the original tissue. They should enable nutrition supply, accelerate tissue regeneration, and should not evoke inflammatory reactions. Sufficient cell colonization and appropriate cell behavior is crucial for successful integration of the implants into the patient's body. The cell behavior and colonization of the biomaterial is critically regulated by its properties.

In this thesis, we evaluated the cell response to various modifications of materials. The main goal was to improve the physical and chemical properties of the materials, and thus to increase their attractiveness for cell colonization. The first two studies are focused on the interaction of materials with vascular cells. They discuss the impact of plasma modification and subsequent functionalization of the plasma-activated surface by bioactive molecules on the behavior of VSMC. The following three studies are concentrated on skin tissue engineering. In the third study, the effect of plasma treatment and the fiber density of nanofibrous membranes on keratinocyte adhesion, spreading, migration, and proliferation is investigated. In the last two studies, desirable cell behavior is afforded to be achieved by modifying the nanofibrous scaffold by the ECM molecules naturally present in the skin or occurring during tissue regeneration. These studies discuss the different behavior of skin cells on these protein-modified materials.

The clinically used vascular prostheses do not favor sufficient cellular colonization. Their relatively high hydrophobic properties do not allow the reconstruction of a continuous layer of endothelial cells and phenotypically matured smooth muscle cells (Chlupac et al. 2009; Ravi and Chaikof 2010). For this reason, vascular prostheses of better chemical and physical properties are needed for more successful implantation. In our studies, we focused on the surface modification of PE by plasma treatment followed by its functionalization with bioactive substances. PE in its pristine (i.e., non-treated) form has high hydrophobicity (its water drop contact angle is about 100°) and does not support the adsorption of the cell adhesion-mediating ECM molecules in a flexible form or in the appropriate geometrical conformation needed for binding cells. The result is that the cells adhere poorly to the polymer surface (Bacakova and Svorcik 2008). Plasma treatment leads to splitting the bonds in the polymer chain,

and creates free radicals, double bonds, and new functional chemical groups (mainly oxygen-containing groups) on the polymer surface. The oxygen-containing groups increase surface wettability, and this supports the adsorption of cell-adhesion-mediating molecules on the polymer surface in a near-physiological and bioactive conformation (for a review, see Bacakova et al. 2011). In our studies, the adhesion, spreading, proliferation, and phenotypic maturation of the VSMC was significantly improved by plasma treatment due to the presence of a higher concentration of oxygen-containing groups, and thus the higher wettability of the PE.

The free radicals and unsaturated bonds created during plasma discharge easily bind various chemical molecules. Thus, these features can be used for functionalizing the material surface with various biomolecules, e.g., grafting amino acids, oligopeptides, or protein molecules, which can also influence cell adhesion and growth (for a review, see (Bacakova and Svorcik 2008; Bacakova et al. 2011). We functionalized the plasma-treated HDPE or LDPE surface with Gly, PEG, BSA, colloidal C nanoparticles or BSA+C (Parizek et al. 2013) or by Fn and BSA (Novotna et al. 2013).

In our studies, the bioactive substance had an important impact on cell behavior. Glycine is a component of a well-known ligand for integrin cell adhesion receptors – RGD (Arg-Gly-Asp). Glycine alone cannot be bound by cell adhesion receptors, but Gly enriches the irradiated polymer surface with oxidized and amino groups. These groups are well-known to improve the adsorption of cell-adhesion mediating proteins and cell colonization (Heitz et al. 2003; Bacakova et al. 2011). Although on the samples grafted with Gly, the lowest contact angle (i.e. the highest wettability) and oxygen content was measured, the cell proliferation was comparable with only plasma-treated samples. However, Gly slightly increased the cell spreading area of the cells which suggests the improved adsorption of cell adhesion molecules. PEG grafted on the plasma-activated LDPE surface did not show a positive effect on cell proliferation but improved cell adhesion and spreading. On these samples, the number of cells was even slightly lower than on non-treated samples. This result contrasts with our previous finding on HDPE foils (Parizek et al. 2009). These differences in cell behavior on the HDPE and LDPE can be explained by the different arrangement of the PEG chains on the polymer surfaces. The PEG chains can be attached to the surface only by one end and dangle on the surface in a water environment (in our case, in the cell culture medium). This PEG behavior has a repulsive effect on cell adhesion, because the

adsorption of cell adhesion molecules is hampered on this mobile surface (Bacakova et al. 2007). On the other hand, PEG can also be attached to the material surface through several sites on a single chain. In this case, the PEG chains are not mobile and can support the adsorption of adhesive molecules and cell adhesion and growth (Kasalkova et al. 2010). In our study, the cell-repulsive effect of the PEG probably prevails on LDPE, whereas on HDPE, PEG promoted the cell adhesion by secondary adsorption of cell adhesion-mediating molecules (Parizek et al. 2009). In spite of the weaker cell proliferation on Gly-grafted LDPE, the spreading area of cells was larger than on other modified samples. This finding implies that the PEG-grafted LDPE surface allowed the adsorption of cell adhesion molecules. However, this adsorption was probably non-homogenous because on some sample regions, the cells were well-spread, while on the other sites, the cells remained round. In addition, grafting the plasma-treated LDPE surface with Gly and PEG significantly increased the concentration of the focal adhesion proteins talin and vinculin, which also indicate the stimulating effect of Gly and PEG on cell adhesion.

The BSA and BSA+C-grafted LDPE surface significantly increased the concentration of α-actin or SM1 and SM2 in the cells, i.e. important markers of the phenotypic maturation of VSMC. The cells on these samples reached a relatively high cell population density. Moreover, they displayed well-developed talin- and vinculin-containing focal adhesion plaques. These factors, i.e. good cell adhesion and growth, are associated with cell differentiation (Bacakova et al. 2004). Nevertheless, albumin is a protein that is non-adhesive for cells and has been used for constructing cell-repulsive surfaces. From this point of view, our finding of the supportive effect of BSA on cell adhesion and growth might be surprising. However, albumin has previously been reported to enable the adsorption of cell adhesion molecules from the serum supplement of the cell culture medium in the appropriate spatial conformation for cell adhesion receptors (Koenig et al. 2003; Koblinski et al. 2005). This indicates the masking effect of the serum in the culture medium. Thus, in order to enhance the effect of grafted BSA on a plasma-activated PE surface, the serum-free medium was used for cultivating the cells. The serum-free medium did not contain cell adhesion-mediating molecules (fibronectin and vitronectin). In the serum-free medium, the cell non-adhesive properties of BSA were revealed. Cell proliferation was significantly weaker than on non-treated samples and the cells were poorly adhered and mainly assumed a spherical shape.

The effect of grafted fibronectin, the protein playing an important role in cell adhesion, was controversial. We expected high adhesion and subsequent growth of the cells on these samples, due to the binding of specific oligopeptide sequences (i.e., RGD-containing sequences) present in these molecules, by cell adhesion receptors. However, the cell proliferation was similar to the only plasma-activated surfaces. The relatively low cell proliferation activity on Fn-grafted samples could be explained by the relatively low quantity and non-homogenous distribution of the Fn molecules attached to the polymer surface. In addition, the geometrical conformation of the Fn immobilized on the polymer surface might be inappropriate for binding by the cells (Burmeister et al. 1996).

In the field of skin tissue engineering, we focused on the modification of the polymer biodegradable nanofibrous membrane in order to enhance its colonization by skin cells. We modified the membrane by plasma treatment or coated it with proteins normally present in the natural skin (collagen, fibronectin) or occurring during wound healing (fibrin).

Biodegradable materials are advantageously used in skin tissue engineering, because they can be slowly resorbed in the organism and finally replaced by newly formed tissue. In the case of the PLA or PLGA, which were used in our studies, the polylactide or polyglycolide is slowly transformed to lactide or glycolide by hydrolysis of the aliphatic ester linkages in the molecules. The lactic and glycolic acid are further metabolized and removed from the body as carbon monoxide and water (Pandey 2013). In our studies, we prepared nanofibrous membranes from these biodegradable polymers. Recently, nanostructured materials have become promising for the construction of tissue substitutes. The nanostructure of the materials better mimics the nanofibrous components of the natural ECM than flat or microstructured surfaces (Sun et al. 2012). Nanostructured materials are capable of adsorbing the cell adhesion-mediating molecules in an appropriate geometrical conformation. Thus, the nanofibrous materials can promote skin regeneration by improving the adhesion and proliferation of the skin cells and the neovascularization of a tissue-engineered skin implant. They enable cells to be supplied with oxygen and nutrition and prevent fluid accumulation at the wound site (Sridhar et al. 2015). In addition, the nanofibrous membranes can be used for developing a bilayer of skin cells, i.e. fibroblasts and keratinocytes situated on opposite sides of the nanofibrous membrane. The pores in the carriers can enable physical and

biochemical communication between the fibroblasts and keratinocytes together with the diffusion of nutrients, growth factors, and other biologically active molecules from the culture medium or the surrounding tissue (McMillan et al. 2007).

In order to further improve the adhesion and growth of skin cells, we treated PLA nanofibrous membranes with oxygen plasma. The plasma-treated membranes better supported the adhesion, spreading (as indicated by a larger cell cluster spreading area), and proliferation of keratinocytes. We revealed a higher amount of oxygen-containing groups (mainly C=O groups) on the membranes after the plasma treatment, which resulted in an increase of surface wettability. These changes of physicochemical properties of the membranes probably led to the enhancement of the cell adhesion and growth observed on these membranes. Previous studies also showed the positive effect of oxygen plasma treatment on cell behavior. For example, Wan et al. treated poly (lactide-co-glycolide) films (PLGA) with oxygen plasma. They observed the incorporation of polar groups into the material surface, an increase in its hydrophilicity, and an improvement in the adhesion and growth of mouse fibroblasts (Wan et al. 2004). Gugala and Gogolewski reported that the oxygen plasma-treated PLA porous membrane better supported the attachment and growth of osteoblasts than the non-treated membrane (Gugala and Gogolewski 2006). Other factors that might improve the colonization of plasma-treated membranes with keratinocytes are an increase of material stiffness and the formation of additional nanostructures on the membrane. SEM images revealed changes in surface morphology, due to the degradation of the fiber surface.

Although the rate of fiber degradation increased with increasing plasma power and exposure time, cell behavior was not significantly affected by these conditions of plasma treatment. Only the differences between the mild and strong plasma conditions were noticed. The samples treated under mild plasma conditions (plasma power less than 50W and exposure time shorter than 30 s) did not show significantly better cell adhesion and proliferation than non-treated membranes. An analysis of the material properties showed that no significant chemical or morphological changes in these samples occurred. It seems that the mild plasma condition did not have an important effect on the physical and chemical properties of the material or on cell behavior. Stronger plasma treatment (plasma power ranging from 50W to 100W and exposure time ranging from 30 s to 120 s) enhanced cell attachment, spreading, and proliferation in comparison to the non-treated membranes. However, we observed no clear dependence of cell behavior on the modulation of plasma power and exposure time.

This observation indicates that an increase in plasma power and exposure time above a specific effective plasma treatment condition limit does not have a significant influence on cell behavior.

However, we found that the fiber density had a significant influence on keratinocyte adhesion and growth. This effect was mainly manifested on plasma-treated membranes. The cells adhered in higher densities and the cell cluster area was larger on plasma-treated membranes with lower fiber densities (5 or 9 g/m^2) than on plasma-treated membranes with higher fiber densities (16 or 30 g/m^2). This result can be explained by the presence of larger pores between the fibers in the membranes with a lower fiber density, which may have provided more space for the cells to migrate into deeper layers of the membranes and to proliferate. They may also enable a better oxygen and nutrient supply for the cells. Soliman et al. described a similar effect of the fiber packing density of nanofibrous membranes on cell behavior. Higher fiber packing density resulted in smaller pores and weaker cell proliferation (Soliman et al. 2011). Moreover, plasma treatment led to a decrease in the size of the pores between fibers and an increase in the rigidity and fragility of the membranes. This effect could further enhance the dependence of cell behavior on fiber density.

Another way to improve the attractiveness of nanofibrous membranes for cell colonization is to modify them with specific biomolecules. In our study, we coated the PLA and PLGA nanofibrous membranes with molecules physiologically present in skin (collagen and fibronectin) or by fibrin, a molecule playing an important role during wound healing. The protein nanocoating strongly influenced the behavior of human dermal fibroblasts and HaCaT keratinocytes.

Fibrin deposition on nanofibrous membranes markedly improved the adhesion and proliferation of dermal fibroblasts. Fibrin mediates adhesion through integrin cell adhesion receptors, namely $\alpha_5\beta_1$, $\alpha_v\beta_3$ and $\alpha_v\beta_3$ integrins, which recognize the RGD motifs present in the fibrin molecule (Gailit et al. 1997; Laurens et al. 2006). We revealed that fibrin increased the mRNA level for β_1-integrins and enhanced the development of typical focal adhesion plaques in cells. In addition, through its αC domain, fibrin attracts the ECM molecules from the serum supplement of the cell culture medium, such as fibronectin or vitronectin, thus further supporting cell adhesion (Laurens et al. 2006). Fibrin can stimulate cell proliferation by the alpha and beta chains present in fibrinogen and fibrin molecules (Gray et al. 1993). Other mechanisms of growth stimulation could be the mitogenic activity of the thrombin molecules present in

fibrin (Dawes et al. 1993) or stimulating the autocrine production of growth factors in cells by fibrin (Yamamoto et al. 2005). In contrast to fibroblasts, the adhesion and growth of keratinocytes was not significantly improved by fibrin nanocoating. The explanation could be that keratinocytes naturally do not come in direct contact with fibrin as fibroblasts. After skin damage, fibroblasts migrate into a fibrin clot, start to produce ECM, and as the first cell type, they contribute to the wound healing. Keratinocytes migrate to the wound secondarily, attach to the ECM matrix, and create new cell layers of epidermis. Many previous studies tried to reveal the role of fibrin in the adhesion and proliferation of keratinocytes, but did not come to a consistent consensus. For example, Kubo et al. showed that fibrin and fibrinogen were non-adhesive for keratinocytes due to the lack of $\alpha_v\beta_3$ integrin receptors important for binding cells to fibrin molecule on keratinocytes (Kubo et al. 2001). In our study, the HaCaT keratinocytes were able to adhere to the fibrin-coated membranes, although they were not so well flattened as on collagen-coated membranes. This may be explained by the relatively long exposure of fibrin coating to the adhering keratinocytes, i.e. more than 24 hours, which is sufficient time for these cells to alter or remove the protein coat in order to enhance their adhesion (Kubo et al. 2001). On the other hand, Sese et al. observed that keratinocyte adhesion and proliferation was influenced by the concentration of thrombin (i.e., an enzyme converting fibrinogen into fibrin). They found that the optimal thrombin concentration for the stimulation of keratinocyte proliferation was about 1 U/ml (Sese et al. 2011). The proliferation of fibroblasts was not strongly dependent on the thrombin concentration. In our study, for the fabrication of the fibrin nanocoating, we used thrombin at a concentration of 2.5 U/ml. This concentration was optimal for creating the fibrin nanocoating on the membrane and for supporting the proliferation of fibroblasts but probably not convenient for keratinocyte growth.

Our experiments also revealed that fibrin stimulated the fibroblasts to produce important ECM molecules. Dermal fibroblasts are responsible for synthesizing the ECM, such as collagen or fibronectin, in the skin dermis. On our fibrin-coated membranes, the fibroblasts formed a well-developed network of collagen or fibronectin fibers compared to the non-coated membranes. Other authors described the stimulatory effect of fibrin on the synthesis of collagen (Mazlyzam et al. 2007; Sclafani and McCormick 2012) and fibronectin (Trombetta-eSilva et al. 2013) by fibroblasts. Our experiments proved that ascorbic acid (AA) was important for the formation of collagen

fibers. For this purpose we added AA into the cell culture medium. The cells cultivated on the membrane in a standard cell culture medium (i.e., without AA) did not form well-developed collagen fibers deposited on the membrane. These results are in accordance with a study by Murad et al. They revealed that cells cultivated without ascorbic acid are incapable of forming stable collagen fibers deposited on the material surface, but form only unstable collagen that remain inside the cells (Murad et al. 1981). It is known that AA helps to catalyze the hydroxylation of lysine and proline amino acids, important components that form stable mature collagen with a triple-helical structure outside the cells (de Clerck and Jones 1980; Tajima and Pinnell 1996). In addition, AA added into the cell culture medium increased fibroblast proliferation on our membranes.

Collagen nanocoating on nanofibrous membranes also enhances the attachment, spreading, and proliferation of cells, particularly keratinocytes. Collagen is the main component of the ECM with the oligopeptide sequence DGEA (Asp-Gly-Glu-Ala) which is bound by most of the cells, mainly the $\alpha_2\beta_1$ or $\alpha_3\beta_1$ integrin receptors (Marchisio et al. 1990; Staatz et al. 1991). The mentioned receptors are also expressed in HaCaT keratinocytes (Scharffetter-Kochanek et al. 1992). HaCaT keratinocytes in our study adhered, spread, and proliferated faster on collagen-coated membranes compared to fibrin-coated or non-coated membranes. After a skin injury, the keratinocytes physiologically migrate into the wound and interact through their integrin receptors with molecules of the ECM, mainly with collagen I nanofibers (O'Toole 2001). It seems to be beneficial to modify nanofibrous scaffolds using collagen or directly fabricate collagen nanofibrous scaffolds (Rho et al. 2006; Mahjour et al. 2015). Compared to keratinocytes, dermal fibroblasts adhere to and proliferate on collagen-coated membranes, in a similar manner as on non-coated membranes. During wound healing, the fibroblasts produce strong ECM fibers made of collagen and elastin which resist the traction forces of the cells (Eastwood et al. 1996). However, on our membranes, the collagen mostly created a gel that was probably too soft and was deformed by the traction forces generated by fibroblasts. Thus, the collagen gel was probably not capable of providing an appropriate substrate for the attachment and migration of dermal fibroblasts. Agis et al. compared the fibroblast behavior on collagen gel and on a collagen porous sponge. They found that the collagen sponge better supported cell migration, proliferation, and ECM production compared to collagen gel (Agis et al. 2014).

In order to further enhance cell attachment, spreading, and proliferation, fibronectin was deposited onto the fibrin or collagen nanocoatings. Fibronectin is not only one of the most important ECM proteins participating in cell adhesion, but it is also involved in the mechanism of cell proliferation and migration (Ruoslahti and Pierschbacher 1987). The fibronectin further enhanced the adhesion and proliferation of dermal fibroblasts. This positive effect was more pronounced on collagen-coated membranes, i.e. on the material where the adhesion and growth of fibroblasts were less stimulated than on fibrin. In addition, on the collagen-coated membrane, fibronectin further improved the spreading of keratinocytes.

6. Conclusion and future perspectives

Modifications of the biomaterials developed in our projects with potential applications in vascular or skin tissue engineering significantly affected the cell colonization of materials. Changes in the biomaterial properties after their specific modifications, and their effect on cell behavior, are summarized in four impacted publications and in one submitted manuscript.

In the field of vascular tissue engineering, we treated the polymer foils by plasma discharge, and subsequently grafted these materials with bioactive substances. The plasma treatment positively influenced the adhesion and growth of vascular smooth muscle cells (VSMC). The beneficial effect of the plasma treatment on cell behavior could be attributed to the formation of new oxygen-containing chemical functional groups on the material surface and its increased wettability. Grafting with Gly or PEG enhanced cell spreading and the formation of focal adhesion plaques. The functionalization of the polymer foils with BSA or BSA+C tended to promote the growth and phenotypic maturation of the VSMC. However, in the serum-free medium (medium without a serum supplement), grafting with BSA poorly supported the cell colonization of materials due to the non-adhesive cell properties of BSA, which were not masked by the adsorption of the cell adhesion-mediating molecules normally present in the serum.

In the field of skin tissue engineering, degradable nanofibrous membranes were modified by plasma discharge or by biomolecules naturally present in the skin and occurring during skin regeneration. The plasma treatment again positively influenced cell behavior which was manifested by the better adhesion, spreading, and higher proliferation of HaCaT keratinocytes. The modification of degradable materials with biomolecules played an important role in cell behavior. The fibrin-coated membranes preferentially stimulated dermal fibroblasts to adhere, proliferate, and produce important molecules of ECM. The collagen-coated membranes enhanced the attachment, spreading, and proliferation of HaCaT keratinocytes. This finding indicates that a degradable nanofibrous membrane with protein nanocoating could be promising for the construction of a bilayered skin substitute. On one side of the membrane, the fibrin-coated nanofibers could support the adhesion, proliferation, and ECM synthesis of fibroblasts. The opposite side of the membrane - with collagen nanocoating - could serve as an appropriate carrier for keratinocytes.

7. References

Adams J. C. Schematic view of an arterial wall in cross-section. Expert Reviews in Molecular Medicine © Cambridge University Press 2002 [cited. Available from http://journals.cambridge.org/fulltext_content/ERM/ERM4_01/S1462399402004039sup006.htm.

Agis H., Collins A., Taut A. D., Jin Q., Kruger L., Gorlach C., Giannobile W. V. Cell population kinetics of collagen scaffolds in ex vivo oral wound repair. *PLoS One,* 2014, 9 (11): e112680.

Andukuri A., Minor W. P., Kushwaha M., Anderson J. M., Jun H. W. Effect of endothelium mimicking self-assembled nanomatrices on cell adhesion and spreading of human endothelial cells and smooth muscle cells. *Nanomedicine (Lond),* 2010, 6 (2): 289-297.

Auxenfans C., Fradette J., Lequeux C., Germain L., Kinikoglu B., Bechetoille N., Braye F., Auger F. A., Damour O. Evolution of three dimensional skin equivalent models reconstructed in vitro by tissue engineering. *Eur J Dermatol,* 2009, 19 (2): 107-113.

Bacakova L., Filova E., Kubies D., Machova L., Proks V., Malinova V., Lisa V., Rypacek F. Adhesion and growth of vascular smooth muscle cells in cultures on bioactive RGD peptide-carrying polylactides. *J Mater Sci Mater Med,* 2007, 18 (7): 1317-1323.

Bacakova L., Filova E., Parizek M., Ruml T., Svorcik V. Modulation of cell adhesion, proliferation and differentiation on materials designed for body implants. *Biotechnol Adv,* 2011, 29 (6): 739-767.

Bacakova L., Filova E., Rypacek F., Svorcik V., Stary V. Cell adhesion on artificial materials for tissue engineering. *Physiol Res,* 2004, 53: S35-45.

Bacakova L., Lisa V., Pellicciari C., Mares V., Bottone M. G., Kocourek F. Sex related differences in the adhesion, migration, and growth of rat aortic smooth muscle cells in culture. *In Vitro Cell Dev Biol Anim,* 1997, 33 (6): 410-413.

Bacakova L., Svorcik V. Cell colonization control by physical and chemical modification of materials. In *Cell Growth Processes: New Research*, edited by D. Kimura. USA: Nova Science Publishers, Inc., 5-56, 2008.

Bacakova M., Lopot F., Hadraba D., Varga M., Zaloudkova M., Stranska D., Suchy T., Bacakova L. Effects of fiber density and plasma modification of nanofibrous membranes on the adhesion and growth of HaCaT keratinocytes. *J Biomater Appl,* 2015, 29 (6): 837-853.

Bacakova M., Musilkova J., Riedel T., Stranska D., Brynda E., Zaloudkova M., Bacakova L. The potential applications of fibrin-coated electrospun polylactide nanofibers in skin tissue engineering. *Int J Nanomedicine,* 2016, 11: 771-789.

Bacakova M., Pajorova J., Stranska D., Riedel T., Brynda E., Zaloudkova M., Bacakova L. Protein nanocoatings on synthetic polymeric nanofibrous membranes as carriers for skin cells. submitted.

Balasundaram G., Webster T. J. Increased osteoblast adhesion on nanograined Ti modified with KRSR. *J Biomed Mater Res A,* 2007, 80 (3): 602-611.

Boukamp P., Petrussevska R. T., Breitkreutz D., Hornung J., Markham A., Fusenig N. E. Normal keratinization in a spontaneously immortalized aneuploid human keratinocyte cell line. *J Cell Biol,* 1988, 106 (3): 761-771.

Burmeister J. S., Vrany J. D., Reichert W. M., Truskey G. A. Effect of fibronectin amount and conformation on the strength of endothelial cell adhesion to HEMA/EMA copolymers. *J Biomed Mater Res,* 1996, 30 (1): 13-22.

Dadsetan M., Pumberger M., Casper M. E., Shogren K., Giuliani M., Ruesink T., Hefferan T. E., Currier B. L., Yaszemski M. J. The effects of fixed electrical charge on chondrocyte behavior. *Acta Biomater,* 2011, 7 (5): 2080-2090.

Dai N. T., Williamson M. R., Khammo N., Adams E. F., Coombes A. G. Composite cell support membranes based on collagen and polycaprolactone for tissue engineering of skin. *Biomaterials,* 2004, 25 (18): 4263-4271.

de Clerck Y. A., Jones P. A. The effect of ascorbic acid on the nature and production of collagen and elastin by rat smooth-muscle cells. *Biochem J,* 1980, 186 (1): 217-225.

Dvorankova B., Smetana K., Jr., Vacik J., Jelinkova M. Cultivation of keratinocytes on poly HEMA and their migration after inversion. *Folia Biol,* 1996, 42 (3): 83-86.

Eaglstein W. H., Falanga V. Tissue engineering and the development of Apligraf, a human skin equivalent. *Clin Ther,* 1997, 19 (5): 894-905.

Eastwood M., Porter R., Khan U., McGrouther G., Brown R. Quantitative analysis of collagen gel contractile forces generated by dermal fibroblasts and the relationship to cell morphology. *J Cell Physiol,* 1996, 166 (1): 33-42.

Eisenbud D., Huang N. F., Luke S., Silberklang M. Skin substitutes and wound healing: current status and challenges *Wounds,* 2004, 16 (1): 2-17.

El-Ghalbzouri A., Lamme E. N., van Blitterswijk C., Koopman J., Ponec M. The use of PEGT/PBT as a dermal scaffold for skin tissue engineering. *Biomaterials,* 2004, 25 (15): 2987-2996.

Engler A., Bacakova L., Newman C., Hategan A., Griffin M., Discher D. Substrate compliance versus ligand density in cell on gel responses. *Biophys J,* 2004, 86 (1 Pt 1): 617-628.

Fager G., Hansson G. K., Gown A. M., Larson D. M., Skalli O., Bondjers G. Human arterial smooth muscle cells in culture: inverse relationship between proliferation and expression of contractile proteins. *In Vitro Cell Dev Biol,* 1989, 25 (6): 511-520.

Filova E., Brynda E., Riedel T., Chlupac J., Vandrovcova M., Svindrych Z., Lisa V., Houska M., Pirk J., Bacakova L. Improved adhesion and differentiation of endothelial cells on surface-attached fibrin structures containing extracellular matrix proteins. *J Biomed Mater Res A,* 2014, 102 (3): 698-712.

Gailit J., Clarke C., Newman D., Tonnesen M. G., Mosesson M. W., Clark R. A. Human fibroblasts bind directly to fibrinogen at RGD sites through integrin alpha(v)beta3. *Exp Cell Res,* 1997, 232 (1): 118-126.

Glaser D. E., Gower R. M., Lauer N. E., Tam K., Blancas A. A., Shih A. J., Simon S. I., McCloskey K. E. Functional characterization of embryonic stem cell-derived endothelial cells. *J Vasc Res,* 2011, 48 (5): 415-428.

Glukhova M. A., Koteliansky V. E. Integrins, cytoskeletal and extracellular matrix proteins in developing smooth muscle cells of human aorta. In *The Vascular Smooth Muscle Cell. Molecular and Biological Responses to the Extracellular Matrix.*, edited by S. M. Schwartz and R. P. Mecham. USA: Acad. Press., 37-79, 1995.

Gobin A. S., West J. L. Val-ala-pro-gly, an elastin-derived non-integrin ligand: smooth muscle cell adhesion and specificity. *J Biomed Mater Res A,* 2003, 67 (1): 255-259.

Grausova L., Kromka A., Burdikova Z., Eckhardt A., Rezek B., Vacik J., Haenen K., Lisa V., Bacakova L. Enhanced growth and osteogenic differentiation of human osteoblast-like cells on boron-doped nanocrystalline diamond thin films. *PLoS One,* 2011, 6 (6): e20943.

Gray A. J., Bishop J. E., Reeves J. T., Laurent G. J. A alpha and B beta chains of fibrinogen stimulate proliferation of human fibroblasts. *J Cell Sci,* 1993, 104 (Pt 2): 409-413.

Groeber F., Holeiter M., Hampel M., Hinderer S., Schenke-Layland K. Skin tissue engineering--in vivo and in vitro applications. *Adv Drug Deliv Rev,* 2011, 63 (4-5): 352-366.

Gugala Z., Gogolewski S. Attachment, growth, and activity of rat osteoblasts on polylactide membranes treated with various low-temperature radiofrequency plasmas. *J Biomed Mater Res A,* 2006, 76 (2): 288-299.

Harris P. A., di Francesco F., Barisoni D., Leigh I. M., Navsaria H. A. Use of hyaluronic acid and cultured autologous keratinocytes and fibroblasts in extensive burns. *Lancet,* 1999, 353 (9146): 35-36.

Heitz J., Svorcik V., Bacakova L., Rockova K., Ratajova E., Gumpenberger T., Bauerle D., Dvorankova B., Kahr H., Graz I., Romanin C. Cell adhesion on polytetrafluoroethylene modified by UV-irradiation in an ammonia atmosphere. *J Biomed Mater Res A,* 2003, 67 (1): 130-137.

Hu J., Sun X., Ma H., Xie C., Chen Y. E., Ma P. X. Porous nanofibrous PLLA scaffolds for vascular tissue engineering. *Biomaterials,* 2010, 31 (31): 7971-7977.

Chan-Park M. B., Shen J. Y., Cao Y., Xiong Y., Liu Y., Rayatpisheh S., Kang G. C., Greisler H. P. Biomimetic control of vascular smooth muscle cell morphology and phenotype for functional tissue-engineered small-diameter blood vessels. *J Biomed Mater Res A,* 2009, 88 (4): 1104-1121.

Chen G., Sato T., Ohgushi H., Ushida T., Tateishi T., Tanaka J. Culturing of skin fibroblasts in a thin PLGA-collagen hybrid mesh. *Biomaterials,* 2005, 26 (15): 2559-2566.

Chlupac J., Filova E., Bacakova L. Blood vessel replacement: 50 years of development and tissue engineering paradigms in vascular surgery. *Physiol Res,* 2009, 58 Suppl 2: S119-139.

Chlupac J., Filova E., Riedel T., Houska M., Brynda E., Remy-Zolghadri M., Bareille R., Fernandez P., Daculsi R., Bourget C., Bordenave L., Bacakova L. Attachment of human endothelial cells to polyester vascular grafts: pre-coating with adhesive protein assemblies and resistance to short-term shear stress. *Physiol Res,* 2014, 63 (2): 167-177.

Imahara S. D., Klein M. B. Skin grafts. In *Biomaterials for Treating of Skin Loss*, edited by D. Orgill and C. Blanco, 58-80, 2009.

Iwai R., Nemoto Y., Nakayama Y. The effect of electrically charged polyion complex nanoparticle-coated surfaces on adipose-derived stromal progenitor cell behaviour. *Biomaterials,* 2013, 34 (36): 9096-9102.

Jeong S. I., Jun I. D., Choi M. J., Nho Y. C., Lee Y. M., Shin H. Development of electroactive and elastic nanofibers that contain polyaniline and poly(L-lactide-co-epsilon-caprolactone) for the control of cell adhesion. *Macromol Biosci,* 2008, 8 (7): 627-637.

Jirka I., Vandrovcova M., Frank O., Tolde Z., Plsek J., Luxbacher T., Bacakova L., Stary V. On the role of Nb-related sites of an oxidized beta-TiNb alloy surface in its interaction with osteoblast-like MG-63 cells. *Mater Sci Eng C Mater Biol Appl,* 2013, 33 (3): 1636-1645.

Kasalkova N., Makajova Z., Parizek M., Slepicka P., Kolarova K., Bacakova L., Hnatowicz V., Svorcik V. Cell Adhesion and Proliferation on Plasma-Treated and Poly(ethylene glycol)-Grafted Polyethylene. *Journal of Adhesion Science and Technology,* 2010, 24 (4): 743-754.

Koblinski J. E., Wu M., Demeler B., Jacob K., Kleinman H. K. Matrix cell adhesion activation by non-adhesion proteins. *J Cell Sci,* 2005, 118 (Pt 13): 2965-2974.

Koenig A. L., Gambillara V., Grainger D. W. Correlating fibronectin adsorption with endothelial cell adhesion and signaling on polymer substrates. *J Biomed Mater Res A,* 2003, 64 (1): 20-37.

Kotal V., Svorcik V., Slepicka P., Sajdl P., Blahova O., Sutta P., Hnatowicz V. Gold Coating of Poly(ethylene terephthalate) Modified by Argon Plasma. *Plasma Process Polym,* 2007, 4 (1): 69-76.

Kromka A., Grausova L., Bacakova L., Vacik J., Rezek B., Vanecek M., Williams O. A., Haenen K. Semiconducting to metallic-like boron doping of nanocrystalline diamond films and its effect on osteoblastic cells. *Diamond and Related Materials,* 2010, 19 (2-3): 190-195.

Kubo M., Van de Water L., Plantefaber L. C., Mosesson M. W., Simon M., Tonnesen M. G., Taichman L., Clark R. A. Fibrinogen and fibrin are anti-adhesive for keratinocytes: a mechanism for fibrin eschar slough during wound repair. *J Invest Dermatol,* 2001, 117 (6): 1369-1381.

Kubova O., Svorcik V., Heitz J., Moritz S., Romanin C., Matejka P., Mackova A. Characterization and cytocompatibility of carbon layers prepared by photo-induced chemical vapor deposition. *Thin Solid Films,* 2007, 515 (17): 6765-6772.

Lacroix S., Bouez C., Vidal S., Cenizo V., Reymermier C., Justin V., Vicanova J., Damour O. Supplementation with a complex of active nutrients improved dermal and epidermal characteristics in skin equivalents generated from fibroblasts from young or aged donors. *Biogerontology,* 2007, 8 (2): 97-109.

Langer R., Vacanti J. P. Tissue engineering. *Science,* 1993, 260 (5110): 920-926.

Laurens N., Koolwijk P., de Maat M. P. Fibrin structure and wound healing. *J Thromb Haemost,* 2006, 4 (5): 932-939.

Li X., Chu J. L., Wang A. J., Zhu Y. Q., Chu W. K., Yang L., Li S. Uniaxial Mechanical Strain Modulates the Differentiation of Neural Crest Stem Cells into Smooth Muscle Lineage on Micropatterned Surfaces. *PLoS One,* 2011, 6 (10).

Liu H., Mao J., Yao K., Yang G., Cui L., Cao Y. A study on a chitosan-gelatin-hyaluronic acid scaffold as artificial skin in vitro and its tissue engineering applications. *J Biomater Sci Polym Ed,* 2004, 15 (1): 25-40.

Liu L., Chen S., Giachelli C. M., Ratner B. D., Jiang S. Controlling osteopontin orientation on surfaces to modulate endothelial cell adhesion. *J Biomed Mater Res A,* 2005, 74 (1): 23-31.

Mahjour S. B., Fu X., Yang X., Fong J., Sefat F., Wang H. Rapid creation of skin substitutes from human skin cells and biomimetic nanofibers for acute full-thickness wound repair. *Burns,* 2015, 41 (8): 1764-1774.

Malin E. W., Galin C. M., Lairet K. F., Huzar T. F., Williams J. F., Renz E. M., Wolf S. E., Cancio L. C. Silver-Coated Nylon Dressing Plus Active DC Microcurrent for Healing of Autogenous Skin Donor Sites. *Ann Plast Surg,* 2013, 71 (5): 481-484.

Marchisio P. C., Cancedda R., De Luca M. Structural and functional studies of integrin receptors in cultured human keratinocytes. *Cell Differ Dev,* 1990, 32 (3): 355-359.

Marston W. A., Hanft J., Norwood P., Pollak R., Dermagraft Diabetic Foot Ulcer Study G. The efficacy and safety of Dermagraft in improving the healing of chronic diabetic foot ulcers: results of a prospective randomized trial. *Diabetes Care,* 2003, 26 (6): 1701-1705.

Mazlyzam A. L., Aminuddin B. S., Fuzina N. H., Norhayati M. M., Fauziah O., Isa M. R., Saim L., Ruszymah B. H. Reconstruction of living bilayer human skin equivalent utilizing human fibrin as a scaffold. *Burns,* 2007, 33 (3): 355-363.

McMillan J. R., Akiyama M., Tanaka M., Yamamoto S., Goto M., Abe R., Sawamura D., Shimomura M., Shimizu H. Small-diameter porous poly (epsilon-caprolactone) films enhance adhesion and growth of human cultured epidermal keratinocyte and dermal fibroblast cells. *Tissue Eng,* 2007, 13 (4): 789-798.

Moiseeva E. P. Adhesion receptors of vascular smooth muscle cells and their functions. *Cardiovasc Res,* 2001, 52 (3): 372-386.

Monami M., Vivarelli M., Desideri C. M., Ippolito G., Marchionni N., Mannucci E. Autologous skin fibroblast and keratinocyte grafts in the treatment of chronic foot ulcers in aging type 2 diabetic patients. *J Am Podiatr Med Assoc,* 2011, 101 (1): 55-58.

Morimoto N., Suzuki S., Kim B. M., Morota K., Takahashi Y., Nishimura Y. In vivo cultured skin composed of two-layer collagen sponges with preconfluent cells. *Ann Plast Surg,* 2001, 47 (1): 74-81; discussion 81-72.

Murad S., Grove D., Lindberg K. A., Reynolds G., Sivarajah A., Pinnell S. R. Regulation of collagen synthesis by ascorbic acid. *Proc Natl Acad Sci U S A,* 1981, 78 (5): 2879-2882.

Murphy P. S., Evans G. R. Advances in wound healing: a review of current wound healing products. *Plast Surg Int,* 2012, 2012: 190436.

Mutsaers S. E., Bishop J. E., McGrouther G., Laurent G. J. Mechanisms of tissue repair: from wound healing to fibrosis. *Int J Biochem Cell Biol,* 1997, 29 (1): 5-17.

Nguyen D. T., Orgill D. P., Murphy G. F. The pathofysiologic basis for wound healing regeneration. In *Biomaterials for Treating Skin Loss*, edited by D. Orgill and c. Bianco, 25-58, 2009.

Novotna K., Bacakova M., Kasalkova N., Slepicka P., Lisa V., Svorcik V., Bacakova L. Adhesion and Growth of Vascular Smooth Muscle Cells on Nanostructured and Biofunctionalized Polyethylene. *Materials,* 2013, 6 (5): 1632-1655.

O'Toole E. A. Extracellular matrix and keratinocyte migration. *Clin Exp Dermatol,* 2001, 26 (6): 525-530.

Orr A. W., Hastings N. E., Blackman B. R., Wamhoff B. R. Complex regulation and function of the inflammatory smooth muscle cell phenotype in atherosclerosis. *J Vasc Res,* 2010, 47 (2): 168-180.

Pajoum Shariati S. R., Shokrgozar M. A., Vossoughi M., Eslamifar A. In vitro co-culture of human skin keratinocytes and fibroblasts on a biocompatible and biodegradable scaffold. *Iran Biomed J,* 2009, 13 (3): 169-177.

Pandey A. K. Recent advancements of biodegradable polylactic acid/ polylactide: A review on synthesis, characterization and applications. *Advanced Materials Letters,* 2013, in press.

Parizek M., Kasalkova N., Bacakova L., Slepicka P., Lisa V., Blazkova M., Svorcik V. Improved adhesion, growth and maturation of vascular smooth muscle cells on polyethylene grafted with bioactive molecules and carbon particles. *Int J Mol Sci,* 2009, 10 (10): 4352-4374.

Parizek M., Novotna K., Bacakova L. The role of smooth muscle cells in vessel wall pathophysiology and reconstruction using bioactive synthetic polymers. *Physiol Res,* 2011, 60 (3): 419-437.

Parizek M., Slepickova Kasalkova N., Bacakova L., Svindrych Z., Slepicka P., Bacakova M., Lisa V., Svorcik V. Adhesion, growth, and maturation of vascular

smooth muscle cells on low-density polyethylene grafted with bioactive substances. *Biomed Res Int,* 2013: 371430.

Pereira R. F., Barrias C. C., Granja P. L., Bartolo P. J. Advanced biofabrication strategies for skin regeneration and repair. *Nanomedicine (Lond),* 2013, 8 (4): 603-621.

Peschel G., Dahse H. M., Konrad A., Wieland G. D., Mueller P. J., Martin D. P., Roth M. Growth of keratinocytes on porous films of poly(3-hydroxybutyrate) and poly(4-hydroxybutyrate) blended with hyaluronic acid and chitosan. *J Biomed Mater Res A,* 2008, 85 (4): 1072-1081.

Ravi S., Chaikof E. L. Biomaterials for vascular tissue engineering. *Regen Med,* 2010, 5 (1): 107-120.

Ravi S., Qu Z., Chaikof E. L. Polymeric materials for tissue engineering of arterial substitutes. *Vascular,* 2009, 17: S45-54.

Reno F., Traina V., Gatti S., Battistella E., Cannas M. Functionalization of a poly(D,L)lactic acid surface with galactose to improve human keratinocyte behavior for artificial epidermis. *Biotechnol Bioeng,* 2008, 100 (1): 195-202.

Reznickova A., Novotna Z., Kasalkova N. S., Svorcik V. Gold nanoparticles deposited on glass: physicochemical characterization and cytocompatibility. *Nanoscale Res Lett,* 2013, 8 (1): 252.

Rho K. S., Jeong L., Lee G., Seo B. M., Park Y. J., Hong S. D., Roh S., Cho J. J., Park W. H., Min B. M. Electrospinning of collagen nanofibers: effects on the behavior of normal human keratinocytes and early-stage wound healing. *Biomaterials,* 2006, 27 (8): 1452-1461.

Riedel T., Brynda E., Dyr J. E., Houska M. Controlled preparation of thin fibrin films immobilized at solid surfaces. *J Biomed Mater Res A,* 2009, 88 (2): 437-447.

Rimpelova S., Kasalkova N. S., Slepicka P., Lemerova H., Svorcik V., Ruml T. Plasma treated polyethylene grafted with adhesive molecules for enhanced adhesion and growth of fibroblasts. *Mater Sci Eng C Mater Biol Appl,* 2013, 33 (3): 1116-1124.

Rockova-Hlavackova K., Svorcik V., Bacakova L., Dvorankova B., Heitz J., Hnatowicz V. Bio-compatibility of ion beam-modified and RGD-grafted polyethylene. *Nuclear Instruments & Methods in Physics Research Section B-Beam Interactions with Materials and Atoms,* 2004, 225 (3): 275-282.

Rudijanto A. The role of vascular smooth muscle cells on the pathogenesis of atherosclerosis. *Acta Med Indones,* 2007, 39 (2): 86-93.

Ruoslahti E., Pierschbacher M. D. New perspectives in cell adhesion: RGD and integrins. *Science,* 1987, 238 (4826): 491-497.

Sclafani A. P., McCormick S. A. Induction of dermal collagenesis, angiogenesis, and adipogenesis in human skin by injection of platelet-rich fibrin matrix. *Arch Facial Plast Surg,* 2012, 14 (2): 132-136.

Seet W. T., Manira M., Khairul Anuar K., Chua K. H., Ahmad Irfan A. W., Ng M. H., Aminuddin B. S., Ruszymah B. H. Shelf-life evaluation of bilayered human skin equivalent, MyDerm. *PLoS One,* 2012, 7 (8): e40978.

Selig H. F., Keck M., Lumenta D. B., Mittlbock M., Kamolz L. P. The use of a polylactide-based copolymer as a temporary skin substitute in deep dermal burns: 1-year follow-up results of a prospective clinical noninferiority trial. *Wound Repair Regen,* 2013, 21 (3): 402-409.

Sese N., Cole M., Tawil B. Proliferation of human keratinocytes and cocultured human keratinocytes and fibroblasts in three-dimensional fibrin constructs. *Tissue Eng Part A,* 2011, 17 (3-4): 429-437.

Shevchenko R. V., James S. L., James S. E. A review of tissue-engineered skin bioconstructs available for skin reconstruction. *J R Soc Interface,* 2010, 7 (43): 229-258.

Shin H., Jo S., Mikos A. G. Biomimetic materials for tissue engineering. *Biomaterials,* 2003, 24 (24): 4353-4364.

Scharffetter-Kochanek K., Klein C. E., Heinen G., Mauch C., Schaefer T., Adelmann-Grill B. C., Goerz G., Fusenig N. E., Krieg T. M., Plewig G. Migration of a human keratinocyte cell line (HACAT) to interstitial collagen type I is mediated by the alpha 2 beta 1-integrin receptor. *J Invest Dermatol,* 1992, 98 (1): 3-11.

Soliman S., Sant S., Nichol J. W., Khabiry M., Traversa E., Khademhosseini A. Controlling the porosity of fibrous scaffolds by modulating the fiber diameter and packing density. *J Biomed Mater Res A,* 2011, 96 (3): 566-574.

Sprague A. H., Khalil R. A. Inflammatory cytokines in vascular dysfunction and vascular disease. *Biochem Pharmacol,* 2009, 78 (6): 539-552.

Sridhar S., Venugopal J. R., Ramakrishna S. Improved regeneration potential of fibroblasts using ascorbic acid-blended nanofibrous scaffolds. *J Biomed Mater Res A,* 2015, 103 (11): 3431-3440.

Staatz W. D., Fok K. F., Zutter M. M., Adams S. P., Rodriguez B. A., Santoro S. A. Identification of a tetrapeptide recognition sequence for the alpha 2 beta 1 integrin in collagen. *J Biol Chem,* 1991, 266 (12): 7363-7367.

Stenmark K. R., Davie N., Frid M., Gerasimovskaya E., Das M. Role of the adventitia in pulmonary vascular remodeling. *Physiology (Bethesda),* 2006, 21: 134-145.

Stiebellehner L., Frid M. G., Reeves J. T., Low R. B., Gnanasekharan M., Stenmark K. R. Bovine distal pulmonary arterial media is composed of a uniform population of well-differentiated smooth muscle cells with low proliferative capabilities. *Am J Physiol Lung Cell Mol Physiol,* 2003, 285 (4): L819-828.

Sun L., Stout D. A., Webster T. J. The nano-effect: improving the long-term prognosis for musculoskeletal implants. *J Long Term Eff Med Implants,* 2012, 22 (3): 195-209.

Sung H. J., Eskin S. G., Sakurai Y., Yee A., Kataoka N., McIntire L. V. Oxidative stress produced with cell migration increases synthetic phenotype of vascular smooth muscle cells. *Ann Biomed Eng,* 2005, 33 (11): 1546-1554.

Svorcik V. Cell proliferation on UV-excimer lamp modified and grafted polytetrafluoroethylene. *Nucl Instrum Methods Phys Res B,* 2004, 217 (2): 307-313.

Svorcik V., Chaloupka A., Rezanka P., Slepicka P., Kolska Z., Kasalkova N., Hubacek T., Siegel J. Au-nanoparticles grafted on plasma treated PE. *Radiation Physics and Chemistry,* 2010, 79 (3): 315-317.

Svorcik V., Kasalkova N., Slepicka P., Zaruba K., Kral V., Bacakova L., Parizek M., Lisa V., Ruml T., Gbelcova H., Rimpelova S., Mackova A. Cytocompatibility of Ar+ plasma treated and Au nanoparticle-grafted PE. *Nucl Instrum Methods Phys Res B,* 2009, 267 (11): 1904-1910.

Svorcik V., Kolarova K., Slepicka P., Mackova A., Novotna M., Hnatowicz V. Modification of surface properties of high and low density polyethylene by Ar plasma discharge. *Polym Degrad Stab,* 2006, 91 (6): 1219-1225.

Tajima S., Pinnell S. R. Ascorbic acid preferentially enhances type I and III collagen gene transcription in human skin fibroblasts. *J Dermatol Sci,* 1996, 11 (3): 250-253.

Thyberg J. Differentiated properties and proliferation of arterial smooth muscle cells in culture. *Int Rev Cytol,* 1996, 169: 183-265.

Trombetta-eSilva J., Eadie E. P., Zhang Y., Norris R. A., Borg T. K., Bradshaw A. D. The effects of age and the expression of SPARC on extracellular matrix production by cardiac fibroblasts in 3-D cultures. *PLoS One,* 2013, 8 (11): e79715.

Ucuzian A. A., Brewster L. P., East A. T., Pang Y., Gassman A. A., Greisler H. P. Characterization of the chemotactic and mitogenic response of SMCs to PDGF-BB and FGF-2 in fibrin hydrogels. *J Biomed Mater Res A,* 2010, 94 (3): 988-996.

van Kooten T. G., Spijker H. T., Busscher H. J. Plasma-treated polystyrene surfaces: model surfaces for studying cell-biomaterial interactions. *Biomaterials,* 2004, 25 (10): 1735-1747.

Vandrovcova M., Jirka I., Novotna K., Lisa V., Frank O., Kolska Z., Stary V., Bacakova L. Interaction of human osteoblast-like Saos-2 and MG-63 cells with thermally oxidized surfaces of a titanium-niobium alloy. *PLoS One,* 2014, 9 (6): e100475.

Vanscheidt W., Ukat A., Horak V., Bruning H., Hunyadi J., Pavlicek R., Emter M., Hartmann A., Bende J., Zwingers T., Ermuth T., Eberhardt R. Treatment of recalcitrant venous leg ulcers with autologous keratinocytes in fibrin sealant: a multinational randomized controlled clinical trial. *Wound Repair Regen,* 2007, 15 (3): 308-315.

Wan Y., Qu X., Lu J., Zhu C., Wan L., Yang J., Bei J., Wang S. Characterization of surface property of poly(lactide-co-glycolide) after oxygen plasma treatment. *Biomaterials,* 2004, 25 (19): 4777-4783.

Wang C., Cen L., Yin S., Liu Q. H., Liu W., Cao Y. L., Cui L. A small diameter elastic blood vessel wall prepared under pulsatile conditions from polyglycolic acid mesh and smooth muscle cells differentiated from adipose-derived stem cells. *Biomaterials,* 2010, 31 (4): 621-630.

Wang W., Guo L., Yu Y., Chen Z., Zhou R., Yuan Z. Peptide REDV-modified polysaccharide hydrogel with endothelial cell selectivity for the promotion of angiogenesis. *J Biomed Mater Res A,* 2014.

Winfrey M. E., Cochran M., Hegarty M. T. A new technology in burn therapy: INTEGRA artificial skin. *Dimens Crit Care Nurs,* 1999, 18 (1): 14-20.

Yamamoto M., Yanaga H., Nishina H., Watabe S., Mamba K. Fibrin stimulates the proliferation of human keratinocytes through the autocrine mechanism of transforming growth factor-alpha and epidermal growth factor receptor. *Tohoku J Exp Med,* 2005, 207 (1): 33-40.

8. Publications

8.1 Publications related to PhD thesis

Parizek M., Slepickova Kasalkova N., Bacakova L., Svindrych Z., Slepicka P., Bacakova M., Lisa V., Svorcik V. Adhesion, growth, and maturation of vascular smooth muscle cells on low-density polyethylene grafted with bioactive substances. *BioMed Research International,* 2013, 371430

IF = 1.579 (2014)

Novotna K.*, Bacakova M.*, Kasalkova N., Slepicka P., Lisa V., Svorcik V., Bacakova L. Adhesion and Growth of Vascular Smooth Muscle Cells on Nanostructured and Biofunctionalized Polyethylene. *Materials,* 2013, 6 (5): 1632-1655.

IF = 2.651 (2014)

***** These authors contributed equally to this work.

Bacakova M., Lopot F., Hadraba D., Varga M., Zaloudkova M., Stranska D., Suchy T., Bacakova L. Effects of fiber density and plasma modification of nanofibrous membranes on the adhesion and growth of HaCaT keratinocytes. *Journal of Biomaterials Applications,* 2015, 29 (6): 837-853.

IF = 2.197 (2014)

Bacakova M., Musilkova J., Riedel T., Stranska D., Brynda E., Zaloudkova M., Bacakova L. The potential applications of fibrin-coated electrospun polylactide nanofibers in skin tissue engineering. *International Journal of Nanomedicine*, 2016, 11: 771-789.

IF = 4.383 (2014)

8.2 Manuscript related to PhD thesis

Bacakova M., Pajorova J., Stranska D., Riedel T., Brynda E., Zaloudkova M., Bacakova L. **Protein nanocoatings on synthetic polymeric nanofibrous membranes as carriers for skin cells**. Submitted to PLoS ONE

8.3 Publications non-related to PhD thesis

Bacakova L., Beranek L., Bacakova M., Soukup D., Lisa V., Dvorak R. Human bone-derived cells on C-C composites treated by grinding, a-C:H coating, laser irradiation

and laser perforation. *Engineering of Biomaterials (Inzynieria Biomaterialów)*, 2008, 11 (75): 2-6.

Grausova L., Vacik J., Bilkova P., Vorlicek V., Svorcik V., Soukup D., Bacakova M., Lisa V., Bačáková L. Regionally-selective adhesion and growth of human osteoblast-like MG 63 cells on micropatterned fullerene C60 layers. *Journal of Optoelectronics and Advanced Materials*, 2008, 10: 2071-2076.

IF = 0.577 (2008), **IF = 0.429 (2014)**

Catros S., Guillotin B., Bacakova M., Fricain J.C., Guillemot F. Effect of laser energy, substrate film thickness and bioink viscosity on viability of endothelial cells printed by Laser-Assisted Bioprinting. *Applied Surface* Science, 2011, 257 (12): 5142-5147.

IF = 2.103 (2011), IF = 2.711 (2014)

Harcuba P., Bacakova L., Stransky J., Bacakova M., Novotna K., Janecek M. Surface treatment by electric discharge machining of Ti-6Al-4V alloy for potential application in orthopaedic. *Journal of the Mechanical Behavior of Biomedical Materials*, 2012, 7: 96-105.

IF = 2.368 (2012), IF = 3.417 (2014)

9. Conferences

9.1 International Conferences

Bacakova M. et al.: Polymer Carriers Modified by Plasma and Functionalized with Au Nanoparticles as Substrates for Mouse 3T3 Fibroblasts. *Biomaterials in Medicine and Veterinary Medicine*, Rytro, Poland, 13. – 16. 10. 2011. Oral presentation.

Bacakova M. et al.: Plasma modified polylactide nanofibers as carriers for skin cells. *The 9th World Biomaterials Congress (WBC),* Chengdu, China, 1. – 5. 6. 2012. Poster.

Bacakova M. et al.: Plasma-Modified Polylactide Nanofibers for Skin Tissue Engineering. *Biomaterials in Medicine and Veterinary Medicine*, Rytro, Poland, 11. – 14. 10. 2012. Oral and poster presentation.

Bacakova M. et al.: Plasma-Modified Polylactide Nanofibers as Carriers for Skin Cells. *The 9th Asian - European International Conference on Plasma Surface Engineering (AEPSE),* Jeju, South Korea, 25. – 30. 8. 2013. Oral presentation.

Bacakova M. et al.: Fibrin and Collagen Structures on Nanofibrous Membranes as Carriers for Skin Cells. *Tissue Engineering Congress*, London, England, 2. – 4. 6. 2014. Oral presentation.

Bacakova M. et al.: Nanofibrous Membranes with Fibrin and Collagen Structures as Carriers for Skin Cells. *Biomaterials in Medicine and Veterinary Medicine*, Rytro, Poland, 9. – 12. 10. 2014. Oral presentation.

Bacakova M. et al.: Nanofibrous Membranes with Fibrin and Collagen Structures as Carriers for Skin Cells. *V International Conference on Tissue Engineering (ICTE2015)*, Lisbon, Portugal, 25. – 27. 6. 2015. Oral presentation.

Bacakova M et al.: Fibrin Structures on nanofibrous membranes as carriers for dermal fibroblasts. *World Conference on Regenerative Medicine*, Leipzig, Germany, 21. – 23. 10. 2015. Poster

Bacakova M. et al.: Fibrin and Collagen Structures on Nanofibrous Membranes as Carriers for Skin Cells. *The 10th World Biomaterials Congress (WBC)*, Montreal, Canada, 17. – 22. 5. 2016. Poster

Bacakova M. et al.: The potential application of fibrin-coated polylactide nanofibers in skin tissue engineering. *Nano In Bio*, Guadeloupe, France, 31. 5. – 5. 6. 2016. Oral presentation.

9.2 Czech Conferences

Bacakova M. et al.: Vliv fyzikálně-chemických parametrů bioprintingu na buněčnou viabilitu, *Biomateriály a jejich povrchy IV*, Herbertov, Czech Republic, 14. – 17. 9. 2011. Oral presentation.

Bacakova M. et al.: Plasmovaná polylaktidová nanovlákna jako nosiče kožních buněk. *Biomateriály a jejich povrchy V*, Herbertov, Czech Republic, 12. – 15. 9. 2012. Oral presentation.

Bacakova M. et al.: Nanovlákenné materiály v kožním tkáňovém inženýrství. *Bioimplantologie*, Brno, Czech Republic, 11. – 12. 4. 2013. Oral presentation.

Bacakova M. et al.: Kolagenové a fibrinové vrstvy na nanovlákenných membránách pro kožní tkáňové inženýrství. *Biomateriály a jejich povrchy VI*, Herbertov, Czech Republic, 11. – 14. 9. 2013. Oral presentation.

Bacakova M. et al.: Modifikovanné nanovlákenné membrány pro kožní tkáňové inženýrství. *Biomateriály a jejich povrchy VII*, Herbertov, Czech Republic, 16. – 19. 9. 2013. Oral presentation.

10. Appendix

Hindawi Publishing Corporation
BioMed Research International
Volume 2013, Article ID 371430, 18 pages
http://dx.doi.org/10.1155/2013/371430

Research Article

Adhesion, Growth, and Maturation of Vascular Smooth Muscle Cells on Low-Density Polyethylene Grafted with Bioactive Substances

Martin Parizek,[1] Nikola Slepickova Kasalkova,[2] Lucie Bacakova,[1] Zdenek Svindrych,[1] Petr Slepicka,[2] Marketa Bacakova,[1] Vera Lisa,[1] and Vaclav Svorcik[2]

[1] *Institute of Physiology, Academy of Sciences of the Czech Republic, Videnska 1083, 142 20 Prague 4-Krc, Czech Republic*
[2] *Institute of Chemical Technology, Technicka 5, 166 28 Prague 6-Dejvice, Czech Republic*

Correspondence should be addressed to Lucie Bacakova; lucy@biomed.cas.cz

Received 28 August 2012; Accepted 14 February 2013

Academic Editor: Benaissa El Moualij

The attractiveness of synthetic polymers for cell colonization can be affected by physical, chemical, and biological modification of the polymer surface. In this study, low-density polyethylene (LDPE) was treated by an Ar^+ plasma discharge and then grafted with biologically active substances, namely, glycine (Gly), polyethylene glycol (PEG), bovine serum albumin (BSA), colloidal carbon particles (C), or BSA+C. All modifications increased the oxygen content, the wettability, and the surface free energy of the materials compared to the pristine LDPE, but these changes were most pronounced in LDPE with Gly or PEG, where all the three values were higher than in the only plasma-treated samples. When seeded with vascular smooth muscle cells (VSMCs), the Gly- or PEG-grafted samples increased mainly the spreading and concentration of focal adhesion proteins talin and vinculin in these cells. LDPE grafted with BSA or BSA+C showed a similar oxygen content and similar wettability, as the samples only treated with plasma, but the nano- and submicron-scale irregularities on their surface were more pronounced and of a different shape. These samples promoted predominantly the growth, the formation of a confluent layer, and phenotypic maturation of VSMC, demonstrated by higher concentrations of contractile proteins alpha-actin and SM1 and SM2 myosins. Thus, the behavior of VSMC on LDPE can be regulated by the type of bioactive substances that are grafted.

1. Introduction

Construction of tissue replacements and tissue engineering are very important areas of contemporary medicine and biotechnology. They have great potential for the future, due to increased life expectancy, civilization disorders, and thus increased requirements for medical care. Advanced tissue replacements consist of two basic components: cells and cell carriers. Artificial materials are usually applied as cell carriers, and for this purpose they should be adapted to act as analogues of the extracellular matrix, that is, to control the adhesion, growth, phenotypic maturation, and proper functioning of the cells. Synthetic polymers are an important type of materials that can be used for constructing substitutes for various tissues of the human body. These materials have a wide range of advantages, such as relatively easy availability and low cost, defined and versatile chemical composition, tunable mechanical properties, and tailored biodegradability at physiological conditions. These properties have made these polymers an obvious choice of material for many biotechnological and medical applications, for example, as growth supports for cell cultures *in vitro* or for constructing nonresorbable, fully resorbable, or semiresorbable vascular prostheses [1–4], artificial heart valves [5], bone and joint replacements [6, 7], implants for plastic surgery [8], bioartificial skin [9], and carriers for cell, drug or gene delivery [10]; for a review, see [11–14].

For biomedical applications, it is generally accepted that synthetic polymeric materials have to be biocompatible; that is, they must match the mechanical properties of the replaced tissue and not act as cytotoxic, mutagenic, or immunogenic. In addition, the physicochemical characteristics of the surface

of these biomaterials are of great importance, because they can directly influence and control the cell adhesion, spreading, and signaling events that further regulate a wide range of biological functions, for example, cell growth, differentiation, and extracellular matrix synthesis [15].

However, in their pristine state, many polymeric materials have unfavorable physical and chemical surface properties, which are limiting for their colonization with cells and for their integration with the surrounding tissues in the patient's organism. A typical example is the high hydrophobicity of synthetic polymers; that is, the water drop contact angle on the material surface is often higher than 90°. Fortunately, a wide range of physical and chemical modifications is available that can be used to create more hydrophilic bioactive surfaces attractive for cell colonization. For example, the polymers can be irradiated with ions [2, 3], with ultraviolet light [14, 16, 17], or exposed to plasma [18]. These treatments induce degradation of the polymer chains, release of noncarbon atoms, and creation of radicals. These radicals react with oxygen in the ambient atmosphere, leading to the formation of oxygen-containing functional chemical groups on the polymer surface (i.e., carbonyl, carboxyl, hydroxyl, ether, or ester groups). These groups enhance the polymer polarity and wettability and promote the adsorption of cell adhesion-mediating molecules in appropriate geometrical conformations, which enable specific amino acid sequences (e.g., RGD) in these molecules to be reached by cell adhesion receptors. In addition, conjugated double bonds between carbon atoms are created, and this renders the polymer surface electrically conductive. It is known that the electrical conductivity of a material surface enhances its attractiveness for cell colonization, even without active electrical stimulation (for a review, see [11–13, 19]).

In addition, the radicals, oxygen-containing groups, and double bonds that provide chemically reactive sites on the material surface can subsequently be grafted with various bioactive molecules, such as amino acids, proteins, other synthetic polymers, or nanoparticles. The grafted substances can further enhance the attractiveness of the modified polymer surface for cell adhesion and growth [18, 20–22].

In this study, we have therefore evaluated the adhesion, growth, and phenotypic maturation of vascular smooth muscle cells (VSMC) derived from rat aorta and cultured on low-density polyethylene (LDPE) modified by an Ar^+ plasma discharge and subsequent grafting with glycine (Gly), bovine serum albumin (BSA), polyethylene glycol (PEG), colloidal carbon nanoparticles (C), or BSA+C. The aim of these modifications was to create surfaces attractive for cell colonization, and furthermore to be able to control the extent of cell adhesion, cell growth activity, and cell differentiation. Growth supports of this kind are particularly important for VSMC, in order to prevent their so-called phenotypic modulation, that is, transition from their quiescent differentiated state to a synthetic and proliferative phenotype (for a review, see [23]). This modulation is associated with the risk of restenosis of an artificial vascular graft. For this reason, VSMCs have been avoided in the construction of vascular replacements. However, VSMCs are the most numerous cell component of the natural blood vessel wall. Thus, these cells have to be included in advanced bioartificial vascular replacements, provided their phenotype, and proliferation activity is controlled by appropriate cell culture conditions, including the physical and chemical properties of their material carrier.

LDPE was chosen as a carrier for VSMC in this study. Unlike other polymers, namely, polytetrafluoroethylene (PTFE) and polyethylene terephthalate (PET), LDPE is not used for constructing clinically applied vascular prostheses. However, due to its relatively simple and well-defined chemical composition, polyethylene provides a good model for studying the correlations between physicochemical changes of the material surface and the cell behavior. This model has been used with success in numerous earlier studies that we have carried out (e.g., [18, 20–22]).

Another aim of this study was to compare the sensitivity of LDPE and high-density polyethylene (HDPE), used in most of our earlier studies, to plasma treatment and subsequent grafting, and the influence of these modifications on cell behavior.

2. Experimental

2.1. Preparation of the Polymer Samples. The experiments were carried out on low-density polyethylene foils (LDPE) of Granoten S^*H type (thickness 0.04 mm, density 0.922 $g{\cdot}cm^{-3}$, and melt flow index 0.8 g/10 minutes), made by the Granitol Joint-Stock Company, Moravsky Beroun, Czech Republic. The polyethylene samples were cut into circles (diameter 2 cm) using a metallic perforator. The foils were modified by an Ar^+ plasma discharge (gas purity: 99.997%) using a Balzers SCD 050 device. The time of modification was 50 seconds, and the discharge power was 1.7 W. The chamber parameters were: Ar flow 0.3 $l\,s^{-1}$, Ar pressure 10 Pa, electrode area 48 cm^2, interelectrode electrode distance 50 mm, chamber volume 1000 cm^3, and plasma volume 240 cm^3. After this process, the samples were immersed in water solutions of glycine (Gly; Merck, Darmstadt, Germany, product number 104201), bovine serum albumin (BSA; Sigma-Aldrich, Germany, product number A9418) or polyethylene glycol (PEG; Merck, Darmstadt, Germany, product number 817018, m.w. 20000). Some plasma-treated samples and samples grafted with BSA were exposed to a suspension of colloidal carbon particles (C; Spezial Schwartz 4, Degussa AG, Germany) [18, 24]. All substances mentioned here were used in a concentration of 2 wt.%, and the time of the grafting process was 12 hours at room temperature [18]. Unmodified LDPE and standard cell culture polystyrene dishes were used as reference samples.

2.2. Characterization of the Polymer Samples. It is known that after plasma treatment changes occur in a wide range of parameters in the modified layer during the aging process [25]. For this reason, all analyses (and also cell culture experiments) were performed 20 days after modification (i.e., on aged samples).

The surface wettability was determined by measuring the contact angle using the static water drop method. The measurement was performed by distilled water in 10 different positions at room temperature with error 5% on the Surface

Energy Evaluation System (SEE System, Advex Instruments, Czech Republic).

The surface free energy (SFE) was evaluated on the basis of the contact angle of two liquids (water and glycerol). From these values, the SEE System calculates the surface energy according to the Owens-Wendt model [26].

The concentration profile of oxygen in the modified surface was determined by Rutherford Backscattering Spectroscopy (RBS). The RBS analysis was performed in a vacuum target chamber with 2.72 MeV He^+ ions. The elemental depth profiles were inspected at an accessible depth of a few hundred nm. The RBS spectra were evaluated by the GISA 3.99 code. The typical RBS detection limit is 0.1 at.% for oxygen.

The changes in surface morphology and roughness were determined by Atomic Force Microscopy (AFM), using a VEECO CP II in tapping mode. We used an RTESPA-CP Si probe, with spring constant 20–80 N/m. By repeated measurements of the same region ($1 \times 1\,\mu m^2$), it was proven that the surface morphology did not change after three consecutive scans. The mean roughness value (R_a) is the arithmetic average of the deviations from the centre plane of the sample.

2.3. Cells and Culture Conditions. Each LDPE sample 2 cm in diameter was cut into four smaller parts of equal size, and these parts were used for evaluating the cell number and the cell morphology and for immunofluorescence staining. Whole samples were used for an evaluation of the molecular markers of cell adhesion and differentiation by enzyme-linked immunofluorescence assay (ELISA). All LDPE samples were sterilized with 70% ethanol for one hour. The smaller samples were inserted into 24-well plates (TPP, Switzerland; well diameter 1.5 cm), while for the bigger (i.e., whole) samples, 12-well plates from the same company (diameter 2.1 cm) were used. After sterilization, the samples were air-dried for 12 hours in a sterile environment in order to prevent possible negative effects of ethanol on the cells. After the drying process, the samples were fixed to the bottom of the culture wells by plastic rings (inner area 0.38 cm^2 for the smaller samples and 1.77 cm^2 for the bigger samples) in order to prevent the samples floating in the cell culture media. The samples were seeded with VSMC isolated by an explantation method from rat aorta. The cells were used in the third passage, and their seeding density was 17000 cells per cm^2 [18]. The cells were cultivated in Dulbecco's Modified Eagle Minimum Essential Medium (DMEM, Sigma, USA), supplemented with 10% foetal bovine serum (Sebak GmbH, Aidenbach, Germany) and gentamicin (40 μg/mL, LEK, Slovenia), for 1, 2, 4, 5, or 7 days (temperature 37°C, humidified atmosphere of 5% of CO_2 in the air). For the smaller samples, 1.5 mL of the medium was used, and for the bigger samples, 3 mL of the medium. For the evaluation of the cell numbers and the cell spreading area, 4 smaller samples for each experimental group and time interval were used. For ELISA, 8 large samples for each experimental group were used, and the cultivation time was 7 days. For immunofluorescence staining, the time of cultivation was 4 days, and the cells were grown on the smaller samples.

2.4. Evaluation of the Cell Number and Cell Morphology. The cells on the smaller polymer samples were rinsed in phosphate-buffered saline (PBS). On one sample per each experimental group, the cells were fixed by 70% cold ethanol (−20°C) and stained with a combination of Texas Red C_2-maleimide fluorescent membrane dye (Molecular Probes, Invitrogen, Cat. number T6008; concentration 20 ng/mL in PBS) and Hoechst nuclear dye number 33342 (Sigma, USA; 5 μg/mL in PBS). The cell number and cell morphology were then evaluated using an Olympus IX 51 microscope equipped with an Olympus DP 70 digital camera.

The size of the cell spreading area was measured using Atlas software (Tescan Ltd, Czech Republic) on pictures taken on days 1 and 2 after seeding.

On the three remaining smaller samples, the cells were counted in a Cell Viability Analyzer (Vi-cell XR, Beckman Coulter). After rinsing with PBS, the cells were harvested by 5 min treatment in a trypsin-EDTA solution (Sigma, Cat. number T4174). The device performed an automatic analysis of the number of viable and dead cells, based on the trypan blue exclusion test.

2.5. Construction of Growth Curves and Calculation of Cell Population Doubling Time. The cell numbers obtained on days 1, 2, 5, and 7 after seeding were expressed as cells per cm^2 (i.e., the cell population densities) and were used for constructing growth curves. The cell population doubling time (DT) was determined by the equation

$$\mathrm{DT} = \log(2)\,\frac{t - t_0}{\log N_t - \log N_{t_0}}, \tag{1}$$

where N_{t_0} and N_t are the cell population densities at the beginning and at the end of the studied culture interval [2, 3].

2.6. Immunofluorescence Staining. On day 4 after seeding, the cells were rinsed twice in PSB, fixed with precooled 70% ethanol (−20°C, 15 min), and pretreated with 1% bovine serum albumin in PBS containing 0.05% Triton X-100 (Sigma) for 20 minutes at room temperature, in order to block nonspecific binding sites and permeabilize the cell membrane. The cells were then incubated with primary antibodies against several molecular markers of adhesion and phenotypic maturation of VSMC, namely, integrin-associated focal adhesion proteins talin vinculin and paxillin, α-actinin, a protein present in focal adhesions and also binding the actin cytoskeleton, cytoskeletal protein β-actin, and contractile proteins α-actin and SM1 and SM2 myosins, markers of VSMC phenotypic maturation (Table 1).

The primary antibodies were diluted in PBS to concentrations of 1 : 200 and applied overnight at 4°C. After rinsing with PBS, the secondary antibodies (dilution 1 : 400) were added for 1 hour at room temperature. These antibodies were goat anti-mouse or goat anti-rabbit F(ab′)2 fragments of IgG (H + L), both conjugated with Alexa Fluor 488 and purchased from Molecular Probes, Invitrogen (Cat. number A11017 and A11070, resp.). The cells were then rinsed twice in PBS, mounted under microscopic glass coverslips in a Gel/Mount permanent fluorescence-preserving aqueous

Table 1: Primary antibodies used for immunofluorescence staining (Immf.) and enzyme-linked immunosorbent assay (ELISA) of markers of adhesion and phenotypic maturation of VSMCs.

Antibody against	Developed in, type	Company, Cat. number	Dilution	Incubation
Chicken talin	Mouse, monoclonal	Sigma[a] T 3287	Immf.: 1 : 200 ELISA: 1 : 500	Immf.: overnight, 4°C ELISA: 60 min, RT[c]
Human vinculin	Mouse, monoclonal	Sigma[a] V9131	Immf.: 1 : 200 ELISA: 1 : 400	Immf.: overnight, 4°C ELISA: 60 min, RT[c]
Recombinant human paxillin	Rabbit, polyclonal	Chemicon[b] P1093	Immf.: 1 : 200 ELISA: 1 : 400	Immf.: overnight, 4°C ELISA: 60 min, RT[c]
Chicken α-actinin	Rabbit, polyclonal	Sigma[a] A2543	Immf.: 1 : 200 ELISA: 1 : 500	Immf.: overnight, 4°C ELISA: 60 min, RT[c]
Synthetic peptide of α-smooth muscle actin	Mouse, monoclonal	Sigma[a] A2547	Immf.: 1 : 200 ELISA: 1 : 400	Immf.: overnight, 4°C ELISA: 60 min, RT[c]
Synthetic peptide of β-actin	Mouse, monoclonal	Sigma[a] A 5441	Immf.: 1 : 200 ELISA: 1 : 400	Immf.: overnight, 4°C ELISA: 60 min, RT[c]
Human smooth muscle SM1 and SM2 myosin	Mouse, monoclonal	Sigma[a] M7786	Immf.: 1 : 200 ELISA: 1 : 500	Immf.: overnight, 4°C ELISA: 60 min, RT[c]

[a]Sigma, St. Louis, MO, USA; Czech Dealer: Sigma-Aldrich S.R.O., Prague, Czech Republic.
[b]Chemicon International Inc., Temecula, CA, USA; Czech dealer: Scintilla S.R.O., Jihlava, Czech Republic.
[c]Room temperature (RT).

mounting medium (Biomeda Corporation, Foster City, CA, U.S.A.), and evaluated under an Olympus IX 51 microscope (obj. 100x), using an Olympus DP 70 digital camera [18].

2.7. Enzyme-Linked Immunosorbent Assay (ELISA). The differences in the concentration of the adhesion and differentiation molecules on the tested materials were evaluated semiquantitatively, using enzyme-linked immunosorbent assay (ELISA) in homogenized cells per mg of protein.

For this purpose, the cells were cultured for 7 days and then rinsed with PBS, released with trypsin-EDTA solution (Sigma, Cat. number T4174, incubation 5 min at 37°C), and counted in the Cell Viability Analyzer (Vi-CELL XR, Beckman Coulter). Trypsinized cells were resuspended in PBS, centrifuged, resuspended in distilled and deionized water (10^6 cells/in 200 μL), and kept in a freezer at −70°C overnight. The cells were then homogenized by ultrasonication for 40 seconds (cycle 1, amplitude 70%) in a sonicator (UP 100 H, Dr. Hielscher GmbH), and the total protein content was measured using a modified method originally developed by Lowry [18, 27]. Aliquots of the cell homogenates corresponding to 1–50 μg of protein in 50 μL of water were adsorbed on 96-well microtiter plates (Maxisorp, Nunc) at 4°C overnight. After washing twice with PBS (100 μL/well), the nonspecific binding sites were blocked by 0.02% gelatin in PBS (100 μL/well, 60 min) and then treated by 1% Tween (Sigma, Cat. number P1379, 100 μL/well, 20 min). The primary antibodies (Table 1) were diluted in PBS (1 : 200 to 1 : 500) and applied for 60 minutes at room temperature (50 μL/well). The secondary antibodies, that is, goat anti-mouse IgG Fab specific (dilution 1 : 1000) or goat anti-rabbit IgG whole molecule (dilution 1 : 1000), both conjugated with peroxidase and purchased from Sigma (Cat. number A3682 and A0545, resp.), were applied for 45 min at room temperature (50 μL/well). This step was followed by double washing in PBS and an orthophenylenediamine reaction (Sigma, Cat. number P1526, concentration 2.76 mM) using 0.05% H_2O_2 in 0.1 M phosphate buffer (pH 6.0, dark place, 100 μL/well). The reaction was stopped after 10–30 minutes by 2 M H_2SO_4 (50 μL/well), and the absorbance was measured at 490 and 690 nm by a Versa Max Microplate Reader (Molecular Devices Corporation, Sunnyvale, CA, USA). The absorbance of the cell samples taken from modified LDPE foils was given as a percentage of the value obtained in the cells on pure LDPE [18].

2.8. Statistics. The biological results were presented as mean ± SEM (Standard Error of Mean). The statistical significance was evaluated by the One-Way Analysis of Variance (ANOVA), Student-Newman-Keuls method. For the cell number and the size of the cell spreading area, multiple comparisons of values obtained on all tested samples were performed. For the data obtained from ELISA, values on tested samples were compared only with values on the control unmodified LDPE. For ELISA, Dunnett's posttest was also used. Values $P \leq 0.05$ were considered significant.

3. Results and Discussion

3.1. Physicochemical Properties of Polymer Samples. It is known that Ar plasma discharge can cause changes in the chemical structure and surface morphology of a modified layer. These changes significantly affect the surface wettability [28]. The degree of wettability, characterized by the contact angle, is shown in Figure 1 for pristine LDPE, plasma-treated LDPE, and plasma treated and subsequently grafted with biomolecules. The contact angle decreases dramatically after plasma treatment. This is due to the creation of free radicals and subsequent oxidation of the layer exposed to the air [29]. This leads to the formation of new oxygen

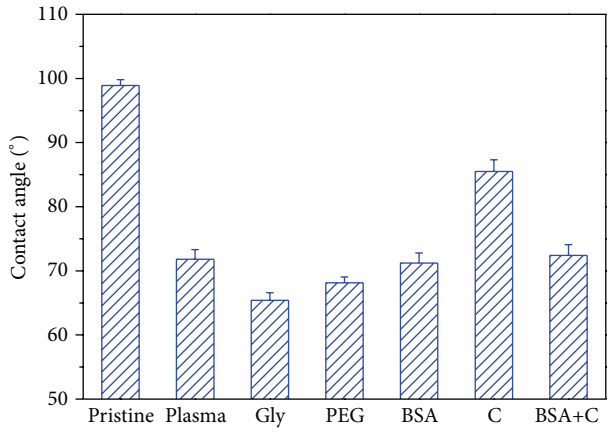

Figure 1: The water drop contact angle of pristine LDPE (pristine), plasma-treated LDPE (plasma), LDPE treated with plasma and then grafted with glycine (Gly), polyethylene glycol (PEG), bovine serum albumin (BSA), colloidal carbon particles (C), or a combination of BSA and C (BSA+C).

Table 2: Surface free energy (SFE, in $mJ \cdot m^{-2}$) of pristine LDPE, plasma-treated LDPE (plasma), LDPE treated with plasma and then grafted with glycine (Gly), polyethylene glycol (PEG), bovine serum albumin (BSA), colloidal carbon particles (C), or with a combination of BSA and C (BSA+C). γ_{total} is the total SFE of the polymer and consists of nonpolar (γ_{LW}) and polar components (γ_{AB}).

	γ_{total}	γ_{LW}	γ_{AB}
Pristine	24.54	23.16	1.37
Plasma	28.56	25.01	3.55
Gly	36.20	31.89	4.31
PEG	34.91	5.01	29.90
BSA	26.56	20.28	6.28
C	26.59	19.22	7.37
BSA+C	25.58	12.86	12.72

The values are the mean of 10 to 15 measurements for each experimental group and were calculated automatically by the Surface Energy Evaluating System (SEE System, Masaryk University, Brno, Czech Rep.).

structures, for example, carbonyl, carboxyl, and ester groups [30]. Subsequent grafting of glycine and PEG to the plasma-activated surface resulted in a further decrease in the contact angles on these samples. The molecules of Gly and PEG contain polar groups, which increase the hydrophilicity of the material surface. However, the presence of BSA and BSA+C had no significant effect on the wettability of LDPE, because the contact angles on these samples were comparable with the values on samples treated only with plasma. Different behavior was observed in samples after modification with colloidal C particles. These samples had much lower wettability than the plasma-treated samples. This result is in accordance with the previous finding by ourselves and by other authors that carbon-based coatings, for example, with amorphous diamond-like carbon, graphite or nonfunctionalized fullerenes, are often hydrophobic (for a review, see [19]). Nevertheless, the wettability of C-modified LDPE in this study still remained higher than on pristine LDPE.

The total surface free energy (SFE) of the LDPE samples was inversely correlated with the water contact angle; that is, samples with a relatively low contact angle had a higher total SFE (LDPE grafted with Gly or PEG), while samples with a high contact angle had lower total SFE (pristine LDPE, Table 2). In other words, the total SPE was positively correlated with the hydrophilicity of the material surface. On all modified samples, the total SFE and its polar component increased in comparison with pristine LDPE. Similar differences between pristine and UV light-treated LDPE were described by O'Connell et al. [31]. The highest polar component of SFE was found on samples modified with plasma and subsequently grafted with PEG. This result is consistent with relatively high hydrophilicity of this sample (Figure 1), and also with the results obtained by RBS, which revealed a high concentration of oxygen in PEG-grafted LDPE (Figure 2). Surprisingly, the increase in the polar component was relatively small in LDPE grafted with Gly (Table 2), which exhibited the lowest water drop contact angle and the highest oxygen concentration at the material surface (Figures 1 and 2). In addition, the changes in the nonpolar component were variable. This component increased on samples modified in plasma or on samples subsequently grafted with glycin, while on samples grafted with BSA, C, or BSA+C, this value decreased. Similar variability has been described on LDPE, UHMWPE, and Sarlink polymers after treatment with UV light and has been explained by configuration changes of chemical functional groups at the material surface during its modification [31].

The concentration depth profile of oxygen modified LDPE was determined from RBS measurements. The concentration of oxygen in a modified layer and the oxygen depth profile is shown in Figure 2. The highest concentration of oxygen was found in the surface layers of all modified substrates. With increasing depth from the surface, the oxygen concentration decreased, and at a depth of 80 nm the amount of oxygen was minimal. Most oxygen in the modified layer was determined on a sample treated by plasma and grafted with glycine. More oxygen was also detected on a sample modified with plasma discharge and PEG. A comparable amount of oxygen was measured on substrates exposed to plasma or exposed to plasma and subsequently grafted with BSA or BSA+C. These results, obtained by the RBS method, are consistent with the results determined by goniometry, except that the samples grafted with C showed a similar oxygen content as the samples grafted with BSA and BSA+C, although their water drop contact angle was higher.

Changes in surface morphology and surface roughness that occurred due to plasma exposure and the subsequent grafting process were studied by the AFM method. AFM scans of pristine and modified samples are shown in Figure 3. Plasma modification leads to ablation of the surface layer. Its amorphous phase is ablated preferably [32]. This leads to enhanced branching of LDPE structures. Subsequent grafting with glycine and PEG on the plasma modified surface does not significantly change the surface morphology, but it slightly increases the surface roughness. Figure 3 shows that the bonding of carbon particles highlights the fine details of the structure and also leads to the formation of small

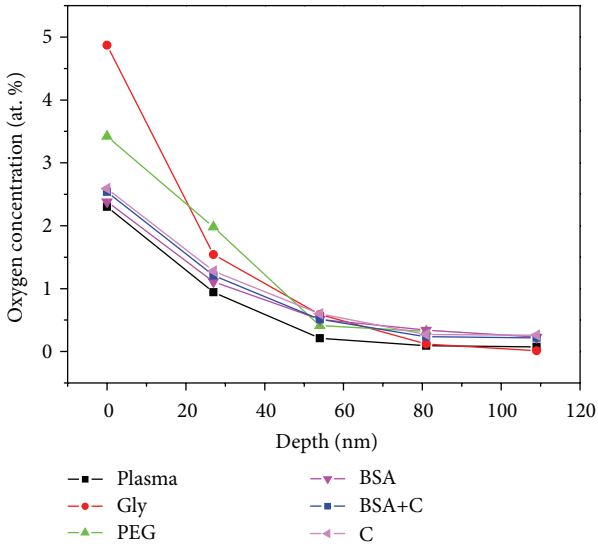

Figure 2: Oxygen concentration in the modified layer and depth concentration profile of oxygen, determined from RBS measurements, on plasma-treated LDPE (plasma), LDPE treated with plasma and then grafted with glycine (Gly), polyethylene glycol (PEG), bovine serum albumin (BSA), colloidal carbon particles (C), or a combination of BSA and C (BSA+C).

spherical units corresponding to carbon nanoparticles. In the case of BSA and BSA+C grafting, large cluster formations that strongly affect the surface roughness were detected, in agreement with previous observations for BSA published by Wang et al. [33].

3.2. Initial Adhesion and Subsequent Growth of Cells on Polymer Samples. On the first day of the experiment, the highest number of initially adhered cells was found on the control PS dishes (17,100 ± 3,300 cells/cm^2). The cell numbers on all LDPE samples showed no statistically significant differences, when compared with each other (Figure 4(a)). Nevertheless, the highest average cell number was observed on LDPE grafted with BSA (10,950 ± 1,030 cells/cm^2), while the lowest number was found on LDPE grafted with PEG (4,770 ± 1,400 cells/cm^2). This number was even slightly lower than the value found on pristine LDPE (5,720 ± 1,780 cells/cm^2). This result contrasts with our earlier findings on HDPE foils [18], where the lowest initial cell number was found on the control PS, and the highest values were found on HDPE grafted with PEG. This disproportion in the cell behavior on LDPE and on HDPE could be explained by the different arrangements of the PEG chains on the surfaces of LDPE and HDPE samples. It is known that if PEG chains are attached to a surface only by one end, and dangle on the surface in a water environment (including cell culture media), this has a repulsive effect on cell adhesion. Cell adhesion on artificial materials *in vitro* is mediated by specific proteins adsorbed on the material surface from the serum supplement of the culture medium, mainly fibronectin and vitronectin. This adsorption is hampered or even disabled on mobile surfaces, especially if the surface mobility is combined with relatively high hydrophilicity, which occurs in PEG due to the presence of -OH groups in its molecules and which was also proven in this study (Figure 1). PEG—also known as polyethylene oxide (PEO), if its molecular mass is above 20,000—has been widely used for constructing surfaces that are nonadhesive for cells, especially those which were designed for the attachment of oligopeptidic ligands for cell adhesion receptors in defined types, concentrations, and distributions and which should prevent uncontrolled protein adsorption and aberrant cell adhesion [4, 34]; for a review, see [11–13]. PEG can also be attached to the material surface through several sites on one chain. In this case, PEG chains are not mobile and can support the adsorption of cell adhesion-mediating proteins and subsequent cell adhesion and growth [21]; for a review, see [18]. In our experiments, the cell-repulsive effects of PEG probably prevailed on LDPE, while PEG promoted cell adhesion on HDPE. This topic needs further investigation, but it can be supposed that the different behavior of PEG was due to the different structure of LDPE and HDPE. For example, LDPE molecules have more branching than HDPE molecules, so their intermolecular forces are weaker. The tensile strength of LDPE is lower, but its resilience is higher. Because of the side branches, LDPE molecules are less tightly packed and less crystalline than HDPE molecules. All these factors may lead to different attachment, distribution, and mobility of PEG chains on LDPE and HDPE surfaces, particularly if the branched LDPE structure is further enhanced by plasma treatment, as mentioned previously.

In spite of the relatively low number of initially adhered cells on PEG-grafted LDPE, the spreading area of cells on day 1 after seeding on this material (1,527 ± 98 μm^2) was on an average larger than the areas on the other modified LDPE samples (which ranged from 1,282 ± 49 μm^2 to 1,361 ± 60 μm^2), significantly larger than the areas on unmodified LDPE (687 ± 57 μm^2) and similar to those found on PS (1,664 ± 104 μm^2; Figure 4(b)). One explanation is that the cells had more space for spreading due to the lower number of adhering cells. In any case, the cell spreading implies that PEG-grafted LDPE surfaces allowed adsorption of cell adhesion molecules. However, this adsorption may be nonhomogeneous. On some regions, the cells were well spread and polygonal, while on other sites, the cells remained round (Figure 5).

From day 1 to 2 after seeding, the cells on all LDPE-based samples started to enter the exponential phase of growth and proliferated with doubling times ranging on an average from 14.1 to 46.1 hours (Table 3), while the cells on polystyrene dishes remained rather in the lag phase and proliferated more slowly (doubling time 59.0 hours). As a result, the statistically significant differences between the LDPE samples and PS, observed on day 1, disappeared on day 2 after seeding (Figure 4(c)). Only on LDPE grafted with PEG did the cell number still remain significantly lower than on PS (10,000 ± 1,800 cells/cm^2 versus 22,700 ± 2,300 cells/cm^2 on PS).

The cell spreading area on day 2 after seeding was (similarly as on day 1) significantly larger on all modified LDPE samples (1,037 ± 36 μm^2–1,714 ± 71 μm^2) than on unmodified LDPE (441 ± 18 μm^2), but at the same time

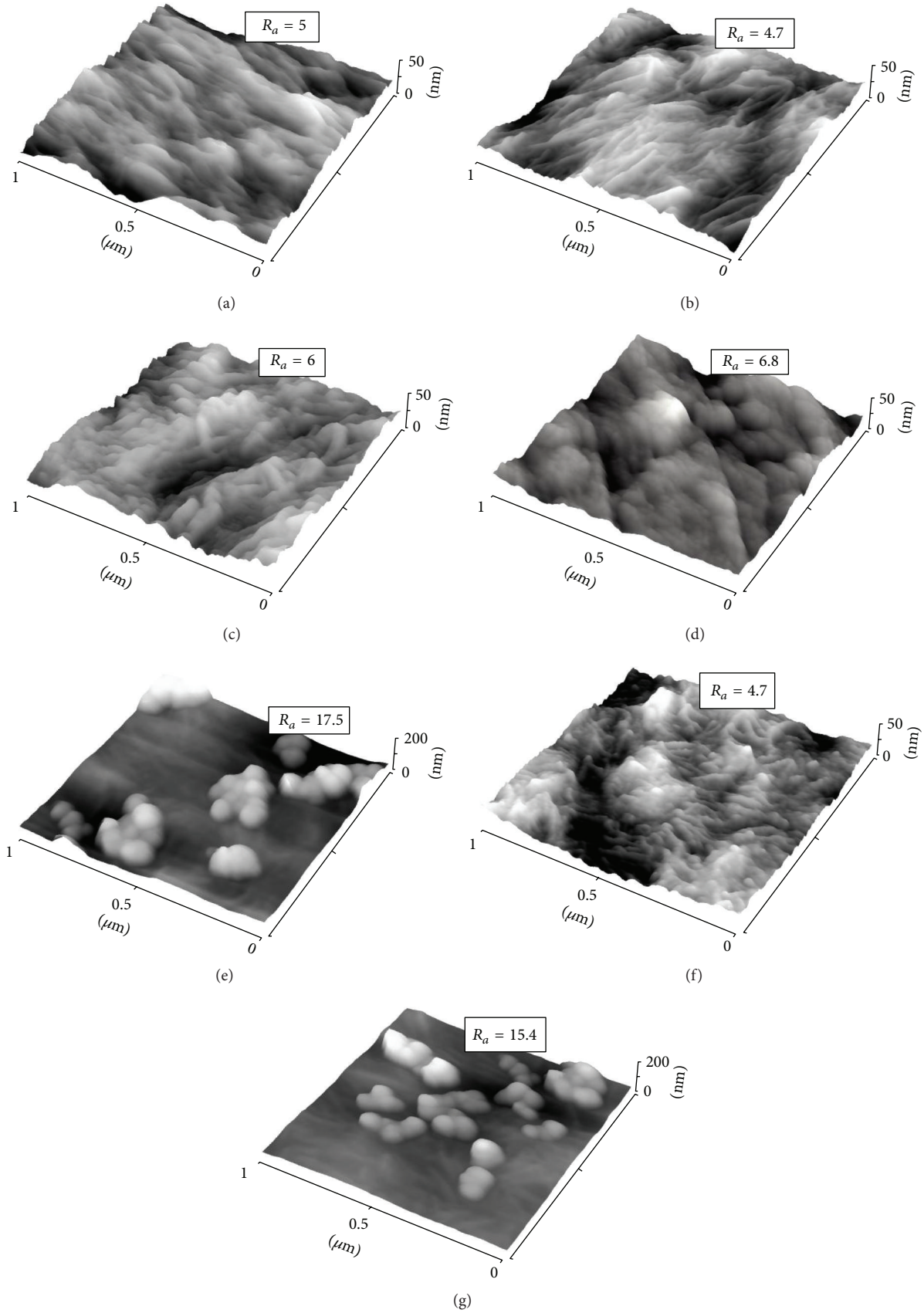

Figure 3: AFM scans of pristine LDPE (a), plasma-treated LDPE (b), LDPE treated with plasma and grafted with glycine (c), PEG (d), BSA (e), C (f), or BSA+C (g). R_a is the surface roughness in nm.

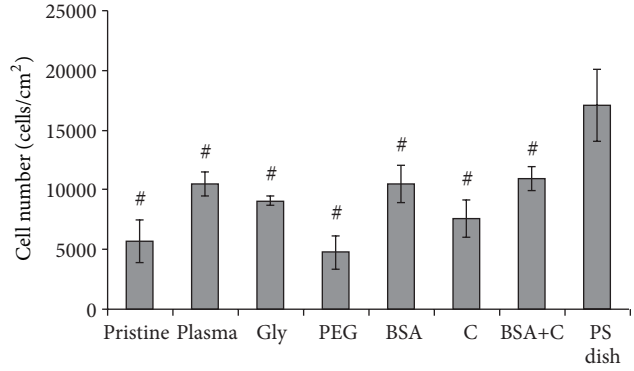

(a) Cell number, day 1

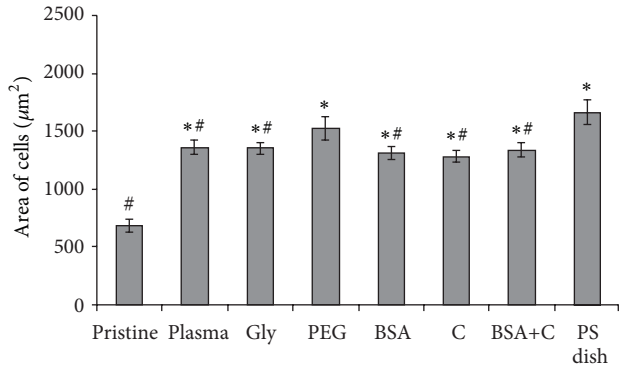

(b) Spreading area, day 1

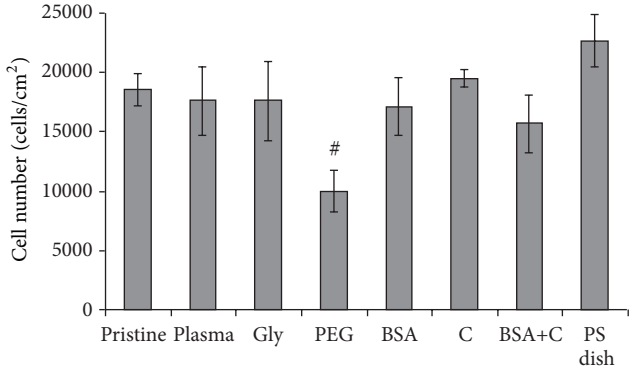

(c) Cell number, day 2

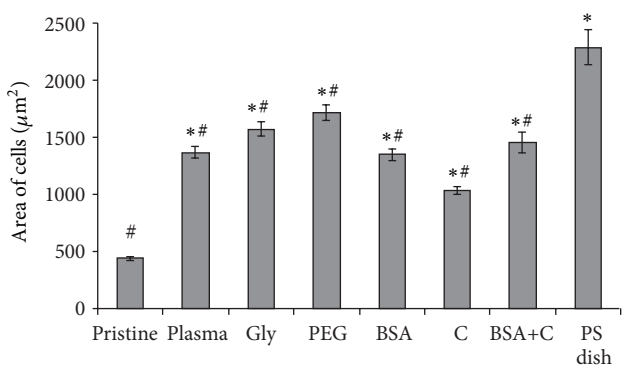

(d) Spreading area, day 2

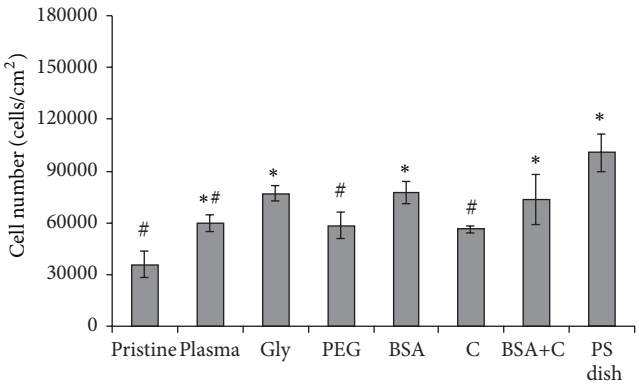

(e) Cell number, day 5

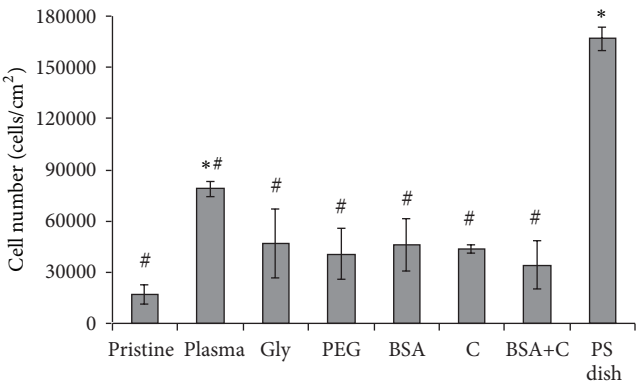

(f) Cell number, day 7

Figure 4: The number (a, c, e, and f) and the size of the spreading area (b, d) of rat aortic smooth muscle cells in cultures on nonmodified LDPE (pristine), on LDPE irradiated with plasma (plasma), on LDPE irradiated with plasma and grafted with glycine (Gly), on polyethylene glycol (PEG), on bovine serum albumin (BSA), on colloidal carbon particles (C), or on bovine serum albumin and C (BSA+C). A tissue culture polystyrene dish (PS dish) was used as a reference material. Days 1, 2, 5, and 7 after seeding. Mean ± SEM from 3 samples, each measured 50 times (cell number, Vi-CELL Analyser) or from 119 to 229 cells for each experimental group (spreading area). ANOVA, Student-Newman-Keuls method. Statistical significance: $^{*,\#}P \leq 0.05$ compared to the value on pristine PE and a polystyrene dish, respectively.

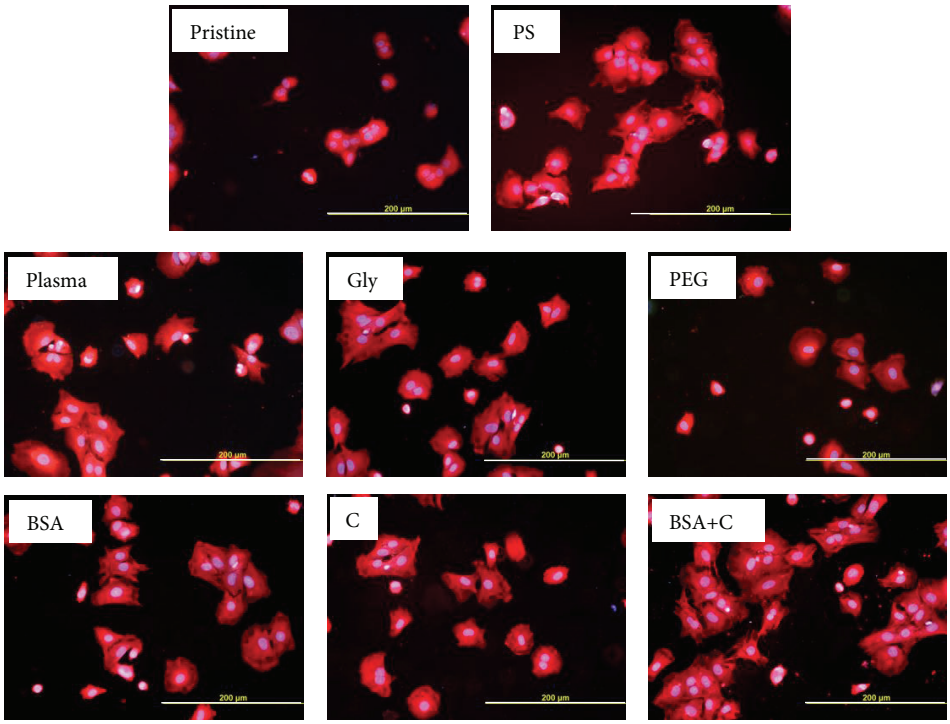

Figure 5: Morphology of rat aortic smooth muscle cells on day 1 after seeding on pristine LDPE (pristine), on a tissue culture polystyrene dish (PS), on LDPE irradiated with Ar^+ plasma (plasma), on LDPE irradiated with plasma and grafted with glycine (Gly), on polyethyleneglycol (PEG), on bovine serum albumin (BSA), on colloidal carbon particles (C), or on bovine serum albumin and carbon particles (BSA+C). Cell membrane and cytoplasm stained with Texas Red C_2-maleimide (red fluorescence), cell nuclei with Hoechst 33342 (blue fluorescence). Olympus IX 51 microscope, DP 70 digital camera, obj. 20x, bar = 200 μm.

it was significantly smaller than on PS (2,289 ± 149 μm^2; Figure 4(d)). Similar results were obtained in our earlier study performed on cultures on HDPE. The cell spreading areas of VSMC on HDPE treated with the same modifications as LDPE in the present study were larger than the spreading areas of the unmodified polymer. This can be explained by the increase in oxygen concentration on the surface of the modified polymer samples, their optimized wettability, and also changes in their surface roughness and morphology (Figures 1–3; [18]).

It is known that the size of the spreading area correlates positively with cell proliferation activity, at least to a certain extent [35, 36]; for a review, see [11–13]. In accordance with this, from day 2 to 5 after seeding, the cells on all modified samples proliferated more quickly (doubling time from 9.4 to 13.6 hours) than the cells on pristine LDPE (doubling time 25.5 hours); see Table 3, Figure 6. On day 5 after seeding, the cells on the modified LDPE samples (except the samples grafted with PEG and C) reached a significantly higher cell population density (59,940 ± 4,850–77,530 ± 6,460 cells/cm^2) than the cells on pristine LDPE (35,680 ± 7,760 cells/cm^2). On LDPE grafted with Gly, BSA, or BSA+C, the cell population densities reached values not significantly different from those obtained on the PS dishes (100,740 ± 10,930 cells/cm^2), which are considered as the "gold standard" for cell cultivation (Figure 4(e)). The samples grafted with BSA or BSA+C were covered by almost confluent cell layers (Figure 7). Similar results were also obtained in our earlier study performed on HDPE, but the cell population densities on BSA and BSA+C significantly exceeded the values on the PS dishes [18].

The improved spreading and growth of VSMC on LDPE irradiated with plasma can be explained by physicochemical changes in the polymer surface which lead to an increased oxygen content and increased wettability of the surface. These surfaces are then more susceptible to adsorption of adhesion-mediating extracellular matrix proteins, for example, vitronectin, fibronectin, collagen, or laminin, in a near physiological and bioactive conformations, suitable for binding by the cell adhesion receptors (for a review, see [11–13]).

The reactive sites formed in a polymer when it is exposed to plasma can be used for grafting various molecules which further modulate the effects of polymer treatment on cell adhesion, growth, phenotypic maturation, and functioning. Glycine, used for grafting the plasma-activated LDPE in this study, is a component of a well-known ligand for integrin cell adhesion receptors, that is, Arg-Gly-Asp (RGD), though Gly alone cannot be bound by these receptors. Nevertheless, Gly grafting enriches the irradiated polymer surface with additional oxygen-containing and also amine groups, which are known to improve the adsorption of cell adhesion-mediating proteins and cell colonization [16]; for a review, see [12]. In addition, Gly and PEG slightly increased the size of the nanoscale irregularities on the polymer surface; that is, they enhanced the material nanostructure, which has been

Table 3: Cell population doubling time (hours) of rat aortic smooth muscle cells from day 1 to 2, day 2 to 5, and day 5 to 7 after seeding on nonmodified LDPE (pristine), LDPE irradiated with plasma (plasma), LDPE irradiated with plasma and grafted with glycine (Gly), polyethyleneglycol (PEG), bovine serum albumin (BSA), colloidal carbon particles (C), bovine serum albumin and C (BSA+C), and polystyrene dishes (PS dish).

Material/time interval	Pristine	Plasma	Gly	PEG	BSA	C	BSA+C	PS dish
Days 1-2	14.1	32.0	25.0	22.5	33.8	17.7	46.1	59.0
Days 2–5	25.5	13.6	11.3	9.4	11.0	15.7	10.8	11.2
Days 5–7	−21.8*	60.3	−33.6*	−45.5*	−32.1*	−66.9*	−21.9*	33.0

*Nonproliferating cells.

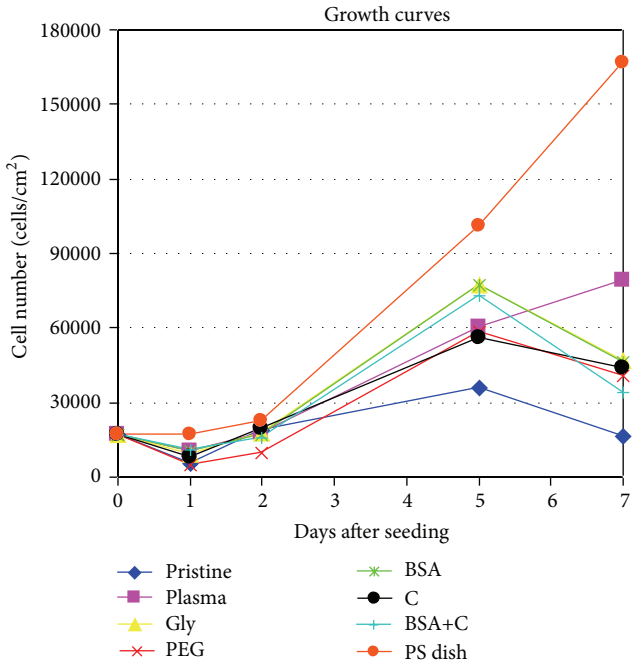

Figure 6: Growth dynamics of rat aortic smooth muscle cells in cultures on nonmodified PE (pristine), on PE irradiated with plasma (plasma), on PE irradiated with plasma and grafted with glycine (Gly), on polyethyleneglycol (PEG), on bovine serum albumin (BSA), on colloidal carbon particles (C), or on bovine serum albumin and C (BSA+C). A tissue culture polystyrene dish (PS dish) was used as the reference material. Means from three samples for each experimental group and time interval (each sample measured 50 times).

shown, like surface wettability, to optimize the spectrum and the geometrical conformations of adsorbed cell adhesion-mediating molecules (for a review, see [12]).

Albumin, a protein that is nonadhesive for cells, has been used for constructing cell-repulsive surfaces. From this point of view, our result that albumin grafting improved the colonization of LDPE with cells might be surprising. However, albumin preadsorbed on the material surfaces improved the geometrical conformation of the cell adhesion-mediating molecules, for example, fibronectin and vitronectin, and their accessibility for cell adhesion receptors [37, 38]; for a review, see [12, 18]. In addition, BSA grafted on the LDPE formed nanosized (i.e., smaller than 100 nm) and submicron-sized (i.e., smaller than 1 μm) cluster structures (Figure 3). Irregularities of this size are believed to promote the adsorption of cell adhesion-mediating molecules in a more physiological conformation than the conventional flat surfaces, and this markedly improves the adhesion and further functioning of the cells [39, 40].

From day 5 to 7 after seeding, the cells on most modified LDPE samples stopped proliferating (i.e., entered the stationary phase of growth), and they even decreased in number. Cell proliferation continued only on the polystyrene dishes and on the plasma-irradiated LDPE (Figure 6, Table 3). On all LDPE samples, the final cell population density was significantly lower than on the PS dishes (Figure 4(f)). However, the cell proliferation on all modified HDPE samples in our earlier study continued from day 5 to 7, and the final cell population density on these samples was similar to or even higher than on the PS dishes [18].

Thus, the positive effects of plasma treatment and subsequent grafting on the adhesion and growth of VSMC were more apparent in HDPE than in LDPE. Analogous results were obtained when a terpolymer of polytetrafluoroethylene, polyvinyldifluoride and polypropylene (PTFE/PVDF/PP), and polysulfone (PSU) was mixed with carbon nanotubes. The addition of nanotubes significantly improved the adhesion and growth of human osteoblast-like MG 63 cells on the terpolymer, while this effect was much less apparent on PSU. This difference was explained by the high hydrophobicity of pristine PTFE/PVDF/PP (water drop contact angle ~100°), while the pristine PSU was more hydrophilic (contact angle ~85°). In addition, PSU contains bioactive sulphone groups, which can also mediate the positive effects of this polymer on cell adhesion. Sulphonated polystyrene promoted the adsorption of fibronectin in an advantageous geometrical conformation for cell adhesion [41]. Thus, pristine PSU is more suitable for cell colonization, and thus the cells were less sensitive to the modifications, further improving the cell adhesion and growth (for a review, see [42]). However, in our studies, both LDPE and HDPE were relatively hydrophobic, having a similar water drop contact angle of 98.6 ± 1.90° and 102.5 ± 2.31°, respectively. Thus, the different sensitivity of cells to modifications of LDPE and HDPE may be due to other differences in the physical and chemical properties of these polymers (see above), for example, differences in chain branching, tensile strength, resilience, crystallinity, packing density, and so forth. A further investigation of this topic is needed.

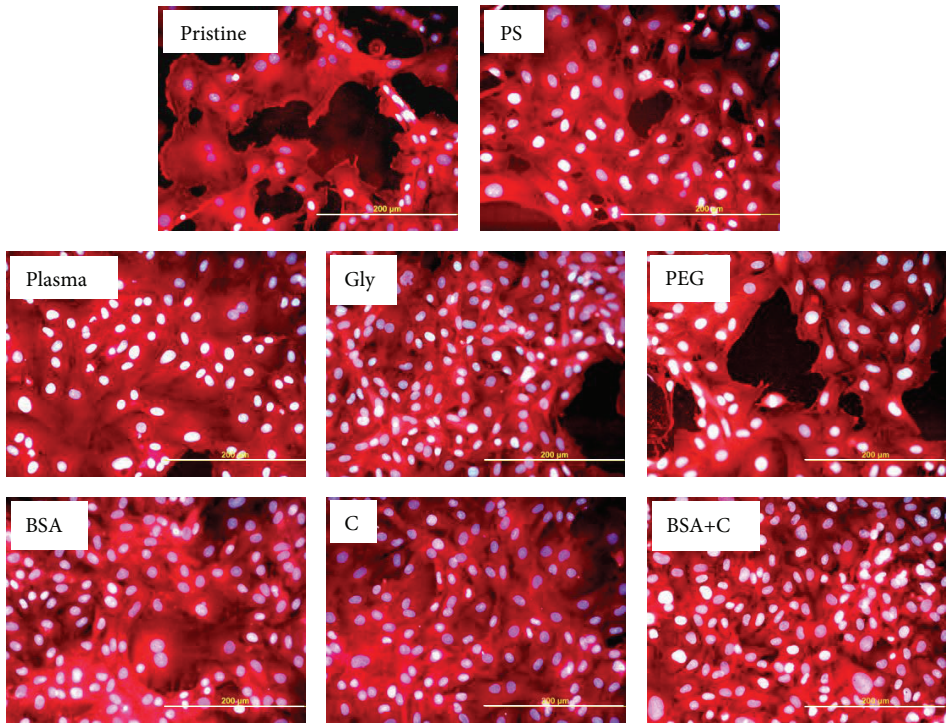

Figure 7: Morphology of rat aortic smooth muscle cells on day 5 after seeding on pristine LDPE (pristine), on a tissue culture polystyrene dish (PS), on LDPE irradiated with Ar^+ plasma (plasma), on LDPE irradiated with plasma and grafted with glycine (Gly), on polyethyleneglycol (PEG), on bovine serum albumin (BSA), on colloidal carbon particles (C), or on bovine serum albumin and carbon particles (BSA+C). Cell membrane and cytoplasm stained with Texas Red C_2-maleimide (red fluorescence), cell nuclei with Hoechst mumber 33342 (blue to white fluorescence). Olympus IX 51 microscope, DP 70 digital camera, obj. 20x, bar = 200 μm.

3.3. Distribution and Concentration of Molecular Markers of Cell Adhesion and Phenotypic Maturation. Immunofluorescence staining showed that the cells on all modified LDPE samples had better developed focal adhesion plaques containing talin and vinculin than the cells on pristine LDPE samples (Figure 8). This result correlates well with the size of the cell spreading area, which was generally larger on all modified samples than on pristine LDPE.

ELISA revealed that the concentration of talin in cells on LDPE modified with plasma, or plasma with subsequent grafting of Gly or PEG, was significantly higher than in cells on pristine LDPE. The concentration of vinculin, which stabilizes focal adhesion plaques (for a review, see [12]), was also higher in cells on LDPE grafted with Gly or PEG (Figure 9). In accordance with these findings, the cells on LDPE modified with plasma, Gly, and particularly PEG achieved on an average the largest cell spreading areas (Figures 4(b) and 4(d)).

However, the concentration of paxillin (i.e., another protein of focal adhesion plaques) was lower in cells on LDPE modified with plasma, Gly, PEG, and BSA+C than in cells on pristine LDPE (Figure 9). Only in cells on LDPE modified with BSA or C the concentration of paxillin was similar as in the cells on pristine polymer. This result corresponded, at least partly, with immunofluorescence staining of paxillin (Figure 10). In cells on LDPE modified with plasma, Gly, or PEG, the paxillin-containing focal adhesions were equally developed or even worse developed than in cells on pristine LDPE, while the paxillin focal adhesions on polymer modified with BSA or C were similarly developed or better developed than in cells on pristine LDPE. Only in cells on BSA+C the paxillin-containing focal adhesions were well-developed, though the concentration of paxillin in these cells was relatively low (Figures 9 and 10). In this context, it should be pointed out that the ELISA method used in our study measured the total number of focal adhesion molecules in the cells, and not only the molecules located in focal adhesion plaques. A more exact method might be to extract the cytosolic fraction of the focal adhesion proteins (i.e., not bound in the focal adhesion plaques) by detergents [43] or to use antibodies against phosphorylated antigens. It can be supposed that phosphorylated paxillin (i.e., activated paxillin exerting its function in cell adhesion) is located in the focal adhesion plaques, while in the cytosolic fraction, nonactive paxillin is not phosphorylated [44–46].

Alpha-actinin is associated with both focal adhesion plaques and the actin cytoskeleton, in which it acts as a crosslinker and stabilizer of the contractile apparatus [47, 48]. In cells on the modified LDPE samples and on PS, its concentration was usually similar to that in cells on pristine LDPE (Figure 9). Only in cells on plasma-irradiated LDPE the concentration of α-actinin was significantly lower. From the cells on all modified samples, only the cells on plasma-modified LDPE continued their proliferation from day 5 to 7 (Figure 6,

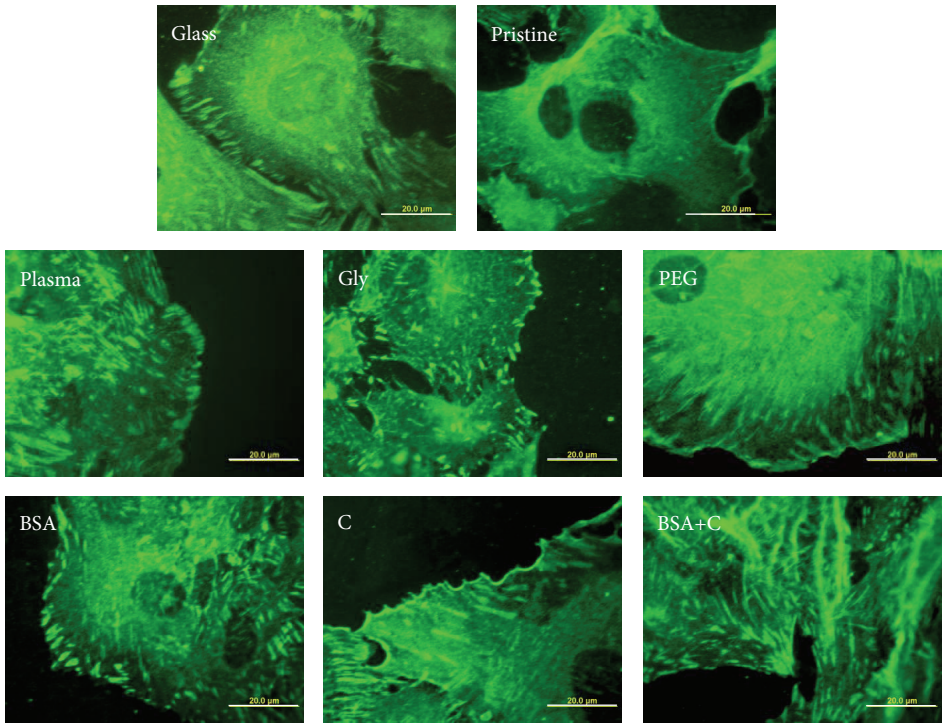

Figure 8: Immunofluorescence of talin, an integrin-associated protein of focal adhesion plaques, in rat aortic smooth muscle cells on day 4 after seeding on a microscopic glass coverslip (glass), on pristine LDPE (pristine), on LDPE irradiated with plasma (plasma), on LDPE irradiated with Ar^+ plasma and grafted with glycine (Gly), on polyethylene glycol (PEG), on bovine serum albumin (BSA), on colloidal carbon particles (C), and on bovine serum albumin with C (BSA+C). Olympus IX 51 microscope, DP 70 digital camera, obj. 100x, bar = 20 μm.

Table 3). Thus, the decreased concentration of α-actinin may be a sign of certain instability of the actin cytoskeleton, which is reorganized during cell division. This presumption is further supported by the immunofluorescence staining pattern of α-actinin. In cells on plasma-modified LDPE, the structures containing α-actinin are relatively short and are located predominantly at the cell periphery, while in the cells on the other samples, the α-actinin-containing structures are long, filament like, often running in parallel through the entire cell (Figure 11).

VSMCs exist in two basic phenotypes, referred to as contractile and synthetic. The contractile phenotype occurs in mature healthy blood vessels and is characterized by the presence of desmin, that is, a protein of intermediate filaments, muscle type of tropomyosin, T-troponin, h-caldesmon, h1-calponin, and metavinculin, and particularly by contractile proteins α-actin and SM1 and SM2 isoforms of myosin. On the other hand, the synthetic phenotype is characterized by the accumulation of cell organelles involved in proteosynthesis, such as endoplasmic reticulum, ribosomes or Golgi complex, and predominance of β- and γ-isoforms of actin and nonmuscle myosin. This phenotype occurs physiologically in immature blood vessels under development, pathologically in diseased blood vessels, for example, during atherosclerosis and hypertension, and artificially after disintegration of the vascular wall and seeding VSMC *in vitro* (for a review, see [48]). However, the synthetic phenotype of VSMC *in vitro* can be reversed, at least partly, to the contractile phenotype by appropriate cell culture conditions, such as the use of serum-free media, dynamic stimulation of VSMC, and particularly the physical and chemical properties of the adhesion substrate. In cells on our materials, the distribution and concentration of α-actin or SM1 and SM2 myosins were therefore evaluated as markers of phenotypic maturation of VSMC, that is, their transition toward a more differentiated contractile phenotype.

We found that α-actin formed thick and brightly stained filament bundles in cells on all samples, including pristine LDPE (Figure 12), while bundles containing SM1 and SM2 myosins were more apparent in cells on modified LDPE than on pristine LDPE (Figure 13). However, as revealed by ELISA, the concentration of α-actin and SM1 and SM2 myosins was significantly higher only in cells on LDPE grafted with BSA and BSA+C, respectively, compared to cells on pristine LDPE (Figure 9). The cells on the samples grafted with BSA or BSA+C had a relatively high cell population density on day 5 after seeding, approaching the value found on cell culture PS, and reached confluence. In addition, these cells had relatively large spreading areas and well-developed talin- and vinculin-containing focal adhesion plaques (Figures 4(b), 4(d), and 8). These factors, that is, good cell-cell adhesion in confluent cultures together with good cell-matrix adhesion, are associated with cell differentiation (for a review, see [11–13]). At the same time, the concentration of β-actin, that is,

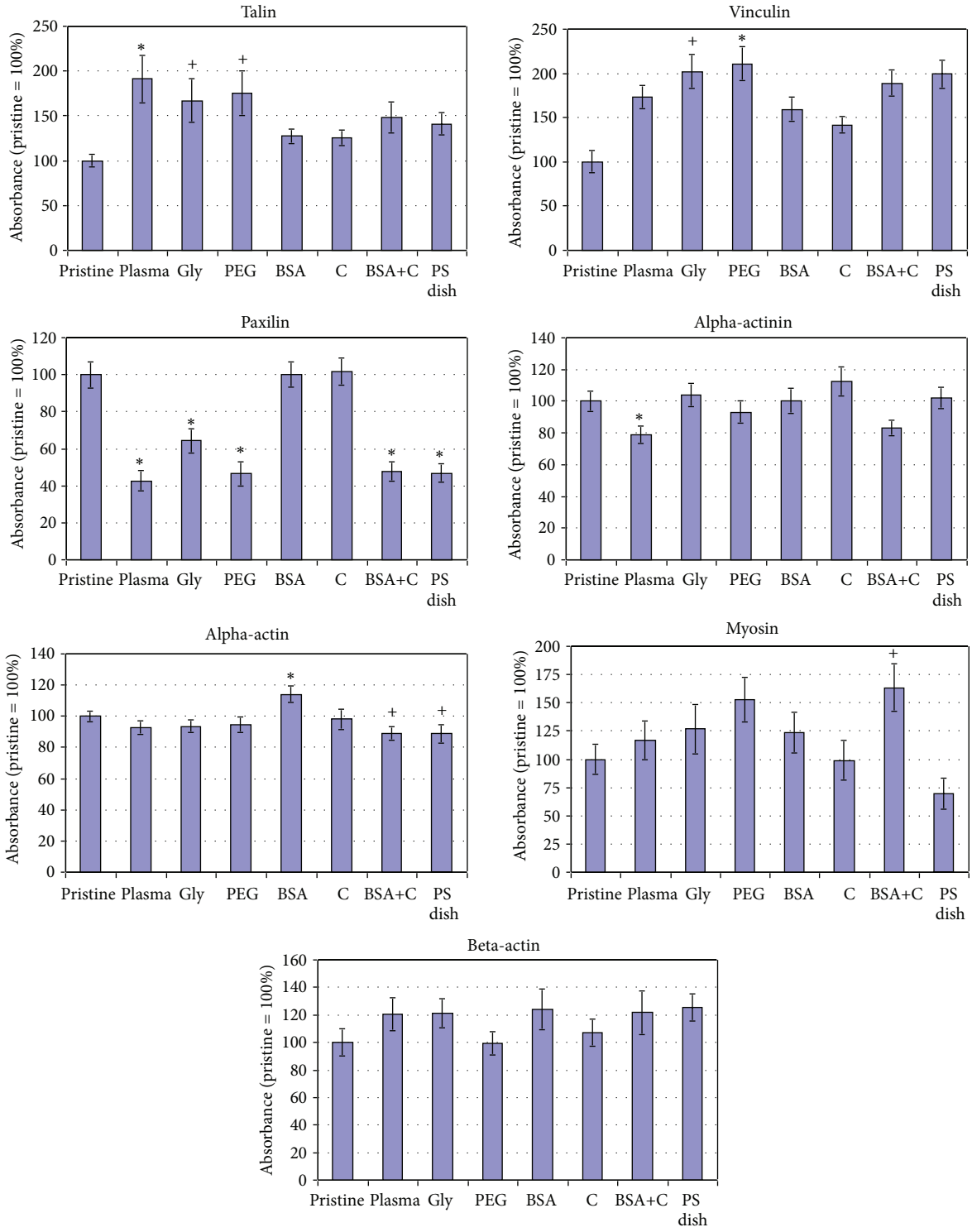

Figure 9: Concentration of focal adhesion, cytoskeletal, and contractile proteins in rat aortic smooth muscle cells in 7-day-old cultures on pristine PE (pristine), on PE activated with plasma (plasma), on PE grafted with glycine (Gly), on polyethylene glycol (PEG), on bovine serum albumin (BSA), on colloidal carbon particles (C), or on BSA with C (BSA+C), and on a tissue culture polystyrene dish (PS dish). Measured by ELISA per mg of protein. Means ± SEM from three to seven experiments, each performed in duplicate or in triplicate. Absorbance values were normalized to the values obtained in cell samples from pristine PE, that is, given as a percentage of the values on pristine PE. ANOVA, statistical significance: $^{*,+}P \leq 0.05$ compared to the value on pristine PE (Student-Newman Keuls method and Dunnett's posttest, resp.).

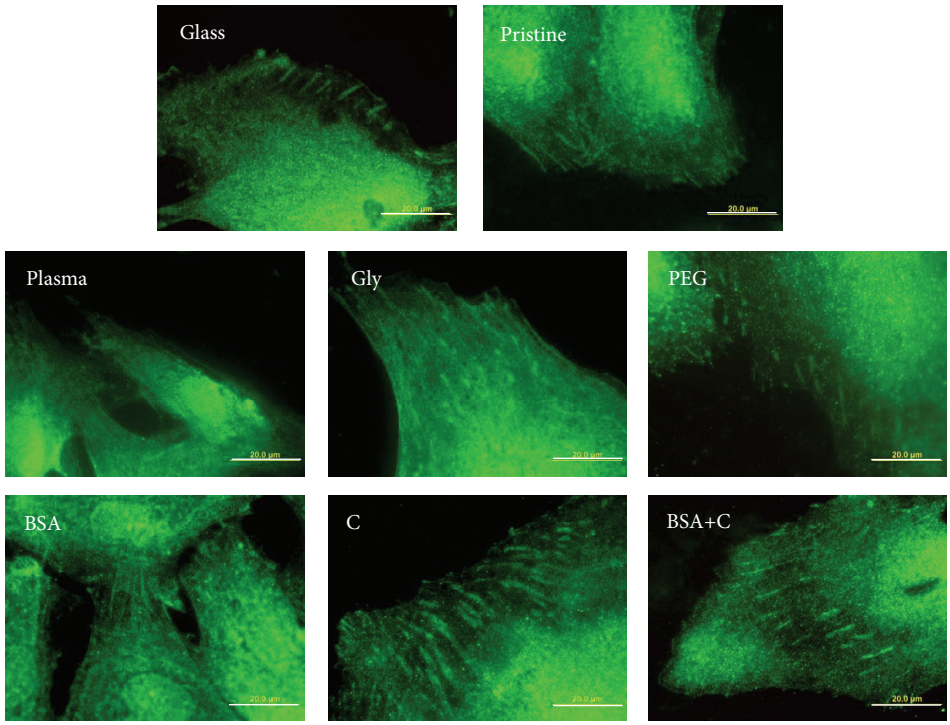

Figure 10: Immunofluorescence of paxillin, an integrin-associated protein of focal adhesion plaques, in rat aortic smooth muscle cells on day 4 after seeding on a microscopic glass coverslip (glass), on pristine LDPE (pristine), on LDPE irradiated with plasma (plasma), on LDPE irradiated with Ar^+ plasma and grafted with glycine (Gly), on polyethylene glycol (PEG), on bovine serum albumin (BSA), on colloidal carbon particles (C), and on bovine serum albumin with C (BSA+C). Olympus IX 51 microscope, DP 70 digital camera, obj. 100x, bar = 20 μm.

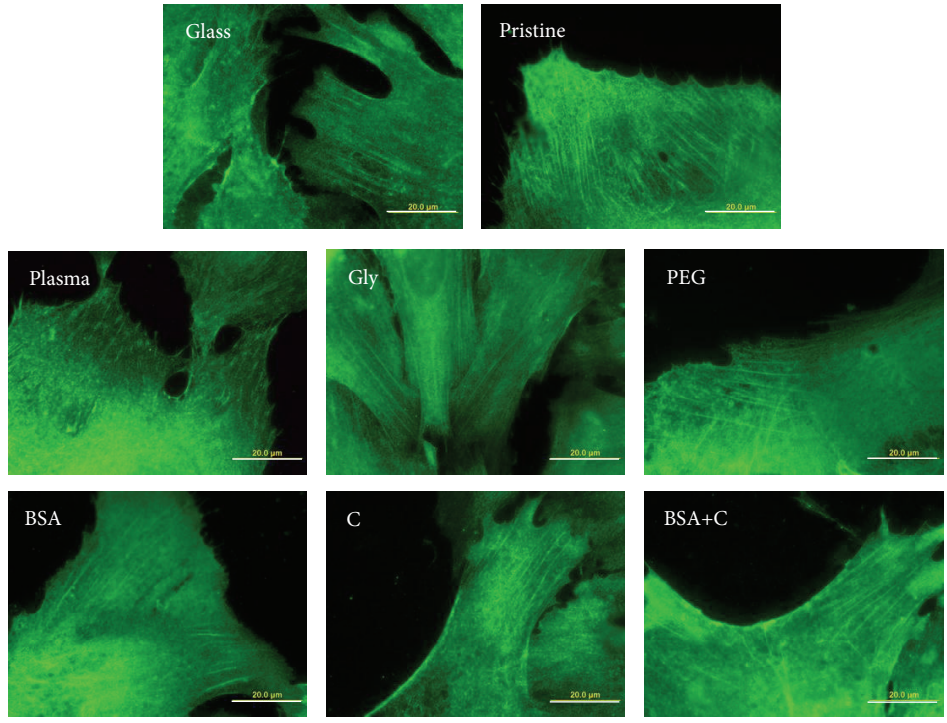

Figure 11: Immunofluorescence of α-actinin, a protein associated with both focal adhesion plaques and the actin cytoskeleton, in rat aortic smooth muscle cells on day 4 after seeding on a microscopic glass coverslip (glass), on pristine LDPE (pristine), on LDPE irradiated with plasma (plasma), on LDPE irradiated with Ar^+ plasma and grafted with glycine (Gly), on polyethylene glycol (PEG), on bovine serum albumin (BSA), on colloidal carbon particles (C), and on bovine serum albumin with C (BSA+C). Olympus IX 51 microscope, DP 70 digital camera, obj. 100x, bar = 20 μm.

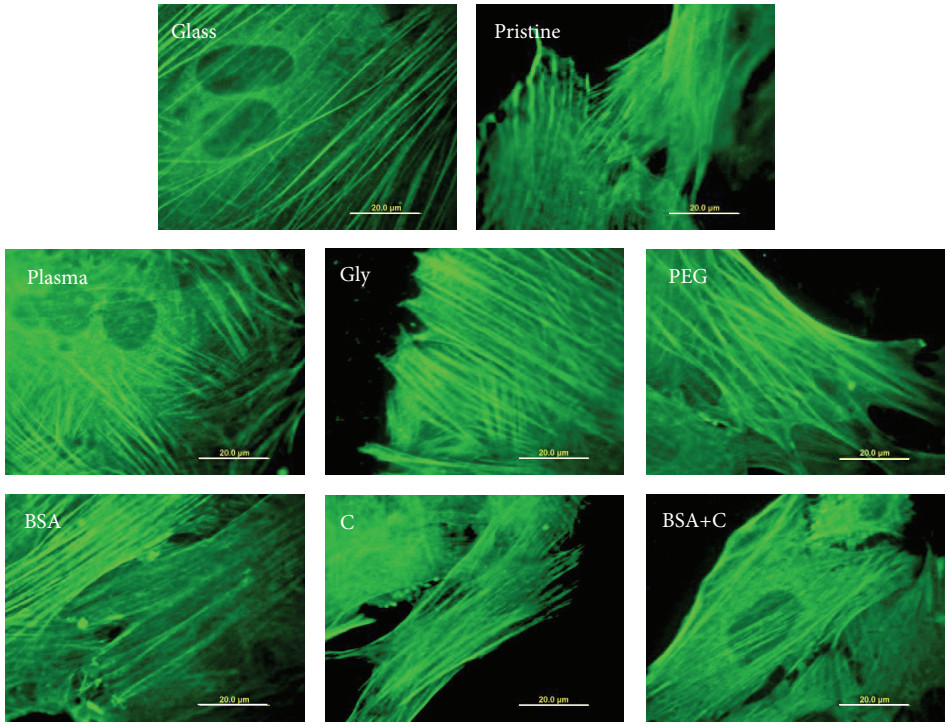

Figure 12: Immunofluorescence of contractile protein α-actin in rat aortic smooth muscle cells on day 4 after seeding on a microscopic glass coverslip (glass), on pristine LDPE (pristine), on LDPE irradiated with plasma (plasma), on LDPE irradiated with Ar^+ plasma and grafted with glycine (Gly), on polyethylene glycol (PEG), on bovine serum albumin (BSA), on colloidal carbon particles (C), and on bovine serum albumin with C (BSA+C). Olympus IX 51 microscope, DP 70 digital camera, obj. 100x, bar = 20 μm.

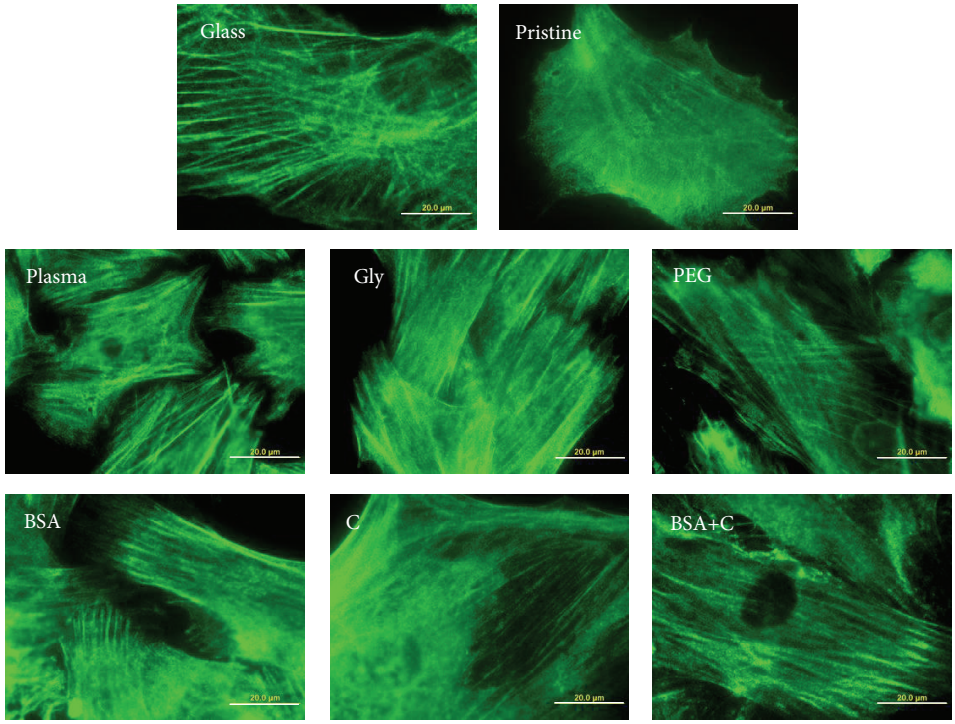

Figure 13: Immunofluorescence of contractile proteins SM1 and SM2 myosins in rat aortic smooth muscle cells on day 4 after seeding on a microscopic glass coverslip (glass), on pristine LDPE (Pristine), on LDPE irradiated with plasma (plasma), on LDPE irradiated with Ar^+ plasma and grafted with glycine (Gly), on polyethylene glycol (PEG), on bovine serum albumin (BSA), on colloidal carbon particles (C), and on bovine serum albumin with C (BSA+C). Olympus IX 51 microscope, DP 70 digital camera, obj. 100x, bar = 20 μm.

an actin isoform nonspecific for VSMC and also present in nonmuscle cell types, was similar in the cells on all tested samples (Figure 9).

Taken together, like the changes in cell number and in spreading area, the changes in the concentration of molecular markers of the adhesion and maturation of VSMC were also generally less apparent on LDPE than on HDPE, after the same modifications of the two polymers (for comparison, see [18]). LDPE grafted with Gly or PEG supported mainly the cell spreading and formation of talin- and vinculin-containing focal adhesion plaques, while the functionalization of LDPE with BSA or BSA+C tended to promote the growth of VSMC to high population densities and their phenotypic maturation, manifested by a higher concentration of α-actin and SM1 and SM2 myosins.

4. Conclusion and Further Perspectives

Modifications of LDPE samples with an Ar^+ plasma discharge and subsequent grafting with glycine, PEG, BSA, C particles, and BSA with C particles improved the colonization of LDPE with VSMC. Grafting with glycine or PEG mainly increased the cell spreading and the concentration of focal adhesion proteins talin and vinculin, which could be attributed to the relatively high oxygen content and wettability of these samples. Grafting LDPE with BSA and BSA+C supported the growth of VSMC to confluence and increased the concentration of α-actin and myosins (SM1 and SM2) in these cells. This could be explained by an enhanced nano- and submicron-scale structure and also by the wettability of the samples. Thus, the plasma treatment and grafting with bioactive substances used in this study improved the adhesion, growth, and phenotypic maturation of VSMC, though these changes were less pronounced than those observed on HDPE in our earlier study [18]. Nevertheless, the polymer modifications developed in this study have a potential for creating a bioartificial vascular wall with reconstructed *tunica media*.

Conflict of Interests

There is no conflict of interests in this study.

Acknowledgments

This study was supported by the Grant Agency of the Czech Republic Grant no. P108/12/G108 ("Center of Excellence"). Mr. Robin Healey (Czech Technical University, Prague, Czech Republic) is gratefully acknowledged for his language revision. The authors also thank Mrs. Ivana Zajanova and Mrs. Jana Vobornikova for their technical assistance.

References

[1] H. P. Greisler, C. W. Tattersall, J. J. Klosak, E. A. Cabusao, J. D. Garfield, and D. U. Kim, "Partially bioresorbable vascular grafts in dogs," *Surgery*, vol. 110, no. 4, pp. 645–654, 1991.

[2] L. Bacakova, V. Mares, M. G. Bottone, C. Pellicciari, V. Lisa, and V. Svorcik, "Fluorine-ion-implanted polystyrene improves growth and viability of vascular smooth muscle cells in culture," *Journal of Biomedical Materials Research*, vol. 49, no. 3, pp. 369–379, 2000.

[3] L. Bačáková, V. Mareš, V. Lisá, and V. Švorčík, "Molecular mechanisms of improved adhesion and growth of an endothelial cell line cultured on polystyrene implanted with fluorine ions," *Biomaterials*, vol. 21, no. 11, pp. 1173–1179, 2000.

[4] L. Bacakova, E. Filova, D. Kubies et al., "Adhesion and growth of vascular smooth muscle cells in cultures on bioactive RGD peptide-carrying polylactides," *Journal of Materials Science*, vol. 18, no. 7, pp. 1317–1323, 2007.

[5] S. H. Daebritz, B. Fausten, B. Hermanns et al., "New flexible polymeric heart valve prostheses for the mitral and aortic positions," *The Heart Surgery Forum*, vol. 7, no. 5, pp. E525–532, 2004.

[6] N. Saito and K. Takaoka, "New synthetic biodegradable polymers as BMP carriers for bone tissue engineering," *Biomaterials*, vol. 24, no. 13, pp. 2287–2293, 2003.

[7] S. A. Atwood, D. W. Van Citters, E. W. Patten, J. Furmanski, M. D. Ries, and L. A. Pruitt, "Tradeoffs amongst fatigue, wear, and oxidation resistance of cross-linked ultra-high molecular weight polyethylene," *Journal of the Mechanical Behavior of Biomedical Materials*, vol. 4, no. 7, pp. 1033–1045, 2011.

[8] C. F. Schierle and L. A. Casas, "Nonsurgical rejuvenation of the aging face with injectable poly-L-lactic acid for restoration of soft tissue volume," *Aesthetic Surgery Journal*, vol. 31, no. 1, pp. 95–109, 2011.

[9] K. W. Ng, D. W. Hutmacher, J. T. Schantz et al., "Evaluation of ultra-thin poly(ε-caprolactone) films for tissue-engineered skin," *Tissue Engineering*, vol. 7, no. 4, pp. 441–455, 2001.

[10] T. Garg, O. Singh, S. Arora, and R. Murthy, "Scaffold: a novel carrier for cell and drug delivery," *Critical Reviews in Therapeutic Drug Carrier Systems*, vol. 29, no. 1, pp. 1–63, 2012.

[11] L. Bacakova, E. Filova, F. Rypacek, V. Svorcik, and V. Stary, "Cell adhesion on artificial materials for tissue engineering," *Physiological Research*, vol. 53, supplement 1, pp. S35–S45, 2004.

[12] L. Bacakova, E. Filova, M. Parizek, T. Ruml, and V. Svorcik, "Modulation of cell adhesion, proliferation and differentiation on materials designed for body implants," *Biotechnology Advances*, vol. 29, no. 6, pp. 739–767, 2011.

[13] L. Bacakova and V. Svorcik, "Cell colonization control by physical and chemical modification of materials," in *Cell Growth Processes: New Research*, D. Kimura, Ed., pp. 5–56, Nova Science, Hauppauge, NY, USA, 2008.

[14] I. Pashkuleva, A. P. Marques, F. Vaz, and R. L. Reis, "Surface modification of starch based biomaterials by oxygen plasma or UV-irradiation," *Journal of Materials Science*, vol. 21, no. 1, pp. 21–32, 2010.

[15] S. Tajima, J. S. F. Chu, S. Li, and K. Komvopoulos, "Differential regulation of endothelial cell adhesion, spreading, and cytoskeleton on low-density polyethylene by nanotopography and surface chemistry modification induced by argon plasma treatment," *Journal of Biomedical Materials Research A*, vol. 84, no. 3, pp. 828–836, 2008.

[16] J. Heitz, V. Svorcik, L. Bacakova et al., "Cell adhesion on polytetrafluoroethylene modified by UV-irradiation in an ammonia atmosphere," *Journal of Biomedical Materials Research A*, vol. 67, no. 1, pp. 130–137, 2003.

[17] R. Mikulikova, S. Moritz, T. Gumpenberger et al., "Cell microarrays on photochemically modified polytetrafluoroethylene," *Biomaterials*, vol. 26, no. 27, pp. 5572–5580, 2005.

[18] M. Parizek, N. Kasalkova, L. Bacakova et al., "Improved adhesion, growth and maturation of vascular smooth muscle cells on polyethylene grafted with bioactive molecules and carbon particles," *International Journal of Molecular Sciences*, vol. 10, no. 10, pp. 4352–4374, 2009.

[19] L. Bacakova, L. Grausova, J. Vacik et al., "Nanocomposite and nanostructure carbon-based films as growth substrates for bone cells," in *Advances in Diverse Industrial Applications of Nanocomposites*, B. Reddy, Ed., pp. 399–435, Intech, 2011.

[20] V. Svorcik, N. Kasalkova, P. Slepicka et al., "Cytocompatibility of Ar^+ plasma-treated and Au nanoparticle-grafted PE," *Nuclear Instruments and Methods in Physics Research B*, vol. 267, no. 11, pp. 1904–1910, 2009.

[21] N. Kasalkova, Z. Makajova, M. Parizek et al., "Cell adhesion and proliferation on plasma-treated and poly(ethylene glycol)-grafted polyethylene," *Journal of Adhesion Science and Technology*, vol. 24, no. 4, pp. 743–754, 2010.

[22] N. Slepickova, N. Kasalkova, P. Slepicka et al., "Cell adhesion and proliferation on polyethylene grafted with Au nanoparticles," *Nuclear Instruments and Methods in Physics Research B*, vol. 272, pp. 391–395, 2012.

[23] M. Parizek, K. Novotná, and L. Bačáková, "The role of smooth muscle cells in vessel wall pathophysiology and reconstruction using bioactive synthetic polymers," *Physiological Research*, vol. 60, no. 3, pp. 419–437, 2011.

[24] A. Van Amerongen, J. H. Wichers, L. B. J. M. Berendsen et al., "Colloidal carbon particles as a new label for rapid immunochemical test methods—quantitative computer image analysis of results," *Journal of Biotechnology*, vol. 30, no. 2, pp. 185–195, 1993.

[25] P. Slepicka, S. Trostova, N. Slepickova-Kasalkova, Z. Kolska, P. Sajdl, and P. V. Svorcik, "Surface modification of biopolymers by argon plasma and thermal treatment," *Plasma Processes and Polymers*, vol. 9, no. 2, pp. 197–206, 2012.

[26] V. Bursikova, P. Stahel, Z. Navratil, J. Bursik, and J. Janca, *Surface Energy Evaluation of Plasma Treated Materials By Contact Angle Measurement*, Masaryk University, Brno, Czech Republic, 2004.

[27] O. H. Lowry, N. J. Rosebrough, A. L. Farr, and R. J. Randall, "Protein measurement with the Folin phenol reagent," *The Journal of Biological Chemistry*, vol. 193, no. 1, pp. 265–275, 1951.

[28] K. Rockova, V. Svorcik, L. Bacakova, B. Dvorankova, J. Heitz, and V. Hnatowicz, "Bio-compatibility of ion beam-modified and RGD-grafted polyethylene," *Nuclear Instruments and Methods in Physics Research B*, vol. 225, no. 3, pp. 275–282, 2004.

[29] V. Švorčík, V. Rybka, V. Hnatowicz, and K. Smetana, "Structure and biocompatibility of ion beam modified polyethylene," *Journal of Materials Science*, vol. 8, no. 7, pp. 435–440, 1997.

[30] V. Svorcik and V. Hnatowicz, "Properties of polymers modified by plasma discharge and ion beam," in *Polymer Degradation and Stability Research Developments*, L. B. Albertov, Ed., pp. 171–216, Nova Science, New York, NY, USA, 2008.

[31] C. O'Connell, R. Sherlock, M. D. Ball et al., "Investigation of the hydrophobic recovery of various polymeric biomaterials after 172 nm UV treatment using contact angle, surface free energy and XPS measurements," *Applied Surface Science*, vol. 255, no. 8, pp. 4405–4413, 2009.

[32] V. Švorčík, K. Kolářová, P. Slepička, A. Macková, M. Novotná, and V. Hnatowicz, "Modification of surface properties of high and low density polyethylene by Ar plasma discharge," *Polymer Degradation and Stability*, vol. 91, no. 6, pp. 1219–1225, 2006.

[33] Q. Wang, Y. X. Guan, S. J. Yao, and Z. Q. Zhu, "Controllable preparation and formation mechanism of BSA microparticles using supercritical assisted atomization with an enhanced mixer," *Journal of Supercritical Fluids*, vol. 56, no. 1, pp. 97–104, 2011.

[34] Y.-S. Lin, S.-S. Wang, T.-W. Chung et al., "Growth of endothelial cells on different concentrations of Gly-Arg-Gly-Asp photochemically grafted in polyethylene glycol modified polyurethane," *Artificial Organs*, vol. 25, no. 8, pp. 617–621, 2001.

[35] S. Huang, C. S. Chen, and D. E. Ingber, "Control of cyclin D1, p27(Kip1), and cell cycle progression in human capillary endothelial cells by cell shape and cytoskeletal tension," *Molecular Biology of the Cell*, vol. 9, no. 11, pp. 3179–3193, 1998.

[36] S. Huang and D. E. Ingber, "Shape-dependent control of cell growth, differentiation, and apoptosis: switching between attractors in cell regulatory networks," *Experimental Cell Research*, vol. 261, no. 1, pp. 91–103, 2000.

[37] A. L. Koenig, V. Gambillara, and D. W. Grainger, "Correlating fibronectin adsorption with endothelial cell adhesion and signaling on polymer substrates," *Journal of Biomedical Materials Research A*, vol. 64, no. 1, pp. 20–37, 2003.

[38] J. E. Koblinski, M. Wu, B. Demeler, K. Jacob, and H. K. Kleinman, "Matrix cell adhesion activation by non-adhesion proteins," *Journal of Cell Science*, vol. 118, no. 13, pp. 2965–2974, 2005.

[39] T. J. Webster, C. Ergun, R. H. Doremus, R. W. Siegel, and R. Bizios, "Specific proteins mediate enhanced osteoblast adhesion on nanophase ceramics," *Journal of Biomedical Materials Research*, vol. 51, no. 3, pp. 475–483, 2000.

[40] J. Lu, C. Yao, L. Yang, and T. J. Webster, "Decreased platelet adhesion and enhanced endothelial cell functions on nano and submicron-rough titanium stents," *Tissue Engineering A*, vol. 18, no. 13-14, pp. 1389–1398, 2012.

[41] H. M. Kowalczyńska, M. Nowak-Wyrzykowska, R. KoThlos, J. Dobkowski, and J. Kamiński, "Semiquantitative evaluation of fibronectin adsorption on unmodified and sulfonated polystyrene, as related to cell adhesion," *Journal of Biomedical Materials Research A*, vol. 87, no. 4, pp. 944–956, 2008.

[42] L. Bacakova, L. Grausova, M. Vandrovcova et al., "Carbon nanoparticles as substrates for cell adhesion and growth," in *Nanoparticles: New Research*, S. L. Lombardi, Ed., pp. 39–107, Nova Science, Hauppauge, NY, USA, 2008.

[43] H. Mao, Y. Wang, Z. Li et al., "Hsp72 interacts with paxillin and facilitates the reassembly of focal adhesions during recovery from ATP depletion," *The Journal of Biological Chemistry*, vol. 279, no. 15, pp. 15472–15480, 2004.

[44] C. A. Carter and T. Bellido, "Decrease in protein tyrosine phosphorylation is associated with F-actin reorganization by retinoic acid in human endometrial adenocarcinoma (RL95-2) cells," *Journal of Cellular Physiology*, vol. 178, no. 3, pp. 320–332, 1999.

[45] C. E. Turner, "Paxillin interactions," *Journal of Cell Science*, vol. 113, part 23, pp. 4139–4140, 2000.

[46] R. Zaidel-Bar, R. Milo, Z. Kam, and B. Geiger, "A paxillin tyrosine phosphorylation switch regulates the assembly and

form of cell-matrix adhesions," *Journal of Cell Science*, vol. 120, part 1, pp. 137–148, 2007.

[47] N. F. Worth, B. E. Rolfe, J. Song, and G. R. Campbell, "Vascular smooth muscle cell phenotypic modulation in culture is associated with reorganisation of contractile and cytoskeletal proteins," *Cell Motility and the Cytoskeleton*, vol. 49, no. 3, pp. 130–145, 2001.

[48] B. Sjöblom, A. Salmazo, and K. Djinović-Carugo, "Alpha-actinin structure and regulation," *Cellular and Molecular Life Sciences*, vol. 65, no. 17, pp. 2688–2701, 2008.

Materials **2013**, *6*, 1632-1655; doi:10.3390/ma6051632

OPEN ACCESS

materials

ISSN 1996-1944

www.mdpi.com/journal/materials

Article

Adhesion and Growth of Vascular Smooth Muscle Cells on Nanostructured and Biofunctionalized Polyethylene

Katarina Novotna [1,†], Marketa Bacakova [1,†], Nikola Slepickova Kasalkova [2], Petr Slepicka [2], Vera Lisa [1], Vaclav Svorcik [2] and Lucie Bacakova [1,*]

[1] Department of Biomaterials and Tissue Engineering, Institute of Physiology, Academy of Sciences of the Czech Republic, Videnska 1083, CZ-14220 Prague 4, Czech Republic; E-Mails: k.novotna@biomed.cas.cz (K.N.); marketa.bacakova@biomed.cas.cz (M.B.); lisa.v@biomed.cas.cz (V.L.)

[2] Department of Solid State Engineering, Institute of Chemical Technology, Technicka 5, CZ-16628 Prague 6, Czech Republic; E-Mails: nikola.kasalkova@vscht.cz (N.S.K.); petr.slepicka@vscht.cz (P.S.); vaclav.svorcik@vscht.cz (V.S.)

† These authors contributed equally to this work.

* Author to whom correspondence should be addressed; E-Mail: lucy@biomed.cas.cz; Tel.: +420-2-9644-3742; Fax: +420-2-9644-2844.

Received: 8 January 2013; in revised form: 21 March 2013 / Accepted: 11 April 2013 / Published: 29 April 2013

Abstract: Cell colonization of synthetic polymers can be regulated by physical and chemical modifications of the polymer surface. High-density and low-density polyethylene (HDPE and LDPE) were therefore activated with Ar^+ plasma and grafted with fibronectin (Fn) or bovine serum albumin (BSA). The water drop contact angle usually decreased on the plasma-treated samples, due to the formation of oxidized groups, and this decrease was inversely related to the plasma exposure time (50–300 s). The presence of nitrogen and sulfur on the polymer surface, revealed by X-ray photoelectron spectroscopy (XPS), and also by immunofluorescence staining, showed that Fn and BSA were bound to this surface, particularly to HDPE. Plasma modification and grafting with Fn and BSA increased the nanoscale surface roughness of the polymer. This was mainly manifested on HDPE. Plasma treatment and grafting with Fn or BSA improved the adhesion and growth of vascular smooth muscle cells in a serum-supplemented medium. The final cell population densities on day 6 after seeding were on an average higher on LDPE than on HDPE. In a serum-free medium, BSA grafted to the polymer surface hampered cell adhesion. Thus, the

cell behavior on polyethylene can be modulated by its type, intensity of plasma modification, grafting with biomolecules, and composition of the culture medium.

Keywords: plasma treatment; biocompatibility; bioactivity; wettability; nanoscale surface roughness; albumin; fibronectin; cell spreading area; tissue engineering

1. Introduction

The use of artificial materials in medicine and biology has become very important, especially their application as substitutes for damaged tissues and organs, or as carriers for drug or gene delivery [1–4]. These materials have to be biocompatible, *i.e.*, they have to match the mechanical properties of the replaced tissue, and not act as cytotoxic, mutagenic or immunogenic. For specific applications, biocompatible materials can behave as bioinert and not as promoting cell adhesion and growth. For example, materials of these types have been applied in the construction of artificial eye lenses [5] or in the articular surfaces of joint prostheses [6], which are implants requiring transparency or smoothness, and are thus completely cell-free surfaces. Bioinert materials have also been used for fabricating polymeric vascular prostheses in order to prevent the adhesion and activation of thrombocytes and immunocompetent cells on the inner surface of these grafts [7].

However, adhesion, spreading, growth and phenotypic maturation of cells are required for constructing advanced bioartificial tissue replacements, including replacements for blood vessels or for bone. In these replacements, the artificial materials should act as analogs of the natural extracellular matrix, and thus they should support regeneration of the damaged tissue. For example, in vascular tissue engineering, this means that the material should enable reconstruction of the *tunica intima*, formed by a confluent layer of endothelial cells, and also reconstruction of the *tunica media*, which contain vascular smooth muscle cells. For these purposes, advanced artificial materials should not just be passively tolerated by the cells, but should act as bioactive or biomimetic, which means that they induce the required cell responses in a controllable manner (for a review, see [8,9]).

It is generally known that the cell–material interaction is strongly dependent on the physical and chemical properties of the material surface, such as wettability, roughness and topography, or the presence of various chemical functional groups and biomolecules. From this point of view, the surfaces of most materials currently used for constructing tissue replacements are not optimal for integrating with the surrounding tissues, and need further modification in order to improve their physicochemical surface properties and thus enhance the cell colonization and new tissue formation (for a review, see [3,4]). A typical example is provided by synthetic polymers (polyethylene, polypropylene, polystyrene, polyethyleneterephthalate or polytetrafluoroethylene), which are biomaterials widely used in various biotechnologies, including cell cultivation and construction of tissue replacements. In their non-treated state, however, some materials usually form inadequate scaffolds for cell colonization, often due to their relatively high hydrophobicity (water drop contact angle in the range of about 90–120°). These materials can be rendered more hydrophilic by several techniques, particularly by irradiation with ultraviolet (UV) light [10], an ion beam [11–13] or exposure to plasma discharge [14–16]. In addition to the changes in surface wettability, these

treatments also affect the roughness, morphology, electrical conductivity, stability, mechanical properties and chemical composition of the material surface. A common feature of irradiation with UV light, ion beam or plasma treatment is splitting of the bonds within the polymer molecules, which results in the creation of free radicals, double bonds and new functional groups (especially oxygen-containing groups) on the polymer surface. Oxidized groups increase the wettability of polymers, and this supports the adsorption of cell adhesion-mediating extracellular matrix (ECM) molecules in an appropriate spatial conformation, increasing the accessibility of specific sites in these molecules for cell adhesion receptors. Free radicals and unsaturated bonds can then be used for functionalizing the material surface with various biomolecules, e.g., grafting amino acids, oligopeptides or protein molecules, which can also influence (mediate or attenuate) the cell adhesion and growth (for a review, see [3,4]). This grafting occurs spontaneously after exposure of the irradiated material to biological environments, including biological fluids such as blood, intercellular liquid or cell culture media.

Polyethylene has been used in several tissue engineering applications. For example, composites of HDPE with hydroxyapatite [17] or tricalcium phosphate [18] have been developed for the construction of bone replacements, composites of HDPE with graphite for the construction of joint replacements [19], and copolymers of HDPE with hyaluronan for the reconstruction of osteochondral defects [20]. HDPE was also clinically applied for calvarial reconstruction [21]. LDPE is used for producing intravascular catheters for arteriography and angioplasty, due to its advantageous mechanical properties, such as elasticity and flexibility [22].

In our study, two types of polyethylene, namely high density polyethylene (HDPE) and low density polyethylene (LDPE), were modified by Ar^+ plasma discharge of various exposure times (50, 100 and 300 s), and were subsequently exposed to solutions of two important components of fetal serum, namely fibronectin (Fn) and bovine serum albumin (BSA). We expected the biomolecules from these fluids to graft spontaneously to the plasma-activated polyethylene and to influence cell adhesion and growth, which were studied using rat vascular smooth muscle cells in cultures on these materials. Polyethylene was chosen as a model material for studies of cell–material interaction, due to its easy availability and particularly its relatively simple molecule, consisting only of carbon and hydrogen, which enables clear and reproducible results to be obtained. A comparison was also made for the cell behavior on HDPE and LDPE.

2. Results and Discussion

2.1. Physical and Chemical Properties of the Polyethylene Samples

2.1.1. Surface Wettability

The water drop contact angle decreased after plasma modification of the polymers, which means that the surface wettability increased (Figure 1). The highest decrease in the contact angle was observed on samples irradiated for 50 s, and as the exposure time was prolonged the decrease was less apparent. On HDPE irradiated for 300 s, the contact angle even increased (Figure 1A). A similar observation on HDPE was published earlier, and can be explained by the different rearrangement of HDPE after plasma irradiation in comparison with LDPE [23]. It is generally known that the increase in wettability is due to the formation of new oxidized groups on the polymer surface after plasma

modification [4,24]. However, surface wettability is also associated with rearrangement of the surface structure, mainly of the oxidized groups, during the aging period of the polymer after plasma exposure. During this period, the oxidized groups are reoriented from the surface to the inside of the polymer. This causes an increase in the contact angle, though in most cases the contact angle of a modified polymer after the aging period still remains lower than the contact angle of the non-treated polymer. The rearrangement of the oxidized groups during aging is influenced by the degree of crosslinking of the polymer structure and the time of plasma modification. A less crosslinked structure and longer modification times lead to greater mobility of these groups. The structure of HDPE is less crosslinked than the structure of LDPE, probably due to the fact that HDPE molecules are more linear and less branched than LDPE molecules, and these differences are further enhanced by plasma irradiation. Thus, the less crosslinked structure of HDPE and relatively long plasma irradiation (300 s) led to higher rotation of the oxidized groups into the polymer, their burrowing into the polymer, their lower exposure on the polymer surface, and thus to lower wettability of the polymer, manifested by a relatively high contact angle (119°), which became even higher than on non-treated HDPE. Moreover, the lesser branching of HDPE creates less opportunity for oxidized groups to occur on this polymer, which might be another important factor influencing the contact angle.

Figure 1. Water drop contact angle on (**A**) HDPE; and (**B**) LDPE in non-treated form (**N**), treated with plasma for 50, 100 or 300 s (**Plasma**), and subsequently grafted with fibronectin (**Fn**) or bovine serum albumin (**BSA**). Mean ± S.D. from 30 measurements performed on 3 samples (10 measurements on each).

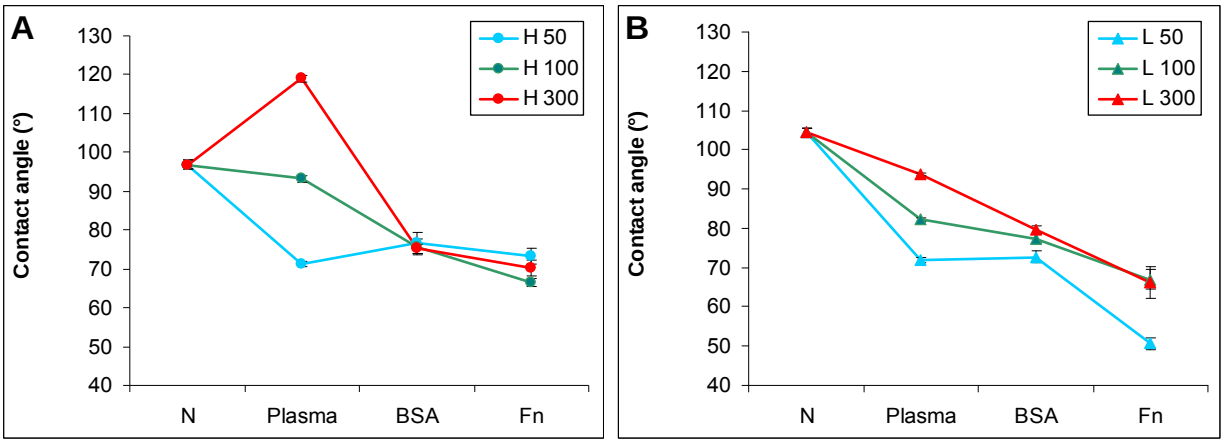

Subsequent grafting of Fn or BSA onto the plasma-activated polymer surface usually resulted in a further decrease in the contact angle. This phenomenon was well apparent, particularly on HDPE and LDPE irradiated with plasma for 100 and 300 s. The increase in surface wettability could be explained by the polar groups present in fibronectin and albumin molecules, oxygen-containing and amine groups. However, on the polymers irradiated for 50 s, the presence of BSA and Fn on an HDPE surface and BSA on an LDPE surface did not have significant effects on the surface wettability, as indicated by the contact angles on these polymers, which were comparable with the values on the samples treated only with plasma. Similar results for BSA on HDPE and LDPE have been published earlier [25,26]. In these studies focused on grafting bioactive substances onto HDPE and LDPE surfaces, only glycin and polyethylene glycol further decreased the contact angle on the

plasma-irradiated polymers, while the contact angle remained similar after grafting of BSA, colloidal carbon particles and a combination of BSA and these particles. Similarly, in the present study, grafting the plasma-treated PE with Fn was more efficient in decreasing the contact angle than grafting with BSA, except in the case of HDPE irradiated for 50 s.

2.1.2. XPS Analysis and Immunofluorescence Staining of Grafted Biomolecules

Fibronectin and albumin are proteins which contain nitrogen and disulfide bonds [27,28]. The presence of these biomolecules on the PE surface was therefore tested using X-ray photoelectron spectroscopy analysis (XPS) by determining the concentration of nitrogen and sulfur on the polymer surface. XPS also determined the concentration of oxygen as evidence that oxidized polar groups were formed after plasma irradiation.

XPS analysis showed that the concentration of nitrogen was significantly higher on HDPE and LDPE activated with plasma and subsequently grafted with Fn and BSA than on samples only treated with plasma (Table 1). The nitrogen found in a low amount on the plasma-treated samples was probably bound from the ambient atmosphere after plasma exposure. In addition, sulfur was determined on the samples grafted with Fn and BSA. Due to the higher presence of nitrogen and sulfur on the grafted samples than on the only plasma-treated samples, we can conclude that fibronectin and albumin were successfully bound on the plasma-treated polymer surface. XPS also indicates that the concentration of oxygen increased after the polymer was exposed to plasma, and this led to a decline in the contact angle (Figure 1). The higher concentration of oxygen on the irradiated samples than on the non-treated samples indicated the formation of newly oxidized polar groups after plasma modification.

Table 1. Concentration (in at. %) of carbon (C), oxygen (O), nitrogen (N) and sulfur (S), determined by XPS analysis, on HDPE and LDPE treated with plasma for 50 s (**50**), and subsequently grafted with fibronectin (**Fn**) and bovine serum albumin (**BSA**). Mean from three measurements for each experimental group; the measurement error did not exceed 5%.

Material/	**HDPE**				**LDPE**			
Modification	C (at. %)	O (at. %)	N (at. %)	S (at. %)	C (at. %)	O (at. %)	N (at. %)	S (at. %)
50	82.2	14.2	2.5	0	83.0	14.8	1.5	0
50 Fn	72.9	20.2	6.7	0.2	82.2	13.6	2.8	at limit of detection
50 BSA	74.4	15.3	9.9	0.4	72.7	15.3	10.9	0.4

The presence of fibronectin and albumin was also tested by immunofluorescence staining (Figure 2). The resultant fluorescence intensity was presented as the difference between the fluorescence intensity measured on samples treated with both primary and secondary antibodies and on samples treated with the secondary antibody only (*i.e.*, the staining control). On HDPE and on LDPE grafted with Fn or BSA, the fluorescence intensity reached high positive values, indicating the presence of Fn and BSA on the polymer surface. By contrast, the fluorescence intensity had negative values on the non-treated polymers [Figure 2(A,B)]. This was probably due to non-specific binding of the secondary antibody to the polymer surface, because the fluorescence intensity of the staining control, *i.e.*, the sample incubated only in the secondary antibody, was higher than the fluorescence

intensity after staining the non-treated polymer with both primary and secondary antibodies (Figure 2C). The non-specific binding of the secondary antibody on samples grafted with Fn and BSA was significantly reduced due to the presence of these biomolecules. In this context it should be pointed out that in studies using immunocytochemical methods, BSA [25,26,29], the whole blood serum [30] or solutions of other biomolecules, e.g., gelatin [12] are commonly used for blocking non-specific binding sites for antibodies. In addition, the fluorescence intensity on HDPE grafted with Fn or BSA was higher than on LDPE, which showed that Fn and BSA were grafted in a higher concentration on the HDPE surface than on LDPE [Figure 2(A,B)].

Figure 2. Immunofluorescence staining of (**A**) fibronectin; and (**B**) albumin and their microphotographs (**C**) on HDPE (**H**) and LDPE (**L**), in non-treated form (**N**), treated with plasma for 50 s and subsequently grafted with fibronectin (**50 Fn**) or bovine serum albumin (**50 BSA**). Olympus IX 51 microscope, obj. 10x, DP 70 digital camera. The measurements were performed at the same exposure time for all experimental groups (1.2 s).

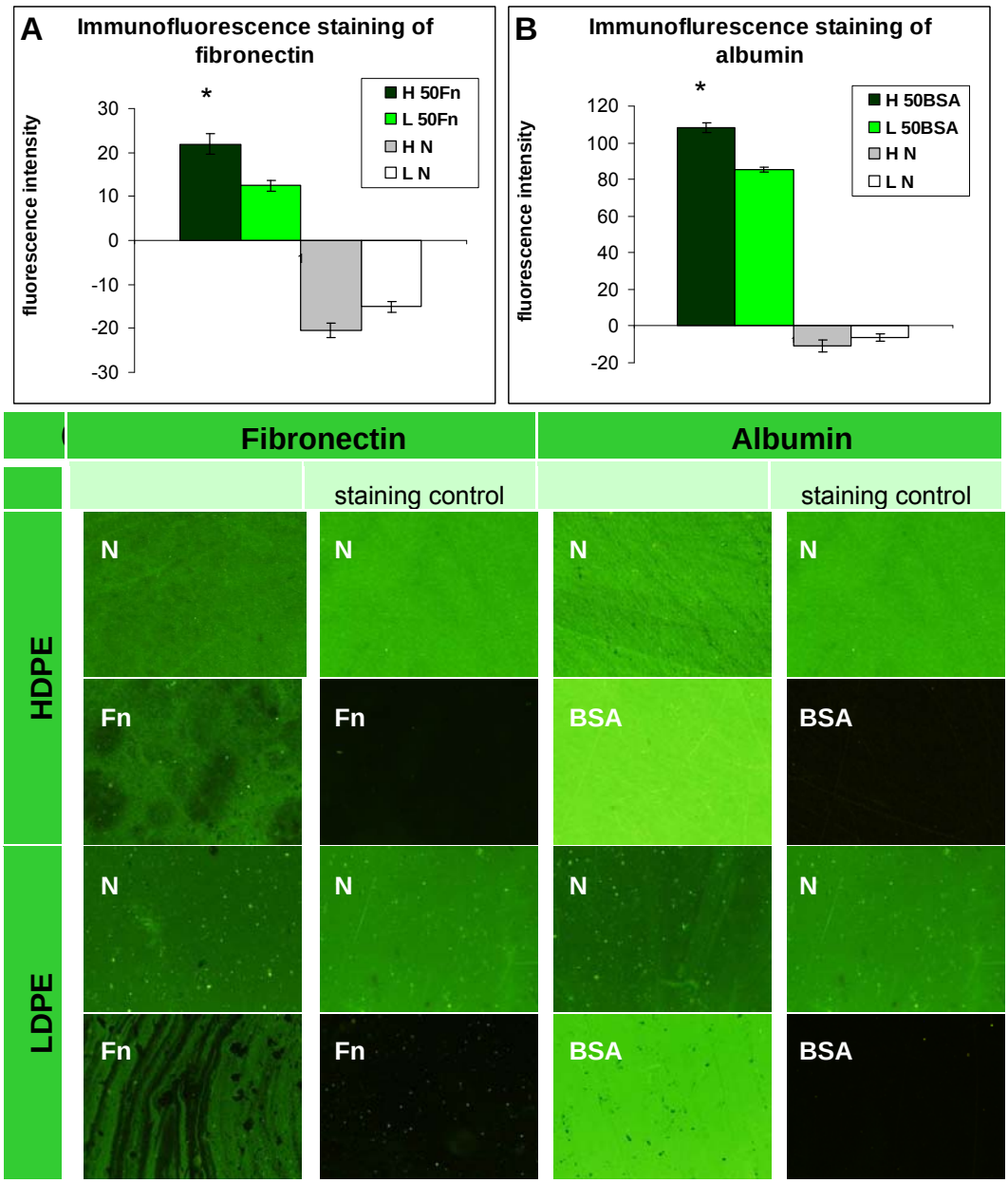

2.1.3. Surface Roughness and Morphology

Changes in surface roughness and morphology after plasma exposure and grafting with biomolecules were studied by the Atomic Force Microscopy (AFM) method (Figure 3, Table 2). Plasma treatment led to ablation of the surface layer [23], which increased the nanoscale surface roughness in proportion to the exposure time. These events were more apparent on HDPE than on LDPE, and could be explained by the different structure of the two polymers. For example, LDPE is more crosslinked than HDPE, and thus it could be more resistant to ablation. In our earlier study, plasma treatment of PE for 400 s resulted in the removal of a surface layer of HDPE that was about 1 μm in thickness, but of a layer of LDPE that was only 0.6 μm in thickness [23].

Figure 3. AFM images of HDPE (**H**) and LDPE (**L**) in non-treated form (**N**), treated in plasma for 50 s, and subsequently grafted with fibronectin (**Fn**) or bovine serum albumin (**BSA**).

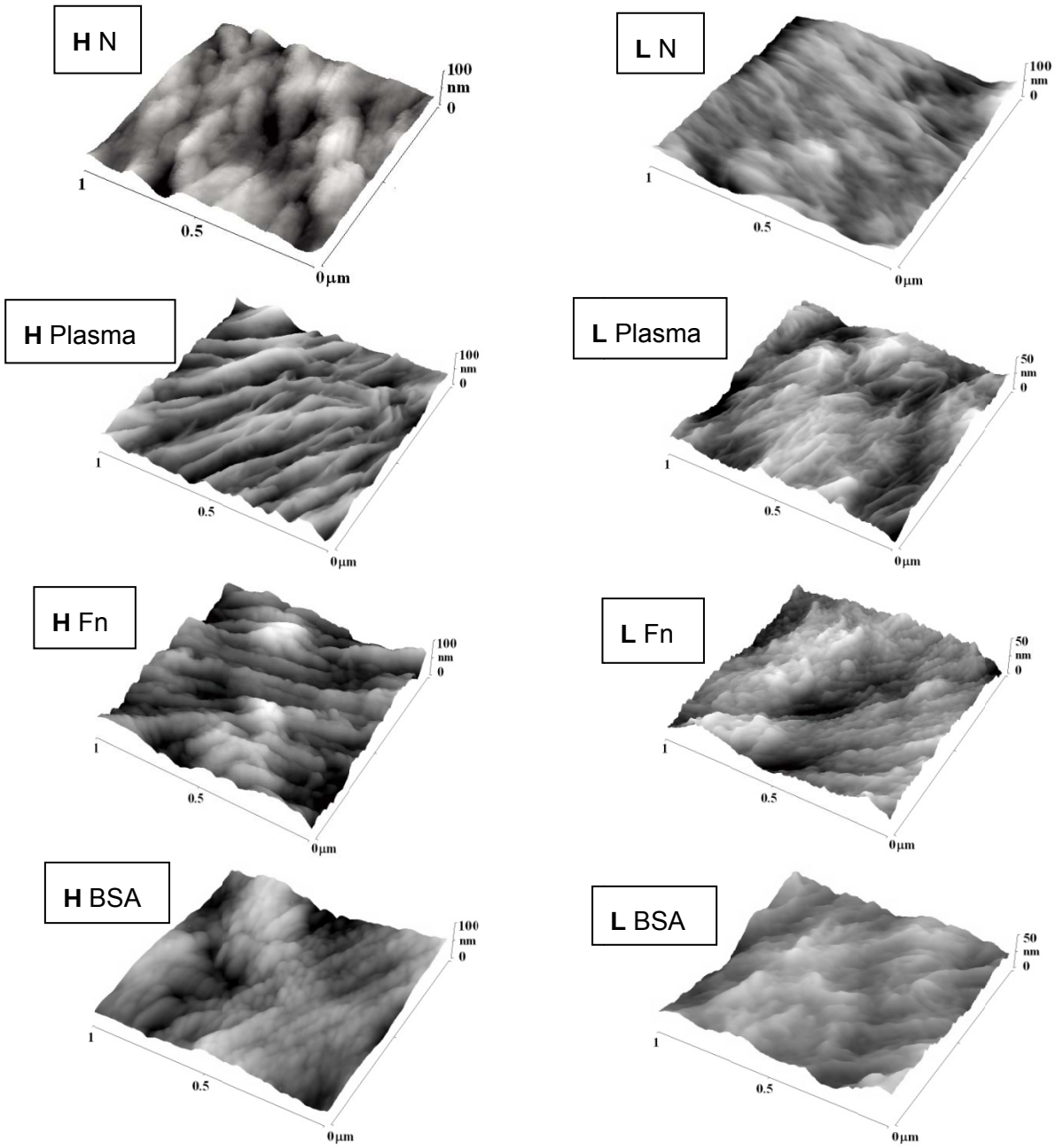

Table 2. The mean surface roughness values (R_a) of LDPE and HDPE in non-treated form (**N**), treated in plasma for 50, 100 or 300 s (**50, 100, 300**), and subsequently grafted with fibronectin (**Fn**) or albumin (**BSA**).

Sample	HDPE	LDPE
N	6.1	5.0
50	7.4	4.7
50 Fn	10.4	5.5
50 BSA	6.9	5.4
100	8.4	6.7
100 Fn	11.7	4.6
100 BSA	9.4	4.7
300	11.5	6.6
300 Fn	12.0	5.6
300 BSA	7.8	4.6

In addition, the surface morphology of both types of PE was changed after plasma modification. A lamellar structure appeared on the polymer surface, perhaps due to the different ablation rate of the amorphous and crystalline phases. The amorphous phase is ablated preferentially [23,31]. The newly created lamellar structure was more apparent on the HDPE surface, while the LDPE surface appeared to be ablated more uniformly (homogeneously). The reason could be a higher proportion of the crystalline phase in HDPE, while the amorphous phase prevails in LDPE [23].

Subsequent grafting with Fn or BSA further changed the surface roughness (see Table 2) and the morphology of PE. Grafting with Fn strongly increased the surface roughness of HDPE, while BSA did not significantly increase, or even reduced, the surface roughness of the plasma-treated surface, although this roughness still remained higher than on the non-treated polymer. The lamellar structure was less apparent on the grafted surface than on the only-treated HDPE surface. Grafting LDPE with Fn or BSA produced rather small and non-significant changes in surface roughness and morphology. On LDPE irradiated for 100 or 300 s, both Fn and BSA showed a tendency to smoothen the material surface (Figure 3).

2.2. Cell Adhesion and Growth

2.2.1. Cell Adhesion and Growth on LDPE and HDPE Samples in a Standard Serum-supplemented Medium

The proliferation of cells in DMEM with fetal bovine serum (FBS) had in general a growing tendency. On day 2 after seeding, there were similar numbers of initially adhered cells on the control polystyrene, on the samples exposed to a plasma discharge, and on all Fn-grafted and BSA-grafted samples (Figure 4). This cell behavior was observed on both LDPE and HDPE, and could be explained by a masking effect of the serum in the culture medium, *i.e.*, secondary adsorption of serum components influencing cell adhesion, particularly vitronectin, fibronectin and albumin on the samples, which occurs within a few minutes after these substrates are exposed to the culture medium (for a review, see [3,4,9]). Significant differences were found only between the non-treated samples and some modified samples, usually with the exception of the BSA-grafted samples

[Figure 4(A,B,D–F)], and in two cases also with the exception of the samples only irradiated with plasma [Figure 4(B,D)].

Figure 4. Growth curves of rat aortic smooth muscle cells cultured in a serum-supplemented medium on HDPE (**A–C**) or LDPE (**D–F**) in non-treated form (**N**), treated with plasma for 50, 100 or 300 s (**50, 100, 300**), and subsequently grafted with fibronectin (**Fn**) or bovine serum albumin (**BSA**). A standard cell culture polystyrene dish (**PS**) was used as a reference material. Mean ± S.E.M. from 20 measurements on microphotographs (day 2 and 4) or 200 measurements on a ViCell XR Analyser (Beckman Coulter, Brea, CA, USA) (day 6). ANOVA, Student–Newman–Keuls Method. Statistical significance: * $p \leq 0.05$ compared to non-modified HDPE or LDPE.

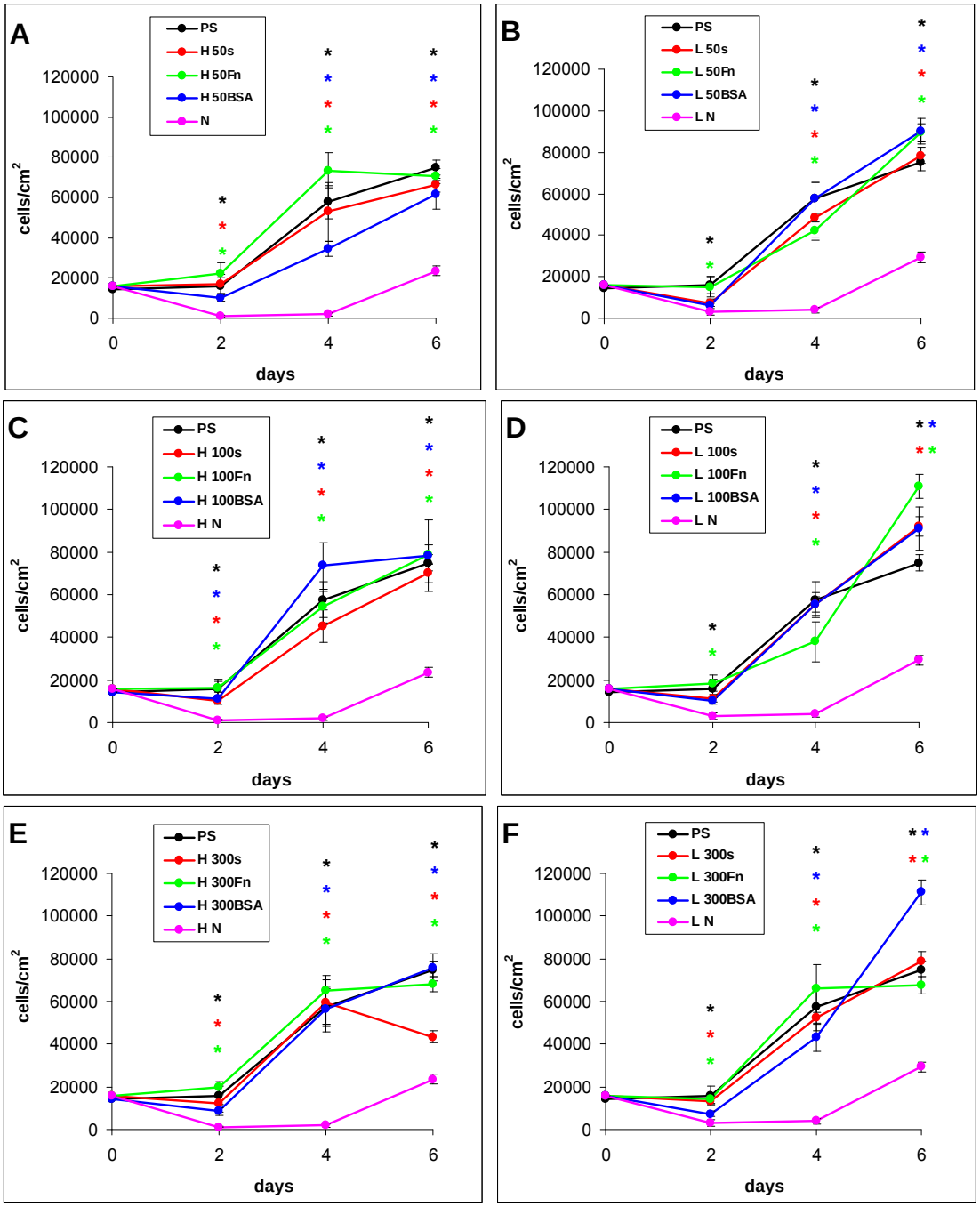

From day 2 to day 4 after seeding, the cells on all modified PE samples showed an intense increase in their growth, while the cell growth on the non-treated PE samples was stagnant. As a result, the cell numbers on all modified samples on day 4 were significantly higher than the values on the non-treated samples. However, the differences among the groups of modified samples still remained non-significant (Figure 4).

From day 4 to day 6 after seeding, the cells on most of the HDPE samples reached confluence, slowed down their proliferation and entered the stationary growth phase, *i.e.*, their number did not increase as rapidly as between day 2 and day 4, and on some samples the number even decreased. By contrast, the cells on the LDPE samples usually continued their growth, and thus reached on an average higher final cell population densities. On day 6 after seeding, these densities ranged from about 78,000 to 111,000 cells·cm^{-2} on LDPE, while there were only 43,000 to 79,000 cells·cm^{-2} on HDPE (Figure 4).

Particularly the cells on the BSA-grafted LDPE samples continued their exponential growth, and on day 6 after seeding their population densities were among the highest values reached on these samples, especially on LDPE activated with plasma for 300 s (Figure 4F). These results can be considered as surprising, because albumin is known as a cell non-adhesive molecule [32], which has been used for creating bioinert cell-free surfaces, applicable e.g., in blood-contacting devices [33,34]. In our study, the non-adhesive properties of albumin are slightly reflected by the relatively low numbers of initially adhered cells on the BSA-grafted samples, which often did not differ significantly from the values on the non-treated polyethylene (Figure 4). Nevertheless, the cell spreading areas were mostly larger than in the cells on non-treated samples, and usually not significantly smaller than on the control polystyrene dishes, except BSA-grafted HDPE treated with plasma for 100 s (Figures 5–7). Albumin has been reported to promote adsorption of ECM molecules, e.g., vitronectin and fibronectin, in advantageous spatial conformations, supporting the accessibility of these molecules by cell adhesion receptors (for a review, see [25]). These molecules cannot only be adsorbed over the albumin from the serum of the culture medium, but are also synthesized and deposited by VSMC themselves [35], especially at later culture intervals. This may account for the relatively high proliferation activity of the cells on BSA-grafted PE (Figure 4).

As for the non-treated HDPE and LDPE samples, the cell number increased from day 4 to 6 on these materials (Figure 4). However, the maximum population densities on these polymers still remained significantly lower (from about 24,000 to 29,000 cells·cm^{-2}) than on the modified samples (from 43,000 to 111,000 cells·cm^{-2}).

In accordance with the weak cell proliferation on non-treated PE, the visualization of the cells on day 2 also showed a lower size of the cell spreading area on non-treated PE than on the modified samples (Figures 5–7). This insufficient cell spreading can be explained by the relatively high hydrophobicity of non-treated HDPE and LDPE. It is known that, on highly hydrophobic surfaces, the cell adhesion-mediating proteins, e.g., fibronectin and vitronectin, present in the serum of the culture medium, are adsorbed in rigid, non-physiological and denatured form, less appropriate for binding the specific sites in the protein molecules by the cell adhesion receptors (for a review, see [3,4,9]). By contrast, the modified polymers were more hydrophilic, with an enhanced nanostructure or grafted with biomolecules. As mentioned above, BSA supports the adsorption of cell adhesion-mediating molecules in a near-physiological conformation, appropriate for binding to the cell adhesion receptors.

In addition, the fibronectin grafted on some samples provided the possibility for direct binding of the cells, e.g., through specific RGD-containing amino acid sequences in the Fn molecules [28].

Figure 5. Morphology of rat aortic smooth muscle cells in two-day-old cultures in a serum-supplemented medium on HDPE in non-treated form (**N**), treated with plasma for 50, 100 or 300 s (**50, 100, 300**), and subsequently grafted with fibronectin (**Fn**) or bovine serum albumin (**BSA**). A standard cell culture polystyrene dish (**PS**) was used as a reference material. Cells stained with Texas Red C_2-Maleimide and Hoechst #33342. Olympus IX 51 microscope, obj. 20, DP 70 digital camera, bar 200 µm or 100 µm (Fn-grafted samples).

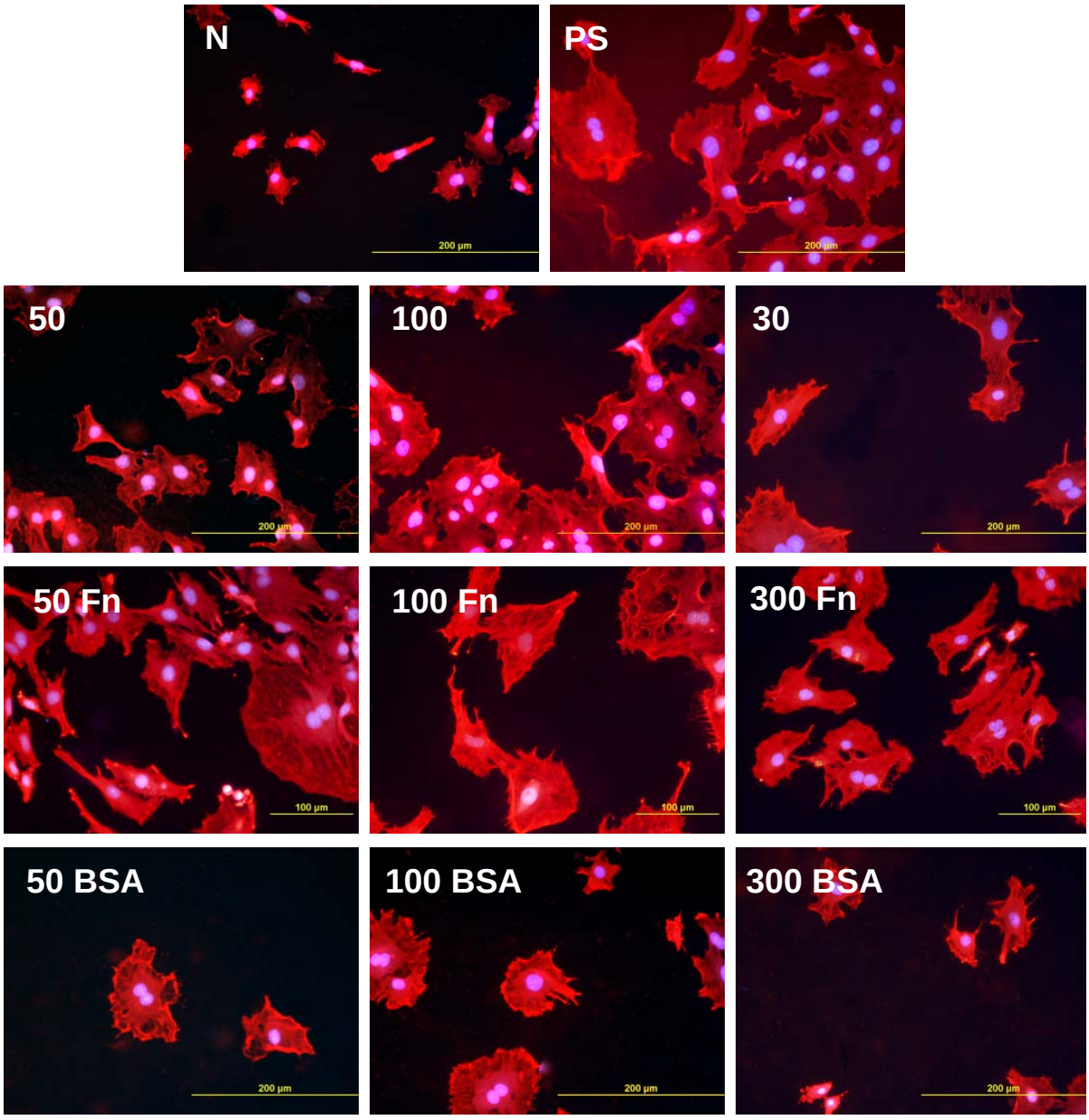

Figure 6. Morphology of rat aortic smooth muscle cells in two-day-old cultures in a serum-supplemented medium on LDPE in non-treated form (**N**), treated with plasma for 50, 100 or 300 s (**50, 100, 300**), and subsequently grafted with fibronectin (**Fn**) or bovine serum albumin (**BSA**). A standard cell culture polystyrene dish (**PS**) was used as a reference material. Cells stained with Texas Red C_2-Maleimide and Hoechst #33342. Olympus IX 51 microscope, obj. 20, DP 70 digital camera, bar 200 µm or 100 µm (Fn-grafted samples).

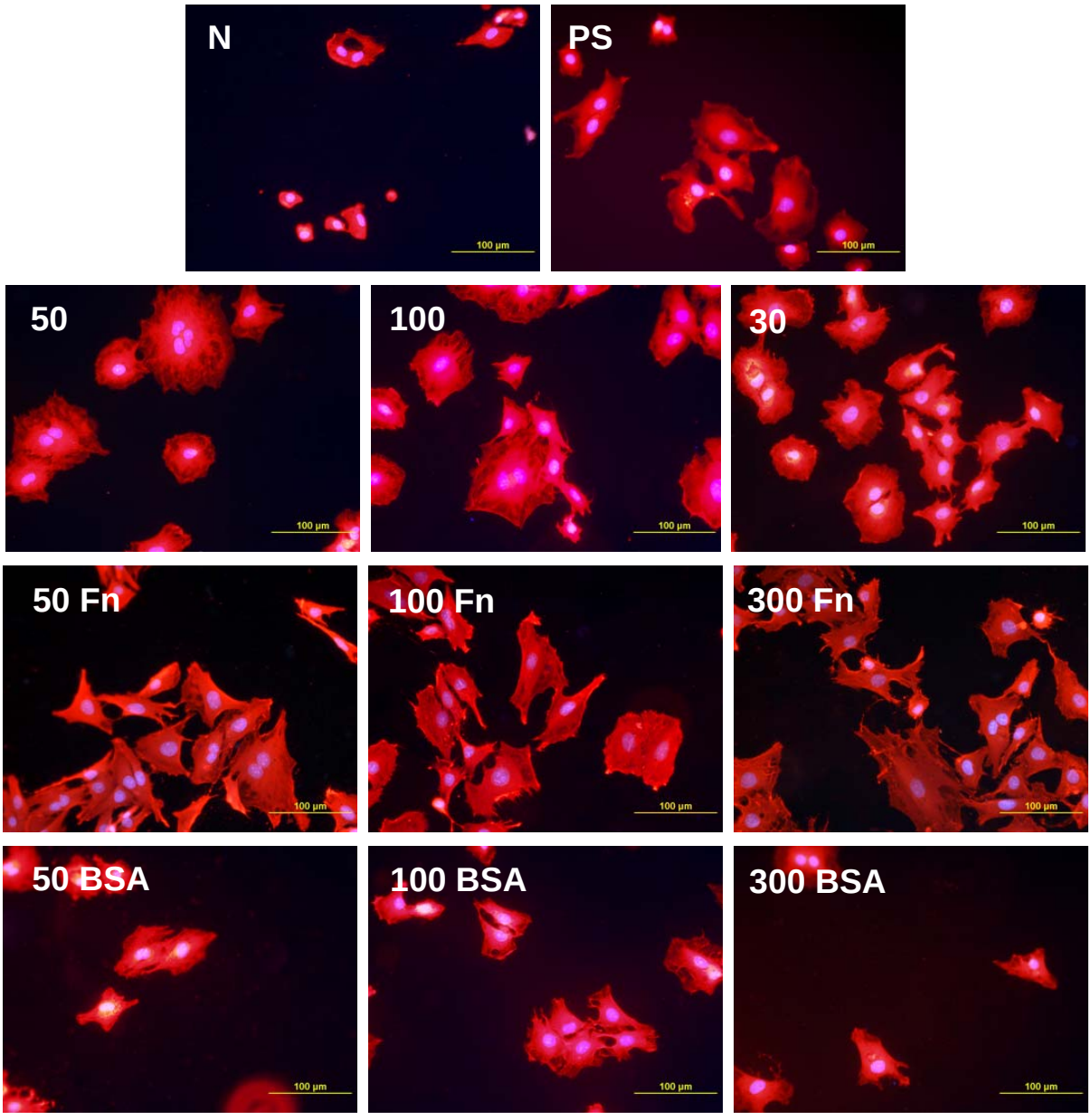

Figure 7. The size of the cell spreading area of rat aortic smooth muscle cells in two-day-old cultures in a serum-supplemented medium on (**A**) HDPE; or (**B**) LDPE in non-treated form (**N**), treated with plasma for 50, 100 or 300 s, and subsequently grafted with fibronectin (**Fn**) or bovine serum albumin (**BSA**). A standard cell culture polystyrene dish (**PS**) was used as a reference material. Mean ± S.E.M. from 32 to 95 measured cells for each experimental group. ANOVA, Student–Newman–Keuls Method. Statistical significance: ▪ $p \leq 0.05$ compared to other experimental groups, indicated by the colors of these groups above the columns.

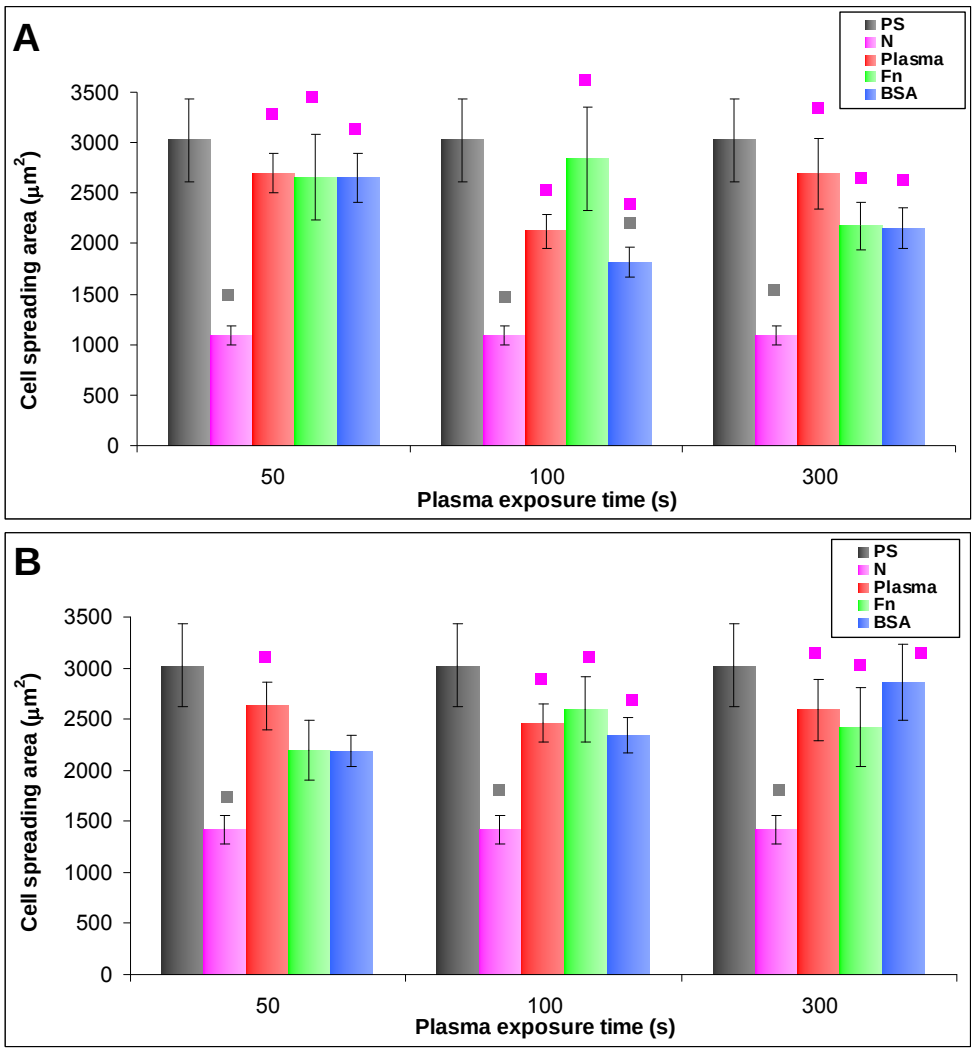

2.2.2. Cell Adhesion and Growth on LDPE and HDPE in a Serum-Free Medium

In the serum-free medium, the differences in the behavior of VSMC on the PE samples with various modifications became more apparent than in the serum-supplemented medium, and the growth dynamics of the cells revealed a different trend. From days 2 to 4 after seeding, the cell number was mostly stagnant, and on some samples it even decreased. There was an increasing tendency only between days 4 and 6 (Figure 8). This stagnancy in cell growth was most likely because there was a limited quantity of the ECM proteins normally present in fetal serum, mainly vitronectin and fibronectin, which ensure proper adhesion, spreading and subsequent growth of cells on the material

surfaces. The serum-free medium used in this study did not contain these proteins. However, cell adhesion-mediating proteins can be present on cells in small quantities even after trypsinization [36], and could be used for cell adhesion after seeding cells on the tested materials, particularly on polystyrene, non-treated PE and plasma-treated PE (on Fn-grafted PE, the Fn molecules could be used directly for cell adhesion). In addition, VSMC are able to synthesize a wide spectrum of cell adhesion-mediating ECM molecules (for a review, see [35]). This takes place especially at later culture intervals. By way of these molecules, the cells adhere to the material surface through the bonds between specific amino acid sequences in these molecules and cell adhesion receptors on the cell membrane, e.g., integrins. Another way for cells to attach to the tested materials is by so-called weak chemical bonding, *i.e.*, hydrogen bonding, electrostatic, polar or ionic interactions between various molecules on the cell membrane and functional chemical groups on the polymers, *etc*., but this type of binding does not transfer specific signals into the cells and does not ensure their survival, growth and other functions (for a review, see [3,4,9,37,38]).

Figure 8. Growth curves of rat aortic smooth muscle cells cultured in a serum-free medium on (**A–C**) HDPE; or (**D–F**) LDPE in non-treated form (**N**), treated with plasma for 50, 100 or 300 s (**50, 100, 300**), and subsequently grafted with fibronectin (**Fn**) and bovine serum albumin (**BSA**). A standard cell culture polystyrene dish (**PS**) was used as a reference material. Mean ± S.E.M. from 20 measurements (day 2 and 4) or 4 measurements (day 6). ANOVA, Student–Newman–Keuls Method. Statistical significance: * $p \leq 0.05$ compared to the non-modified LDPE or HDPE.

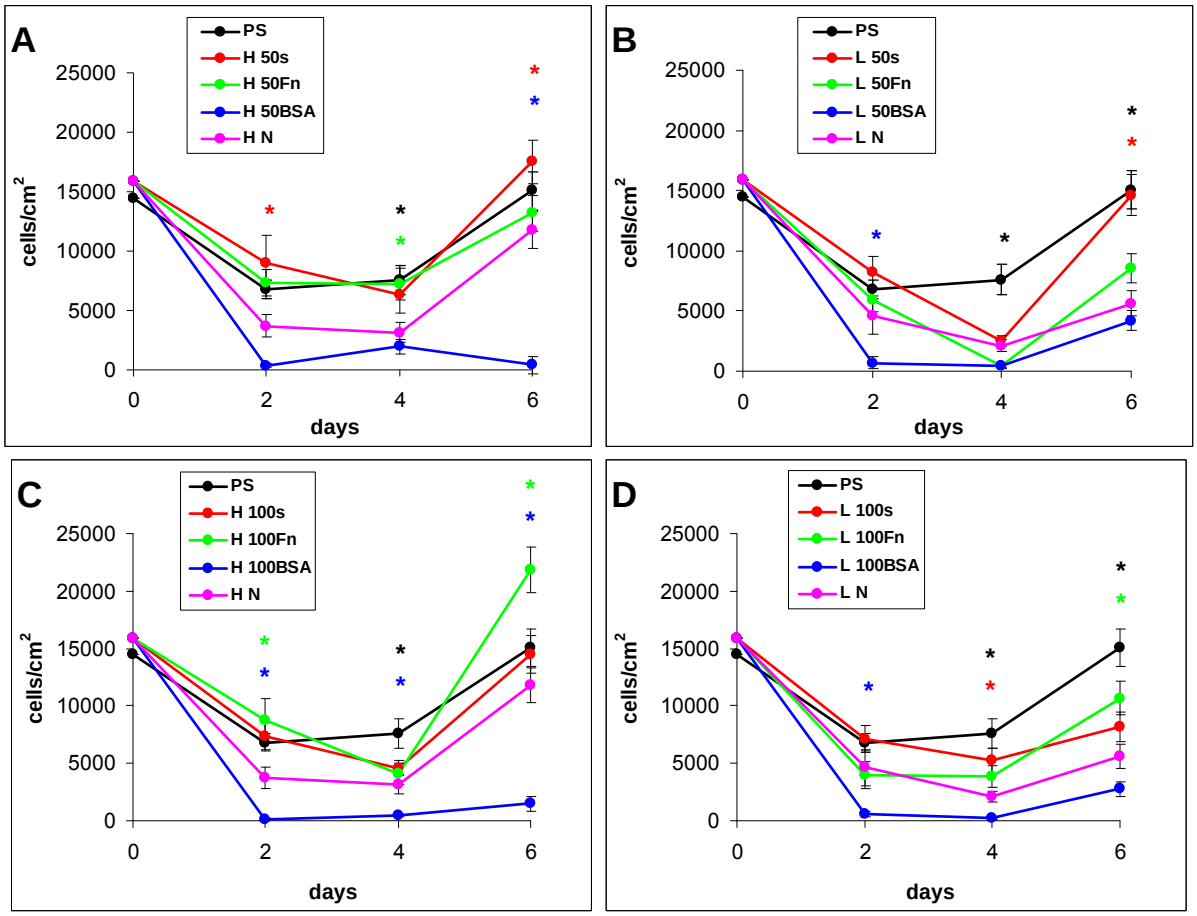

Figure 8. *Cont.*

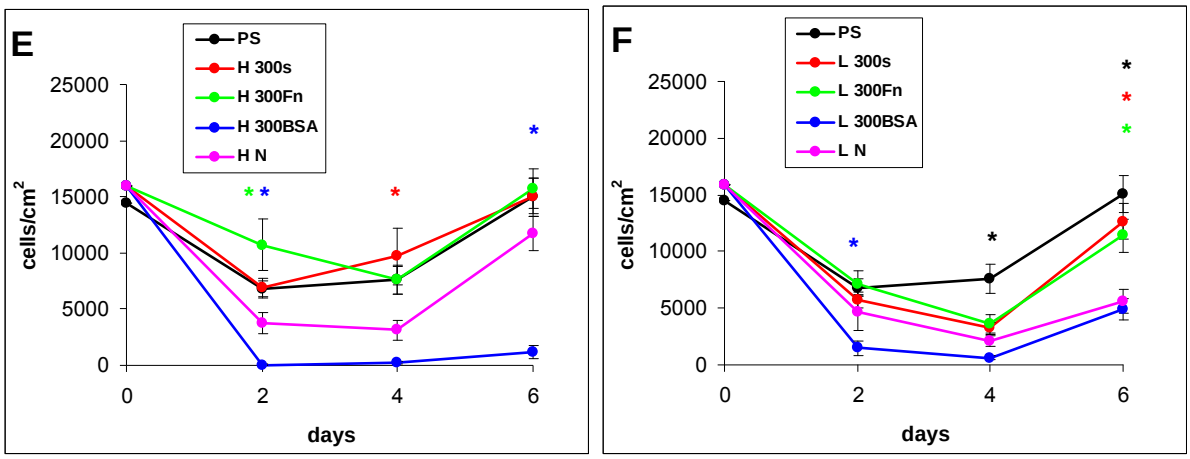

As early as on day 2 after seeding, the cell non-adhesive properties of BSA were completely revealed in the serum-free medium. This effect of albumin was more apparent on HDPE, where the cell densities ranged from 37 to 367 cells·cm^{-2}, while on LDPE the values were slightly higher (551 to 1470 cells·cm^{-2}; Figure 8). Accordingly, the cell spreading was also the lowest on the HDPE samples (Figures 9). The cells mainly assumed a spherical shape on these surfaces, while on the other samples, even on the BSA-grafted LDPE samples (Figure 10) or on non-treated LDPE and HDPE, the cell morphology was spindle-shaped or polygonal.

From day 4 to 6, the cell numbers increased slightly, probably by preferential cell growth on sites with discontinuity of the albumin layer, or secondary deposition of cell adhesion-mediating ECM proteins synthesized by the cells themselves on the albumin layer. On day 6, this increase was slightly more apparent on BSA-grafted LDPE (from 2800 to 4900 cells·cm^{-2}) than on BSA-grafted HDPE (from 400 to 1500 cells·cm^{-2}). However, these samples still displayed the lowest cell population densities, irrespective of plasma exposure time (Figure 8).

The effects of the grafted fibronectin were controversial. We expected high adhesion and subsequent growth of cells on these samples, due to specific receptor-mediated adhesion of cells to Fn grafted on the plasma-activated polymer surfaces. However, the cell densities in general on all Fn-grafted samples were similar to the values on the plasma-irradiated surfaces, or on the control polystyrene culture dishes. Among all Fn-grafted samples, the weakest proliferation was observed on LDPE irradiated with plasma for 50 s (L 50Fn; Figure 8B), where the cell population density on day 4 was lower than on non-treated LDPE, and as low as on the BSA-grafted samples. On day 6, the number of cells increased, but was still significantly lower than on PS or LDPE irradiated for 50 s (Figure 8B). The relatively low cell proliferation activity on Fn-grafted polyethylene could be explained by relatively low quantity of the Fn molecules attached to the polymer surface. As indicated by XPS, the concentrations of nitrogen and sulfur, which are indicators of the presence of protein molecules, were relatively low on the Fn-grafted surfaces in comparison with the BSA-grafted surfaces, particularly on the LDPE samples. On LDPE, the concentration of S was even on the limit of detection (Table 1). In accordance with this, the intensity of fluorescence of antibody-labeled Fn grafted to plasma-activated surfaces is lower than in the case of albumin [Figure 2(A,B)] In addition, the pictures indicate less homogeneous distribution of fibronectin on these surfaces compared to

albumin (Figure 2C). Also the geometrical conformation of Fn, which is more important for cell binding than the absolute amount of Fn immobilized on the material surface ([39], for a review, see [3,4,9]) could be less appropriate for binding by the cell adhesion receptors. In spite of this, the cells on the Fn-grafted HDPE and LDPE samples were of similar polygonal morphology as the cells on the control polystyrene and plasma-irradiated samples (Figures 9 and 10), although their spreading area was often smaller (Figure 11).

Figure 9. Morphology of rat aortic smooth muscle cells in two-day-old cultures in a serum-free medium on HDPE in non-treated form (**N**), treated with plasma for 50, 100 or 300 s (**50, 100, 300**), and subsequently grafted with fibronectin (**Fn**) and bovine serum albumin (**BSA**). A standard cell culture polystyrene dish (**PS**) served as a reference material. Cells stained with Texas Red C_2-Maleimide and Hoechst #33342. Olympus IX 51 microscope, obj. 20, DP 70 digital camera, bar 200 μm or 100 μm (Fn-grafted samples).

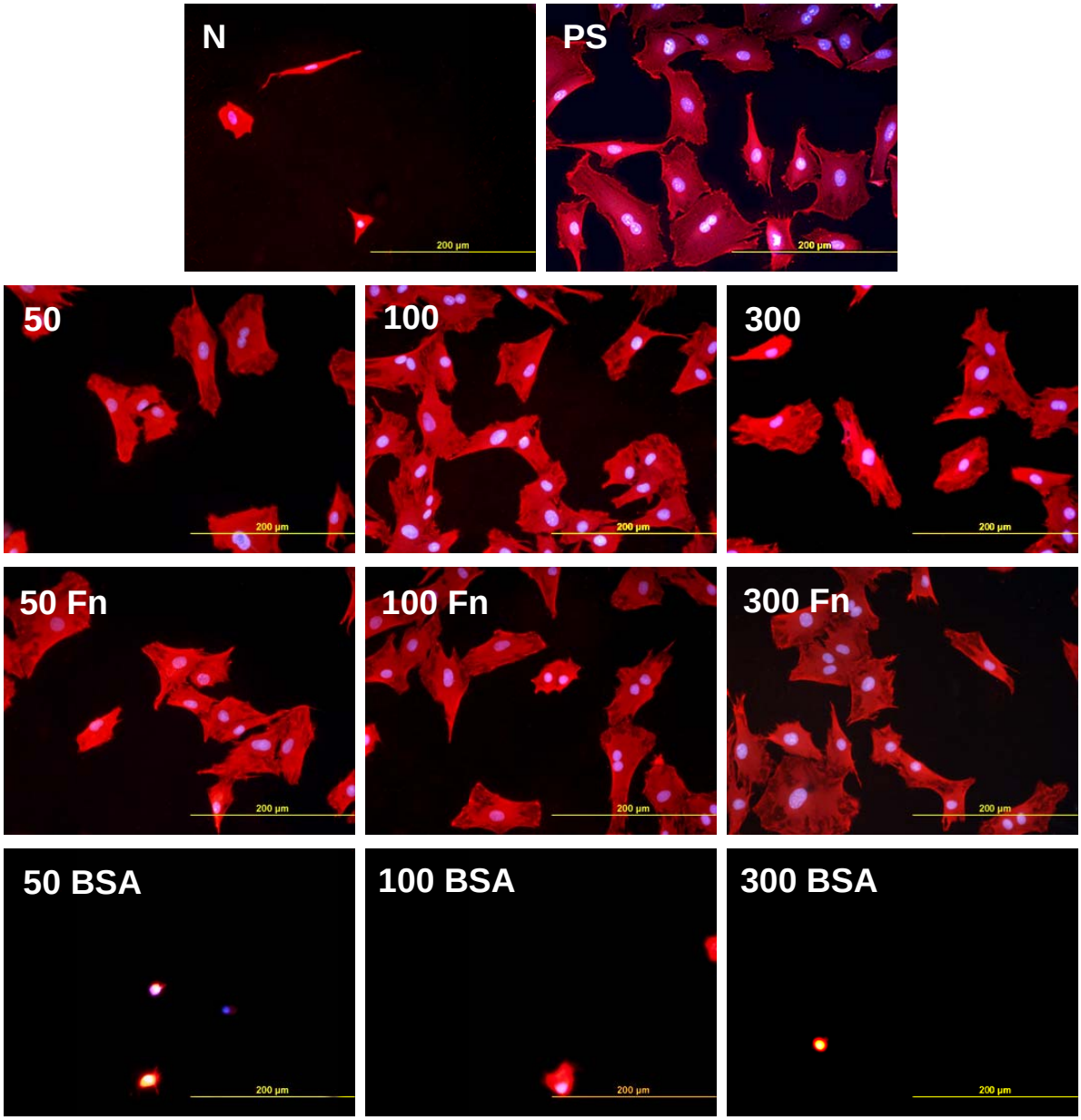

Figure 10. Morphology of rat aortic smooth muscle cells in two-day-old cultures in a serum-free medium on LDPE in non-treated form (**N**), treated with plasma for 50, 100 or 300 s (**50, 100, 300**), and subsequently grafted with fibronectin (**Fn**) and bovine serum albumin (**BSA**). A standard cell culture polystyrene dish (**PS**) was used as a reference material. Cells stained with Texas Red C_2-Maleimide and Hoechst #33342. Olympus IX 51 microscope, obj. 20, DP 70 digital camera, bar 200 μm or 100 μm (Fn-grafted samples).

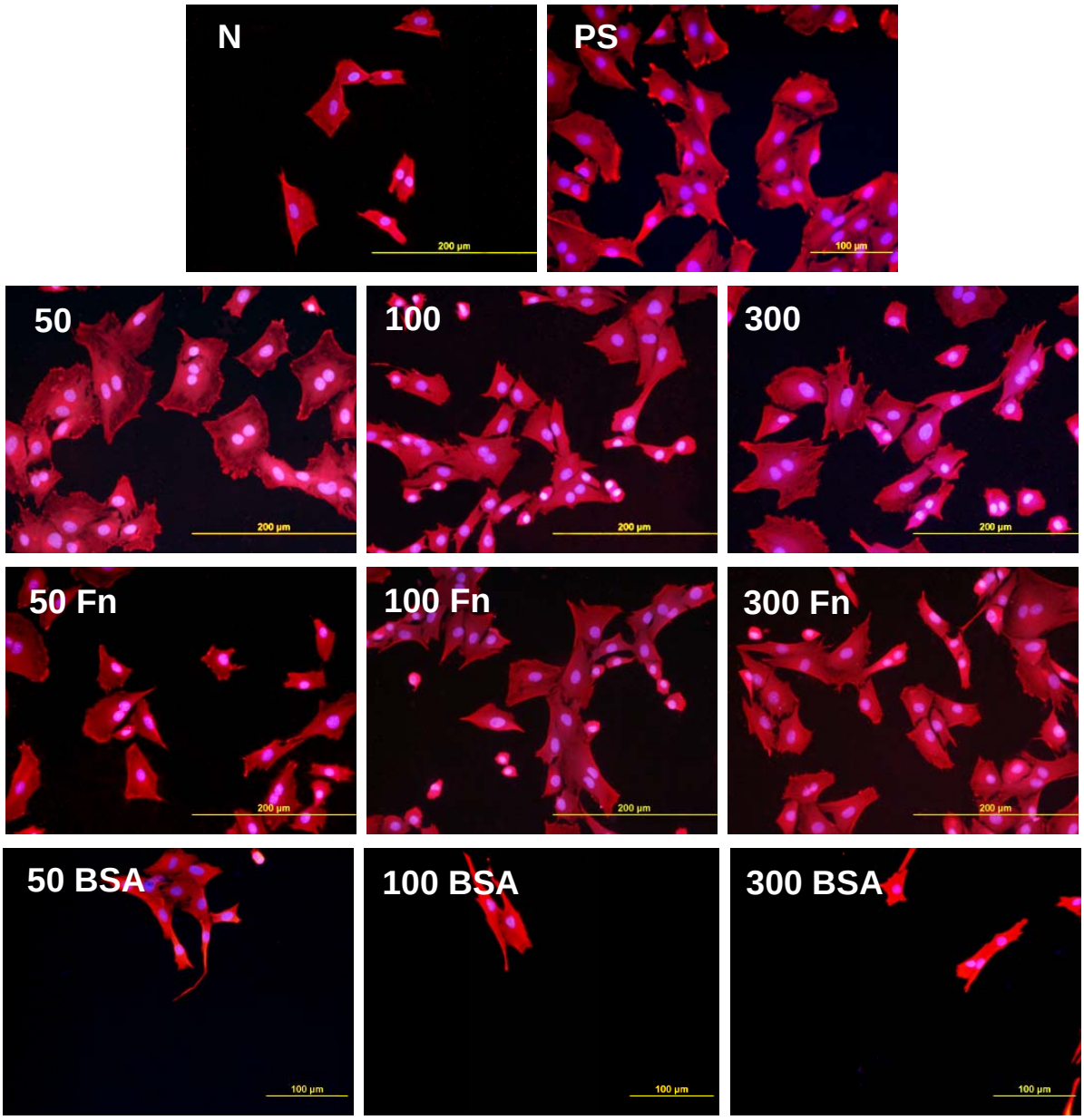

Figure 11. The size of the cell spreading area of rat aortic smooth muscle cells in two-day-old cultures in a serum-free medium on (**A**) HDPE; or (**B**) LDPE in non-treated form (**N**), treated with plasma for 50, 100 or 300 s, and subsequently grafted with fibronectin (**Fn**) or bovine serum albumin (**BSA**). A standard cell culture polystyrene dish (**PS**) was used as a reference material. Mean ± S.E.M. from 4 to 269 measured cells. ANOVA, Student–Newman–Keuls Method. Statistical significance: ▪ $p \leq 0.05$ compared to other experimental groups, indicated by the colors of these groups above the columns.

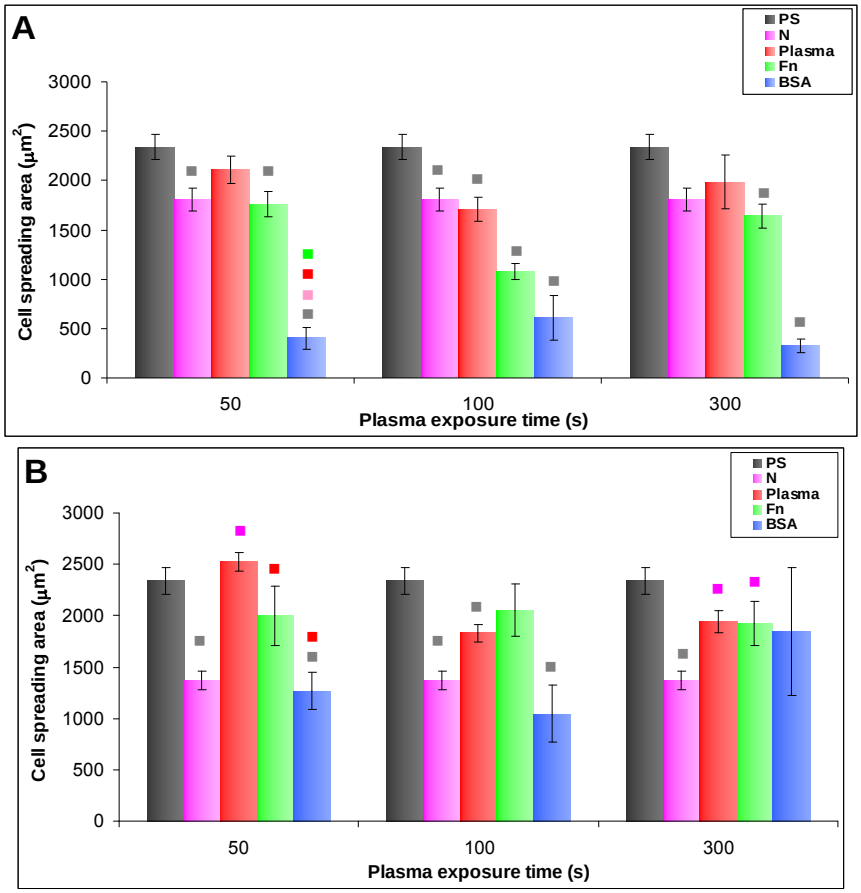

3. Experimental Section

3.1. Preparation and Modification of Polymer Samples

The experiments were carried out on high-density and low-density polyethylene foils (HDPE and LDPE, both purchased from Granitol A. S., Moravsky Beroun, Czech Republic). The HDPE foils were of the Microten M*S type (thickness 40 µm, density 0.951 g·cm^{-3}, melt flow index 0.14 g·10 min^{-1}), and the LDPE was of the Granoten S*H type (thickness 40 µm, specific density 0.922 g·cm^{-3}, melt flow index 0.8 g·10 min^{-1}). Both types of polyethylene were cut into circular samples (diameter 2 cm) using a metallic perforator (punch).

The samples were then treated by an Ar^+ plasma discharge (gas purity 99.997%) using a Balzers SCD 050 device (BalTec Maschinenbau AG, Pfäffikon, Switzerland). The time of exposure was 50, 100 or 300 s, and the discharge power was 3 W. Immediately after the plasma treatment, the samples were immersed in solutions of two components of fetal bovine serum (FBS), namely 2 wt.% of

fibronectin (Fn, Sigma-Aldrich, St. Louis, MI, USA, Cat. No. F2006) or 2 wt.% of bovine serum albumin (BSA, Sigma-Aldrich, Cat. No. A9418), both diluted in phosphate-buffered saline (PBS; Sigma-Aldrich, Cat. N° P4417). The samples were incubated for 24 h at room temperature (RT) in order to allow grafting of biomolecules to the plasma activated polymer surface. The samples were then rinsed in distilled water, air-dried at RT and stored in an air atmosphere for three weeks in order to reorganize and stabilize their surface structure, particularly the orientation of the oxidized structures on the material surface (the so-called aging period) [23].

3.2. Characterization of the Physical and Chemical Properties of the Polymer Surface

3.2.1. Surface Wettability

The sessile water drop contact angle was measured by See System reflection goniometry (Masaryk University, Brno, Czech Republic). The volume of the water drop on the polymer surface was 8 µL. The contact angle was measured after an aging period of three weeks. For each experimental group, three samples were used, and on each sample, 10 measurements were performed in different regions homogeneously distributed on the sample surface. The contact angle was presented as mean ± Standard Deviation (S.D.) from 30 measurements. Statistical analyses were performed using SigmaStat (Jandel Corp., Las Vegas, NV, USA). Multiple comparison procedures were performed by the One Way Analysis of Variance (ANOVA), Student–Newman–Keuls method. p values equal to or less than 0.05 were considered significant.

3.2.2. Chemical Composition of the Polymer Surface

The presence of grafted biomolecules, *i.e.*, fibronectin (Fn) and bovine serum albumin (BSA), on the HDPE and LDPE surface was determined by X-ray photoelectron spectroscopy (XPS, Omicron Nanotechnology ESCAProbeP spectrometer) and by immunofluorescence staining. XPS determined the concentration (at.%) of the main elements present in the grafted polymer surface (oxygen, nitrogen, sulfur and carbon).

For immunofluorescence staining, specific primary antibodies against Fn (monoclonal anti-human fibronectin, Sigma-Aldrich, Cat. No. F0791) and BSA (monoclonal anti-bovine serum albumin, Sigma–Aldrich, Cat. No. B2901, St. Louis, MI, USA) were used. The primary antibodies were diluted in PBS to a concentration of 1:200 and were applied to HDPE and LDPE samples modified in plasma and subsequently grafted with Fn or BSA, and were also applied to the non-modified control samples. The samples were incubated with primary antibodies overnight at 4 °C. After rinsing with PBS, the secondary antibody, *i.e.*, goat anti-mouse F(ab')2 fragments of IgG (H + L), conjugated with Alexa Fluor® 488 (Molecular Probes, Invitrogen, Cat. No. A11017, Eugene, OR, USA), was diluted in PBS to a ratio of 1:400, and was added to the samples for 1 hour at RT. As a staining control, the secondary antibody was applied to samples which had not been treated with the primary antibodies before. The samples were then rinsed twice in PBS. The fluorescence intensity was evaluated from 10 randomly chosen fields homogeneously distributed on the material surface using an epifluorescence microscope (IX 51, Olympus, Tokyo, Japan, obj. 10×) equipped with a digital camera (DP 70, Olympus, Tokyo, Japan) at the same exposure time for all experimental groups (1.2 s). The data was presented as mean

± Standard Error of Mean (S.E.M.). Statistical analyses were performed using SigmaStat (Jandel Corp., Las Vegas, NV, USA). Multiple comparison procedures were made by the One Way Analysis of Variance (ANOVA), Student–Newman–Keuls method. *p* values equal to or less than 0.05 were considered significant.

3.2.3. Surface Morphology and Roughness

The changes in surface morphology and roughness were determined by Atomic Force Microscopy (AFM), using a CP II device (VEECO, Santa Barbara, CA, USA) working in tapping mode. We used an RTESPA-CP Si probe, with spring constant 20–80 N/m. By repeated measurements of the same region (1 × 1 μm), it was proven that the surface morphology did not change after three consecutive scans. The mean roughness value (R_a) represents the arithmetic average of the deviations from the center plane of the sample.

3.3. Cells and Culture Conditions

The samples were sterilized with 70% ethanol for 1 hour, placed into 12-well polystyrene multidishes (TPP, Switzerland, well diameter 2.2 cm) and then air-dried for 12 hours in a sterile environment. The materials were fixed to the bottom of the culture wells by plastic rings in order to prevent them floating in the cell culture media, and were seeded with vascular smooth muscle cells (VSMC), derived from the rat aorta by an explantation method [40]. The cells were used in passage 3. Each well contained 50,000 cells (*i.e.*, about 14,000 cells·cm^{-2}) and 3 mL of serum-supplemented or serum-free medium. The serum-supplemented medium was Dulbecco's modified Eagle's Medium (DMEM; Sigma, Ronkonkoma, NY, USA, Cat. N° D5648) with 10% of fetal bovine serum (FBS; Sebak GmbH, Aidenbach, Germany) and 40 μg/mL of gentamicin (LEK, Ljubljana, Slovenia), and the serum-free medium was SmGM®-2 Smooth Muscle Growth Medium-2 (SmBM; Lonza, Walkersville, MD, USA, Cat. N° CC-3182), supplemented with epithelial growth factor (EGF), fibroblast growth factor-B (FGF-B) and insulin according to the manufacturer's protocol. The serum-free medium was used in order to enhance the effects on cell adhesion and growth of the chemical functional groups and the biomolecules grafted onto the material surface. This influence can be masked, at least partly, by secondary adsorption of various biomolecules on the polymer surface from the serum supplement of the culture medium. The cells were then cultured for 2, 4 and 6 days in a cell incubator at 37 °C and in a humidified atmosphere with 5% of CO_2 in the air.

3.4. Evaluation of the Cell Number and Cell Spreading Area

On days 2 and 4 after seeding, the cells were rinsed with PBS, fixed with cold 70% ethanol (−20 °C, 5 min), and then stained for 2 hours at RT with a combination of the following fluorescent dyes diluted in PBS: Hoechst #33342 nuclear dye (Sigma-Aldrich, 5 μg·mL^{-1}) and Texas Red C_2-maleimide membrane dye (Molecular Probes, Invitrogen, Carlsbad, CA, USA, Cat. No. T6008, 20 ng·mL^{-1}). The cells were counted on microphotographs taken in 10 randomly chosen fields homogeneously distributed on the material surface, using an epifluorescence microscope (Olympus IX 51, Japan, obj. 20×) equipped with a digital camera (DP 70, Japan). This approach was not applicable on day 6,

when the cells on some samples reached confluence and started to overlap each another. The cells were therefore detached from the materials by a trypsin-EDTA solution (Sigma-Aldrich, Cat. N° T4174) and were counted using a Vi-CELL XR Analyser (Beckman Coulter, Brea, CA, USA). The pictures taken on day 2 after seeding were also used for measuring the size of the cell spreading area using Atlas software (Tescan Ltd., Brno, Czech Republic).

Two independent samples were used for each time interval and experimental group. Non-modified polyethylene (HDPE or LDPE) and standard cell culture polystyrene wells were used as reference materials.

The quantitative data was presented as mean ± S.E.M. Statistical analyses were performed using SigmaStat (Jandel Corp., USA). Multiple comparison procedures were made by the One Way Analysis of Variance (ANOVA), Student–Newman–Keuls method. p values equal to or less than 0.05 were considered significant. The cell numbers obtained on day 2, 4 and 6 after seeding were expressed as the number of cells per cm^2 (*i.e.*, the cell population density), and were used for constructing growth curves.

4. Conclusions

Modification of polyethylene (HDPE and LDPE) with Ar^+ plasma and grafting with fibronectin and albumin influenced the cell colonization of both polymers. In the serum-supplemented medium, all modifications improved the adhesion and growth of vascular smooth muscle cells in comparison with the unmodified polymer. The cells reached higher final population densities, on an average, on LDPE than on HDPE. In the serum-free medium, grafting with albumin did not support cell colonization due to its non-adhesive properties, which were not masked by the adsorption of cell adhesion-mediating molecules, normally present in the serum. The beneficial effect of the plasma treatment on cell adhesion and growth could be attributed to the formation of new-oxidized structures on the polymer surface, an increase in surface wettability, changes in surface morphology, and enhanced nanoscale roughness. Changes in the physical and chemical properties of the material surface were more apparent on HDPE than on LDPE. The intensity of the fluorescence indicated that HDPE also contained higher quantities of grafted fibronectin and albumin.

Acknowledgments

This study was supported by the Grant Agency of the Czech Republic (grant No. P108/12/G108 “Center of Excellence”). Robin Healey (Czech Technical University, Prague) is gratefully acknowledged for his language revision of the manuscript.

References

1. Zhang, W.J.; Liu, W.; Cui, L.; Cao, Y. Tissue engineering of blood vessel. *J. Cell. Mol. Med.* **2007**, *11*, 945–957.
2. Yu, H.; Wagner, E. Bioresponsive polymers for nonviral gene delivery. *Curr. Opin. Mol. Ther.* **2009**, *2*, 165–178.
3. Bacakova, L.; Filova, E.; Rypacek, F.; Svorcik, V.; Stary, V. Cell adhesion on artificial materials for tissue engineering. *Physiol. Res.* **2004**, *53*, S35–S45.

4. Bacakova, L.; Svorcik, V. Cell colonization control by physical and chemical modification of materials. In *Cell Growth Processes: New Research*; Kimura, D.; Ed.; Nova Science Publishers, Inc.: Hauppauge, NY, USA, 2008; pp. 5–56.
5. Bozukova, D.; Pagnoulle, C.; de Pauw-Gillet, M.C.; Desbief, S.; Lazzaroni, R.; Ruth, N.; Jerome, R.; Jerome, C. Improved performances of intraocular lenses by poly(ethylene glycol) chemical coatings. *Biomacromolecules* **2007**, *8*, 2379–2387.
6. Poulsson, A.H.; Mitchell, S.A.; Davidson, M.R.; Johnstone, A.J.; Emmison, N.; Bradley, R.H. Attachment of human primary osteoblast cells to modified polyethylene surfaces. *Langmuir* **2009**, *25*, 3718–3727.
7. Granke, K.; Ochsner, J.L.; McClugage, S.G.; Zdrahal, P. Analysis of graft healing in a new elastomer-coated vascular prosthesis. *Cardiovasc. Surg.* **1993**, *1*, 254–261.
8. Bacakova, L.; Filova, E.; Kubies, D.; Machova, L.; Proks, V.; Malinova, V.; Lisa, V.; Rypacek, F. Adhesion and growth of vascular smooth muscle cells in cultures on bioactive RGD peptide-carrying polylactides. *J. Mater. Sci. Mater. Med.* **2007**, *18*, 1317–1323.
9. Bacakova, L.; Filova, E.; Parizek, M.; Ruml, T.; Svorcik, V. Modulation of cell adhesion, proliferation and differentiation on materials designed for body implants. *Biotechnol. Adv.* **2011**, *29*, 739–767.
10. Heitz, J.; Svorcik, V.; Bacakova, L.; Rockova, K.; Ratajova, E.; Gumpenberger, T.; Bäuerle1, D.; Dvorankova, B.; Kahr, H.; Graz, I.; *et al.* Cell adhesion on polytetrafluoroethylene modified by UV-irradiation in an ammonia atmosphere. *J. Biomed. Mater. Res.* **2003**, *67A*, 130–137.
11. Svorcik, V.; Rybka, V.; Hnatowicz, V.; Smetana, K., Jr. Structure and biocompatibility of ion beam modified polyethylene. *J. Mater. Sci. Mater. Med.* **1997**, *8*, 435–440.
12. Bacakova, L.; Mares, V.; Lisa, V.; Svorcik, V. Molecular mechanisms of improved adhesion and growth of an endothelial cell line cultured on polystyrene implanted with fluorine ions. *Biomaterials* **2000**, *21*, 1173–1179.
13. Walachova, K.; Svorcik, V.; Bacakova, L.; Hnatowicz, V. Colonization of ion-modified polyethylene with vascular smooth muscle cells *in vitro*. *Biomaterials* **2002**, *23*, 2989–2996.
14. Wang, Y.; Lu, L.; Zheng, Y.; Chen, X. Improvement in hydrophilicity of PHBV films by plasma treatment. *J. Biomed. Mater. Res. A* **2006**, *76*, 589–595.
15. Tajima, S.; Chu, J.S.; Li, S.; Komvopoulos, K. Differential regulation of endothelial cell adhesion, spreading, and cytoskeleton on low-density polyethylene by nanotopography and surface chemistry modification induced by argon plasma treatment. *J. Biomed. Mater. Res. A* **2008**, *84*, 828–836.
16. Pareta, R.A.; Reising, A.B.; Miller, T.; Storey, D.; Webster, T.J. Increased endothelial cell adhesion on plasma modified nanostructured polymeric and metallic surfaces for vascular stent applications. *Biotechnol. Bioeng*. **2009**, *103*, 459–471.
17. Zhang, Y.; Tanner, K.E.; Gurav, N.; di Silvio, L. *In vitro* osteoblastic response to 30 vol% hydroxyapatite-polyethylene composite. *J. Biomed. Mater. Res. A* **2007**, *81*, 409–417.
18. Homaeigohar, S.S.; Shokrgozar, M.A.; Javadpour, J.; Khavandi, A.; Sadi, A.Y. Effect of reinforcement particle size on *in vitro* behavior of beta-tricalcium phosphate-reinforced high-density polyethylene: A novel orthopedic composite. *J. Biomed. Mater. Res. A* **2006**, *78*, 129–138.

19. Fouad, H.; Elleithy, R. High density polyethylene/graphite nano-composites for total hip joint replacements: processing and in vitro characterization. *J. Mech. Behav. Biomed. Mater.* **2011**, *4*, 1376–1383.
20. Oldinski, R.A.; Ruckh, T.T.; Staiger, M.P.; Popat, K.C.; James, S.P. Dynamic mechanical analysis and biomineralization of hyaluronan-polyethylene copolymers for potential use in osteochondral defect repair. *Acta Biomater*. **2011**, *7*, 1184–1191.
21. Mokal, N.J.; Desai, M.F. Calvarial reconstruction using high-density porous polyethylene cranial hemispheres. *Indian J. Plast. Surg.* **2011**, *44*, 422–431.
22. Caldwell, R.A.; Woodell, J.E.; Ho, S.P.; Shalaby, S.W.; Boland, T.; Langan, E.M.; LaBerge, M. *In vitro* evaluation of phosphonylated low-density polyethylene for vascular applications. *J. Biomed. Mater. Res.* **2002**, *62*, 514–524.
23. Svorcik, V.; Kolarova, K.; Slepicka, P.; Mackova, A.; Novotna, M.; Hnatowicz, V. Modification of surface properties of high and low density polyethylene by Ar plasma discharge. *Polym. Degrad. Stabil*. **2006**, *91*, 1219–1225.
24. Svorcik, V.; Kasalkova, N.; Slepicka, P.; Zaruba, K.; Kral, V.; Bacakova, L. Cytocompatibility of Ar + plasma treated and Au nanoparticle-grafted PE. *Nucl. Instrum. Meth. B* **2009**, *267*, 1904–1910.
25. Parizek, M.; Kasalkova, N.; Bacakova, L.; Slepicka, P.; Lisa, V.; Blazkova, M.; Svorcik, V. Improved adhesion, growth and maturation of vascular smooth muscle cells on polyethylene grafted with bioactive molecules and carbon particles. *Int. J. Mol. Sci.* **2009**, *10*, 4352–4374.
26. Parizek, M.; Kasalkova, N.S.; Bacakova, L.; Lisa, V.; Svindrych, Z.; Slepicka, P.; Svorcik, V. Adhesion, growth and maturation of vascular smooth muscle cells on low-density polyethylene grafted with bioactive substance. *J. Biomed. Biotechnol.* **2013**, in press.
27. Kella, N.K.; Kang, Y.J.; Kinsella, J.E. Effect of oxidative sulfitolysis of disulfide bonds of bovine serum albumin on its structural properties: A physiochemical study. *J. Protein Chem.* **1988**, *7*, 535–548.
28. Pankov, R.; Yamada, K.M. Fibronectin at a glance. *J. Cell Sci.* **2002**, *15*, 3861–3863.
29. Xiao, Y.; Isaacs, S.N. Enzyme-linked immunosorbent assay (ELISA) and blocking with bovine serum albumin (BSA)—Not all BSAs are alike. *J. Immunol. Methods* **2012**, *384*, 148–151.
30. Bacakova, L.; Lisa, V.; Kubinova, L.; Wilhelm, J.; Novotna, J.; Eckhart, A.; Herget, J. UV light—Irradiated collagen III modulates expression of cytoskeletal and surface adhesion molecules in rat aortic smooth muscle cells *in vitro*. *Virchows Arch.* **2002**, *440*, 50–62.
31. Kim, K.S.; Ryu, C.M.; Park, C.S.; Sur, G.S.; Park, C.E. Investigation of crystallinity effects on the surface of oxygen plasma treated low density polyethylene using X-ray photoelectron spectroscopy. *Polymer* **2003**, *44*, 6287–6295.
32. Kowalczynska, H.M.; Nowak-Wyrzykowska, M.; Szczepankiewicz, A.A.; Dobkowski, J.; Dyda, M.; Kaminski, J.; Kołos, R. Albumin adsorption on unmodified and sulfonated polystyrene surfaces, in relation to cell-substratum adhesion. *Colloids Surf. B Biointerfaces* **2011**, *84*, 536–544.
33. Brynda, E.; Houska, M.; Jirouskova, M.; Dyr, J.E. Albumin and heparin multilayer coatings for blood-contacting medical devices. *J. Biomed. Mater. Res*. **2000**, *51*, 249–257.
34. Yamazoe, H.; Tanabe, T. Drug-carrying albumin film for blood-contacting biomaterials. *J. Biomater. Sci. Polym. Ed.* **2010**, *21*, 647–657.

35. Glukhova, M.A.; Koteliansky, V.E. Integrins, cytoskeletal and extracellular matrix proteins in developing smooth muscle cells of human aorta. In *The Vascular Smooth Muscle Cell: Molecular and Biological Responses to the Extracellular Matrix*; Schwartz, S.M., Mecham, R.P., Eds.; Academic Press Inc.: Waltham, MA, USA, 1995; pp. 37–79.
36. Shipley, G.D.; Ham, R.G. Multiplication of Swiss 3T3 cells in a serum-free medium. *Exp. Cell Res*. **1983**, *146*, 249–260.
37. Maroudas, N.G. Sulphonated polystyrene as an optimal substratum for the adhesion and spreading of mesenchymal cells in monovalent and divalent saline solutions. *J. Cell. Physiol.* **1976**, *90*, 511–520.
38. Curtis, A.S.G.; Forrester, J.V.; McInnes, C.; Lawrie, F. Adhesion of cells to polystyrene surfaces. *J. Cell. Biol.* **1983**, *97*, 1500–1506.
39. Burmeister, J.S.; Vrany, J.D.; Reichert, W.M.; Truskey, G.A. Effect of fibronectin amount and conformation on the strength of endothelial cell adhesion to HEMA/EMA copolymers. *J. Biomed. Mater. Res*. **1996**, *30*, 13–22.
40. Bacakova, L.; Mares, V.; Lisa, V.; Bottone, M.G.; Pellicciari, C.; Kocourek, F. Sex-related differences in the migration and proliferation of rat aortic smooth muscle cells in short and long term culture. *In Vitro Cell. Develop. Biol. Anim.* **1997**, *33*, 410–413.

JOURNAL OF
biomaterials
applications

Journal of Biomaterials Applications
2015, Vol. 29(6) 837–853

DOI: 10.1177/0885328214546647
jba.sagepub.com
SAGE

Effects of fiber density and plasma modification of nanofibrous membranes on the adhesion and growth of HaCaT keratinocytes

Marketa Bacakova[1], Frantisek Lopot[2], Daniel Hadraba[1,2], Marian Varga[3], Margit Zaloudkova[4], Denisa Stranska[5], Tomas Suchy[4] and Lucie Bacakova[1]

Abstract

It may be possible to regulate the cell colonization of biodegradable polymer nanofibrous membranes by plasma treatment and by the density of the fibers. To test this hypothesis, nanofibrous membranes of different fiber densities were treated by oxygen plasma with a range of plasma power and exposure times. Scanning electron microscopy and mechanical tests showed significant modification of nanofibers after plasma treatment. The intensity of the fiber modification increased with plasma power and exposure time. The exposure time seemed to have a stronger effect on modifying the fiber. The mechanical behavior of the membranes was influenced by the plasma treatment, the fiber density, and their dry or wet state. Plasma treatment increased the membrane stiffness; however, the membranes became more brittle. Wet membranes displayed significantly lower stiffness than dry membranes. X-ray photoelectron spectroscopy (XPS) analysis showed a slight increase in oxygen-containing groups on the membrane surface after plasma treatment. Plasma treatment enhanced the adhesion and growth of HaCaT keratinocytes on nanofibrous membranes. The cells adhered and grew preferentially on membranes of lower fiber densities, probably due to the larger area of void spaces between the fibers.

Keywords

Tissue engineering, nanofibers, needle-less electrospinning, fiber density, plasma-treatment, skin, fibroblasts, keratinocytes

Introduction

Nanofibrous materials are being applied increasingly in tissue engineering, because they can better mimic the structure and the mechanical properties of the fibrous components of natural extracellular matrix (ECM). For this reason, they are considered to be attractive for adhesion and growth of cells. In comparison with conventionally used flat or microstructured surfaces, nanostructured materials enhance the cell–material interaction. This enhancement is due to the adsorption of cell adhesion-mediating ECM molecules from biological fluids in an appropriate spatial conformation. This enables good accessibility of specific sites on these molecules for cell adhesion receptors.[1,2] In addition, nanofibrous membranes are advantageous for constructing the bilayer of skin cells – fibroblasts and keratinocytes – in skin tissue engineering. These membranes will separate the two cell types, but due to the porous structure of the material, they will ensure their physical and humoral communication. The layer of fibroblasts can therefore serve as a nutrient feeder for keratinocytes, similarly as in the native skin.[3]

[1]Institute of Physiology, Academy of Sciences of the Czech Republic, Czech Republic
[2]Dept. of Anatomy and Biomechanics, Faculty of Physical Education and Sport, Charles University, Czech Republic
[3]Institute of Physics, Academy of Sciences of the Czech Republic, Czech Republic
[4]Institute of Rock Structure and Mechanics, Academy of Sciences of the Czech Republic, Czech Republic
[5]Elmarco Ltd., Czech Republic

Corresponding author:
Marketa Bacakova, MSc., Institute of Physiology, Academy of Sciences of the Czech Republic, Videnska 1083, Prague 4 14220, Czech Republic.
Email: marketa.bacakova@biomed.cas.cz

Various artificial and natural materials have been adopted for constructing a scaffold that is suitable for treating skin injuries. Artificial skin substitutes can be made from poly(HEMA),[4,5] polybuthylene terephthalate,[6] nylon,[7,8] hydroxybuthyrate,[9] polycaprolactone,[10] polylactic acid,[11] and polyglycolic acid, or their copolymers.[11,12] The most widely tested and applied natural biomaterials are chitosan,[13,14] collagen,[15] hyaluronic acid,[16,17] and chondroitin sulfate.[18] For our study, we used biodegradable nanofibrous membranes made from polylactic acid (polylactide, PLA). The main advantage of biodegradable materials is their slow resorption in the organism, associated with a decrease in molecular weight. In the case of PLA, this decrease in molecular weight is due to the transformation of polylactide to lactide by hydrolysis of aliphatic ester linkages in PLA molecules.[19] The lactic acid is further metabolized and removed from the body as carbon monoxide and water. Due to their ability to be resorbed, biodegradable materials are finally replaced by regenerated tissue.

Generally, materials used in tissue engineering have to be biocompatible. They cannot be cytotoxic, mutagenic or immunogenic, and their physical and chemical properties should correspond to the properties of the replaced tissue. In advanced tissue engineering, biomaterials used for bioartificial tissue substitutes should be bioactive. They should act as analogs of the natural ECM, i.e. they should promote and control the adhesion, proliferation, differentiation, and maturation of cells, and thus the regeneration of damaged tissue. The bioactivity of materials depends strongly on the physical and chemical properties of the material surface, such as its wettability, electrical charge and conductivity, mechanical properties, surface roughness, and topography. For this reason, some materials do not have optimal physical and chemical properties for fully replacing damaged tissue, and need further modification. These further modifications should enhance cell–material interaction and the formation of new tissue (for a review, see Bacakova et al.[1] and Bacakova and Svorcik[20]).

The physical and chemical properties of the polymer surface can be altered by several physical techniques, particularly by irradiation with an ion beam,[21,22] ultraviolet light,[23] or exposure to plasma discharge.[24–26] The common feature of these techniques is the induction of polymer chain degradation, the creation of free radicals and double bonds, and crosslinking of the polymer chains. These radicals react with oxygen in the ambient atmosphere, leading to the formation of oxygen-containing chemical groups on the material surface (i.e. carbonyl, carboxyl, hydroxyl, ether, or ester groups). The oxygen groups enhance the polarity and wettability of the material and promote the adsorption of cell adhesion-mediating molecules in an appropriate spatial conformation. This enhancement guarantees that the specific amino acid sequences of these molecules are well accessible for cell adhesion receptors – integrins. In addition, conjugated double bonds between carbon atoms are created during plasma treatment, and this influences the electrical conductivity of the polymer surface. It is known that electrical conductivity of the material surface enhances cell colonization.[1]

In this study, we have evaluated the adhesion and growth of immortal human HaCaT keratinocytes on polylactide nanofibrous membranes modified in oxygen plasma under various process conditions. The aim of this modification was to create a nanofibrous membrane surface that would be attractive for keratinocyte colonization. These plasma-treated membranes could be used as temporary carriers for skin cells during wound healing after skin injury.

Materials and methods

Preparation and modification of nanofibrous membranes

Poly(L-lactide) (PLA, Ingeo™ Biopolymer 4032D) was purchased from NatureWorks, Minnetonka, MN, USA. The molecular parameters of the polymer material, determined by size exclusion chromatography, were $M_w = 124{,}000$ g/mol and $M_n = 48{,}000$ g/mol.[27] A 7 wt.% solution of PLA in a mixture of chloroform, dichloroethane, and ethyl acetate was used for the electrospinning process. First, the polymer was diluted only in chloroform, and the two other solvents were added after the dilution. The polymer solution was made electrically conductive with the use of tetraethylammonium bromide, which was first dissolved in dimethylformamide at a concentration of 3 wt.%, and then 3 g of this solution was added to 100 g of the PLA solution.

Nanofibrous membranes were prepared using the novel Nanospider needleless electrospinning technology (NS Lab 500, Elmarco Ltd., Liberec, Czech Republic). The process conditions were: electrode distance: 180 mm; voltage: 60–10 kV; the spinning electrode rotated at 4 rpm; relative humidity: 25–30%, and room temperature. The membranes were prepared at various fiber densities, i.e. the area weight of the prepared nanofibers was 5, 9, 16, 30 g/m^2.

The membranes were then treated by oxygen plasma discharge using the Phantom LT CCP-RIE System, Trion Technology, in two steps. The first step was performed in etching regime with discharge power from 25 W to 100 W, exposure time from 10 s to 120 s, pressure 150 mTorr, and oxygen flow 20 cm^3/s. The first step was followed by blowing the device (second step)

for 30 s with pressure 150 mTorr and argon flow 20 cm^3/s. The nanofibrous membranes were treated on both sides.

Characterization of the physical and chemical properties of nanofibrous membranes

The morphology of the nanofibrous membranes before and after plasma treatment was evaluated by scanning electron microscopy (SEM) using an SEM field-emission gun operating in secondary electron mode (FE-SEM Tescan MIRA3). The diameter of the fibers and the area of the void spaces among the fibers were measured on the SEM images using Atlas software (Tescan Ltd., Brno, Czech Republic). The diameter of the fibers was expressed in nm, and the area of the void spaces among the fibers was expressed in μm^2.

The mechanical properties of the plasma-treated membranes (plasma power 75 W, exposure time 30 s) and the non-treated nanofibrous membranes of two different fiber densities (5 and 16 g/m^2) were tested in the dry state (at normal air atmosphere and room temperature) and in the wet state, i.e. in phosphate-buffered saline (PBS) at room temperature. The uniaxial tensile test was selected because the SEM images had proven isotropy of the materials. The rectangular strips of constant geometry were fastened into the tensile instrument and were stretched at a constant speed of 6 mm/s. The elongation and force were recorded by sampling frequency 20 Hz and calculated into the stress–strain curve. Finally, the Young's modulus was established for each material and condition. The difference between the groups was statistically evaluated by the two-sample *t*-test.

The chemical composition (concentration of oxygen, carbon, and C–C, C–O, C = O) of the membrane surface before and after plasma treatment was determined by X-ray photoelectron spectroscopy (XPS), using an ADES-400 photoelectron spectrometer (V. G. Scientific, UK). The concentration was determined in at.% with sensitivity 0.1 at.%.

Cell culture on nanofibrous membranes

The nanofibrous membranes were cut into square samples (1 × 1 cm) and were fixed in CellCrown inserts (Scaffdex Ltd., Finland). The samples were sterilized in 70% ethanol for 30 min. After sterilization, the samples were rinsed in distilled water for one week to remove residues of the solvents used during the preparation of the nanofibers. The water was changed every day.

The samples fixed in CellCrown inserts were inserted into polystyrene 24-well cell culture plates (TPP, Switzerland, well diameter 1.5 cm). The samples were seeded with human HaCaT keratinocytes[28] (CLS Cell Lines Service) at a density of 30,000 cells per well (i.e. 15,000 cells/cm^2) into 1.5 ml Dulbecco's modified Eagle's Medium (DMEM; Sigma-Aldrich, USA) with 10% of fetal bovine serum (FBS; Sebak GmbH, Germany) and 40 μg/ml of gentamicin (LEK, Slovenia). The cells were cultivated for 1, 3, and 7 days in a cell incubator at 37°C and in a humidified atmosphere with 5% of CO_2 in the air.

Evaluation of cell growth and mitochondrial activity on nanofibrous membranes

On days 1, 3, and 7 after seeding, the number of initially adhered cells and their subsequent growth on the samples were estimated by the amount of cellular DNA, using the Picogreen dsDNA assay kit (Invitrogen®). The assay is based on measurements of the fluorescence of Picogreen, a nucleic acid stain for quantitating double-stranded DNA in solution. The assay was carried out according to the manufacturer's protocol. Fluorescence was measured with the Synergy HT Multi-Mode Reader (BioTek, USA) in black 96-well cell culture plates (96 F Nunclon delta, Black microwell Si) with excitation wavelength of 480 nm and emission wavelength of 520 nm. The amount of cell DNA on each sample in all time intervals was expressed in ng/cm^2.

Cell mitochondrial activity was measured on days 3 and 7 after seeding by the XTT Cell Proliferation Kit (Roche). The principle of this assay is the cleavage of yellow tetrazolium salt XTT to form a water-soluble orange formazan salt by metabolic cell activity. The formazan dye was then quantified by monitoring the absorbance using a spectrophotometer (ELISA reader). The assay was performed according to the manufacturer's protocol. The absorbance was measured using the VersaMax ELISA Microplate Reader (Molecular Devices Corporation, Sunnyvale, CA, USA) in 96-well cell culture plates (F 96 Maxisorp (NUNC –Imunoplate)) with wavelength 470 nm.

For both analyses (the Picogreen assay and the XTT assay), the samples of nanofibrous membranes were moved into unused fresh 24-well plates to avoid the influence of the cells adhered to the bottom of the wells.

Evaluation of cell adhesion, spreading and morphology on nanofibrous membranes

The spreading and the morphology of the cells on the PLA nanofibers were visualized on days 1, 3, and 7 after seeding by staining the cells with a combination of fluorescent dyes (Hoechst #33342 cell nucleus dye, Texas Red C_2-maleimide cell membrane dye) and with scanning electron microscopy (SEM).

For staining the cells with a combination of fluorescent dyes, the cells were rinsed with PBS, fixed with cold (−20°C) 70% ethanol for 10 min, and then stained for 1 h at room temperature with a combination of fluorescent dyes diluted in PBS: Hoechst #33342 cell nucleus dye (Sigma-Aldrich, 5 μg/ml) and Texas Red C_2-maleimide cell membrane dye (Molecular Probes, Invitrogen, 20 ng/ml). Images documenting the cell morphology were taken using an epifluorescence microscope (Olympus IX 51, Japan, obj. 10×) equipped with a digital camera (DP 70, Japan). The cell cluster spreading area (in μm^2) was measured in the images, which were acquired under a fluorescence microscope using Atlas software (Tescan Ltd., Brno, Czech Republic) on day 3 after seeding.

For SEM, the samples were fixed in 3% glutaraldehyde in PBS, washed with PBS buffer, dehydrated in an ethanol series (25, 50, 75, 90, 96 and 100% v/v), transferred to 100% (v/v) acetone, and dried in a BALZERS CPD 010 critical-point dryer. The samples were then sputter-coated with gold and examined with a Quanta 450 scanning electron microscope (FEI, USA). The high vacuum mode was used, and images were taken on an ETD – Everhart-Thornley detector in secondary electrons mode at high voltage 20 kV, magnification 2000×.

Immunofluorescence staining of molecules participating in cell differentiation, adhesion, and spreading

On day 3 after seeding, the presence of the following markers in HaCaT cells was evaluated:

- keratin 5 and filaggrin as early and middle differentiation markers of keratinocytes
- $ß_1$ integrin, an important molecule for mediating cell–material interaction
- vinculin, an integrin-associated protein present in focal adhesion plaques
- F-actin, an important component of the cell cytoplasmic cytoskeleton associated with focal adhesion plaques.

For immunofluorescence staining of keratin 5, filaggrin, $ß_1$ integrin, and vinculin, the cells were rinsed in PBS and fixed with cold (−20°C) 70% ethanol for 10 min at room temperature. After fixation, the cells were treated with 1% bovine serum albumin in PBS containing 0.05% Triton X-100 (Sigma-Aldrich) for 20 min, and then with 1% Tween (Sigma-Aldrich) in PBS for 20 min at room temperature to block nonspecific binding sites and to permeabilize the cell membrane. The cells were then incubated with the following primary monoclonal antibodies overnight at 4°C: basal cell cytokeratin (RCK 103, mouse, MUbioBV), anti-filaggrin (rabbit, Sigma-Aldrich), anti-$ß_1$ integrin (mouse, Millipore), and anti-vinculin (mouse, Sigma-Aldrich). All antibodies were diluted in PBS to a concentration of 1:200. After rinsing with PBS, the secondary antibody, i.e. goat anti-mouse F(ab′)2 fragments of IgG (H + L) or goat anti-rabbit F(ab′)2 fragments of IgG (H + L), conjugated with Alexa Fluor® 488 (Molecular Probes, Invitrogen), was diluted in PBS to a ratio of 1:400 and applied to the samples for 1 h at room temperature in the dark. The cells were rinsed with PBS and scanned using a Leica TCS SPE DM2500 upright confocal microscope, obj. 63 × / 1.3 NA oil.

F-actin, an important component of the cell cytoplasmic cytoskeleton, was stained with phalloidin conjugated with TRITC (Sigma-Aldrich) diluted in PBS to a final concentration of 5 μg/ml for 1 h at room temperature, after rinsing the cells in PBS and fixation with 70% ethanol (−20°C, 10 min). The actin cytoskeleton was imaged using a Leica TCS SPE DM2500 upright confocal microscope, obj. 63 ×/1.3 NA oil.

Statistics

If not stated otherwise in the text above, the quantitative data are presented as mean ± standard error of mean (S.E.M.) or as mean ± standard deviation (SD) from three independent samples for each experimental group and time interval. Statistical significance was evaluated using the analysis of variance, Student–Newman–Keuls method. Values of $p \leq 0.05$ were considered as significant.

Results

Physical and chemical properties of polylactide nanofibrous membranes

The morphology of nanofibrous membranes of four different fiber densities (5 g/m^2, 9 g/m^2, 16 g/m^2, and 30 g/m^2), and the potential fiber modification and degradation after plasma treatment were investigated by scanning electron microscopy (SEM). The nanofibrous membranes consisted of mostly straight and randomly oriented fibers. The thickest fibers were measured on membranes with density of fibers 30 g/m^2 in the non-treated state and also in the plasma-treated state. The area of the void spaces between fibers decreased with the density of the fibers. After plasma treatment, the fiber diameter did not change, or increased slightly and insignificantly; however, the area of the void spaces between the fibers decreased significantly (Table 1).

The SEM images show significant modification of the nanofibers after plasma treatment. The membranes

Table 1. Morphological parameters of PLA membranes of various fiber densities (5 g/m^2, 9 g/m^2, 16 g/m^2 and 30 g/m^2) before and after plasma treatment.

Treatment	Density of fibers (g/m^2)	5	9	16	30
	Fibers				
Non-treated	Diameter, range (nm)	63 to 927	40 to 763	40 to 799	80 to 1073
	Diameter, mean ± S.E.M (nm)	287.0 ± 13.4	218.6 ± 10.2	271.1 ± 10.9	333.9 ± 10.4
Plasma-treated	Diameter, range (nm)	80 to 1107	63 to 701	63 to 847	80 to 1087
	Diameter, mean ± S.E.M (nm)	287.5 ± 13.2	241.5 ± 9.9	276.3 ± 12.9	339.4 ± 19.4
	Void spaces				
Non-treated	Area, range (μm2)	0.09 to 7.29	0.09 to 5.31	0.08 to 4.52	0.1 to 3.16
	Area, mean ± S.E.M (μm2)	1.64 ± 0.11	1.04 ± 0.08	0.90 ± 0.06	0.76 ± 0.05
Plasma-treated	Area, range (μm2)	0.05 to 4.68	0.1 to 3.37	0.07 to 3.57	0.04 to 2.6
	Area, mean ± S.E.M (μm2)	1.28 ± 0.10*	0.77 ± 0.05*	0.63 ± 0.05*	0.43 ± 0.03*

Note: Mean ± S.E.M. from 127 to 215 measurements (fibers) and 131 to 196 measurements (void spaces). ANOVA, Student–Newman–Keuls method. Statistical significance: *$p \leq 0.05$ in comparison with non-treated samples.

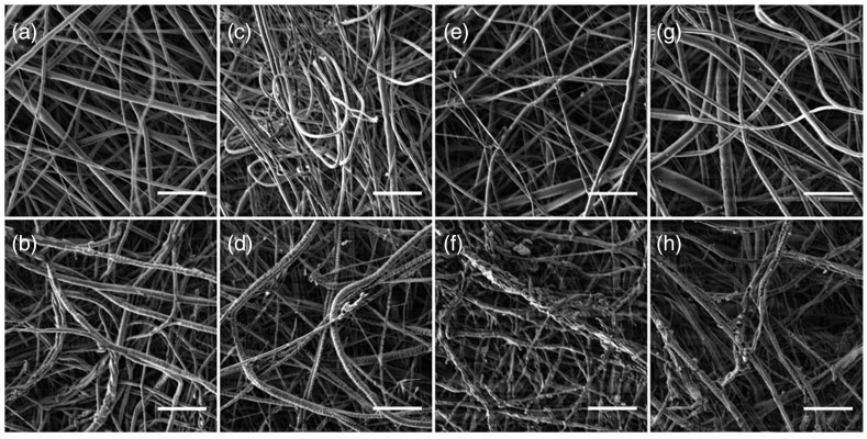

Figure 1. SEM images of PLA membranes of various fiber densities (a, b: 5 g/m^2; c, d: 9 g/m^2; e, f: 16 g/m^2; g, h: 30 g/m^2) before (a, c, e, g) and after the plasma treatment with power 75 W and exposure time 30 s (b, d, f, h). FE-SEM Tescan MIRA3, magnification 10,000×, bar 5 μm.

of higher fiber densities (16 g/m^2 and 30 g/m^2) showed more pronounced modification of the fibers than the membranes of lower fiber densities (5 g/m^2 and 9 g/m^2) after plasma treatment with power 75 W and exposure time 30 s. The fibers in membranes of higher fiber densities seemed to be more degraded than the fibers in membranes of lower fiber densities (Figure 1). We also investigated the influence of various powers and exposure times on the modification of the nanofibers. When low power (25–50 W) and a short exposure time (10–30 s) were used, there was no modification of the fibers (Figure 2). However, if higher power (50–100 W) with a longer exposure time (30–120 s) was applied, modification of the fibers was clearly apparent in the membranes (Figure 3). The SEM data show that the fiber modification increased with power and exposure time. The plasma exposure time seemed to have a more significant effect than the plasma power on fiber modification. For example, nanofibrous membranes treated in plasma with lower power 50 W for a longer exposure time 60 s (Figure 3c) or 120 s (Figure 3d) showed stronger fiber modification and also significant degradation of fibers in a deeper layer of the membrane than membranes treated with higher power 75 W (Figure 3e) or 100 W (Figure 3f) for a shorter exposure time of 30 s (Figure 3(e) and (f)).

We characterized the mechanical properties of the membranes in order to investigate the response of nanofibrous membranes to mechanical stress generated mainly by cell activity (i.e. adhesion, spreading, migration, etc.). The mechanical behavior of the membranes was influenced by fiber density (5 and 16 g/m^2),

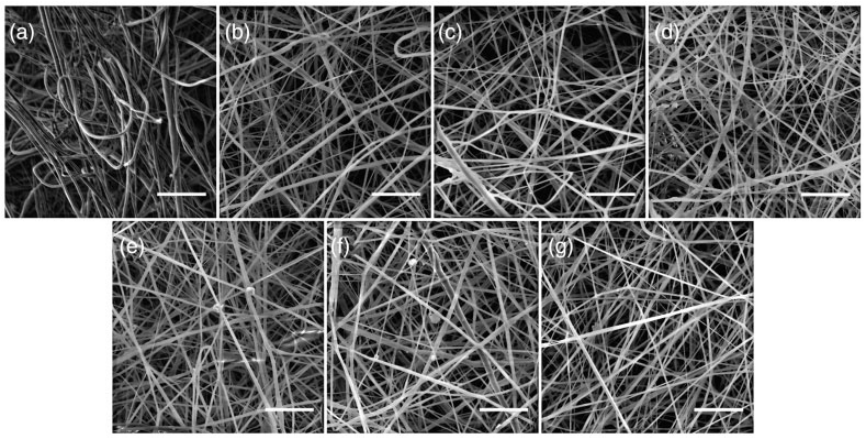

Figure 2. SEM images of PLA membranes of fiber density 9 g/m^2 before (a) and after plasma treatment with various power and exposure times: (b) 25 W 10 s, (c) 25 W 20 s, (d) 25 W 30 s, (e) 50 W 10 s, (f) 50 W 20 s, (g) 50 W 30 s. FE-SEM Tescan MIRA3, magnification 10,000×, bar 5 μm.

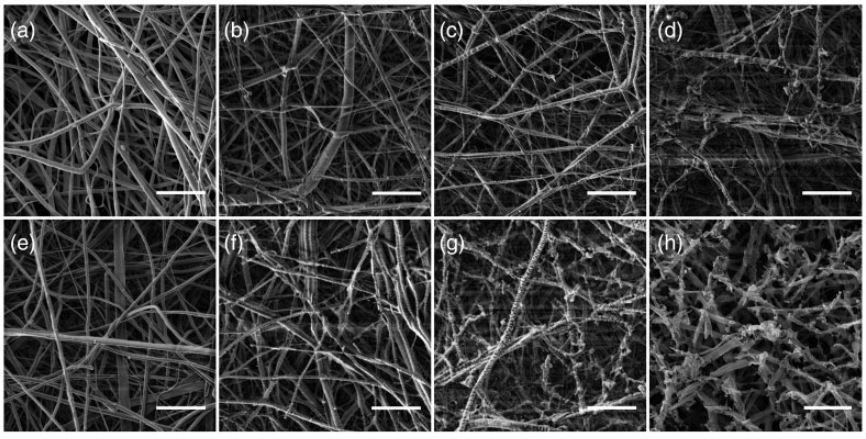

Figure 3. SEM images of PLA membranes of fiber density 16 g/m^2 before (a) and after plasma treatment with various power and exposure times: (b) 50 W 30 s, (c) 50 W 60 s, (d) 50 W 120 s, (e) 75 W 30 s, (f) 100 W 30 s, (g) 100 W 60 s, (h) 100 W 120 s. FE-SEM Tescan MIRA3, objective magnification 10,000×, bar 5μm.

by plasma treatment (plasma power 75 W, exposure time 30 s), and by the conditions under which the mechanical properties were measured (dry or wet conditions) (Table 2). The membranes are mainly used under wet conditions (e.g. immersed in a cell culture medium). These conditions are therefore more relevant for investigating the mechanical properties of the membranes. The dry non-treated membranes displayed elasto-plastic behavior with two different response areas. Young's modulus (E1) in the initial elastic area ($\varepsilon_{el} < 10$ %) and Young's modulus (E2) in the area of high deformations showed that the 16 g/m^2 and 5 g/m^2 fiber density membranes exhibit no difference in stiffness (Table 2) in both areas. The dry membranes became very brittle after plasma treatment, i.e. there was a significant increase in stiffness and no deformation response above ε_{el}, and therefore zero value for Young's modulus E2. The wet non-treated membranes displayed elasto-plastic behavior too, but with a significant decrease at ultimate tensile strength (TS). However, the maximum deformation (ε_{max}) did not change significantly compared to the dry membranes. The trend of the response to stress for the wet 5 g/m^2 plasma-treated membranes was similar to the trend for dry plasma-treated membranes; an even more brittle response with low ultimate strength and almost no deformation. The results for 16 g/m^2 indicate no significant difference between dry plasma-treated and wet plasma-treated membranes.

The changes in the surface elemental composition of the membrane after plasma treatment at various plasma power and exposure times were observed by

Table 2. Young's modulus E1 and E2, ultimate tensile strength TS and maximal deformation ε_{max} of PLA nanofiber membranes of different densities show the dependence of the mechanical response on the different treatment conditions.

	E1 (N/mm^2)			E2 (N/mm^2)			TS (N/mm^2)			ε_{max} (%)		
	Mean	SD	p	Mean	SD	p	Mean	SD	p	Mean	SD	p
5 vs	5.09	0.251	No	0.35	0.016	No	38.97	2.455	No	68.17	3.680	***
16 g/m^2	4.91	0.240		0.35	0.019		36.89	1.948		62.26	2.201	
5 TR vs	12.38	0.090	*	0.00	0.00	–	60.23	4.591	**	7.54	0.563	No
16 g/m^2 TR	7.65	0.824		0.00	0.00		37.79	3.467		8.74	0.409	
5 W vs	3.78	0.865	No	0.26	0.012	No	33.27	2.968	***	67.16	12.254	No
16 g/m^2 W	2.62	0.518		0.24	0.005		24.32	6.270		55.20	5.610	
5 TRW vs	5.68	0.725	No	0.00	0.00	–	19.65	4.270	***	4.43	1.655	–
16 g/m^2 TRW	8.88	0.842		0.00	0.00		44.81	4.283		12.03	2.045	

TR: plasma-treated membranes; W: wet membranes; p – p-value less than the significant level.
*$p < 0.001$.
**$p < 0.01$.
***$p < 0.05$
No ≥ 0.05.

Table 3. Concentration (in at.%) of carbon (C), oxygen (O) and groups C–C, C–O, C = O, determined by XPS on PLA nanofibers of fiber density 16 g/m^2 before (Pristine) and after plasma treatment with power 50–100 W and exposure time 30–120 s.

			C1s		
Sample	C (at.%)	O (at.%)	C–C	C–O	C = O
Pristine	63.8	36.2	39.1	13.9	10.8
50 W 30 s	61.5	38.5	31.7	14.0	15.9
50 W 60 s	60.0	40.0	30.8	15.4	13.7
50 W 120 s	60.0	40.0	27.7	15.3	17.0
75 W 30 s	63.1	36.9	36.8	13.4	12.9
100 W 30 s	62.5	37.5	33.9	14.3	14.3
100 W 60 s	58.7	41.3	30.2	13.3	15.2
100 W 120 s	62.5	37.5	34.5	13.9	14.1

X-ray photoelectron spectroscopy (XPS) (Table 3). The concentration of oxygen and oxygen-containing groups C–O and C = O was mainly determined, because the gas used for plasma discharge was oxygen, which incorporated into and reacted with the membrane surface. The concentration of oxygen was only slightly increased. The concentration of oxygen in non-treated (Pristine) PLA was relatively high, and thus the oxygen incorporated into the membrane surface after plasma treatment probably did not significantly influence the total oxygen concentration. The concentration of oxygen containing groups, mainly C = O, was increased after plasma treatment, but there was no significant dependence on plasma power or exposure time.

Adhesion and growth of HaCaT keratinocytes on polylactide nanofibrous membranes

Cell adhesion, growth, metabolic activity, morphology, and phenotypic maturation on PLA membranes of various fiber densities treated under the same plasma conditions. Nanofibrous membranes of different fiber densities (5, 9, 16 and 30 g/m^2) exposed to a plasma discharge with defined power 75 W and exposure time 30 s strongly influenced the cell behavior. The results indicate that in all three time intervals of cell cultivation, the amount of cell DNA, which correlates with the cell number, was significantly higher on plasma-treated membranes of almost all densities (Figure 4(a) to (c)). In addition, the XTT assay, which determined higher cell mitochondrial enzyme activity on plasma-treated membranes on day 3 after cell seeding, confirmed the positive effect of plasma treatment on cell behavior (Figure 4d). We also observed differences in the cell morphology and the cell cluster spreading area on plasma-treated and non-treated PLA membranes. At first, keratinocytes naturally adhered in clusters and then spread on the whole surface of the material. After a three-day cultivation, the cell cluster area was significantly larger on plasma-treated membranes than on non-treated membranes, with the exception of the membranes with the highest fiber density 30 g/m^2 – there was no significant difference between non-treated and plasma-treated samples (Figures 5 and 6).

The results also showed the influence of the membrane fiber densities on the amount of cell DNA, the cell population density, and the cell morphology. The amount of cell DNA was significantly higher on membranes of lower fiber densities (5 and 9 g/m^2) than on

membranes of higher fiber densities (16 and 30 g/m^2). These differences were clearer on plasma-treated membranes than on non-treated membranes (Figure 4(a) to (c)). The cell cluster area measured on day 3 was not significantly different on non-treated membranes of various fiber densities. However, on plasma-treated membranes of various fiber densities, the cells adhered in larger clusters on PLA membranes with fiber densities of 5 and 9 g/m^2 than on membranes with fiber densities of 16 and 30 g/m^2 (Figures 5 and 6).

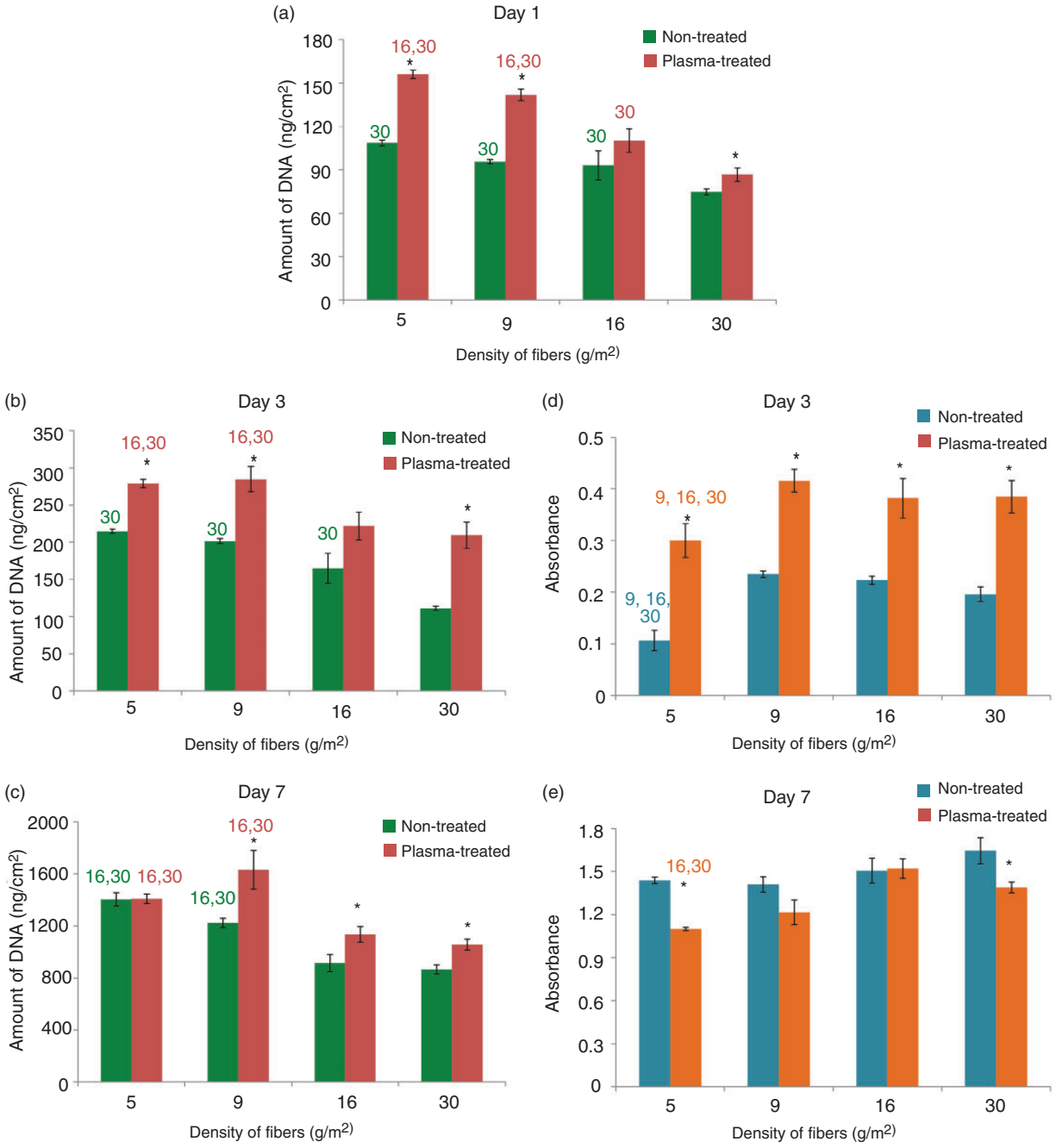

Figure 4. Amount of cell DNA measured by the Picogreen assay kit (a–c) and mitochondrial activity determined by the XTT assay kit (d, e) in human HaCaT keratinocytes on days 1, 3, and 7 on non-treated and plasma-treated (power 75 W, exposure time 30 s) PLA membranes of various fiber density (5, 9, 16, 30 g/m^2). Arithmetic means ± S.E.M. from nine measurements made on three independent samples for each experimental group and time interval. ANOVA, Student–Newman–Keuls method, statistical significance ($p \leq 0.05$): 5, 9, 16, 30 in comparison with the experimental group of the same label and * in comparison with the non-treated sample of the same fiber density.

Scanning electron microscopy, performed on days 3 and 7 after seeding (Figure 7), revealed that the HaCaT cells formed islands located predominantly on top of the nanofibrous membranes. However, in some places, fibers running through or above the cell islands were also observed. On day 7, the cell islands were considerably larger, so that large areas on the nanofibrous membranes were covered with cells, particularly in the case of the plasma-treated membranes (Figure 7(d) and (h)).

On day 3 after cell seeding, we investigated markers for the early and middle stage of keratinocyte differentiation (keratin 5, filaggrin, respectively) and molecules that play an important role in cell adhesion ($ß_1$ integrin receptors, vinculin and actin in the filamentous form, i.e. F-actin) (Figure 8). Immunofluorescence staining showed that the cells had well-developed keratin filaments on non-treated and plasma-treated membranes, and particularly on the control microscopic glass coverslips. On both types of nanofibrous membranes, keratin was located mainly at the cell periphery, while on the glass coverslips the keratin filaments were distributed throughout the entire cells. Filaggrin seemed to be present in a higher quantity on the PLA membranes than on the control glass. The cells adhered well through the adhesion receptors of the $ß_1$ integrin family on both types of PLA membranes and also on the control glass, where they showed a brighter fluorescence signal. Vinculin was distributed diffusely throughout all the cells or was organized into focal adhesion plaques, which were more apparent in the cells on the glass control. F-actin in cells on non-treated membranes, on plasma-treated membranes, and on the control glass was organized into fine fibers running in parallel between the opposite cell edges. These fibers were more apparent in the cells on the control glass, while on the nanofibrous membranes F-actin formed only tiny filaments or was distributed diffusely without forming specific fiber structures.

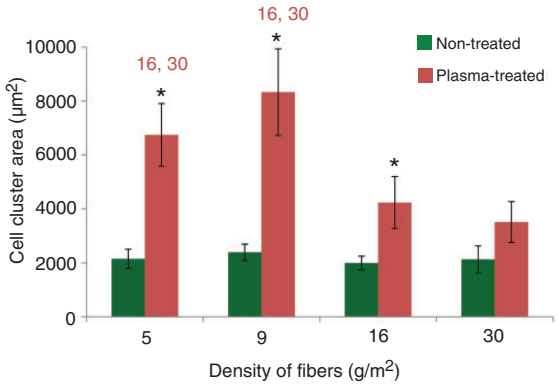

Figure 5. Cell cluster spreading area of HaCaT keratinocytes on day 3 on non-treated and plasma-treated (power 75 W, exposure time 30 s) PLA membranes of various fiber densities (5, 9, 16, 30 g/m^2), measured using Atlas software (Tescan Ltd., Brno, Czech Republic). Arithmetic means ± S.E.M. from 44 to 179 measurements. ANOVA, Student–Newman–Keuls method, statistical significance ($p \leq 0.05$): 5, 9, 16, 30 in comparison with the experimental group of the same label and * in comparison with the non-treated sample of the same fiber density.

Cell adhesion, growth, and morphology on PLA membranes treated under various plasma conditions. In this part of the study, we investigated the influence of various plasma conditions, i.e. various power and exposure times, on cell behavior. First, we treated membranes of fiber density 9 g/m^2 in plasma with power 25 W or 50 W and exposure times from 10 s to 30 s. Then we used higher power from 50 W to 100 W and longer exposure times from 30 s to 120 s. For plasma treatment with higher power and longer exposure times, we used membranes of higher fiber density (16 g/m^2), because more intense plasma treatment parameters (e.g. 100 W, 100 s) could cause serious degradation of membranes of lower fiber density.

Using lower power 25 W or 50 W and exposure times from 10 s to 30 s, we found a significantly higher

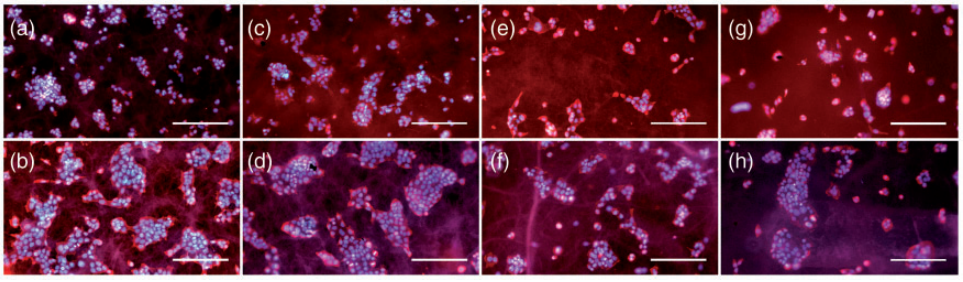

Figure 6. Morphology of human HaCaT keratinocytes after three-day cultivation on non-treated (a, c, e, g) and plasma-treated (power 75 W, exposure time 30 s; b, d, f, h) PLA membranes of various fiber densities (a, b: 5 g/m^2; c, d: 9 g/m^2; e, f: 16 g/m^2, g, h: 30 g/m^2). Cells stained with Texas Red C_2-Maleimide and Hoechst #33342. Olympus IX 51 microscope, obj. 10×, DP 70 digital camera, bar 200 μm.

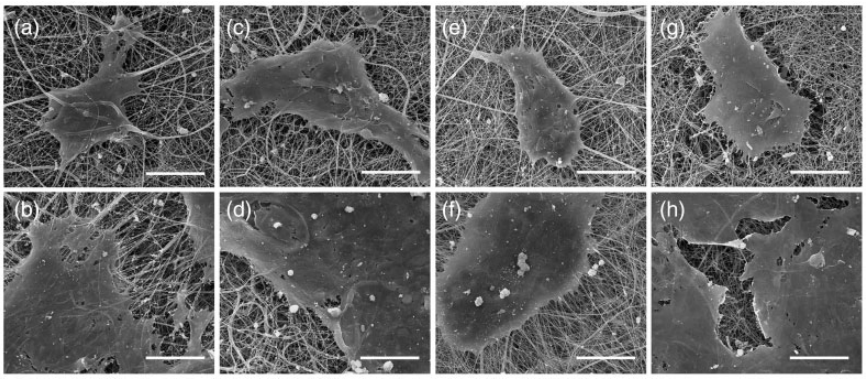

Figure 7. SEM images of the morphology of human HaCaT keratinocytes after three-day cultivation (a, c, e, g) and seven-day cultivation (b, d, f, h) on non-treated (a, b, e, f) and plasma-treated (power 75 W, exposure time 30 s; c, d, g, h) PLA membranes of fiber densities 5 g/m^2 (a–d) and 16 g/m^2 (e–h). Quanta 450 scanning electron microscope (FEI, USA), magnification 2000×, bar 40 μm.

amount of cell DNA, related to the cell number, on all plasma-treated samples than on the non-treated samples only on day 1 (Figure 9a), and on some samples on day 3 after cell seeding (Figure 9b). On day 7 after cell seeding, there were no significant differences in the amount of cell DNA between plasma-treated and non-treated membranes (Figure 9c). However, when we increased the plasma power (50–100 W) and the exposure time (30–120 s), we observed differences of higher significance between plasma-treated and non-treated membranes. On all plasma-treated samples, the cells adhered in higher population densities (as indicated by a higher amount of cell DNA) than on the non-treated samples on days 1 and 3 after seeding (Figure 9 (d) and (e)). On day 7 after seeding, significant differences in cell density between plasma-treated and non-treated membranes were found only on samples treated with power 50 W for 30 s and with power 75 W for 30 s (Figure 9f). Concerning the influence of various plasma conditions – power and exposure time – on the amount of cell DNA, we observed significant differences only among some plasma-treated samples (Figure 9(b), (d) and (f)).

The cell morphology and the size of the cell cluster spreading area on the non-treated and plasma-treated membranes showed a similar trend as the cell number (estimated by the amount of cell DNA). Using lower power (25 W, 50 W) and a shorter exposure time (10–30 s), we observed no differences between plasma-treated and non-treated samples in the cell morphology and the size of the cell cluster spreading area (Figures 10(a) and 11). However, an increase in power and exposure time led to a larger cell cluster area on plasma-treated membranes than on non-treated membranes (Figures 10(b) and 12). The difference in the cell cluster area was not significant between plasma-treated samples with various powers and exposure times.

Discussion

In the first part of the study, we investigated the influence of oxygen plasma and fiber density on the physical and chemical properties of nanofibrous membranes and on the behavior of human HaCaT keratinocytes in cultures on these materials. We observed a higher amount of cell DNA (which correlates with cell population density), higher cell metabolic activity, and larger size of the cell clusters (i.e. islands of cells) on plasma-treated membranes than on non-treated membranes. It was previously reported that plasma treatment changed the chemical and physical properties of the material surface. These alterations are induced by polymer chain degradation,[29] followed by the creation of free radicals and crosslinking between polymer chains. These primary changes lead to the formation of oxygen-containing groups. The oxidized groups enhance material surface wettability and promote adsorption of cell adhesion-mediating molecules in an appropriate spatial conformation. The specific amino acid sequences in these molecules (e.g. RGD) are therefore well accessible for cell adhesion receptors, and the cells can adhere and spread on the material by a considerably large area.[1] In our study, XPS analysis showed that the concentration of oxygen-containing groups, mainly C=O groups, had increased after the oxygen plasma treatment, which could lead to an increase in surface wettability. These changes in the physical properties of the surface could enhance cell adhesion and proliferation. Many previous studies have described a positive effect of plasma treatment on the adhesion and growth of a variety of cells. For example, Gugala and Gogolewski reported that oxygen plasma treatment increased the wettability and the concentration of oxygen on the surface of PLA porous membranes. These changes enhance the attachment and growth of osteoblasts.[30]

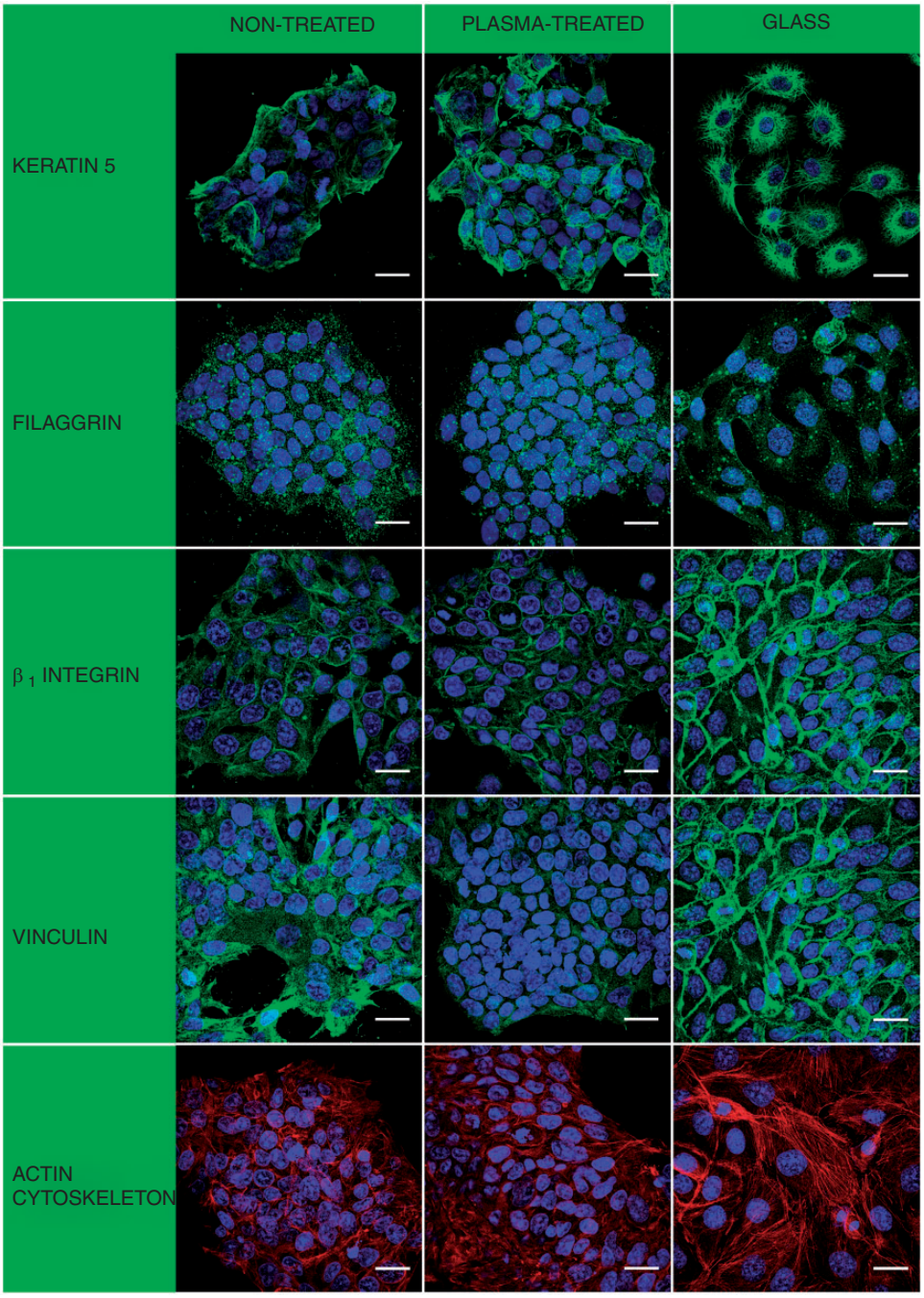

Figure 8. Immunofluorescence staining of cytokeratin 5 and filaggrin (differentiation markers of keratinocytes), $ß_1$ integrin adhesion receptors and vinculin (an integrin-associated protein of focal adhesion plaques), phalloidin staining of F-actin (filamentous cytoskeletal protein) and cell nucleus staining (Hoechst 33342, blue) in human HaCaT keratinocytes after three days of cultivation on non-treated and plasma-treated (power 75 W, exposure time 30 s) PLA membranes of fiber density 9 g/m^2 and on control microscopic glass coverslips (glass). Leica TCS SPE DM2500 confocal microscope, obj. 63 × /1.3 NA oil, bar 25 μm.

Wan *et al*. treated poly (lactide-*co*-glycolide) films (PLGA) with oxygen plasma, and they observed the incorporation of polar groups into the material surface, an increase in its hydrophilicity, and the promotion of adhesion and growth of mouse fibroblasts.[31] Jeong et al. enhanced the cellular activity of human epidermal keratinocytes and fibroblasts by exposing silk fibroin nanofibers to oxygen plasma. The adhesion of the cells was promoted by an increase in the hydrophilicity of the material surface after plasma treatment.[32] Other factors that might improve cell adhesion and growth on plasma-modified nanofibers are an increase in overall

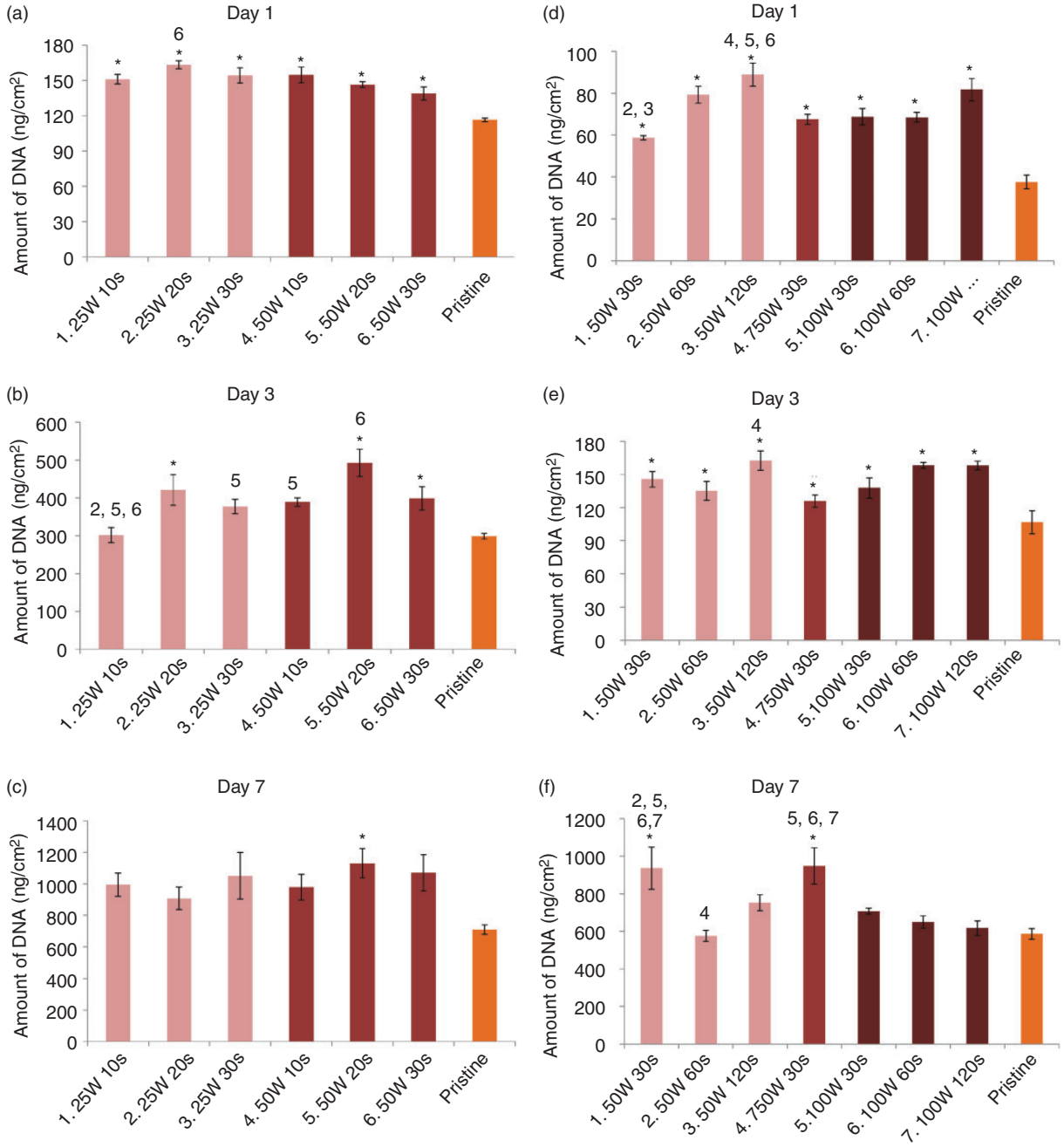

Figure 9. Amount of cell DNA measured by the Picogreen assay kit in human HaCaT keratinocytes on days 1, 3, and 7 on non-treated (Pristine) and plasma-treated (various power 25–50 W and 50–100 W, exposure time 10–30 s and 30–120 s) PLA membranes with fiber density 9 g/m^2 (a–c) and 16 g/m^2 (d–f). Arithmetic means ± S.E.M. from nine measurements made on three independent samples for each experimental group and time interval. ANOVA, Student–Newman–Keuls method, statistical significance ($p \leq 0.05$) in comparison with a certain experimental group are indicated by the number of the group above the column and * in comparison with the non-treated sample (Pristine).

material stiffness and the formation of an additional nanostructure on the material surface. Our earlier studies performed on plasma-treated polymeric foils revealed newly formed nanoscale irregularities on foils that were originally flat, due to partial degradation of the foil surface.[24,25] Also in this study, SEM imaging revealed degradation of the fiber surface, at least at higher plasma powers and longer exposure times. It has been repeatedly shown that the surface nanostructure of various materials has beneficial effects on cell

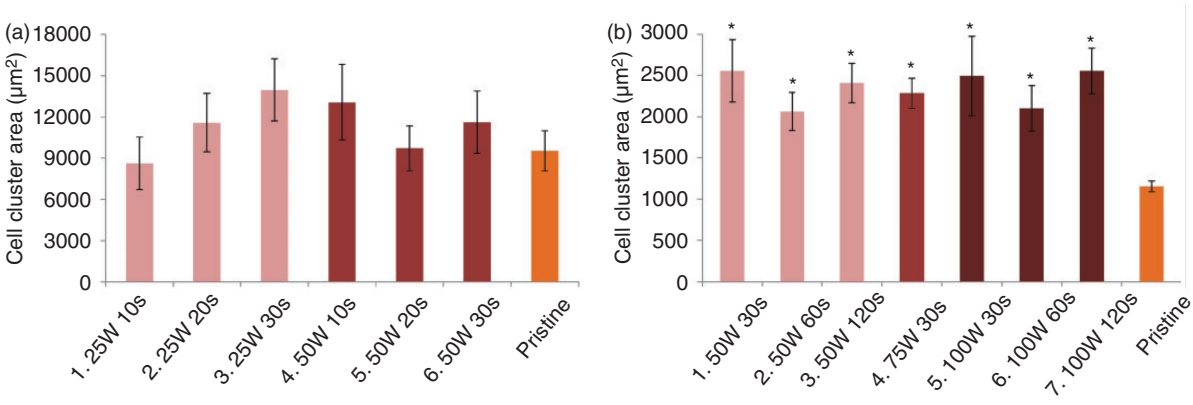

Figure 10. Cell cluster spreading area of HaCaT keratinocytes on day 3 on non-treated and plasma-treated samples (various power 25–50 W and 50–100 W, exposure time 10–30 s and 30–120 s) PLA membranes of fiber density 9 g/m^2 (a) and 16 g/m^2 (b) measured using Atlas software (Tescan Ltd., Brno, Czech Republic). Arithmetic means ± S.E.M. from 44 to 274 measurements. ANOVA, Student-Newman–Keuls method, statistical significance ($p \leq 0.05$): * in comparison with the non-treated sample.

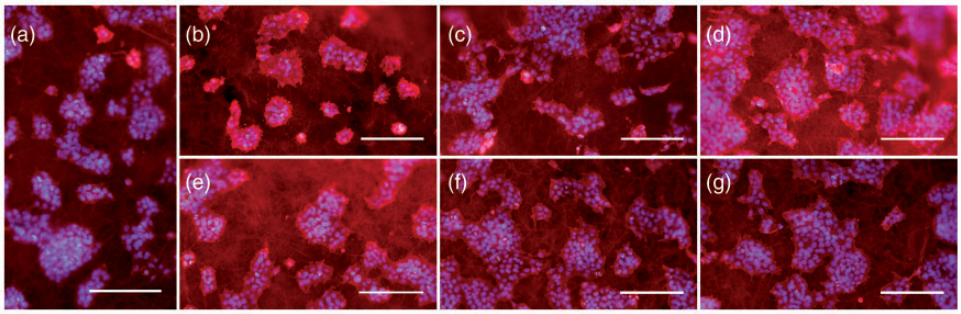

Figure 11. Morphology of human HaCaT keratinocytes after three-day cultivation on non-treated (a) and plasma-treated PLA nanofibers of fiber density 9 g/m^2: (b) 25 W 10 s, (c) 25 W 20 s, (d) 25 W 30 s, (e) 50 W 10 s, (f) 50 W 20 s, (g) 50 W 30 s. Cells stained with Texas Red C_2-Maleimide and Hoechst #33342. Olympus IX 51 microscope, obj. 10×, DP 70 digital camera, bar 200 μm.

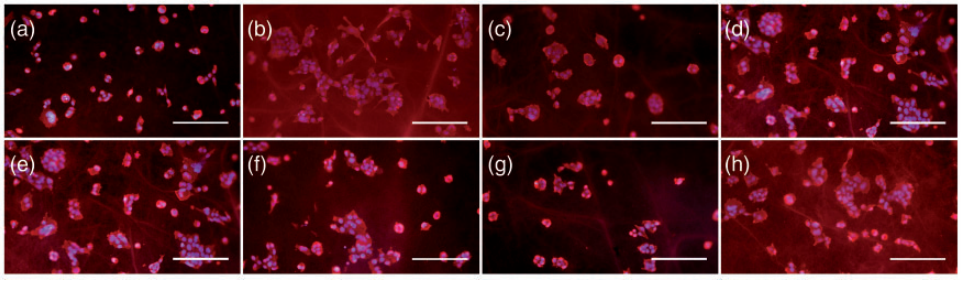

Figure 12. Morphology of human HaCaT keratinocytes after three-day cultivation on non-treated (a) and plasma-treated PLA nanofibrous membranes of fiber density 16 g/m^2: (b) 50 W 30 s, (c) 50 W 60 s, (d) 50 W 120 s, (e) 75 W 30 s, (f) 100 W 30 s, (g) 100 W 60 s, (h) 100 W 120 s. Cells stained with Texas Red C_2-Maleimide and Hoechst #33342. Olympus IX 51 microscope, obj. 10×, DP 70 digital camera, bar 200 μm.

adhesion and growth, which can act synergistically with the material wettability.[1,20]

However, as revealed by immunofluorescence, the plasma treatment appeared to have no significant influence on the presence and distribution of molecular markers of cell adhesion and spreading, namely β_1-integrins, vinculin, and F-actin. The staining pattern of these molecules was similar in cells on non-treated nanofibrous membranes and on plasma-treated nanofibrous membranes. However, this pattern differed

between the cells on nanofibrous membranes and on the control glass coverslips. On the glass coverslips, the intensity of the fluorescence of the β_1-integrins and vinculin was higher, and the F-actin filaments were better developed. Similarly, filamentous organization of keratin 5 was also more apparent on the glass coverslips. This could be explained by the fact that the glass coverslips provided firmer and more continuous support for cell attachment than the relatively loose and porous nanofibrous network, which may not provide sufficient surface area for cell adhesion and spreading.[33] On the other hand, the immunofluorescence of filaggrin in cells on nanofibrous membranes, particularly on less stiff non-treated membranes, appeared brighter than on the glass coverslips. Filaggrin is a structural protein involved in the mechanical resistance and integrity of an epithelial barrier,[34] and this barrier function is probably more difficult to maintain on relatively weak nanofibrous membranes.

Although HaCaT keratinocytes are an immortalized cell line, they conserved markers of keratinocyte differentiation, including markers of terminal keratinocyte differentiation (keratins 1 and 10),[35] late markers involucrin[36] and loricrin,[37] an intermediate marker filaggrin,[38] and an early marker keratin 5.[39,40] In the physiological skin, the terminal, late, and intermediate markers are expressed in suprabasal layers of keratinocytes (i.e. spinous and granular layers), while cytokeratin 5 is expressed in the basal layer.[37,40,41] The expression of differentiation markers in HaCaT cells is influenced by various factors, such as cell population density,[41] the composition of the cell culture media, particularly the concentration of calcium,[36] and also by the time of cultivation.[42] In our system with 7-day cultivation of HaCaT cells on nanofibrous meshes or on glass coverslips, immunofluorescence revealed almost no cytokeratins 1 and 10 (data not shown) but relatively bright signals for keratin 5 and filaggrin, which suggested an early or middle stage of HaCaT cell differentiation. However, immunofluorescence staining did not show striking differences in the presence and distribution of keratin 5 and fillagrin in cells on non-treated and plasma-treated nanofibrous membranes. Therefore, there is a need for a further, deeper investigation, e.g. by biochemical methods capable of quantifying these molecules at protein and mRNA level.

Fiber density had a significant effect on the adhesion and growth of cells. We measured a higher amount of cell DNA, cell metabolic activity and a larger cell cluster spreading area on membranes with lower fiber densities (5 or 9 g/ m^2) than on membranes with higher fiber densities (16 or 30 g/m^2). This effect was more apparent on plasma-treated membranes. Soliman et al. reported on the effect of the fiber packing density of nanofibrous membranes on cell behavior. They showed the dependence of pore size on the fiber packing density and its subsequent effect on cell behavior. Higher fiber packing density resulted in smaller pores and weaker cell proliferation.[33] We observed similar results mainly on plasma-treated membranes. The area of void spaces between the fibers of the membranes increased with decreasing fiber density, which led to better cell adhesion and proliferation. Larger spaces between fibers may have provided more space for the cells to proliferate and migrate into a deeper layer of the membranes. They may also enable a better supply of oxygen and nutrients for the cells, and quicker waste removal.[33] However, the area of void spaces between fibers decreased significantly after plasma treatment, which further enhanced the dependence of cell adhesion and growth on the fiber density of the membranes. Smaller spaces between fibers on plasma-treated membranes of higher fiber densities probably led to significantly lower cell colonization of these membranes. This insufficiency may also have been caused by a decrease in mechanical deformability, and by an increase in the rigidity and fragility of the plasma-treated membranes. In addition, according to SEM analysis, significantly stronger modification of nanofibers of higher fiber densities may not provide sufficient support for cell adhesion and proliferation.

In the second part of the study, we investigated the effect of various plasma conditions (plasma power and exposure time) on altering the physical and chemical properties of the polymer surface, and its influence on cell adhesion and growth. SEM analysis showed that when plasma power less than 50 W and exposure time shorter than 30 s were used, there was no modification of the membranes. However, if higher power (from 50 W to 100 W) and a longer exposure time (from 30 s to 120 s) were applied, the modification of the fibers increased with plasma power and exposure time. We observed that the plasma exposure time seemed to have a more significant effect on the modification and degradation of the fibers. Wan et al. had similar results when they treated a porous PLA scaffold with NH_3 plasma. They showed that the depth of the modification of the scaffold increased mainly with exposure time, while degradation of the scaffold increased with increasing exposure time and plasma power.[43]

Cells cultivated on membranes treated under mild plasma conditions (plasma power less than 50 W and exposure time shorter than 30 s) did not show significantly better adhesion, proliferation, or a larger area of cell clusters than non-treated membranes. As mentioned earlier, SEM analysis did not reveal any significant alteration in the morphology of membranes treated under mild plasma conditions. It therefore seems that these mild plasma treatment conditions did

not have a significant effect on the physical and chemical composition of the membrane surface and on the cell behavior. However, stronger plasma treatment (plasma power ranging from 50 W to 100 W and exposure time ranging from 30 s to 120 s) enhanced cell attachment, proliferation, and spreading in comparison with non-treated membranes. However, we observed no significant dependence of cell behavior on modulation of plasma power and exposure time. XPS analysis showed a slight increase in polar groups on the material surface after plasma treatment, but did not show significant differences in surface chemical composition depending on plasma power and exposure time. This observation indicates that an increase in plasma power and exposure time above a specific effective plasma treatment condition limit does not have a significant influence on cell behavior. The effect of different plasma conditions, plasma power, and exposure time on cell behavior would be more pronounced when there is dynamic cultivation of the cells. Wan et al. showed that different exposure times had a different influences on the detachment of cells enduring shear stress during dynamic cultivation on the material.[44]

Conclusion

Oxygen plasma treatment of PLA nanofibrous membranes had a positive influence on cell colonization of the material. The beneficial effect of plasma treatment on cell adhesion and growth could be attributed to the formation of new oxidized structures on the membrane surface, an increase in surface wettability, and an increase in surface stiffness. No clear dependence of cell behavior on different plasma conditions (plasma power and exposure time) was observed, though higher plasma power and, in particular, longer exposure times resulted in more pronounced improvement of the cell adhesion and growth. The fiber density of the membranes also played an important role in cell adhesion and growth. The cells preferentially adhered to membranes of lower fiber densities, probably due to the larger void spaces between the fibers. This effect was more pronounced on plasma-treated membranes than on non-treated membranes. Thus, PLA nanofibrous membranes are promising materials for the construction of temporary carriers for skin cells, particularly after physical modifications are made to them.

Acknowledgements

The authors would like to acknowledge the kind assistance of Dr Jitka Libertinova (Inst. of Physics, Acad. Sci. CR) for SEM of the nanofiber morphology and Mr Robin Healey (Czech Technical University in Prague) for his language revision of the manuscript.

Declaration of conflicting interests

None declared.

Funding

This study was supported by the Grant Agency of the Czech Republic (grant No. P108/12/G108). Further financial support was provided by the "BIOCEV – Biotechnology and Biomedicine Centre of the Academy of Sciences and Charles University" (CZ.1.05/1.1.00/02.0109), project from the European Regional Development Fund.

References

1. Bacakova L, Filova E, Parizek M, et al. Modulation of cell adhesion, proliferation and differentiation on materials designed for body implants. *Biotechnol Adv* 2011; 29: 739–767.
2. Parizek M, Douglas TE, Novotna K, et al. Nanofibrous poly(lactide-co-glycolide) membranes loaded with diamond nanoparticles as promising substrates for bone tissue engineering. *Int J Nanomed* 2012; 7: 1931–1951.
3. Auxenfans C, Fradette J, Lequeux C, et al. Evolution of three dimensional skin equivalent models reconstructed in vitro by tissue engineering. *Eur J Dermatol* 2009; 19: 107–113.
4. Prasitsilp M, Siriwittayakorn T, Molloy R, et al. Cytotoxicity study of homopolymers and copolymers of 2-hydroxyethyl methacrylate and some alkyl acrylates for potential use as temporary skin substitutes. *J Mater Sci Mater Med* 2003; 14: 595–600.
5. Young CD, Wu JR and Tsou TL. High-strength, ultrathin and fiber-reinforced pHEMA artificial skin. *Biomaterials* 1998; 19: 1745–1752.
6. El-Ghalbzouri A, Lamme EN, van Blitterswijk C, et al. The use of PEGT/PBT as a dermal scaffold for skin tissue engineering. *Biomaterials* 2004; 25: 2987–2996.
7. Malin EW, Galin CM, Lairet KF, et al. Silver-coated nylon dressing plus active DC microcurrent for healing of autogenous skin donor sites. *Ann Plast Surg* 2013; 71: 481–484.
8. Marston WA, Hanft J, Norwood P, et al. The efficacy and safety of dermagraft in improving the healing of chronic diabetic foot ulcers: results of a prospective randomized trial. *Diabetes Care* 2003; 26: 1701–1705.
9. Peschel G, Dahse HM, Konrad A, et al. Growth of keratinocytes on porous films of poly(3-hydroxybutyrate) and poly(4-hydroxybutyrate) blended with hyaluronic acid and chitosan. *J Biomed Mater Res A* 2008; 85: 1072–1081.
10. Dai NT, Williamson MR, Khammo N, et al. Composite cell support membranes based on collagen and polycaprolactone for tissue engineering of skin. *Biomaterials* 2004; 25: 4263–4271.
11. Selig HF, Keck M, Lumenta DB, et al. The use of a polylactide-based copolymer as a temporary skin substitute in deep dermal burns: 1-year follow-up results of a prospective clinical noninferiority trial. *Wound Repair Regen* 2013; 21: 402–409.

12. Chen G, Sato T, Ohgushi H, et al. Culturing of skin fibroblasts in a thin PLGA-collagen hybrid mesh. *Biomaterials* 2005; 26: 2559–2566.
13. Pajoum Shariati SR, Shokrgozar MA, Vossoughi M, et al. In vitro co-culture of human skin keratinocytes and fibroblasts on a biocompatible and biodegradable scaffold. *Iran Biomed J* 2009; 13: 169–177.
14. Ma L, Gao C, Mao Z, et al. Collagen/chitosan porous scaffolds with improved biostability for skin tissue engineering. *Biomaterials* 2003; 24: 4833–4841.
15. Morimoto N, Suzuki S, Kim BM, et al. In vivo cultured skin composed of two-layer collagen sponges with preconfluent cells. *Ann Plast Surg* 2001; 47: 74–81.
16. Harris PA, di Francesco F, Barisoni D, et al. Use of hyaluronic acid and cultured autologous keratinocytes and fibroblasts in extensive burns. *Lancet* 1999; 353: 35–36.
17. Liu H, Mao J, Yao K, et al. A study on a chitosan-gelatin-hyaluronic acid scaffold as artificial skin in vitro and its tissue engineering applications. *J Biomater Sci Polym Ed* 2004; 15: 25–40.
18. Lacroix S, Bouez C, Vidal S, et al. Supplementation with a complex of active nutrients improved dermal and epidermal characteristics in skin equivalents generated from fibroblasts from young or aged donors. *Biogerontology* 2007; 8: 97–109.
19. Pandey AK. Recent advancements of biodegradable polylactic acid/ polylactide: A review on synthesis, characterization and applications. *Adv Mater* 2013 (in press).
20. Bacakova L and Svorcik V. Cell colonization control by physical and chemical modification of materials. In: Kimura D (ed.) *Cell growth processes: new research*. USA: Nova Science Publishers, Inc., 2008, pp.5–56.
21. Svorcik V, Rybka V, Hnatowicz V, et al. Structure and biocompatibility of ion beam modified polyethylene. *J Mater Sci Mater Med* 1997; 8: 435–440.
22. Walachova K, Svorcik V, Bacakova L, et al. Colonization of ion-modified polyethylene with vascular smooth muscle cells in vitro. *Biomaterials* 2002; 23: 2989–2996.
23. Heitz J, Svorcik V, Bacakova L, et al. Cell adhesion on polytetrafluoroethylene modified by UV-irradiation in an ammonia atmosphere. *J Biomed Mater Res A* 2003; 67: 130–137.
24. Novotna K, Bacakova M, Kasalkova N, et al. Adhesion and growth of vascular smooth muscle cells on nanostructured and biofunctionalized polyethylene. *Materials* 2013; 6: 1632–1655.
25. Parizek M, Slepickova Kasalkova N, Bacakova L, et al. Adhesion, growth, and maturation of vascular smooth muscle cells on low-density polyethylene grafted with bioactive substances. *BioMed Res Int* 2013; 2013: 1–18.
26. Pareta RA, Reising AB, Miller T, et al. Increased endothelial cell adhesion on plasma modified nanostructured polymeric and metallic surfaces for vascular stent applications. *Biotechnol Bioeng* 2009; 103: 459–471.
27. Kubies D, Rypacek F, Kovarova J, et al. Microdomain structure in polylactide-block-poly(ethylene oxide) copolymer films. *Biomaterials* 2000; 21: 529–536.
28. Boukamp P, Petrussevska RT, Breitkreutz D, et al. Normal keratinization in a spontaneously immortalized aneuploid human keratinocyte cell line. *J Cell Biol* 1988; 106: 761–771.
29. Nakagawa M, Teraoka F, Fujimoto S, et al. Improvement of cell adhesion on poly(L-lactide) by atmospheric plasma treatment. *J Biomed Mater Res A* 2006; 77: 112–118.
30. Gugala Z and Gogolewski S. Attachment, growth, and activity of rat osteoblasts on polylactide membranes treated with various low-temperature radiofrequency plasmas. *J Biomed Mater Res A* 2006; 76: 288–299.
31. Wan Y, Qu X, Lu J, et al. Characterization of surface property of poly(lactide-co-glycolide) after oxygen plasma treatment. *Biomaterials* 2004; 25: 4777–4783.
32. Jeong L, Yeo IS, Kim HN, et al. Plasma-treated silk fibroin nanofibers for skin regeneration. *Int J Biol Macromol* 2009; 44: 222–228.
33. Soliman S, Sant S, Nichol JW, et al. Controlling the porosity of fibrous scaffolds by modulating the fiber diameter and packing density. *J Biomed Mater Res A* 2011; 96: 566–574.
34. McGrath JA. Filaggrin and the great epidermal barrier grief. *Australas J Dermatol* 2008; 49: 67–73.
35. Prado E, Wurtz T, Ferbus D, et al. Sodium fluoride influences the expression of keratins in cultured keratinocytes. *Cell Biol Toxicol* 2011; 27: 69–81.
36. Micallef L, Belaubre F, Pinon A, et al. Effects of extracellular calcium on the growth-differentiation switch in immortalized keratinocyte HaCaT cells compared with normal human keratinocytes. *Exp Dermatol* 2009; 18: 143–151.
37. Breitkreutz D, Schoop VM, Mirancea N, et al. Epidermal differentiation and basement membrane formation by HaCaT cells in surface transplants. *Eur J Cell Biol* 1998; 75: 273–286.
38. Hong JH, Youm JK, Kwon MJ, et al. K6PC-5, a direct activator of sphingosine kinase 1, promotes epidermal differentiation through intracellular Ca2+ signaling. *J Invest Dermatol* 2008; 128: 2166–2178.
39. Zhou LL, Lin ZX, Fung KP, et al. Ethyl acetate fraction of Radix rubiae inhibits cell growth and promotes terminal differentiation in cultured human keratinocytes. *J Ethnopharmacol* 2012; 142: 241–247.
40. Kitagawa N, Inai Y, Higuchi Y, et al. Inhibition of JNK in HaCaT cells induced tight junction formation with decreased expression of cytokeratin 5, cytokeratin 17 and desmoglein 3. *Histochem Cell Biol* 2014; 1–11.
41. Poumay Y and Pittelkow MR. Cell density and culture factors regulate keratinocyte commitment to differentiation and expression of suprabasal K1/K10 keratins. *J Invest Dermatol* 1995; 104: 271–276.

42. Schoop VM, Mirancea N and Fusenig NE. Epidermal organization and differentiation of HaCaT keratinocytes in organotypic coculture with human dermal fibroblasts. *J Invest Dermatol* 1999; 112: 343–353.
43. Wan Y, Tu C, Yang J, et al. Influences of ammonia plasma treatment on modifying depth and degradation of poly(L-lactide) scaffolds. *Biomaterials* 2006; 27: 2699–2704.
44. Wan Y, Yang J, Yang J, et al. Cell adhesion on gaseous plasma modified poly-(l-lactide) surface under shear stress field. *Biomaterials* 2003; 24: 3757–3764.

International Journal of Nanomedicine

Dovepress
open access to scientific and medical research

Open Access Full Text Article

ORIGINAL RESEARCH

The potential applications of fibrin-coated electrospun polylactide nanofibers in skin tissue engineering

This article was published in the following Dove Press journal:
International Journal of Nanomedicine
25 February 2016
Number of times this article has been viewed

Marketa Bacakova[1,2]
Jana Musilkova[1]
Tomas Riedel[3]
Denisa Stranska[4]
Eduard Brynda[3]
Margit Zaloudkova[5]
Lucie Bacakova[1]

[1]Department of Biomaterials and Tissue Engineering, Institute of Physiology, Czech Academy of Sciences, [2]Second Faculty of Medicine, Charles University in Prague, [3]Institute of Macromolecular Chemistry, Czech Academy of Sciences, Prague, [4]InStar Technologies, Liberec, [5]Institute of Rock Structure and Mechanics, Czech Academy of Sciences, Prague, Czech Republic

Abstract: Fibrin plays an important role during wound healing and skin regeneration. It is often applied in clinical practice for treatment of skin injuries or as a component of skin substitutes. We prepared electrospun nanofibrous membranes made from poly(L-lactide) modified with a thin fibrin nanocoating. Fibrin surrounded the individual fibers in the membrane and also formed a thin fibrous mesh on several places on the membrane surface. The cell-free fibrin nanocoating remained stable in the cell culture medium for 14 days and did not change its morphology. On membranes populated with human dermal fibroblasts, the rate of fibrin degradation correlated with the degree of cell proliferation. The cell spreading, mitochondrial activity, and cell population density were significantly higher on membranes coated with fibrin than on nonmodified membranes, and this cell performance was further improved by the addition of ascorbic acid in the cell culture medium. Similarly, fibrin stimulated the expression and synthesis of collagen I in human dermal fibroblasts, and this effect was further enhanced by ascorbic acid. The expression of beta$_1$-integrins was also improved by fibrin, and on pure polylactide membranes, it was slightly enhanced by ascorbic acid. In addition, ascorbic acid promoted deposition of collagen I in the form of a fibrous extracellular matrix. Thus, the combination of nanofibrous membranes with a fibrin nanocoating and ascorbic acid seems to be particularly advantageous for skin tissue engineering.

Keywords: electrospun nanofibers, nanocoating, skin tissue engineering, fibroblasts, fibrin, ascorbic acid, nanotechnology, nanomedicine, collagen I synthesis, beta1-integrins

Introduction

Nanostructured materials are advantageously applied for constructing a tissue replacement, because they are more attractive for cell adhesion, proliferation, and differentiation than flat or microstructured surfaces. The nanostructure of the material mimics the nanoarchitecture of natural extracellular matrix (ECM), eg, its nanofibrous component, and it enhances the cell–material interaction. Nanostructured materials are capable of adsorbing cell adhesion-mediating ECM molecules from the body fluid or from the cell culture medium in an appropriate spatial conformation. This conformation is important for good accessibility of specific oligopeptidic ligands of ECM molecules to cell adhesion receptors called integrins.[1,2]

Nanostructured materials can promote skin regeneration by improving the adhesion and proliferation of skin cells and the neovascularization of a tissue-engineered skin implant. They enable cells to be supplied with oxygen and nutrition and prevent fluid accumulation at the wound site.[3]

Most models of skin substitutes are based on a nonresorbable artificial material and allogenic cells. These substitutes cannot provide permanent coverage because they will finally be rejected.[4] A promising approach could be to fabricate nanofibrous

Correspondence: Marketa Bacakova
Department of Biomaterials and Tissue Engineering, Institute of Physiology, Czech Academy of Sciences, Videnska 1083, Prague 4, 14220, Czech Republic
Tel +420 2 9644 3765
Email marketa.bacakova@fgu.cas.cz

submit your manuscript | www.dovepress.com
Dovepress
http://dx.doi.org/10.2147/IJN.S99317

biodegradable scaffolds colonized with autologous fibroblasts and keratinocytes. The degradable scaffolds are slowly resorbed in the organism and are finally replaced by a newly formed tissue.

The most widespread technique for preparing nanofibrous scaffold is electrospinning. Due to increasing requirements of the electrospun nanofibrous scaffold for biomedical purposes, several innovative methods of electrospinning have been developed. One approach is the needleless electrospinning enabling the production of nanofibers on a large scale.[5] Another method is the creation of structural nanofibers using multiple-fluid electrospinning such as coaxial,[6,7] triaxial,[8] or side-by-side[9] process. The multiple-fluid electrospinning enables encapsulation of drugs or other biological agents into polymeric nanofibrous scaffold and can be potentially applied for drug delivery. In addition, the electrospinning can be combined with other traditional methods or after-treatment of electrospun nanofibers. Our structural nanofibers were fabricated by coating fibrin on the electrospun polylactide (PLA) nanofibers that were created using a needleless electrospinning technique.

Promising materials for developing nanofibrous degradable scaffolds are synthetic degradable polymers, namely PLAs,[10–12] and their copolymers with glycolides[13] or polyethylene glycol.[14] Other examples include poly (epsilon-caprolactone)[15] or segmented copolymers of polyethylene oxide terephthalate and polybutylene terephthalate.[16]

However, synthetic polymers used for skin tissue engineering often do not favor cellular adhesion, growth, and matrix deposition in their pristine unmodified state.[11] In our earlier study, PLA nanofibrous membranes were modified by plasma treatment in order to enhance the adhesion and growth of human keratinocytes on these carriers.[12] Other modifications included etching of the polymers in NaOH in order to increase their wettability and their electrical charge,[10] copolymerization or blending of the polymers with other more hydrophilic synthetic polymers,[17] and particularly combining synthetic polymers with molecules physiologically present in the skin, such as collagen,[10] hyaluronan,[18] and fibronectin.[17] Another approach is through modification by fibrin.[19,20] Fibrin is a temporary matrix molecule that forms during wound healing. It offers the advantage that fibrinogen, a precursor of fibrin, can be isolated in a considerable amount from the patient's blood in autologous form to prevent unwanted immune reactions.[21,22]

Fibrin plays an important role in skin regeneration. It is a biopolymer resulting from enzymatic reactions of the coagulation cascade. Activation of this cascade leads to the conversion of soluble fibrinogen by thrombin into a network of insoluble fibrin fibers.[23] The fibrin network stabilizes the platelet plug by binding platelets to the fibrin. The platelets secrete growth factors, namely platelet-derived growth factor, which stimulates fibroblasts to proliferate, migrate into the wound site, and produce collagen I and III, glycosaminoglycans, and proteoglycans. Moreover, the fibrin network binds other cell types, such as smooth muscle cells and endothelial cells, through integrin adhesion receptors. In addition, fibrin binds cell adhesion-mediating ECM proteins, fibronectin, and vitronectin, which support the adhesion of fibroblasts.[24]

During the wound healing process, dermal fibroblasts secrete ECM proteins, mainly collagen of types I and III, which are the major component of ECM in the skin dermis.[23] The synthesis of collagen is enhanced by water-soluble ascorbic acid (vitamin C). Ascorbic acid plays a role as a cofactor for enzymes, prolyl, and lysyl hydroxylases, catalyzing the synthesis of hydroxyproline and hydroxylysine in collagen. In addition, ascorbic acid also stimulates collagen biosynthesis by increasing the steady-state level of procollagen mRNA.[25,26] A previous study has shown that the fibroblasts cultivated in a three-dimensional system consisting of ECM molecules not only secreted collagen into the cell culture medium but also deposited it on the cultivation substrate as collagen fibrils.[27] Similarly, human dermal fibroblasts cultured on composite polymeric nanofibrous scaffolds blended with ascorbic acid synthesized more collagen than that synthesized on nonblended scaffolds.[3]

For skin tissue engineering and wound healing, fibrin has been used mostly in the form of self-supporting structures, such as gels,[18,28,29] a glue,[30,31] and microbeads.[30,32] It has been relatively rarely used for surface modification of scaffolds, with the exception of collagen–chitosan porous membranes,[31] or on electrospun poly(lactide-glycolide-caprolactone) nanofibers.[33] To the best of our knowledge, a combination of fibrin and ascorbic acid has not previously been used for constructing potential skin replacements, although this combination has been applied in tissue engineering of tendon and ligament,[34] cartilage,[35] bone,[36] smooth muscle,[37] and heart valves.[38] In these applications, ascorbic acid promoted appropriate differentiation and phenotypic maturation of cells and increased the collagen production in these cells.

The aim of this study is therefore to evaluate the adhesion and growth of human dermal fibroblasts on PLA nanofibrous membranes modified with a cell-degradable fibrin nanocoating. We further investigated the effect of a combination of nanofibrous membranes, fibrin nanocoating, and ascorbic acid on the synthesis of collagen by fibroblasts, mainly in the form of collagen fibrils deposited on the membrane surface as ECM.

Materials and methods

Preparation of nanofibrous membranes

Poly(L-lactide) (PLA; Ingeo™ Biopolymer 4032D) was purchased from NatureWorks, Minnetonka, MN, USA. The molecular parameters of the polymer material, determined by size exclusion chromatography, were M_w=124,000 g/mol and M_n=48,000 g/mol.[39] A 7 wt% solution of PLA in a mixture of chloroform, dichloroethane, and ethyl acetate in the volume ratio of 61:29:10 was used for the electrospinning process. The polymer was diluted only in chloroform, and the other two solvents were added after the dilution. The polymer solution was made electrically conductive with the use of tetraethylammonium bromide, which was first dissolved in dimethylformamide at a concentration of 3 wt%, and then 3 g of this solution was added to 100 g of the PLA solution.[40]

Nanofibrous membranes were prepared using the novel Nanospider needleless electrospinning technology (NS Lab 500; Elmarco Ltd., Liberec, Czech Republic). The process conditions were: electrode distance: 180 mm; voltage: 60–10 kV; the spinning electrode rotated at 4 rpm; relative humidity: 25%–30%, and room temperature. The fiber density, ie, the area weight of the prepared nanofibers, was from 12 to 15 g/m^2.

Preparation of a fibrin nanocoating on PLA membranes

The fibrin nanocoating on a nanofibrous membrane was created by activation of human fibrinogen (EMD Millipore, Billerica, MA, USA) with human thrombin (Sigma-Aldrich Co., St Louis, MO, USA), as published previously.[41] Human fibrinogen and human thrombin are commercially available, and in our study both chemicals were purchased from international well-known companies and therefore no ethical approval was required.

A total of 10 μg/mL of fibrinogen in Tris buffer (consisting of 50 mM Tris–HCl, 100 nM NaCl, and 2.5 mM $CaCl_2$) was adsorbed on the surface of the membrane for 1 hour. The adsorbed fibrinogen was rinsed with Tris buffer and was activated with thrombin (2.5 U/mL in Tris buffer) for 15 minutes. After thrombin activation, the membranes were rinsed with Tris Buffer. Finally, a solution of 200 μg/mL of fibrinogen and 0.5 U/mL of antithrombin III (Chromogenix, Milano, Italy) was added to the membranes for 1 hour. A fibrin network was formed by a catalytic reaction of the surface-attached thrombin with the ambient fibrinogen solution. Antithrombin III blocked unreacted thrombin to form a two-dimensional fibrin layer.

Scanning electron microscopy

The morphology of the PLA membrane in pristine state (nonmodified membrane) was studied by scanning electron microscopy. The membranes were sputter-coated with gold and were evaluated by a Quanta 450 scanning electron microscope (FEI, Hillsboro, OR, USA) in high vacuum mode. The images were taken using ETD – the Everhart–Thornley detector in secondary electrons mode at high voltage of 20 kV and magnification of 2,000× and 10,000×. The diameter of the fibers was measured on the scanning electron microscopy images using Atlas software (Tescan Ltd., Brno, Czech Republic).

Cell culture

The nanofibrous membranes were fixed in Cell Crown inserts (Scaffdex Ltd., Tampere, Finland) and were inserted into polystyrene 24-well or six-well cell culture plates (TPP, Trasadingen, Switzerland; well diameter: 1.56 or 3.38 cm). The samples were seeded with neonatal human dermal fibroblasts, purchased from Lonza (Basel, Switzerland), in passage 5 at a density of 10,000 cells/cm^2. Dulbecco's Modified Eagle's Medium (Sigma-Aldrich Co.) supplemented with 10% of fetal bovine serum (FBS; Sebak GmbH, Aidenbach, Germany) and 40 μg/mL of gentamicin (LEK, Ljubljana, Slovenia) was used for cultivating the cells on the samples. The volume of cell culture medium was 1.5 mL/sample for the 24-well cell culture plate and 6 mL/sample for the six-well cell culture plate. The cells were cultivated for 1, 3, 5, 7, 10, and 14 days in a cell incubator at 37°C and in a humidified atmosphere with 5% of CO_2 in the air. The medium was changed after 1 week of cell cultivation and subsequently every 3 days. Polystyrene culture dishes (24-well or six-well plates) or glass coverslips were used as control materials. On day 1 (for β_1-integrin evaluation) or on day 3 (for other experiments) after cell seeding, 50 μg/mL 2-phospho-L-ascorbic acid trisodium salt (AA) was added into the cell culture medium of one half of the samples to stimulate the cells to produce collagen.

Cell mitochondrial activity

Cell mitochondrial activity was used as an indirect marker of cell proliferation activity, because it usually increases with increasing cell number. This parameter was measured in six intervals of cell cultivation (on days 1, 3, 5, 7, 10, and 14 after cell seeding) by CellTiter 96® AQueous One Solution Cell Proliferation Assay (MTS; Promega Corporation, Madison, WI, USA) on samples of nanofibrous membranes incubated in a 24-well cell culture plate. The principle of this assay is based on the cleavage of yellow tetrazolium salt MTS and on the formation of water-soluble brown formazan salt by the activity of mitochondrial enzymes in cells. The formazan dye is then quantified by measuring the absorbance using a spectrophotometer (ELISA reader).

Four independent samples for each experimental group and time interval were used. One sample without cells for each experimental group and time interval was used as a control to set the background of the measured absorbance. A 24-well polystyrene culture dish was used as a control material for cell proliferation. The samples of nanofibrous membranes were moved into fresh 24-well plates to avoid the influence of the cells adhered to the bottom of the wells. The assay was performed in accordance with the manufacturer's protocol. The absorbance was measured using the VersaMax ELISA Microplate Reader (Molecular Devices LLC, Sunnyvale, CA, USA) in Nunc-Immuno MicroWell 96-well cell culture plates (Sigma-Aldrich Co., St Louis, MO, USA) with wavelength at 490 nm.

Cell morphology and spreading

The spreading and morphology of the cells on PLA nanofibrous membranes with or without fibrin nanocoating were evaluated in six culture intervals (on days 1, 3, 5, 7, 10, and 14 after cell seeding). A 24-well plate polystyrene culture dish was used as a control material. The cells were rinsed with phosphate-buffered saline (PBS), fixed with −20°C cold ethanol for 10 minutes, and then stained for 1 hour at room temperature with a combination of fluorescent dyes diluted in PBS. The cell cytoplasm was stained with Texas Red C_2-maleimide (Molecular Probes, eugene, OR, USA; Thermo Fisher Scientific, Waltham, MA, USA, 20 ng/mL). F-actin, an important molecule of the cell cytoskeleton, was stained with phalloidin conjugated with TRITC (Sigma-Aldrich Co., 5 μg/mL), and cell nucleus was stained with Hoechst #33258 (Sigma-Aldrich Co., 5 μg/mL). Images of the cell morphology were taken using an epifluorescence microscope (IX51, Olympus Corporation, Tokyo, Japan, objective [obj] 10×) equipped with a digital camera (DP 70, Olympus Corporation, Tokyo, Japan) or scanned using a Leica TCS SPE DM2500 upright confocal microscope (Leica Microsystems, Wetzlar, Germany), obj 40×/1.15 numerical aperture (NA) oil.

Real-time polymerase chain reaction

Real-time polymerase chain reaction (real-time PCR) was used for measuring relative mRNA expression of β_1-integrin (important molecule marker of cell adhesion) and collagen I (main component of ECM produced by fibroblasts) on days 7, 10, and 14 after cell seeding. The first evaluated interval was chosen after 1 week of cultivation on the basis of our previous experiments, when fibroblasts started to form collagen fibers after they reached confluence. Moreover, higher cell population density was needed for RNA isolation. Four independent samples of PLA membranes fixed into a six-well cell culture plate for each experimental group and time interval were used. Each membrane sample was pooled in two independent experiments. The polystyrene culture dishes were used as a control material for cell proliferation.

Total RNA was isolated from the samples using the Total RNA Purification Micro Kit (Norgen Biotek Corp., Thorold, ON, Canada), according to the manufacturer's protocol. The cells were rinsed with PBS. The PLA membranes were transferred into 1.5 mL tubes, and RNA was isolated using the lysis solution enriched with mercaptoethanol (1%). The cells on the control polystyrene dish were directly lysed in the plate.

Reverse transcription was performed using the Omniscript Reverse Transcription Kit (Qiagen NV, Venlo, the Netherlands) and random hexamers (New England Biolabs, Inc, Ipswich, MA, USA), according to the manufacturer's protocol.

The mRNA levels were quantified by 5× HOT FIREPol Probe qPCR Mix Plus (ROX) (Solis BioDyne, Tartu, Estonia) and by TaqMan Gene Expression Assays (Thermo Fisher Scientific, Waltham, MA, USA), labeled with FAM reporter dye specific to human β_1-integrin *ITGB1* (Hs00559595_m1) or to human collagen I *COL1A1* (Hs00164004_m1) as a target gene, and glyceraldehyde 3-phosphate dehydrogenase (*GAPDH*) (Hs02758991_g1) as a reference gene, in a final reaction volume of 20 μL on a 96-well optical reaction plate using the iQ5 Multicolor Real-Time PCR Detection System (Bio-Rad Laboratories Inc., Hercules, CA, USA). The amplification conditions consisted of incubation with uracil-DNA glycosylase at 50°C for 2 minutes and initial DNA polymerase enzyme activation at 95°C for 10 minutes, followed by 50 cycles of denaturation at 95°C for 15 seconds and annealing/extension at 60°C for 1 minute.

The data are presented as the mean ± standard error of mean (SEM) from six to eight experimental measurements obtained from three to four independent experiments. Expression values were obtained from C_t numbers. The target gene levels are expressed as a relative value, the ratio of the target gene expression toward the reference *GAPDH* gene. The relative gene expression was calculated as 2^{-num}, where ΔC_t was determined in each sample by subtracting the C_t value of the target gene from the C_t value of the *GAPDH*.

Immunofluorescence staining

The morphology, stability, and degradation of fibrin nanocoating by the cells, distribution of integrin adhesion receptors with β_1 chain, and the total collagen produced by fibroblasts on the PLA membranes were examined with immunofluorescence staining. The morphology of the fibrin nanocoating on the PLA membranes was examined on freshly prepared samples. The stability and degradation

of fibrin nanocoating by the cells was evaluated in six time intervals (on days 1, 3, 5, 7, 10, and 14 after cell seeding). In each time interval, the fibrin nanocoating was stained on PLA membranes seeded with cells and also on membranes without cells, only immersed in the cell culture medium and incubated under the conditions that were used for cell cultivation. The nonmodified membranes incubated in the cell culture medium with and without cells were used as a control to show nonspecific binding of primary or secondary antibody and the cell morphology. The β_1-integrins were visualized in the cells on the investigated substrates on days 3 and 7 after cell seeding. The visualization of total (intracellular and extracellular) collagen produced by fibroblasts on the PLA membranes was performed on days 7, 10, and 14. The cells were cultivated on PLA membranes trapped in CellCrowns and fitted into a 24-well plate. Microscopic glass coverslips were used as a control material. Two samples of each experimental group for each time interval were used.

The membranes cultivated with the cells were incubated with cold (−20°C) 70% ethanol for 10 minutes at room temperature to fix the cells. The membranes without cells or with fixed cells were treated with 1% bovine serum albumin in PBS (Sigma-Aldrich Co.; for the membranes without cells) or with 1% bovine serum albumin in 0.1% triton (Sigma-Aldrich Co.; for the membranes with the cells) for 20 minutes, and then with 1% Tween 20 (Sigma-Aldrich Co.) in PBS for 20 minutes at room temperature to block nonspecific binding sites. Subsequently, the samples were incubated overnight at 4°C with the following primary antibodies diluted in PBS in a ratio of 1:200: rabbit polyclonal antibody against human fibrinogen (Dako Denmark A/S, Glostrup, Denmark), a mouse monoclonal antibody against β_1-integrin chain (Merck Millipore, Billerica, MA, USA), or mouse monoclonal antibody against collagen I (Sigma-Aldrich Co.). After rinsing with PBS, the secondary antibody goat anti-rabbit F(ab')2 fragments of IgG (H + L) or the secondary antibody goat anti-mouse F(ab')2 fragments of IgG (H + L), conjugated with Alexa Fluor® 488 (Molecular Probes; Thermo Fisher Scientific), were applied to the samples (diluted in PBS in a ratio of 1:400) for 1 hour at room temperature in the dark. The cells were rinsed with PBS and were scanned using a Leica TCS SPE DM2500 upright confocal microscope, obj 40×/1.15 NA oil or obj 63×/1.3 NA oil.

Immunofluorescence staining of extracellular collagen

The extracellular collagen, ie, collagen deposited by the cells on the membrane surface, was stained in live cells on days 7, 10, and 14. The cells were cultivated on PLA membranes trapped in CellCrowns and fitted into a 24-well plate. Microscopic glass coverslips were used as a control material.

To stain extracellular type I collagen, the cells were rinsed with a solution of 5% FBS in PBS. The samples were then incubated with primary mouse monoclonal antibody against collagen I (Sigma-Aldrich Co., diluted in PBS in a ratio of 1:200) for 30 minutes on ice. After rinsing the cells with 5% FBS in PBS, they were fixed with 2% paraformaldehyde dissolved in PBS for 20 minutes. The samples were rinsed with PBS, and the nonspecific binding sites were blocked with 1% FBS in PBS. The samples were rinsed with PBS and were incubated with secondary antibody anti-mouse F(ab')2 fragments of IgG (H + L), conjugated with Alexa Fluor® 488 (Molecular Probes, Thermo Fisher Scientific) for 2 hours in the dark. The secondary antibody was diluted in 1% FBS in PBS in a ratio of 1:1,000. The cells were rinsed in PBS, and the cell nucleus was stained with Hoechst #33342, which penetrates through the nonpermeabilized cell membrane.

The cells were scanned using a Leica TCS SPE DM2500 upright confocal microscope, obj 40×/1.15 NA oil.

Sircol™ soluble collagen assay

The total amount of collagen produced by the cells, ie, intracellular collagen and collagen deposited on the PLA membranes, was determined using a Sircol kit (Biocolor Ltd., Carrickfergus, UK) on day 14 after cell seeding. The Sircol assay was carried out only on samples incubated in the cell culture medium with AA. The cells cultivated in the cell standard cultivation medium (without AA) did not deposit collagen as ECM on surface samples in a sufficient amount to enable adequate measurements to be made (the amount of cell collagen was under the detection limit). The Sircol dye binds acid- and pepsin-soluble collagen synthesized by cells and deposited onto the surface as ECM. The Sircol reagent binds to the [Gly-X-Y] helical structure, as found in all types of collagen.

The PLA membranes with cells cultivated in CellCrowns fitted into a six-well plate were removed from the CellCrowns and were transferred into fresh cell culture plates. The polystyrene culture dishes were used as a control material. The membranes and the control polystyrene dishes without cells were used as a control to set a background. Four independent samples for each experimental group were used. The collagen was recovered by acid–pepsin digestion. The cells on the membranes and on the control polystyrene were rinsed with PBS, harvested with a cell scraper in 1 mL of pepsin solution (1 mg/mL dissolved in 0.5 M acetic acid), and lysed overnight at 4°C. The lysates were centrifuged and the supernatants were concentrated according to the Sircol kit manufacturer's protocol.

Finally, the Sircol dye was bound to the isolated collagen, was dissolved, and the absorbance of the colored solution was measured. The absorbance was measured using a VersaMax ELISA Microplate Reader (Molecular Devices LLC) in Nunc-Immuno MicroWell 96-well cell culture plates (Sigma-Aldrich Co.,) with wavelength at 555 nm. The amount of collagen on each type of sample was expressed in μg/cm^2.

The amount of total collagen was adjusted to the cell number estimated by the amount of cellular DNA or to the cell proliferation estimated by the metabolic activity of the cells. The amount of cell DNA was determined using a Picogreen dsDNA assay kit (Thermo Fisher Scientific). The assay is based on measurements of the fluorescence of Picogreen, a nucleic acid stain for quantifying double-stranded DNA in solution. The assay was carried out according to the manufacturer's protocol. Three independent samples of each experimental group were used for the measurements. Fluorescence was measured with the Synergy HT Multi-Mode Reader (BioTek, Winooski, VT, USA) in black 96-well cell culture plates (96 F Nunclon delta; Black Microwell SI) with excitation wavelength at 480 nm and emission wavelength at 520 nm. The amount of cell DNA on each sample was expressed in ng/cm^2. The cell metabolic activity was measured by a CellTiter 96® AQueous One Solution Cell Proliferation Assay (MTS, Promega Corporation), as described in the "Cell mitochondrial activity" section.

Statistics

If not stated otherwise in the text earlier, the quantitative data are presented as mean ± standard deviation from four independent samples for each experimental group and time interval. Statistical significance was evaluated using the analysis of variance and Student–Newman–Keuls method. Values of $P \leq 0.05$ were considered significant.

Results

Morphology of PLA nanofibrous membranes and the fibrin nanocoating on a PLA membrane and its degradation during cell cultivation

The morphology of the nanofibrous membranes in the nonmodified state is shown in Figure 1. The nanofibrous membranes consisted of mostly straight and randomly oriented fibers (Figure 1A, B). The diameter of the fibers varied in a large range from tens of nanometer to >1 μm. The average fiber diameter was ~350 nm (Figure 1C). Thus, the fiber diameter was in the submicron scale rather than in the nanoscale, because the size of nanostructures is defined as ≤100 nm. However, in the scientific literature, submicron-scale fibers are commonly referred to as nanofibers.[40]

The fibrin regularly coated each fiber in the membrane. Moreover, the fibrin randomly formed a thin fibrous mesh on the membrane surface (Figure 2). Tests on the durability of the fibrin nanocoating on the nanofibrous membrane without cells, immersed in the cell culture medium at 37°C for 14 days, showed that the fibrin nanocoating was stable and its morphology was almost unchanged (Figure 3A). The rate of degradation of the fibrin nanocoating on the membrane with cells correlated with the degree of cell proliferation (Figure 3B and C). After 10 days of cell cultivation, the

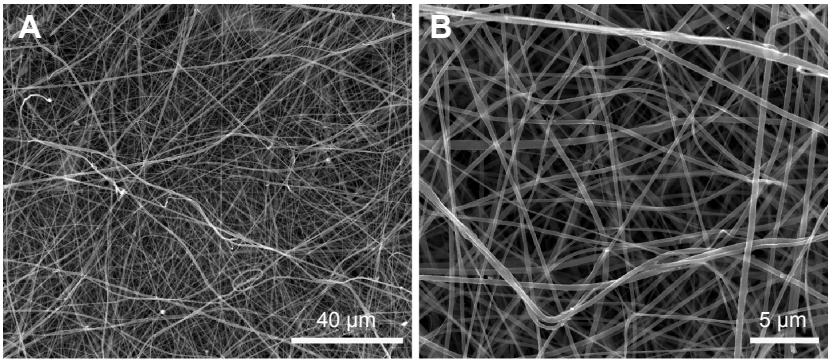

C

Fiber density (g/m^2)	13–15
Fiber diameter, mean ± SD (nm)	352±205
Fiber diameter range (nm)	41–1,747

Figure 1 SEM images of nonmodified PLA membranes.
Notes: Quanta 450 scanning electron microscope FEI, magnification 2,000× (**A**), magnification 10,000× (**B**). Morphological parameters of PLA membranes (**C**). Mean ± SD from 12 SEM images (1,748 measurements in total).
Abbreviations: SEM, scanning electron microscopy; PLA, polylactide; SD, standard deviation.

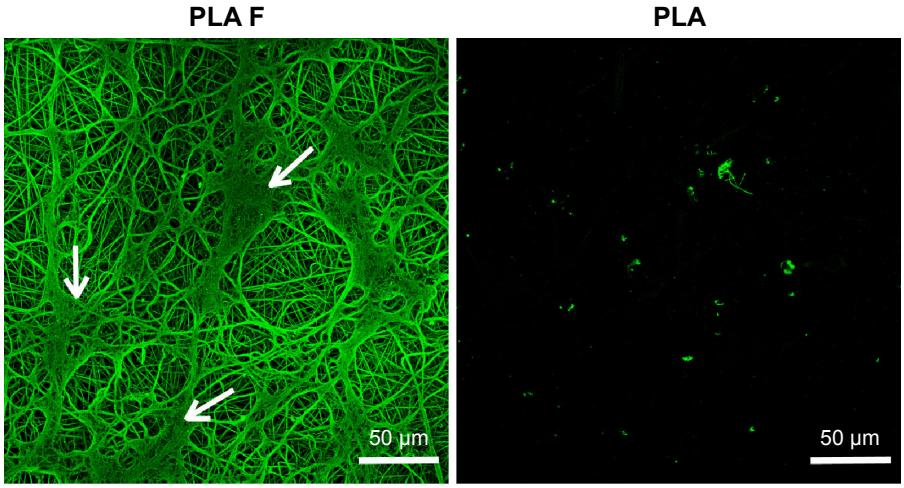

Figure 2 Morphology of the fibrin nanocoating (F) on PLA membranes.
Notes: The fibrin nanocoating stained with primary and secondary antibody. Arrows show the thin fibrous mesh of fibrin at the top of the membrane. The nonmodified membranes (PLA) were used as a control material to show nonspecific binding of primary or secondary antibody. Leica TCS SPE DM2500 confocal microscope, obj 40×/1.15 NA oil.
Abbreviations: PLA, polylactide; obj, objective; NA, numerical aperture; PLA F, fibrin nanocoating on PLA.

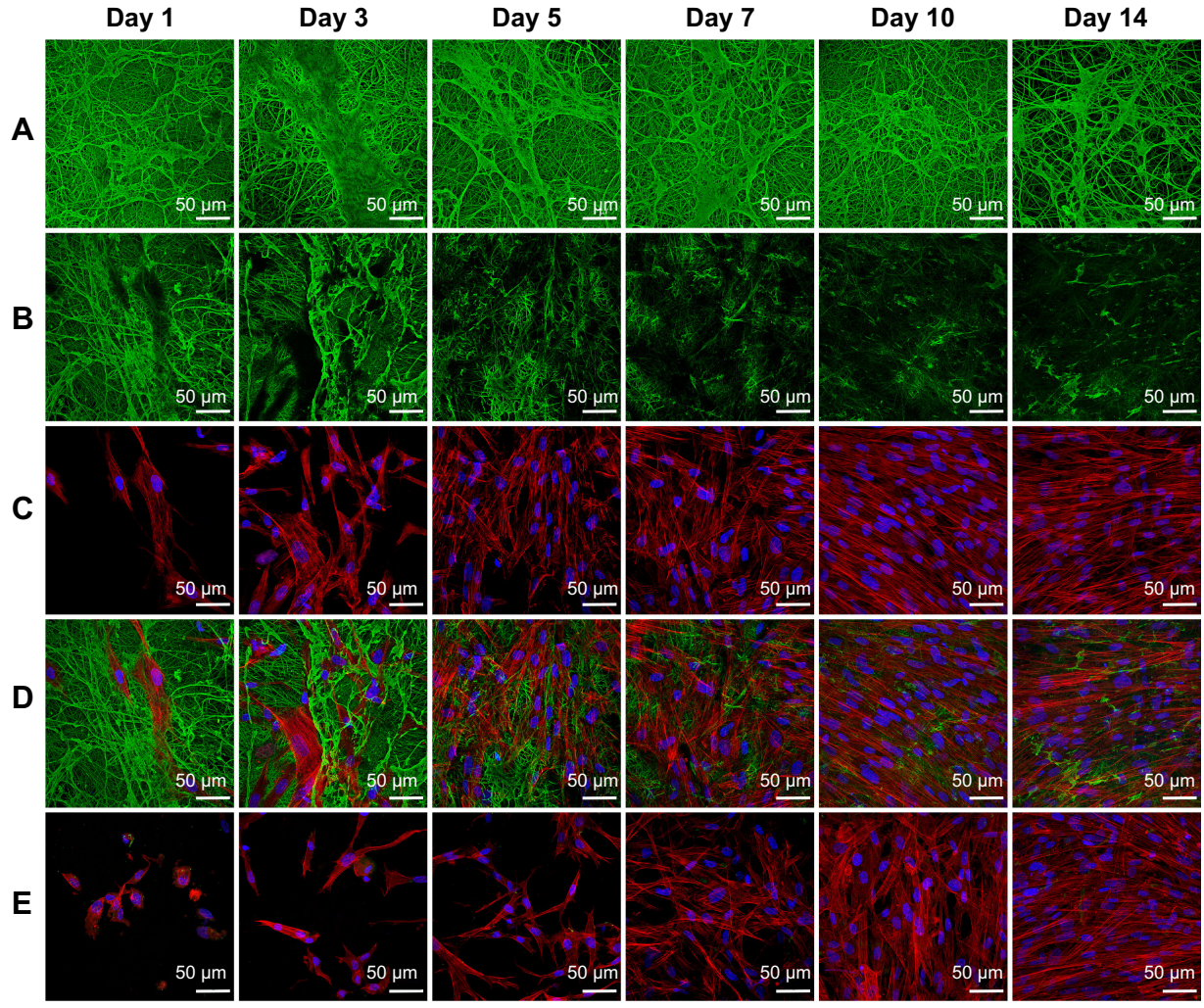

Figure 3 Morphology of the fibrin nanocoating (green) on PLA membranes in six cell culture intervals incubated without cells at 37°C, 5% CO_2 (**A**), incubated with human dermal fibroblasts (**B** – only fibrin nanocoating, **C** – only cells, **D** – fibrin nanocoating with cells). Cells on nonmodified PLA membranes (**E**).
Notes: Cells cultivated in the standard cell culture medium. The fibrin nanocoating was stained by immunofluorescence. The cells were stained with phalloidin conjugated with TRITC and Hoechst #33258. Leica TCS SPE DM2500 confocal microscope, obj 40×/1.15 NA oil.
Abbreviations: PLA, polylactide; obj, objective; NA, numerical aperture; PLA F, fibrin nanocoating on PLA.

fibrin was degraded on the membrane surface. In the deeper layers of the membrane, where the cells did not penetrate, the fibrin remained in unchanged form. The same results were obtained on the samples cultivated in the cell culture medium supplemented with AA (data not shown).

The morphology of the cells was different on nonmodified membranes and on membranes coated with fibrin. On the fibrin-modified membranes, the cells were well-spread already on day 1 after cell seeding, whereas on the nonmodified membrane, some cells were still round in shape even after 3 days of cell cultivation. The cell density was higher on the membranes coated with fibrin than on the nonmodified membranes (Figure 3C and D).

Cell metabolic activity, proliferation, adhesion, and morphology on PLA membranes

The cell mitochondrial metabolic activity, which correlates with cell proliferation, was significantly higher on the membranes coated with fibrin than on the nonmodified membranes from days 1 to 10 after cell seeding. These differences did not become nonsignificant until day 14. Differences in cell proliferation were found on the samples cultivated in the standard cell culture medium and also on the samples cultivated in the medium with AA. On the control polystyrene culture dishes, the cell metabolic activity decreased significantly after 1 week of cell cultivation and was lower than on the membranes coated with fibrin. Moreover, on day 14, the cell proliferation on the control polystyrene was significantly lower than on all types of nanofibrous membranes. AA added into the cell culture medium after 3 days of cell cultivation significantly increased the cell metabolic activity on all types of samples, mainly on days 5, 7, and 10 after cell seeding (Figure 4).

The cell metabolic activity on nonmodified and modified membranes and on the control polystyrene increased with the time of cell cultivation (Figure 4), which indicates increasing density of the cells (Figures 5 and 6). The cells adhered in greater densities on membranes coated with fibrin than on nonmodified membranes (Figures 5 and 6, days 1–7). On day 7, the cells on fibrin were confluent, whereas there were free spaces among the cells on the nonmodified membranes. On day 14, the cells formed confluent monolayers on all types of samples. In addition, the cells on fibrin-coated membranes were better spread than the cells on nonmodified membranes (Figure 5). The addition of AA further stimulated the cell proliferation, which was manifested by their higher population density than that in the medium without AA. This was particularly apparent on the pure PLA (Figure 6).

β_1-Integrins were evaluated as a molecular marker of cell adhesion. Relative mRNA expression of these integrins changed during cell cultivation. On day 7 after seeding, the

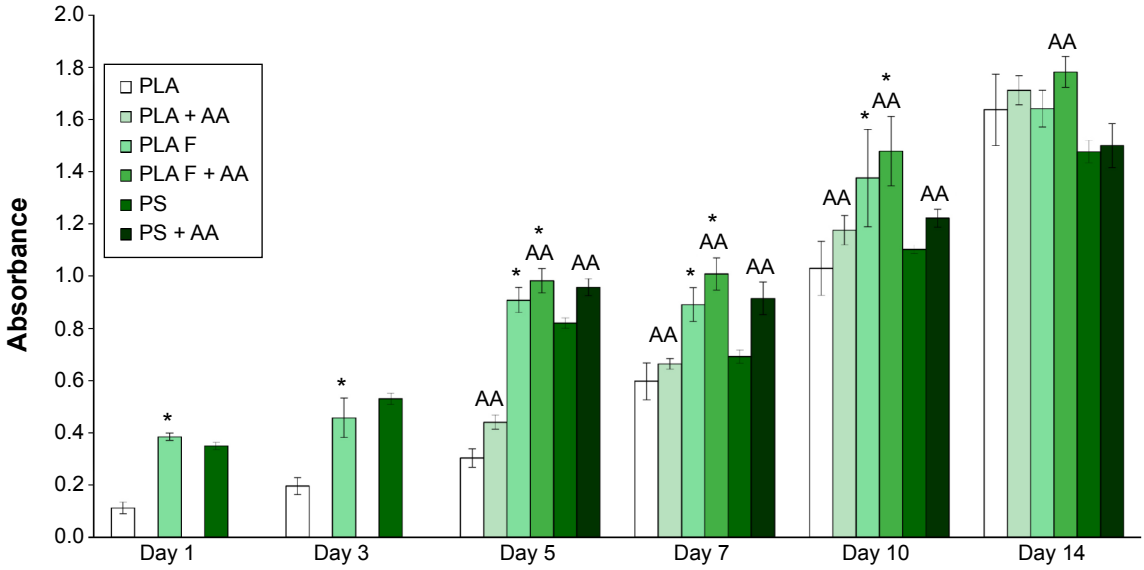

Figure 4 Mitochondrial activity in human dermal fibroblasts determined by an MTS assay in six time intervals (on days 1, 3, 5, 7, 10, and 14 after cell seeding) on nonmodified PLA membranes or on PLA membranes with a fibrin nanocoating (F).

Notes: Cells cultivated in the standard cell culture medium or in a medium supplemented with AA. The PSs were used as a control material. Arithmetic mean ± SD from 16 measurements made on four independent samples for each experimental group and time interval. ANOVA, Student–Newman–Keuls method, statistical significance ($P \leq 0.05$): *compared with a nonmodified PLA membrane in the standard cell culture medium or in the medium with AA, and AA compared with membranes in the standard cell culture medium.

Abbreviations: PLA, polylactide; AA, 2-phospho-L-ascorbic acid trisodium salt; PSs, polystyrene culture dishes; SD, standard deviation; ANOVA, analysis of variance; PLA F, fibrin nanocoating on PLA.

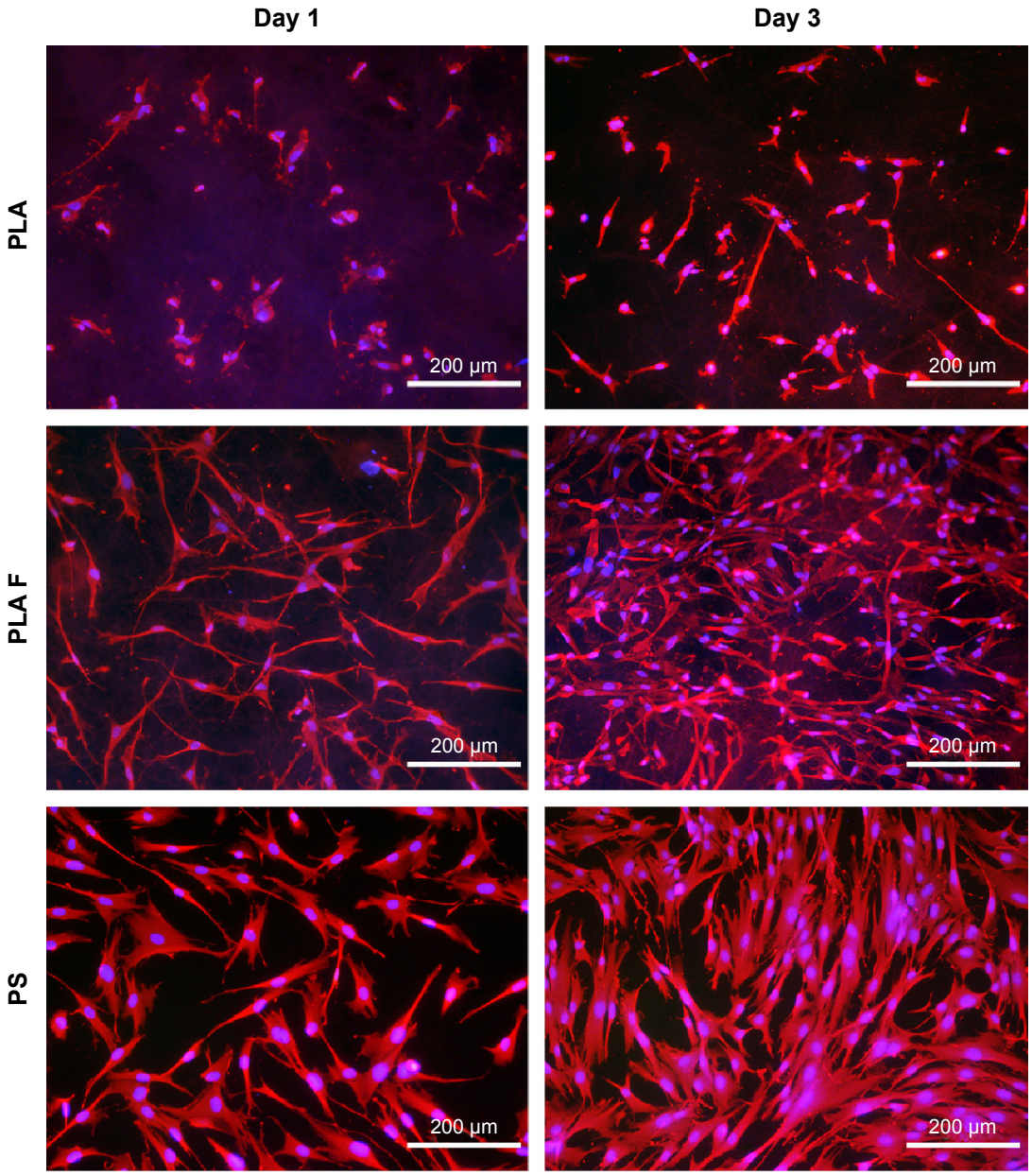

Figure 5 Morphology of human dermal fibroblasts on days 1 and 3 after seeding on nonmodified PLA membranes, or on PLA membranes with a fibrin nanocoating (F).
Notes: Cells cultivated in the standard cell culture medium. The PS was used as a control material. Cells stained with Texas Red C_2-Maleimide and Hoechst #33258. Olympus IX 51 microscope, obj 10×, DP 70 digital camera.
Abbreviations: PLA, polylactide; PS, polystyrene culture dish; obj, objective.

integrin expression was lower on nonmodified membranes compared to membranes coated with fibrin or to control polystyrene. However, on day 10 after seeding, the expression of β_1-integrins was significantly higher on nonmodified membranes than on fibrin-modified membranes. Moreover, on nonmodified membranes, the integrin expression was two times higher on day 10 than on day 7. On day 14 after seeding, the expression on nonmodified membranes, fibrin-modified membranes, and control polystyrene dishes was comparable. AA added into culture medium did not significantly influence β_1-integrin expression. The most apparent (but not significant) positive effect of AA on the increase of β_1-integrin expression was observed in cells on nonmodified membranes on day 10 (Figure 7).

Focal adhesions (FA) containing β_1-integrins were localized preferentially on the cell edges, and thus they were better observable in cells at earlier culture intervals (ie, on day 3, Figure 8) than at later intervals when the cells formed a confluent layer (ie, on day 7, data not shown). On day 3 after seeding (ie, 2 days after adding of AA), FA were better

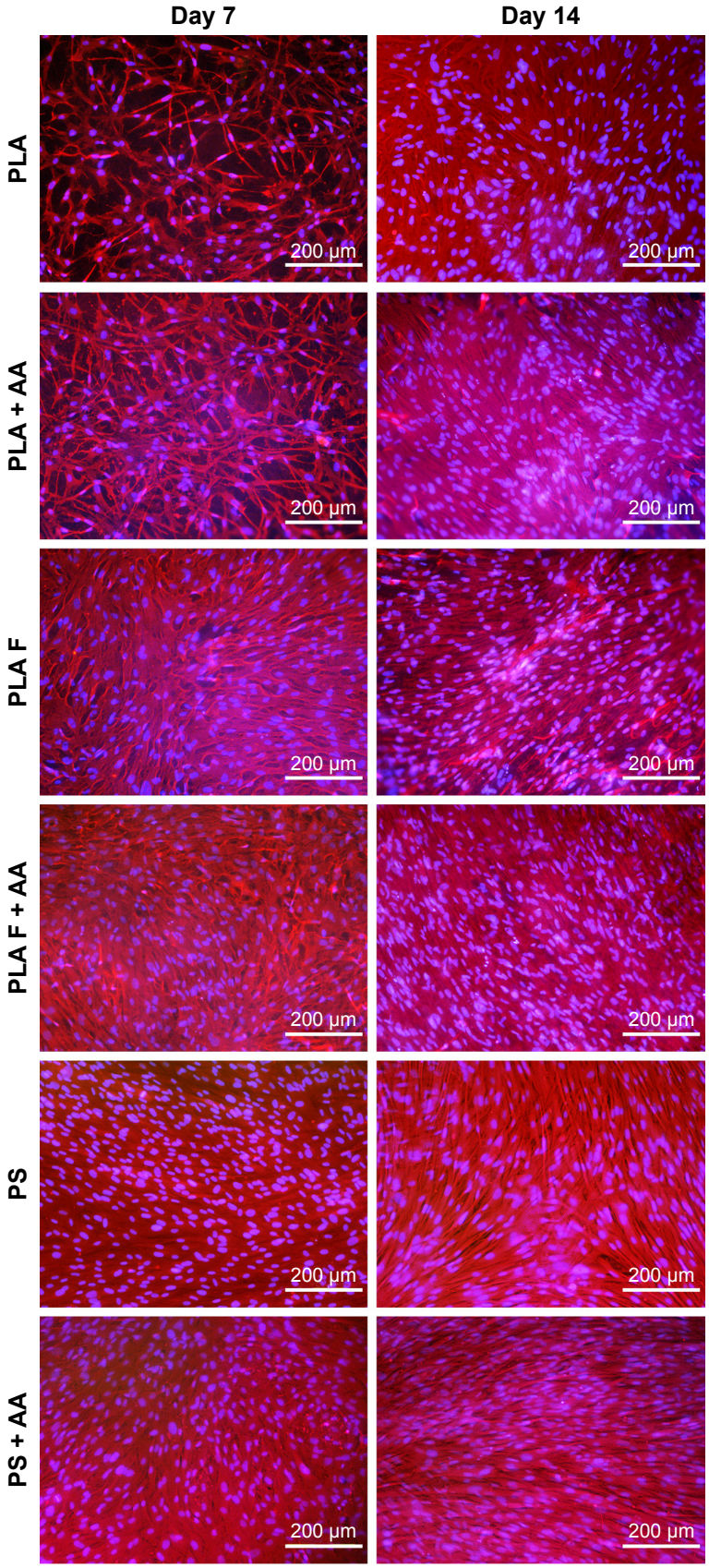

Figure 6 Morphology of human dermal fibroblasts on days 7 and 14 after seeding on nonmodified PLA membranes or on PLA membranes with a fibrin nanocoating (F).
Notes: Cells cultivated in the standard cell culture medium or in the medium supplemented with AA. The PS was used as a control material. Cells stained with Texas Red C2-Maleimide and Hoechst #33258. Olympus IX 51 microscope, obj 10×, DP 70 digital camera.
Abbreviations: PLA, polylactide; AA, 2-phospho-L-ascorbic acid trisodium salt; PS, polystyrene culture dish; obj, objective.

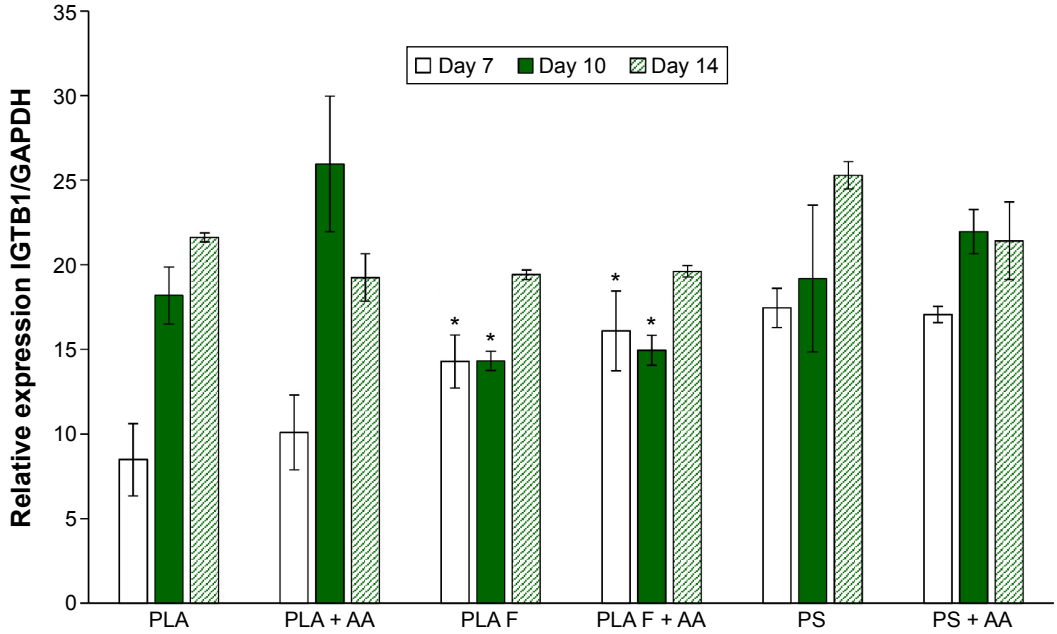

Figure 7 Relative expression of β_1-integrins in human dermal fibroblasts on days 7, 10, and 14 after seeding on nonmodified PLA membranes or on PLA membranes with a fibrin nanocoating (F) determined by real-time PCR.

Notes: The cells were cultivated in the standard cell culture medium or in the medium supplemented with AA. The PS served as a control material. Reference gene GAPDH. ANOVA, Student–Newman–Keuls method, statistical significance ($P \leq 0.05$): *in comparison with the nonmodified PLA membrane in the standard cell culture medium or in the medium with AA.

Abbreviations: PLA, polylactide; PCR, polymerase chain reaction; AA, 2-phospho-L-ascorbic acid trisodium salt; PS, polystyrene culture dish; GAPDH, glyceraldehyde 3-phosphate dehydrogenase; ANOVA, analysis of variance.

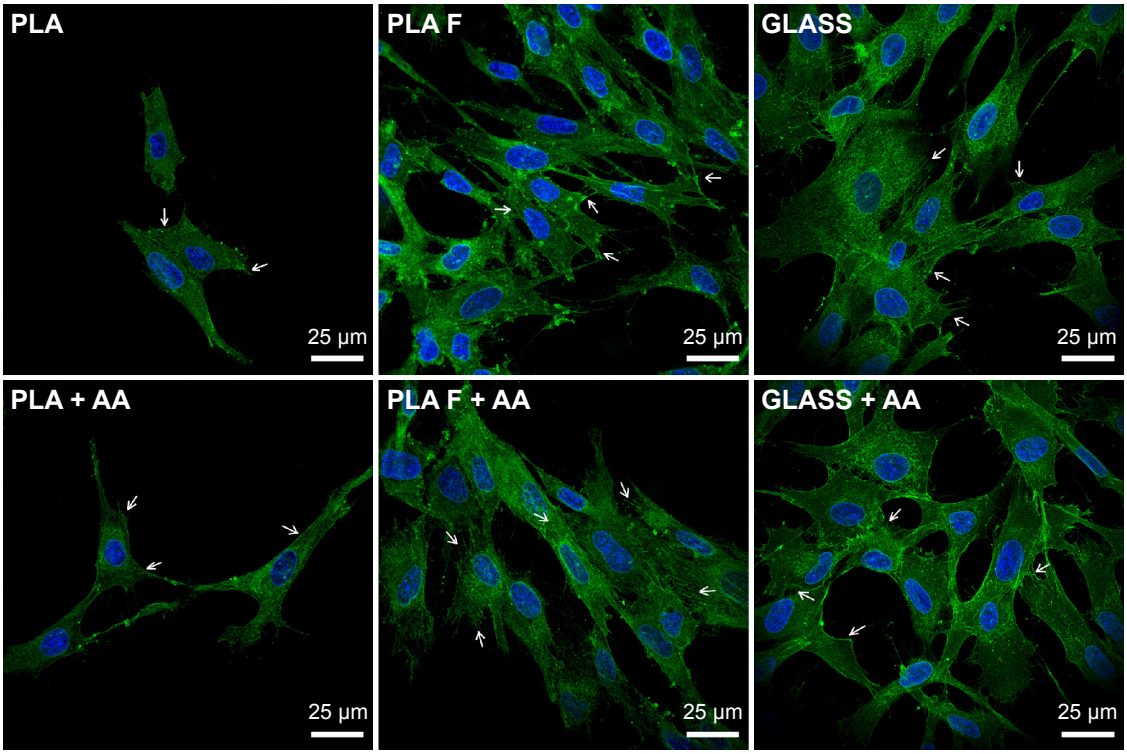

Figure 8 Immunofluorescence staining of β_1-integrins in human dermal fibroblasts on day 3 after seeding on nonmodified PLA membranes or on PLA membranes with a fibrin nanocoating (F).

Notes: Arrows show focal adhesions containing β_1-integrins. The cells were cultivated in the standard cell culture medium or in the medium supplemented with AA. Microscopic glass coverslips (GLASS) served as a control material. Cell nucleus stained with Hoechst #33258 (blue). Leica TCS SPE DM2500 confocal microscope, obj 63×/1.3 NA oil.

Abbreviations: PLA, polylactide; AA, 2-phospho-L-ascorbic acid trisodium salt; obj, objective; NA, numerical aperture.

developed in cells on fibrin-modified membranes than on nonmodified membranes. Positive influence of AA added into the culture medium was slightly apparent on nonmodified membranes, where the FA were better visible in the cells cultured in medium supplemented with AA than in standard medium. On fibrin-modified membranes, the influence of AA was not observed (Figure 8).

Collagen production by human dermal fibroblasts

The relative mRNA expression of collagen I, determined by real-time PCR, was estimated in three time cell culture intervals on days 7, 10, and 14. Collagen I expression was significantly higher on membranes coated with fibrin than on nonmodified membranes at all three time intervals of cell cultivation. After 10 days of cell cultivation, the positive effect of AA on collagen I expression began to be manifested. On day 10 after cell seeding, the expression of collagen I was significantly increased by adding AA into the cell culture medium only on the nonmodified membranes. On day 14, adding AA into the cell culture medium also increased collagen I expression on membranes coated with fibrin. The highest collagen I expression values of all the tested samples were reached on these membranes (Figure 9).

Collagen I expression was significantly lower on the nonmodified membranes than on the control polystyrene dishes. Collagen I expression on the membranes coated with fibrin was comparable to the expression on the control polystyrene dishes, or was slightly lower. However, the difference in expression was not statistically significant. On membranes coated with fibrin and incubated in the cell culture medium with AA for 14 days, the cells expressed the highest quantity of mRNA for collagen I, and this expression was significantly higher than that on the control polystyrene dishes (Figure 9). Collagen I expression increased significantly with the cell cultivation time, except in the case of the cells cultivated on the control polystyrene dishes (Figure 9).

Immunofluorescence staining of collagen I revealed that AA stimulated the cells to form extracellular collagen fibers deposited on the substrate surface after 1 week of cell cultivation (Figure 10). The cells cultivated in the standard cell culture medium without AA synthetized collagen but did not form a fibrous ECM (Figure 11). The collagen remained inside the cells or was probably released into the cell culture medium. After 2 weeks of cultivation, the cells started to deposit small amounts of collagen in ECM on the material surface (Figure 10). On day 14, the expression of collagen I in the cells cultivated in the standard cell culture medium on

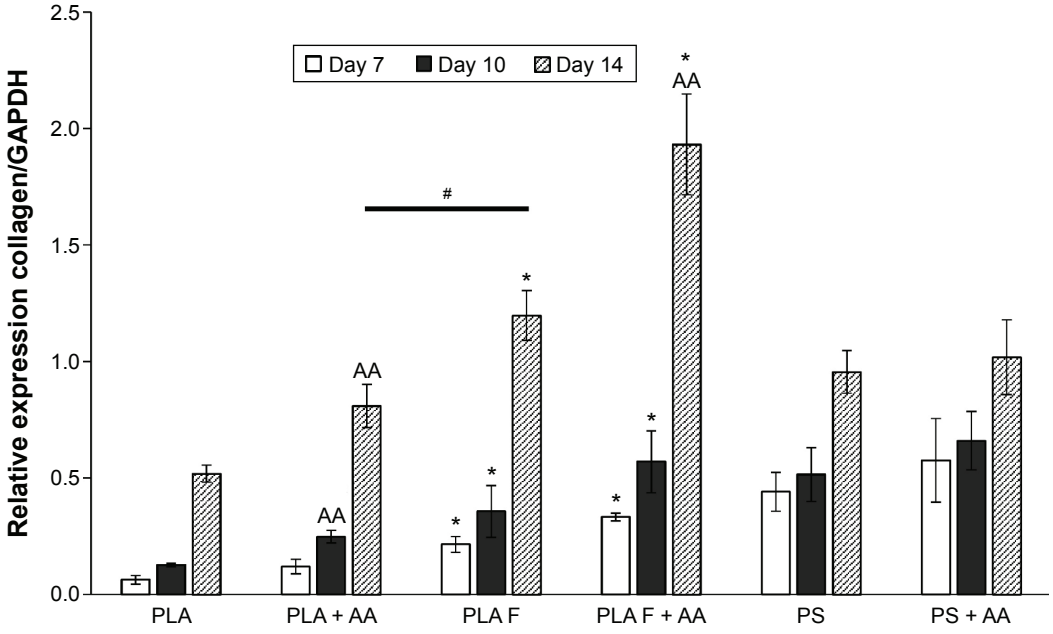

Figure 9 Relative expression of collagen I in human dermal fibroblasts on days 7, 10, and 14 after cell seeding on nonmodified PLA membranes or on PLA membranes with a fibrin nanocoating (F) determined by real-time PCR.

Notes: The cells were cultivated in the standard cell culture medium or in the medium supplemented with AA. The PS served as a control material. Reference gene GAPDH. ANOVA, Student–Newman–Keuls method, statistical significance ($P \leq 0.05$): *in comparison with the nonmodified PLA membrane in the standard cell culture medium or in the medium with AA, AA in comparison with membranes in the standard cell culture medium, and #statistical significance between PLA + AA and PLA F on day 14.

Abbreviations: PLA, polylactide; PCR, polymerase chain reaction; AA, 2-phospho-L-ascorbic acid trisodium salt; PS, polystyrene culture dish; GAPDH, glyceraldehyde 3-phosphate dehydrogenase; ANOVA, analysis of variance.

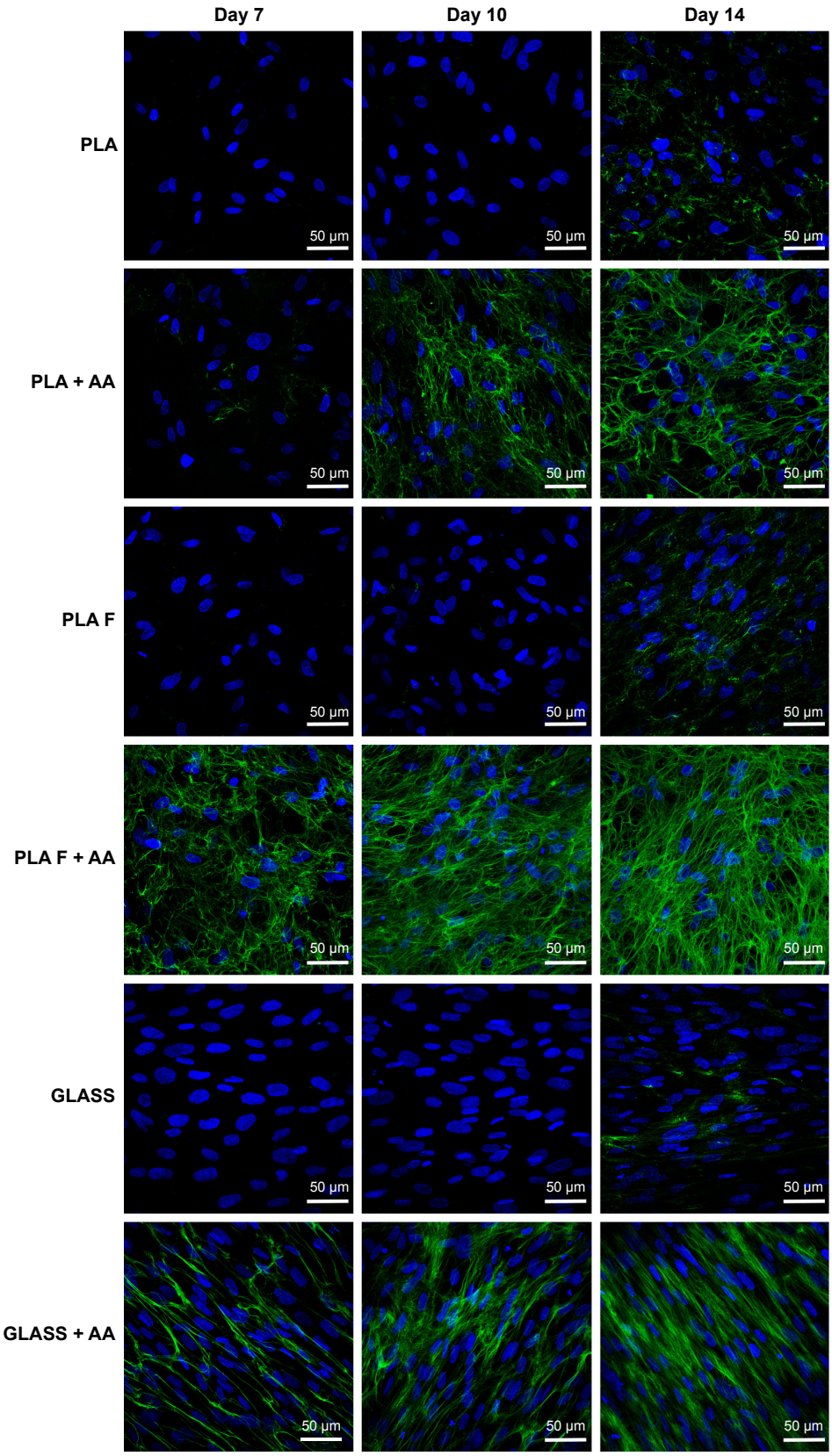

Figure 10 Immunofluorescence staining of extracellular collagen I fibers (green) produced by human dermal fibroblasts on days 7, 10, and 14 after seeding on nonmodified PLA membranes or on PLA membranes with a fibrin nanocoating (F).
Notes: The cells were cultivated in the standard cell culture medium or in the medium supplemented with AA. Microscopic glass coverslips (GLASS) served as a control material. Cell nucleus stained with Hoechst #33258 (blue). Leica TCS SPE DM2500 confocal microscope, obj 40×/1.15 NA oil.
Abbreviations: PLA, polylactide; AA, 2-phospho-L-ascorbic acid trisodium salt; obj, objective; NA, numerical aperture.

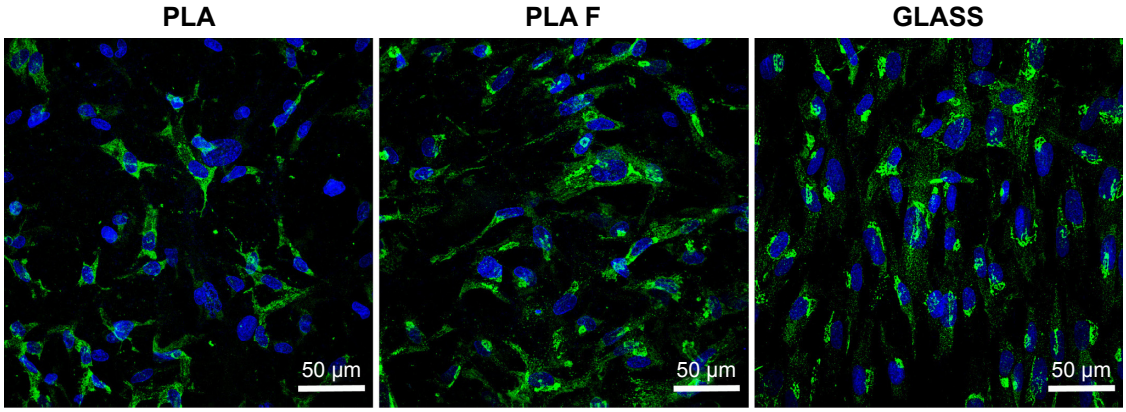

Figure 11 Immunofluorescence staining of total type I collagen (green) in human dermal fibroblasts on day 14 after cell seeding on nonmodified PLA membranes or on PLA membranes with a fibrin nanocoating (F).
Notes: The cells were cultivated in the standard cell culture medium. Microscopic glass coverslips (GLASS) served as a control material. Cell nucleus stained with Hoechst #33342 (blue). Leica TCS SPE DM2500 confocal microscope, obj 40×/1.15 NA oil.
Abbreviations: PLA, polylactide; obj, objective; NA, numerical aperture.

the membranes coated with fibrin was significantly higher than that in the cells cultivated in the medium with AA on the nonmodified membranes (Figure 9). However, the cells did not form well-developed fibrous collagen ECM on the membrane surface (Figure 10).

On day 7 after cell seeding, the cells cultivated with AA on membranes coated with fibrin formed well-developed collagen fibers on the membrane surface. However, the cells cultivated with AA on nonmodified membranes formed only relatively small amounts of collagen ECM. On days 10 and 14 after cell seeding, the fibrin with AA continued to stimulate the cells to form collagen ECM.

The overall (total) collagen production by the cells cultivated in the medium with AA was measured after 14 days of cell cultivation, using a Sircol kit. The amount of collagen was adjusted to the amount of cell DNA (Figure 12A) or

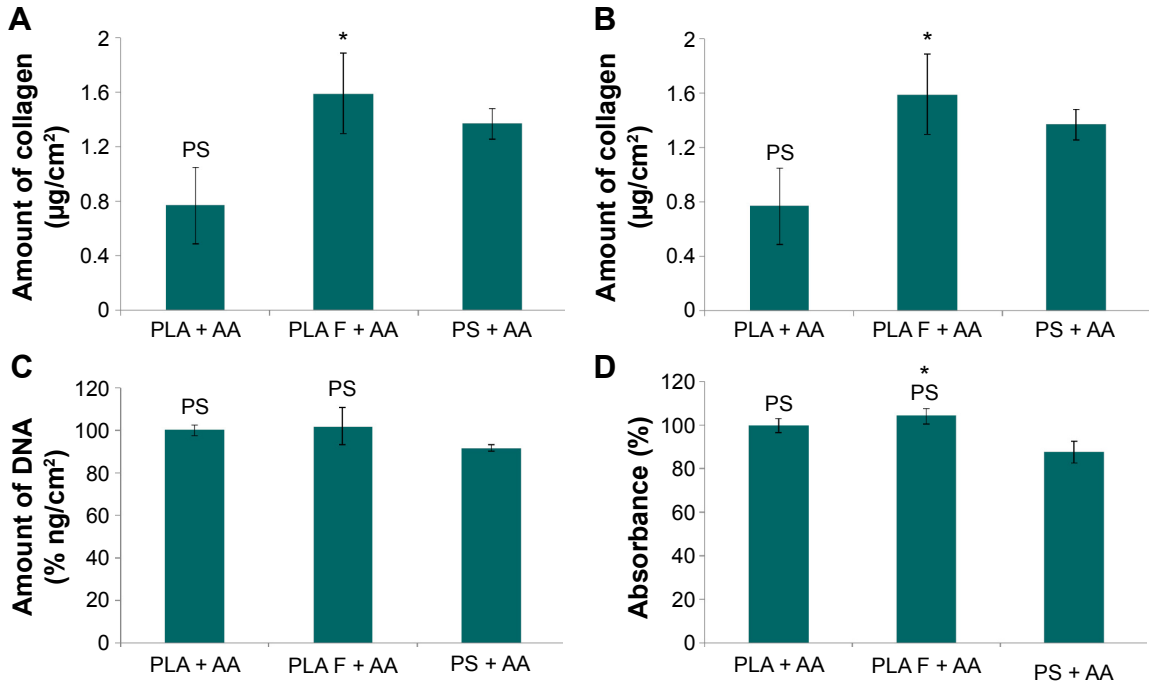

Figure 12 Total amount of type I collagen produced by human dermal fibroblasts on day 14 after seeding on nonmodified PLA membranes or on PLA membranes with a fibrin nanocoating (F).
Notes: Cells cultivated with AA added into the cell culture medium. The PS was used as a control material. Amount of collagen adjusted to the amount of cell DNA (**A**) or to the cell mitochondrial activity (**B**). Amount of cell DNA determined by a Picogreen assay (**C**). Cell mitochondrial activity determined by an MTS assay (**D**). Arithmetic mean ± SEM from 12 measurements made on four independent samples for each experimental group. ANOVA, Student–Newman–Keuls method, statistical significance ($P \leq 0.05$): *compared to a nonmodified PLA membrane, PS compared to the PS.
Abbreviations: PLA, polylactide; AA, 2-phospho-L-ascorbic acid trisodium salt; PS, polystyrene culture dish; SEM, standard error of mean; ANOVA, analysis of variance.

to the cell metabolic activity (Figure 12B). The amount of cell DNA was comparable on nonmodified membranes and on membranes coated with fibrin (Figure 12C), whereas the cell metabolic activity on the membranes coated with fibrin was slightly higher than that on the nonmodified membranes (Figure 12D). The amount of cell DNA and cell metabolic activity on the control polystyrene dishes was significantly lower than that on the PLA membranes (Figure 12C and D).

Collagen production was significantly higher on membranes coated with fibrin than on nonmodified membranes. The amount of collagen on the control polystyrene dishes was significantly higher than that on the nonmodified membranes and was comparable to the amount on the membranes coated with fibrin (Figure 12A and B).

Discussion

The ideal skin substitute mimics the physiology and the mechanical properties of normal skin, enables nutrition supply, accelerates skin tissue regeneration, and is not subject to immune activation. Unfortunately, most of the clinically used skin substitutes have not yet achieved all of these properties. These substitutes mostly serve as a temporary coverage, and they are eventually replaced by scar tissue.[42] A promising approach is to develop inexpensive biodegradable carriers of skin cells with desirable properties available in any quantity needed. This study, including our earlier study,[7] proved that these carriers can be based on modified PLA nanofibrous scaffolds. These scaffolds can be expected to promote the formation of both epidermis and dermis layers. Modification of nanofibrous PLA membranes by plasma in our earlier study enhanced the adhesion and growth of human keratinocytes, while modification with fibrin in this study enhanced the adhesion and growth of human dermal fibroblasts and the synthesis of collagen I by these cells, which is necessary for the additional cell ingrowth.[24] Our further plan is to develop keratinocyte and fibroblast layers on the opposite sides of the same nanofibrous membrane. This membrane will enable physical and biochemical communication between fibroblasts and keratinocytes together with the diffusion of nutrients, growth factors, and other biologically active molecules from the culture medium or from the surrounding tissue.[15] It has been reported that bilayered tissue-engineered skin constructs were more efficient in healing full-thickness skin defects in sheep than single-layer constructs composed of only fibroblasts or keratinocytes.[43]

In the first part of this study, we investigated the influence of fibrin deposited on a nanofibrous membrane, and AA added into the cell culture medium, on the adhesion and proliferation of human dermal fibroblasts. Our results show that fibrin deposition led to markedly improved cell adhesion and spreading compared to the membrane without fibrin. On the membranes with fibrin, the cells were well-spread with well-developed typical FA containing β_1-integrins and polygonal in shape, whereas on the nonmodified membranes, the cells were round until the third day of cell cultivation and with less developed β_1-integrin-containing FA. β_1-Integrins, namely $\alpha_5\beta_1$ integrins (together with $\alpha_v\beta_3$ and $\alpha_v\beta_3$ integrins), mediate the adhesion of fibroblasts to fibrin molecules, in which these adhesion receptors recognize the RGD motifs.[24,44] The group of β_1-integrins also include receptors for collagen, namely $\alpha_1\beta_1$, $\alpha_2\beta_1$, and $\alpha_3\beta_1$ integrins. The expression and production of collagen was increased on fibrin-coated membranes, particularly in the medium with AA, which could contribute to the improved cell adhesion on the modified PLA membranes. Moreover, through the αC domain, the fibrin attracts molecules of ECM from the cell culture medium, such as fibronectin and vitronectin that further support cell adhesion.[24] On nonmodified membranes, cell adhesion is mediated practically only through ECM molecules spontaneously adsorbed from the cell culture medium or deposited on the membrane surface by the cells. In addition, these molecules could be adsorbed in an insufficient quantity and with an inappropriate spatial conformation for recognition by cell adhesion receptors.

The better developed β_1-integrin-containing FA in cells on fibrin-coated membranes correlated with relative mRNA expression of this adhesion receptor. At earlier cell culture interval (on day 7 after seeding), the fibrin nanocoating increased relative β_1-integrin expression. This could be explained by a more intense proliferation of cells on these coatings, which resulted in a higher formation of new cells and their need to express and synthesize integrin receptors in order to adhere to their growth support. In addition, as mentioned earlier, the fibrin coatings (together with increased amount of collagen deposited on these coatings) provided a higher number of adhesion ligands (eg, RGD motifs), which could also increase the β_1-integrin expression. Nevertheless, on day 10, the β_1-integrin expression became higher on nonmodified membranes than that on fibrin-coated membranes. An explanation could be that the cell proliferation and new cell formation, which were delayed on pure PLA membranes, reached their maximum on day 10, while the cells on fibrin-coated PLA membranes reached confluence and slowed down their proliferation. On day 14, the MTS assay indicated that the cell proliferation on fibrin-modified and nonmodified membranes was similar. The β_1-integrin expression was also comparable in cells on both types of

membranes. In addition, the β_1-integrin expression in cells on pure PLA membranes was stimulated, although slightly, by addition of AA into the cell culture medium, which suggests that these cells started focusing on ECM synthesis rather than on cell proliferation.

Fibroblast proliferation was also markedly increased on the fibrin-coated membranes, which is in accordance with many studies published earlier.[19,33] Fibrin can stimulate fibroblast proliferation via the alpha and beta chains present in fibrinogen and fibrin molecules,[45] by the presence of thrombin, a potent mitogen for fibroblasts, in fibrin matrices,[46] and also by stimulating the autocrine production of growth factors in cells by fibrin. In keratinocytes, fibrin stimulated the autocrine production of transforming growth factor alpha through the epidermal growth factor receptor.[47] Fibrin also partially restored the ability of senescent and growth-arrested human dermal fibroblasts to continue replicating.[48]

However, after 2 weeks of cell cultivation, the cell proliferation (measured by cell metabolic activity) on membranes with fibrin became similar to the cell proliferation on the nonmodified membranes, which probably correlated with the degree of fibrin degradation. During cell cultivation, fibrin is physiologically reorganized and is degraded by the cells and replaced by newly synthesized ECM.[28,49] On the membrane surface, the fibrin was degraded by the cells and remained only in the deeper layers of the membrane, where the cells did not penetrate. The degraded fibrin probably suppressed the cell proliferation and stimulated the cells to synthesize ECM molecules and to deposit them on the membrane surface. Similar results were obtained in a fibrin gel after it was contracted and partially degraded by human skin fibroblasts. These cells proliferated more slowly but deposited a greater amount of collagen than the cells in monolayers on culture dishes.[28]

After 1 week of cell cultivation, the cell proliferation on the control polystyrene dishes decreased significantly. On day 14, the cell proliferation on the control polystyrene dishes was even significantly lower than that on all types of samples of nanofibrous membrane. The decline in cell proliferation could be caused by cell contact inhibition on two-dimensional polystyrene dishes,[28] whereas the three-dimensional structure of the nanofibrous membrane enabled cell penetration inside the membrane, ie, it provided more space for cell growth, and thus delayed contact inhibition of the cell growth.

We also found that AA added into the cell culture medium increased cell proliferation but did not significantly influence cell adhesion, as manifested by the expression of β_1-integrins. Increased cell proliferation was apparent already 2 days after AA treatment and continued to day 10 after cell seeding. Previously published results showed that AA increased the proliferation of dermal fibroblasts,[50,51] and this positive effect was more apparent in fibroblasts from elderly donors than in fibroblasts from newborn donors.[52] On day 14, AA had no significant effect on increasing the cell proliferation. This was probably due to the fact that the cells concentrated on ECM synthesis and deposition and stopped proliferating.

In the second part of the study, we focused on collagen production by human dermal fibroblasts stimulated by AA added into the cell culture medium and cultivated on membranes coated with fibrin. We found that fibrin deposited on nanofibrous membranes increased the relative expression and synthesis of type I collagen and the formation of collagen ECM on the material surface. After 1 week of cell cultivation, the cells cultivated on nonmodified membranes deposited collagen ECM only slightly, while the cells cultivated on membranes with fibrin formed a well-developed network of collagen fibers. Sclafani and McCormick found that platelet-rich fibrin matrix injected into the dermis activated dermal fibroblasts to form new collagen.[53] Mazlyzam et al constructed a fibrin scaffold seeded with skin cells. They found newly formed collagen fibers produced by dermal fibroblasts in the dermal layer of the scaffold. The dermal fibroblasts also showed expression of type I collagen at the mRNA level.[19] As mentioned earlier, fibrin-based matrices deposited on poly(lactide-glycolide-caprolactone) nanofibrous scaffolds or on polystyrene dishes also stimulated the production of collagen in dermal fibroblasts.[28,33]

It has been reported repeatedly that ascorbic acid is important for collagen formation by cells. Ascorbic acid helps to catalyze the hydroxylation of lysine and proline amino acids, important components that form stable mature collagen with a triple-helical structure.[25,54] Hydroxyproline stabilizes the collagen triple helix. Its absence results in unstable collagen, which cannot be secreted from the cells at a normal rate. Hydroxylysine is necessary for the crosslinking process of collagen.[55]

Our experiments proved that AA increased the expression of collagen I and stimulated the cells to deposit collagen fibers on the material surface. The cells cultivated in a standard cell culture medium (without AA) did not deposit a significant amount of collagen ECM on the material surface. The cells cultivated in the standard cultivation medium on the membranes coated with fibrin showed a higher expression of collagen I than the cells cultivated in the medium with AA on noncoated membranes. However, these cells did not deposit a considerable amount of fibrous collagen matrix on the material surface. This is in accordance with the study

by Murad et al, mentioned earlier, which revealed that cells cultivated without ascorbic acid are incapable of forming stable collagen fibers deposited on the material surface, but form only unstable collagen that remains inside the cells.[55] However, cells coated with fibrin secreted a greater amount of collagen fibers in the medium with AA than on uncoated membranes in the same medium (Figure 8).

The insoluble extracellular collagen fibers on the material surface did not form directly after the addition of AA into the cell cultivation medium, but formed after 1 week of cell cultivation (ie, after adding AA into the cell cultivation medium for 4 days). The explanation could be that this longer period is needed for the transition of newly synthesized procollagen into insoluble collagen fibrils.[55]

Similarly, the positive effect of AA on collagen I gene expression was not manifested until 10 days of cell cultivation. On day 10, this effect was significant only on nonmodified membranes. On day 14, increased collagen I expression with the addition of AA into the medium was also detected on membranes coated with fibrin. A possible explanation could be that on day 10, collagen I expression was predominantly stimulated by fibrin. However, on day 14, the fibrin nanocoating was almost degraded and AA played a major role in stimulating the cells to collagen expression.

The mRNA collagen I expression and the amount of collagen ECM that was formed increased significantly with the time of cell cultivation, except in the case of the control polystyrene dishes. de Clerck and Jones cultivated rat smooth muscle cells in a cultivation medium with AA and showed that the level of collagen expression increased with time of cultivation.[54] Moreover, it is known that ascorbic acid increased the steady-state level of procollagen mRNA.[25]

Conclusion

The fibrin nanocoating on PLA nanofibrous membranes strongly influenced the behavior of human dermal fibroblasts. Fibrin promoted adhesion and spreading of cells and increased the expression of β_1-integrins, cell proliferation, and collagen synthesis. The beneficial effect of fibrin on the adhesion and proliferation of cells was probably due to its ability to easily bind to cells through the integrin adhesion receptors, to attract the adhesive molecules from the cell culture medium. It was probably also due to its mitogenic effects on the cells. Fibrin increased the mRNA expression of collagen I, the total amount of synthesized collagen, and its deposition as ECM on the membrane surface. AA added into the cell culture medium also promoted cell proliferation, increased collagen I expression, and also slightly improved the expression of β_1-integrins on the uncoated PLA membranes. In addition, ascorbic acid was important for collagen ECM deposition on the membrane surface due to its catalyzing effect for stable collagen fiber formation. Taken together, the combination of fibrin and AA was the most efficient way to stimulate the growth of dermal fibroblasts and the expression, synthesis, and deposition of collagen by these cells.

Acknowledgments

This study was supported by the Grant Agency of Charles University in Prague (Grant No 38214), by the Grant Agency of the Czech Republic (Grant No P108/12/G108) and by the project ''BIOCEV – Biotechnology and Biomedicine Centre of the Academy of Sciences and Charles University'' (CZ.1.05/1.1.00/02.0109). Mr Robin Healey (Czech Technical University in Prague) is gratefully acknowledged for his language revision of the manuscript.

Disclosure

The authors report no conflicts of interest in this work.

References

1. Bacakova L, Filova E, Parizek M, Ruml T, Svorcik V. Modulation of cell adhesion, proliferation and differentiation on materials designed for body implants. *Biotechnol Adv*. 2011;29(6):739–767.
2. Sun L, Stout DA, Webster TJ. The nano-effect: improving the long-term prognosis for musculoskeletal implants. *J Long Term Eff Med Implants*. 2012;22(3):195–209.
3. Sridhar S, Venugopal JR, Ramakrishna S. Improved regeneration potential of fibroblasts using ascorbic acid-blended nanofibrous scaffolds. *J Biomed Mater Res A*. 2015;103(11):3431–3440.
4. Seet WT, Manira M, Khairul Anuar K, et al. Shelf-life evaluation of bilayered human skin equivalent, MyDerm. *PLoS One*. 2012;7(8):e40978.
5. Niu HT, Lin T. Fiber generators in needleless electrospinning. *J Nanomater*. 2012;2012:13.
6. Yu DG, Zhu LM, Branford-White CJ, et al. Solid dispersions in the form of electrospun core-sheath nanofibers. *Int J Nanomedicine*. 2011;6:3271–3280.
7. Yu DG, Zhou J, Chatterton NP, Li Y, Huang J, Wang X. Polyacrylonitrile nanofibers coated with silver nanoparticles using a modified coaxial electrospinning process. *Int J Nanomedicine*. 2012;7:5725–5732.
8. Yu DG, Li XY, Wang X, Yang JH, Bligh SW, Williams GR. Nanofibers fabricated using triaxial electrospinning as zero order drug delivery systems. *ACS Appl Mater Interfaces*. 2015;7(33):18891–18897.
9. Chen G, Xu Y, Yu DG, Zhang DF, Chatterton NP, White KN. Structure-tunable Janus fibers fabricated using spinnerets with varying port angles. *Chem Commun (Camb)*. 2015;51(22):4623–4626.
10. Garric X, Moles JP, Garreau H, Guilhou JJ, Vert M. Human skin cell cultures onto PLA50 (PDLLA) bioresorbable polymers: influence of chemical and morphological surface modifications. *J Biomed Mater Res A*. 2005;72(2):180–189.
11. Hoveizi E, Nabiuni M, Parivar K, Rajabi-Zeleti S, Tavakol S. Functionalisation and surface modification of electrospun polylactic acid scaffold for tissue engineering. *Cell Biol Int*. 2014;38(1):41–49.
12. Bacakova M, Lopot F, Hadraba D, et al. Effects of fiber density and plasma modification of nanofibrous membranes on the adhesion and growth of HaCaT keratinocytes. *J Biomater Appl*. 2015;29(6):837–853.

13. Mo Y, Guo R, Liu J, et al. Preparation and properties of PLGA nanofiber membranes reinforced with cellulose nanocrystals. *Colloids Surf B Biointerfaces*. 2015;132:177–184.
14. Garric X, Vert M, Moles JP. Development of new skin substitutes based on bioresorbable polymer for treatment of severe skin defects. *Ann Pharm Fr*. 2008;66(5–6):313–318.
15. McMillan JR, Akiyama M, Tanaka M, et al. Small-diameter porous poly (epsilon-caprolactone) films enhance adhesion and growth of human cultured epidermal keratinocyte and dermal fibroblast cells. *Tissue Eng*. 2007;13(4):789–798.
16. El-Ghalbzouri A, Lamme EN, van Blitterswijk C, Koopman J, Ponec M. The use of PEGT/PBT as a dermal scaffold for skin tissue engineering. *Biomaterials*. 2004;25(15):2987–2996.
17. Altankov G, Albrecht W, Richau K, Groth T, Lendlein A. On the tissue compatibility of poly(ether imide) membranes: an in vitro study on their interaction with human dermal fibroblasts and keratinocytes. *J Biomater Sci Polym Ed*. 2005;16(1):23–42.
18. Monteiro IP, Gabriel D, Timko BP, et al. A two-component pre-seeded dermal-epidermal scaffold. *Acta Biomater*. 2014;10(12):4928–4938.
19. Mazlyzam AL, Aminuddin BS, Fuzina NH, et al. Reconstruction of living bilayer human skin equivalent utilizing human fibrin as a scaffold. *Burns*. 2007;33(3):355–363.
20. Helmedag MJ, Weinandy S, Marquardt Y, et al. The effects of constant flow bioreactor cultivation and keratinocyte seeding densities on prevascularized organotypic skin grafts based on a fibrin scaffold. *Tissue Eng Part A*. 2015;21(1–2):343–352.
21. Meana A, Iglesias J, Del Rio M, et al. Large surface of cultured human epithelium obtained on a dermal matrix based on live fibroblast-containing fibrin gels. *Burns*. 1998;24(7):621–630.
22. Rajangam T, An SS. Fibrinogen and fibrin based micro and nano scaffolds incorporated with drugs, proteins, cells and genes for therapeutic biomedical applications. *Int J Nanomedicine*. 2013;8:3641–3662.
23. Mutsaers SE, Bishop JE, McGrouther G, Laurent GJ. Mechanisms of tissue repair: from wound healing to fibrosis. *Int J Biochem Cell Biol*. 1997;29(1):5–17.
24. Laurens N, Koolwijk P, de Maat MP. Fibrin structure and wound healing. *J Thromb Haemost*. 2006;4(5):932–939.
25. Tajima S, Pinnell SR. Ascorbic acid preferentially enhances type I and III collagen gene transcription in human skin fibroblasts. *J Dermatol Sci*. 1996;11(3):250–253.
26. Park HJ, Ock SM, Kim HJ, et al. Vitamin C attenuates ERK signalling to inhibit the regulation of collagen production by LL-37 in human dermal fibroblasts. *Exp Dermatol*. 2010;19(8):E258–E264.
27. Geesin JC, Gordon JS, Berg RA. Regulation of collagen synthesis in human dermal fibroblasts by the sodium and magnesium salts of ascorbyl-2-phosphate. *Skin Pharmacol*. 1993;6(1):65–71.
28. Tuan TL, Song A, Chang S, Younai S, Nimni ME. In vitro fibroplasia: matrix contraction, cell growth, and collagen production of fibroblasts cultured in fibrin gels. *Exp Cell Res*. 1996;223(1):127–134.
29. Mazzone L, Pontiggia L, Reichmann E, Ochsenbein-Kolble N, Moehrlen U, Meuli M. Experimental tissue engineering of fetal skin. *Pediatr Surg Int*. 2014;30(12):1241–1247.
30. Ahmed TA, Dare EV, Hincke M. Fibrin: a versatile scaffold for tissue engineering applications. *Tissue Eng Part B Rev*. 2008;14(2):199–215.
31. Han CM, Zhang LP, Sun JZ, Shi HF, Zhou J, Gao CY. Application of collagen-chitosan/fibrin glue asymmetric scaffolds in skin tissue engineering. *J Zhejiang Univ Sci B*. 2010;11(7):524–530.
32. Gorodetsky R, Clark RA, An J, et al. Fibrin microbeads (FMB) as biodegradable carriers for culturing cells and for accelerating wound healing. *J Invest Dermatol*. 1999;112(6):866–872.
33. Nair RP, Joseph J, Harikrishnan VS, Krishnan VK, Krishnan L. Contribution of fibroblasts to the mechanical stability of in vitro engineered dermal-like tissue through extracellular matrix deposition. *Biores Open Access*. 2014;3(5):217–225.
34. Paxton JZ, Wudebwe UN, Wang A, Woods D, Grover LM. Monitoring sinew contraction during formation of tissue-engineered fibrin-based ligament constructs. *Tissue Eng Part A*. 2012;18(15–16):1596–1607.
35. Rampichova M, Buzgo M, Krizkova B, Prosecka E, Pouzar M, Strajtova L. Injectable hydrogel functionalised with thrombocyte-rich solution and microparticles for accelerated cartilage regeneration. *Acta Chir Orthop Traumatol Cech*. 2013;80(1):82–88.
36. Gurevich O, Vexler A, Marx G, et al. Fibrin microbeads for isolating and growing bone marrow-derived progenitor cells capable of forming bone tissue. *Tissue Eng*. 2002;8(4):661–672.
37. Adebayo O, Hookway TA, Hu JZ, Billiar KL, Rolle MW. Self-assembled smooth muscle cell tissue rings exhibit greater tensile strength than cell-seeded fibrin or collagen gel rings. *J Biomed Mater Res A*. 2013;101(2):428–437.
38. Williams C, Johnson SL, Robinson PS, Tranquillo RT. Cell sourcing and culture conditions for fibrin-based valve constructs. *Tissue Eng*. 2006;12(6):1489–1502.
39. Kubies D, Rypacek F, Kovarova J, Lednicky F. Microdomain structure in polylactide-block-poly(ethylene oxide) copolymer films. *Biomaterials*. 2000;21(5):529–536.
40. Novotna K, Zajdlova M, Suchy T, et al. Polylactide nanofibers with hydroxyapatite as growth substrates for osteoblast-like cells. *J Biomed Mater Res A*. 2014;102(11):3918–3930.
41. Riedel T, Brynda E, Dyr JE, Houska M. Controlled preparation of thin fibrin films immobilized at solid surfaces. *J Biomed Mater Res A*. 2009;88(2):437–447.
42. Eisenbud D, Huang NF, Luke S, Silberklang M. Skin substitutes and wound healing: current status and challenges. *Wounds*. 2004;16(1):2–17.
43. Idrus RB, Rameli MA, Low KC, et al. Full-thickness skin wound healing using autologous keratinocytes and dermal fibroblasts with fibrin: bilayered versus single-layered substitute. *Adv Skin Wound Care*. 2014;27(4):171–180.
44. Gailit J, Clarke C, Newman D, Tonnesen MG, Mosesson MW, Clark RA. Human fibroblasts bind directly to fibrinogen at RGD sites through integrin alpha(v)beta3. *Exp Cell Res*. 1997;232(1):118–126.
45. Gray AJ, Bishop JE, Reeves JT, Laurent GJ. A alpha and B beta chains of fibrinogen stimulate proliferation of human fibroblasts. *J Cell Sci*. 1993;104(pt 2):409–413.
46. Dawes KE, Gray AJ, Laurent GJ. Thrombin stimulates fibroblast chemotaxis and replication. *Eur J Cell Biol*. 1993;61(1):126–130.
47. Yamamoto M, Yanaga H, Nishina H, Watabe S, Mamba K. Fibrin stimulates the proliferation of human keratinocytes through the autocrine mechanism of transforming growth factor-alpha and epidermal growth factor receptor. *Tohoku J Exp Med*. 2005;207(1):33–40.
48. Acevedo CA, Brown DI, Young ME, Reyes JG. Senescent cultures of human dermal fibroblasts modified phenotype when immobilized in fibrin polymer. *J Biomater Sci Polym Ed*. 2009;20(13):1929–1942.
49. Nguyen DT, Orgill DP, Murphy GF. The pathofysiologic basis for wound healing regeneration. In: Orgill D, Bianco C, editors. *Biomaterials for Treating Skin Loss*. Cambridge: Woodhead Publishing; 2009:25–58.
50. Lima CC, Pereira AP, Silva JR, et al. Ascorbic acid for the healing of skin wounds in rats. *Braz J Biol*. 2009;69(4):1195–1201.
51. Taniguchi M, Arai N, Kohno K, Ushio S, Fukuda S. Anti-oxidative and anti-aging activities of 2-O-alpha-glucopyranosyl-L-ascorbic acid on human dermal fibroblasts. *Eur J Pharmacol*. 2012;674(2–3):126–131.
52. Phillips CL, Combs SB, Pinnell SR. Effects of ascorbic acid on proliferation and collagen synthesis in relation to the donor age of human dermal fibroblasts. *J Invest Dermatol*. 1994;103(2):228–232.
53. Sclafani AP, McCormick SA. Induction of dermal collagenesis, angiogenesis, and adipogenesis in human skin by injection of platelet-rich fibrin matrix. *Arch Facial Plast Surg*. 2012;14(2):132–136.
54. de Clerck YA, Jones PA. The effect of ascorbic acid on the nature and production of collagen and elastin by rat smooth-muscle cells. *Biochem J*. 1980;186(1):217–225.
55. Murad S, Grove D, Lindberg KA, Reynolds G, Sivarajah A, Pinnell SR. Regulation of collagen synthesis by ascorbic acid. *Proc Natl Acad Sci U S A*. 1981;78(5):2879–2882.

Protein nanocoatings on synthetic polymeric nanofibrous membranes designed as carriers for skin cells

Marketa Bacakova[1, 2], Julia Pajorova[1, 2], Denisa Stranska[3], Tomas Riedel[4], Eduard Brynda[4], Margit Zaloudkova[5], Lucie Bacakova[1]

[1]Dept. of Biomaterials and Tissue Engineering, Institute of Physiology, Czech Academy of Sciences, Czech Republic

[2]2nd Faculty of Medicine, Charles University in Prague, Czech Republic

[3]InStar Technologies, Czech Republic

[4]Institute of Macromolecular Chemistry, Czech Academy of Sciences, Czech Republic

[5]Institute of Rock Nanocoating and Mechanics, Czech Academy of Sciences, Czech Republic

Corresponding author

Marketa Bacakova, MSc., Institute of Physiology, Academy of Sciences of the Czech Republic, Videnska 1083, Prague 4, 14220, Czech Republic, Tel: +420 296 443 765, E-mail: marketa.bacakova@fgu.cas.cz

Key words: tissue engineering, nanocoating, nanofibers, needle-less electrospinning, skin, fibroblasts, keratinocytes, fibrin, collagen, fibronectin

Abstract

Protein-coated resorbable synthetic polymeric nanofibrous membranes are promising for the fabrication of advanced skin substitutes. We fabricated electrospun poly(L-lactide) and poly(L-lactide)-co-glycolide nanofibrous membranes and coated them with fibrin or collagen I. Fibronectin was attached to a fibrin or collagen nanocoating in order to further enhance the cell adhesion and spreading. Fibrin regularly formed a coating around individual nanofibers in the membranes, and also formed a thin fibrous mesh on several places on the membrane surface. Collagen also coated most of the fibers of the membrane and randomly created a soft gel on the membrane surface. Fibronectin predominantly adsorbed onto a thin fibrin mesh or a collagen gel and

formed a thin nanofibrous structure. Fibrin nanocoating greatly improved the attachment, spreading and proliferation of human dermal fibroblasts, whereas collagen nanocoating had a positive influence on the behavior of human HaCaT keratinocytes. In addition, fibrin stimulated the fibroblasts to synthesize fibronectin and to deposit it as an extracellular matrix. Fibronectin attached to fibrin or to a collagen coating further enhanced the adhesion, spreading and proliferation of both cell types.

1. Introduction

Advanced skin substitutes should mimic the morphology, the composition and the functions of the original tissue. They have to accelerate tissue regeneration, i.e. they have to support the formation of dermis and epidermis layers with a well-developed extracellular matrix (ECM). Moreover, they should enable nutrition supply and should not cause unwanted immune reactions. However, clinically-used skin substitutes have not yet met all these requirements, and they have several limiting factors. These substitutes mostly serve as temporary wound coverages or as carriers for skin cells, and ultimately they are rejected by the organism [1]. This transplant rejection is caused mainly by the use of non-resorbable materials or allogenic cells that are subject to inflammatory reactions.

Advanced tissue engineering lays emphasis on the formation of two of the most important layers of natural skin, the dermis and the epidermis. Fibrous or porous membranes or films of nanoscale thickness can be advantageously used for developing a bilayer of fibroblasts and keratinocytes. The pores in the carriers can enable physical and biochemical communication between fibroblasts and keratinocytes, together with diffusion of nutrients, growth factors and other biologically active molecules from the culture medium or from the surrounding tissue [2]. Moreover, nanostructured materials better mimic the nanofibrous component of natural ECM than flat or microstructured surfaces [3]. They enable the adsorption of cell adhesion-mediating ECM molecules from body fluid or from cell culture media in an appropriate spatial conformation. This orientation of ECM molecules enables good accessibility of their specific bioactive amino acid sequences to cell adhesion receptors, e.g. integrins [4].

Synthetic polymers or natural polymers have been used for constructing carriers for skin cells [5]. However, these two types of materials are still rarely applied in combination. Degradable synthetic polymers, mainly polyesters (polylactide,

polylactide-*co*-glycolide, polycaprolactone), are relatively easily spinnable, e.g. nanofibres can be formed by a process referred as to electrospinning [6]. Moreover, nanofibrous membranes made of these synthetic polymers can provide stable mechanical support for cells. However, synthetic polymers often do not favor cellular adhesion, growth and extracellular matrix deposition in their pristine state [7, 8]. In these cases, synthetic polymers could be combined with molecules physiologically present in the skin, such as collagen, hyaluronan and fibronectin, or with molecules occurring during wound healing, particularly fibrin. These molecules improve the colonization of matrices by cells (for a review, see [9]). In addition, natural molecules, e.g. fibrinogen as the precursor of fibrin, can be isolated in an autologous form from the patient's body fluids or tissues to prevent immune rejection of the implant [10].

Collagen is an important component of ECM in the skin dermis. It is mainly produced by fibroblasts, and is organized into fibers running throughout the dermis [11]. In skin substitutes, collagen is often applied in the form of a gel [12, 13], or it is used in composites with other natural or synthetic materials [14, 15]. Previous studies revealed that collagen supported wound healing. Niiyama and Kuroyanagi combined collagen with hyaluronic acid and functionalized this composite with epidermal growth factor [16]. Butler and Orgill observed improved growth of epidermal keratinocytes on a collagen-glycosaminoglycan matrix [17]. Wang et al. prepared collagen/chitosan-based scaffolds with vascular endothelial growth factor and gentamicin encapsulated into PLGA microspheres, and observed positive effects of these scaffolds on the adhesion and growth of mouse fibroblasts [18].

Fibrin is a provisional matrix molecule that plays an important role during wound healing. Fibrin fibers are formed from fibrinogen, a soluble precursor, in the last step of the coagulation cascade [19]. Cells can bind directly to fibrin(ogen) *via* integrin cell adhesion receptors, or *via* non-integrin receptors (e.g. VE-cadherin, ICAM-1 or P-selectin). Fibrin is also able to bind cell adhesion-mediating proteins (e.g. fibronectin and vitronectin) or growth factors [20]. Fibrin has been used mostly in the form of a glue, a gel or microbeads [21-23]. For better regenerative potential and mechanical stability, fibrin matrices have been combined with other biological or synthetic molecules, e.g. collagen [24, 25], hyaluronic acid with a cell adhesion-promoting peptide [26], basic fibroblast growth factor [27] or epidermal growth factor [28]. Fibrin has relatively rarely been deposited on supporting substrates, although fibrin self-

supporting matrices are usually fragile. In our previous study, we deposited a fibrin nanocoating on polylactide nanofibrous membranes and observed its positive influence on the behavior of dermal fibroblasts [9].

In our study we prepared electrospun polylactide (PLA) and polyactide-*co*-glycolide nanofibrous (PLGA) membranes, coated with fibrin or collagen I, and then with fibronectin attached to the surface of these proteins. First, we compared the behavior of human dermal fibroblasts and human HaCaT keratinocytes on these two protein-modified biodegradable polymer matrices. Although the physical and chemical properties and the biocompatibility of PLA and PLGA are generally considered as very close, some differences have been reported between these polymers as regards their degradability, mechanical integrity [29] porosity, wettability, protein adsorption [30] and the cell behavior on their surfaces [31, 32] Then we evaluated the influence of newly-developed protein nanocoatings on the adhesion and growth of dermal fibroblasts and HaCaT keratinocytes.

2. Materials and Methods

2.1 Preparation of nanofibrous membranes

The experiments were carried out on nanofibrous membranes made of a poly(L-lactide-*co*-glycolide) copolymer (PLGA, ratio 85:15) Purasorb PLG 8531 (Purac Biomaterials, Frankfurt, Germany) or made of poly(L-lactide) (PLA) Ingeo™ Biopolymer 4032D (NatureWorks, Minnetonka, Minnesota, USA). Both polymers were dissolved in chloroform. Solvents - dichloroethane and ethyl acetate - were added into a PLA solution to a final concentration of 7 wt.% of PLA. The volume ratio of the chloroform, dichloroethane and ethyl acetate solvents was 61:29:10. The solution of the two polymers was made electrically conductive with the use of tetraethylammonium bromide, which was first dissolved in dimethylformamide to a concentration of 3 wt%, and then 3 g of this solution was added to 100 g of the PLGA or PLA solution [9].

Nanofibrous membranes were prepared using the novel Nanospider needleless electrospinning technology (NS Lab 500, Liberec, Czech Republic). The process conditions were: electrode distance 145 - 180 mm; voltage 50 kV - 60 kV; relative humidity 20 – 30%, and room temperature. The fiber density, i.e. the area weight of the prepared nanofibers, was from 10 to 20 g/m^2.

124 *2.2 Preparation of fibrin and collagen nanocoating with attached fibronectin*

125 The fibrin nanocoating on the polymeric nanofibrous membranes was formed by
126 activating human fibrinogen (EMD Millipore, Billerica, MA, USA, Cat. No. 341576)
127 with human thrombin (Sigma-Aldrich Co., St Louis, MO, USA, Cat. No. T6884) [33].
128 Fibrinogen at a concentration of 10 μg/ml in Tris Buffer (consisting of 50 mM Tris-
129 HCl, 100 nM NaCl and 2.5 mM $CaCl_2$) was adsorbed on the membrane surface for 1
130 hour. The adsorbed fibrinogen was rinsed with Tris Buffer and was activated with
131 thrombin (2.5 U/ml in Tris Buffer) for 15 minutes. After activation with thrombin, the
132 membranes were rinsed with Tris Buffer. Finally, a solution of 200 μg/ml of fibrinogen
133 in Tris Buffer and 0.5 U/ml of antithrombin III in deionized water was added to the
134 membranes for 1 hour. A fibrin network was formed by a catalytic reaction of the
135 surface-attached thrombin with the ambient fibrinogen solution. The antithrombin III
136 blocked the unreacted thrombin in order to form a 2D fibrin layer.

137 The collagen nanocoating was formed from a collagen solution by changing the
138 pH. The collagen solution (Corning, New York, USA, rat tail, 3.37 mg/ml) was diluted
139 in 0.02 M acetic acid to a final concentration of 200 μg/ml, and was applied to the
140 samples. The samples were immersed into ammonia vapor for 10 minutes to change the
141 acid pH to basic pH. After collagen precipitation, the solution was sucked out and the
142 samples were rinsed with deionized water.

143 Fibronectin was attached to the surface of the fibrin and collagen nanocoating.
144 Fibronectin powder (Roche, Basel, Switzerland, human, Cat. No. 11051407001) was
145 dissolved in deionized water at a concentration of 1 mg/ml. The fibronectin solution
146 was subsequently diluted in Phosphate-Buffered Saline (PBS; Sigma-Aldrich Co., St
147 Louis, MO, USA) to a final concentration of 50 μg/ml and was incubated with the
148 samples overnight at 4°C. The samples were then rinsed twice with PBS.

149 *2.3 Morphology of the nanofibrous membranes*

150 The morphology of the PLGA and PLA nanofibrous membranes in their pristine
151 state (i.e., non-coated membranes) was studied by scanning electron microscopy (SEM).
152 The membranes were sputter-coated with gold and were evaluated by a Quanta 450
153 scanning electron microscope (FEI, Hillsboro, OR, USA) in high vacuum mode. The
154 images were taken using an Everhart-Thornley detector (ETD) in secondary electrons
155 mode at high voltage 20 kV, magnification 2 000x and 10 000x.

156 The diameter of the fibers was measured on the SEM images using Atlas software
157 (Tescan Ltd., Brno, Czech Republic).

158 *2.4 Cell culture*

159 The nanofibrous membranes were fixed in Cell Crown inserts (Scaffdex Ltd.,
160 Tampere, Finland) in order to prevent them floating in the cell culture medium, and
161 were inserted into the wells of 24-well plates (TPP, Trasadingen, Switzerland, well
162 diameter 1.56 cm). The samples were seeded with neonatal human dermal fibroblasts,
163 purchased from Lonza (Basel, Switzerland), passage 3 to 6, or with human
164 keratinocytes of the line HaCaT, purchased from CLS Cell Lines Service (Eppelheim,
165 Germany) [34]. The cells were seeded at a density of approx. 10 000 cells/cm^2 (i.e.
166 20 000 cells/well) and were cultivated in Dulbecco's modified Eagle's Medium
167 (DMEM; Sigma-Aldrich Co., St Louis, MO, USA) with 10% of fetal bovine serum
168 (FBS; Sebak GmbH, Aidenbach, Germany) and 40 μg/ml of gentamicin (LEK,
169 Ljubljana, Slovenia). The volume of cell culture medium was 1.5 ml/well. The cells
170 were cultivated for three time intervals (1, 3 and 7 days) in a cell incubator at 37°C and
171 in a humidified atmosphere with 5% of CO_2 in the air. Polystyrene culture wells (24-
172 well plate) were used as a control material.

173 *2.5 Morphology of the protein nanocoatings*

174 The morphology of the fibrin, collagen and fibronectin nanocoatings was studied
175 by immunofluorescence staining on freshly prepared samples, on cell-free samples
176 incubated for two time intervals (i.e., on days 3 and 7) in the DMEM medium under the
177 conditions used for the cell cultivation, and on samples with cells on days 3 or 7 after
178 seeding. Non-coated membranes were used as control samples to evaluate possible non-
179 specific binding of the primary and secondary antibodies. Two samples of each
180 experimental group for each time interval were used.

181 The membranes were treated with 1% bovine serum albumin in PBS for 20
182 minutes, and then with 1% Tween (Sigma-Aldrich Co., St Louis, MO, USA) in PBS for
183 20 minutes at room temperature to block non-specific binding sites. The samples were
184 subsequently incubated overnight at 4°C with primary antibodies against human
185 fibrinogen (Dako Denmark A/S, Glostrup, Denmark, polyclonal rabbit antibody),
186 collagen I (Sigma-Aldrich Co., St Louis, MO, USA, monoclonal mouse antibody) or

fibronectin (Sigma-Aldrich Co., St Louis, MO, USA, mouse monoclonal antibody) diluted in PBS in a ratio of 1:200. The samples were then rinsed twice with PBS and were incubated with secondary antibodies, namely goat anti-rabbit or goat anti-mouse F(ab')2 fragments of IgG (H + L), conjugated with Alexa Fluor® 488 (Molecular Probes, Eugene, OR, USA; Thermo Fisher Scientific, diluted in PBS in a ratio 1:400) for 1 hour at room temperature in the dark.

The fibrin- or collagen-coated membranes with attached fibronectin were also stained for fibrin + fibronectin or collagen + fibronectin on the same sample. The samples were incubated overnight at 4°C with primary antibodies against human fibrinogen (Dako Denmark A/S, Glostrup, Denmark, rabbit polyclonal antibody) or with collagen I (Cosmo Bio Co., LTD., Tokyo, Japan, rabbit polyclonal antibody) diluted in PBS in a ratio of 1:200. Subsequently, after rinsing with PBS, the primary antibody against fibronectin (Sigma-Aldrich Co., St Louis, MO, USA, mouse monoclonal antibody) was added for 3 hours. The samples were rinsed with PBS and were incubated with a secondary antibody goat anti-rabbit F(ab')2 fragment of IgG (H + L), conjugated with Alexa Fluor® 488 (Molecular Probes; Thermo Fisher Scientific, diluted in PBS in a ratio of 1:400) for 1 hour (in order to visualize the fibrin or collagen), and then with a secondary antibody goat anti-mouse F(ab')2 fragment of IgG (H + L), conjugated with Alexa Fluor® 633 (Molecular Probes; Thermo Fisher Scientific, diluted in PBS in a ratio of 1:400) for 1 hour (in order to visualize fibrinogen). The samples were rinsed with PBS and were scanned using a Leica TCS SPE DM2500 upright confocal microscope, obj. 40x/1.15 NA oil.

2.6. Cell spreading and morphology

The spreading and the morphology of the cells on non-coated or protein-coated nanofibrous membranes were visualized on day 1, 3 and 7 after seeding by staining the cells with a combination of fluorescent dyes diluted in PBS (Hoechst #33258 cell nucleus dye, Sigma-Aldrich Co., St Louis, MO, USA, 5 μg/ml and Texas Red C_2-maleimide, cell membrane dye, Molecular Probes; Thermo Fisher Scientific, 20 ng/ml) for 1 hour at room temperature in the dark. Instead of using Texas Red staining, the F-actin cytoskeleton of the cells was stained with phalloidin conjugated with TRITC fluorescent dye (Sigma-Aldrich), diluted in PBS to a final concentration of 5 μg/ml, for 1 hour at room temperature in the dark. Before staining, the cells were rinsed with PBS

and were fixed with -20°C cold ethanol for 10 minutes. Images of the cells were taken using an epifluorescence microscope (Olympus IX 51, Tokyo, Japan, obj. 10x) equipped with a digital camera (DP 70, Olympus, Tokyo, Japan), or using a Leica TCS SPE DM2500 upright confocal microscope, obj. 40x/1.15 NA oil.

On day 1 after seeding of the cells, the spreading area of islands formed by human HaCaT keratinocytes was measured on images taken under a fluorescence microscope, using Atlas software (Tescan Ltd., Brno, Czech Republic).

2.7 Cell mitochondrial activity

The activity of mitochondrial enzymes was measured in three intervals of cell cultivation (on day 1, 3 and 7 after cell seeding) for the dermal fibroblasts, and in two time intervals (on day 3 and 7 after cell seeding) for the HaCaT keratinocytes by CellTiter 96® AQueous One Solution Cell Proliferation Assay (MTS, Promega Corporation, Madison, WI, USA) on samples of nanofibrous membranes incubated in 24-well cell culture plates. The mitochondrial activity of the HaCaT keratinocytes was measured only on day 3 and on day 7, but not on day 1 after cell seeding. The reason was that our preliminary measurements, using the MTS assay, revealed that on day 1 after seeding, when the cell number is relatively low, the measured absorbance was on the limit of detection and showed no significant differences among the tested samples. This was probably due to the relatively low activity of the mitochondrial enzymes in the HaCaT cells. In cell culture and in human skin sections, the activities of mitochondrial enzymes were lower in keratinocytes than in fibroblasts [35]. The principle of an MTS assay is based on cleavage of the yellow tetrazolium salt MTS and on the formation of a water-soluble brown formazan salt by the activity of mitochondrial enzymes (i.e., dehydrogenases) in the cells. The formazan dye was then quantified by measuring the absorbance using a spectrophotometer (e.g., an ELISA reader).

The samples of membranes were moved into fresh 24-well plates to avoid the influence of the cells adhered to the bottom of the well. The assay was performed according the manufacturer's protocol. The absorbance was measured using the VersaMax ELISA Microplate Reader (Molecular Devices Corporation, Sunnyvale, CA, USA) in Nunc-Immuno MicroWell 96-well cell culture plates (Sigma-Aldrich Co., St Louis, MO, USA) with wavelength 490 nm. Three independent samples for each experimental group and time interval were used. One sample without cells for each

experimental group and time interval was used as a control to set the background for the measured absorbance. A polystyrene culture dish (24-well plate) was used as a control material for the cell mitochondrial activity.

2.8 Cell viability

The cell viability was determined using a LIVE/DEAD Viability/Cytotoxicity Kit (Molecular Probes, Life Technologies). The principle of this assay is based on the different ability of two fluorescent dyes to penetrate though the cell membrane of live and dead cells. Calcein AM penetrates into the live cells, where it is converted by esterases to calcein, which emits a green fluorescence. Ethidium homodimer-1(EthD-1) penetrates though the membrane of the dead cells and stains them with a red fluorescence.

The samples were carefully rinsed with PBS and were stained with a solution of $2 \cdot 10^{-3}$ μM calcein AM and $6 \cdot 10^{-3}$ μM EthD-1. After 10 minutes of incubation in the cell incubator, the cells were rinsed with PBS and were evaluated using an epifluorescence microscope (Olympus IX 51, Tokyo, Japan, obj. 10x) equipped with a digital camera (DP 70, Olympus, Tokyo, Japan).

2.9 Statistics

The quantitative data is presented as mean ± standard deviation (S.D.) or as the standard error of the mean (S.E.M) from three independent samples for each experimental group and time interval. Statistical significance was evaluated using the analysis of variance, Student-Newman-Keuls method. Values of $p \leq 0.05$ were considered as significant.

3. Results

3.1 Morphology of nanofibrous membranes

The fibers of both types of nanofibrous membranes were mostly straight and randomly oriented. The diameter of the fibers was within a large range, from tens of nm to more than 1 μm. The average fiber diameter was more than 300 nm (Fig. 1), similarly as in our earlier study [9]. The material nanostructures are defined to be equal to or less than 100 nm, in at least one dimension. The fiber diameter in our study was therefore in

submicron- and micron-scale rather than in nanoscale. However, such fibers are frequently referred to in the literature as nanofibers [4, 36-38].

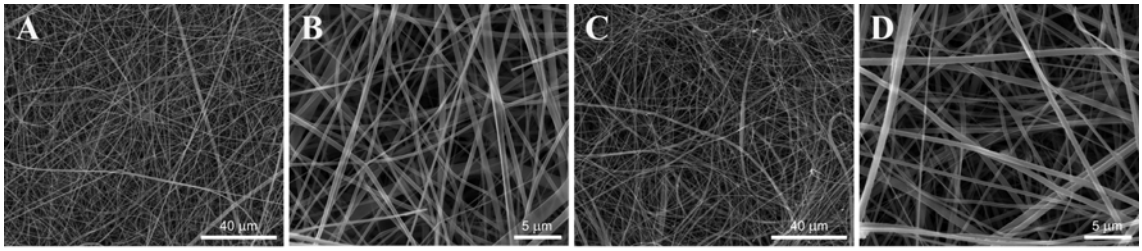

E

	PLGA	PLA
Fiber density (g/m²)	10.5 – 19.6	13.0 - 15.0
Fiber diameter, mean ± SD (nm)	341 ± 203	352 ± 205
Fiber diameter range (nm)	28 – 2 054	41 - 1747

Fig. 1: SEM images of non-modified PLGA membranes (A, B) and PLA membranes (C, D). Quanta 450 scanning electron microscope (FEI, USA), original magnification 2 000x (A, C) or 10 000x (B, D). Morphological parameters of PLGA and PLA membranes (E). Mean ± SD from 12 SEM images (1748 measurements in total).

3.2 The morphology of the protein nanocoating and its stability and degradation during cell cultivation

Fibrin regularly formed a coating around individual nanofibers and also formed a thin nanofibrous mesh on the membrane surface. However, this mesh did not form homogeneously on the whole surface of the membrane. Collagen also coated most of the fibers in the membranes, but not regularly. Moreover, collagen randomly formed a soft gel on the membrane surface (Fig. 2).

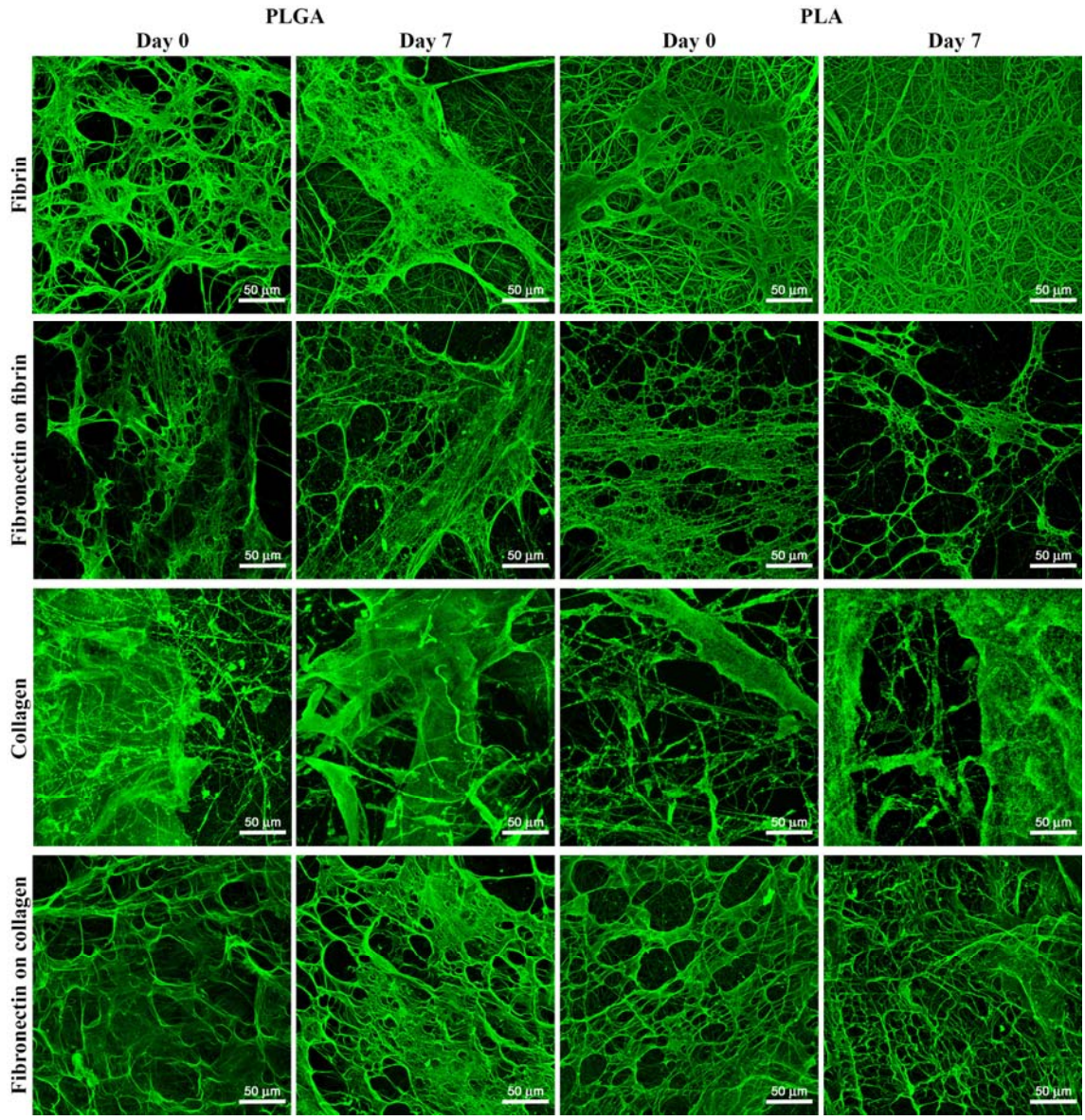

Fig. 2: Immunofluorescence staining of fibrin (row 1), fibronectin deposited on fibrin (row 2), collagen I (row 3) and fibronectin deposited on collagen (row 4), freshly prepared on PLGA and PLA membranes (Day 0) or after 7 days of incubation in DMEM at 37°C and 5% CO_2 (Day 7). Leica TCS SPE DM2500 confocal microscope, obj. 40x/1.15 NA oil.

Fibronectin was bound on the fibrin and collagen nanocoating. Fibronectin formed an additional nanofibrous mesh on the thin fibrin mesh or on the collagen gel (Fig. 3). Fibronectin also adsorbed on fibers coated with fibrin or collagen, but it was hardly visible using immunofluorescence. There was no apparent difference in the morphology of the protein nanocoating on PLGA membranes and on PLA membranes (Fig. 2).

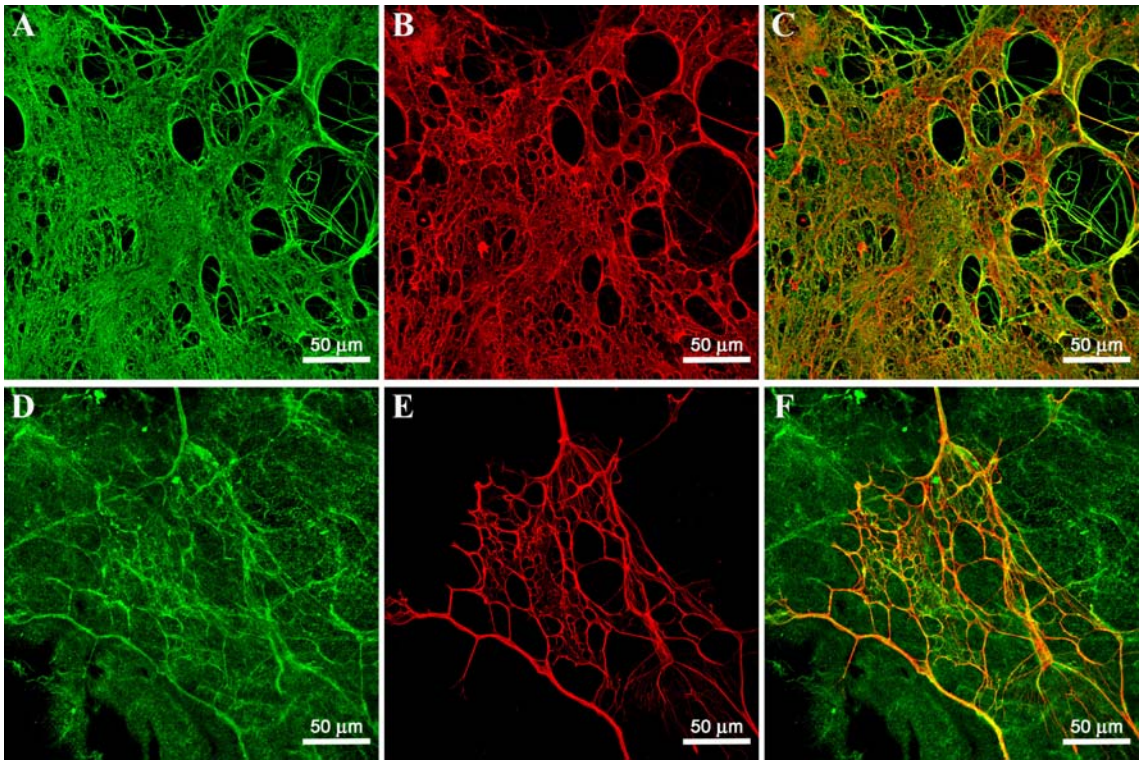

Fig. 3: Immunofluorescence staining of a fibrin nanocoating (A) and a collagen nanocoating (D), and fibronectin on a fibrin nanocoating (B) and on a collagen nanocoating (E), freshly deposited on PLGA membranes. Image A with B and image D with E were merged (C, F). The secondary antibodies were conjugated with Alexa 488 (fibrin, collagen, green fluorescence) or with Alexa 633 (fibronectin, red fluorescence). Leica TCS SPE DM2500 confocal microscope, obj. 40x/1.15 NA oil.

The durability of the protein nanocoatings on the nanofibrous membranes was tested during 7 days under the same conditions as those used for cell cultivation. The results showed that the fibrin, collagen or fibronectin nanocoatings on both polymer membranes were stable in a cell-free environment, and their morphology was almost unchanged after one week (Fig. 2).

However, the cells altered the morphology of the protein nanocoatings during their cultivation. Both types of cells degraded and reorganized the protein nanocoating (Fig. 4). Fibroblasts penetrated into the fibrin mesh and gradually degraded the fibrin nanocoating. Nevertheless, on day 7, some fibrin-coated fibers and some remains of the thin fibrin nanofibrous mesh were still apparent. Collagen was less degraded than fibrin by fibroblasts. However, the collagen gel that formed on the membrane surface appeared to be too soft for the adhesion and growth of fibroblasts, and the cells were often detached from the surface of the material. The fibronectin mesh was degraded

faster on the fibrin nanocoatings than on the collagen nanocoatings. In addition, the fibrin-coated membranes apparently stimulated the fibroblasts to produce fibronectin and to deposit it as ECM in the cell surroundings (Fig. 5).

HaCaT keratinocytes degraded the protein nanocoating in a different way. Thin nanofibrous fibrin and fibronectin meshes on the fibrin-coated membranes were almost completely degraded on day 3 after seeding. Only fibers coated with fibrin and the remains of fibronectin meshes remained until the 7^{th} day of seeding. The degradation process started already on the 1^{st} day of cell cultivation (data not shown here). In Fig. 4, it is apparent that the keratinocytes adhered on the membrane surface did not penetrate into the membrane but remained on the surface of the fibrin or fibronectin meshes, and these meshes were pulled down, probably by cell traction forces. Surprisingly, the fibronectin attached to the collagen gel was not degraded in a similar manner as the fibronectin on the fibrin. The fibronectin attached to the collagen, and also the collagen itself, were only slightly changed and degraded after 7 days of cell cultivation.

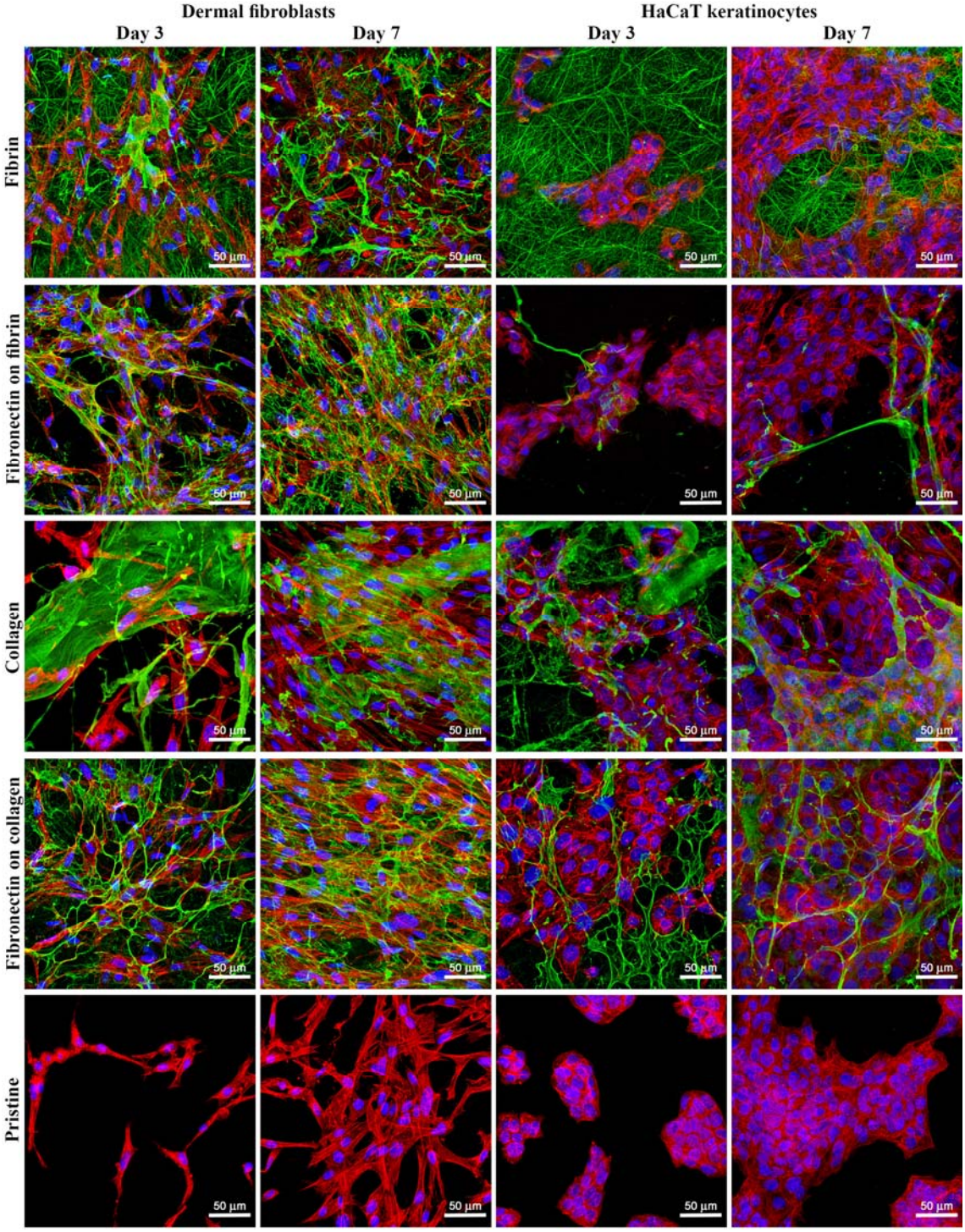

Fig. 4: Immunofluorescence staining (green) of fibrin (row 1), fibronectin deposited on fibrin (row 2), collagen I (row 3) and fibronectin deposited on collagen (row 4) on PLGA membranes after 3 and 7 days of cultivation of human dermal fibroblasts and HaCaT keratinocytes. Row 5: control cells on pristine uncoated membranes. The cells were stained with Phalloidin-TRITC (red; actin cytoskeleton) and with Hoechst #33258 (blue; cell nuclei). Leica TCS SPE DM2500 confocal microscope, obj. 40x/1.15 NA oil.

345 *3.3 Cell adhesion, spreading and morphology*

346 The differences in cell morphology among the various types of samples and cells
347 were observed. On the coated samples, the fibroblasts were well-spread with a spindle-
348 like or polygonal shape already on day 1 after cell seeding. However, on the non-coated
349 membranes, the cells tended to be round and not well adhered (Fig. 6). After one week
350 of cell cultivation, the fibroblasts on the fibrin-coated samples, and also on the collagen-
351 coated samples, were almost confluent. On the non-coated membranes, however, there
352 were considerably large free spaces among the cells. On the membranes with fibrin, the
353 cells were able to penetrate into the fibrin mesh and into deeper layers of the membrane
354 (seen mainly on day 7 after seeding). By contrast, on membranes with collagen, the
355 cells adhered only on the surface of the protein nanocoating or on the surface of the
356 membrane (Fig. 4).

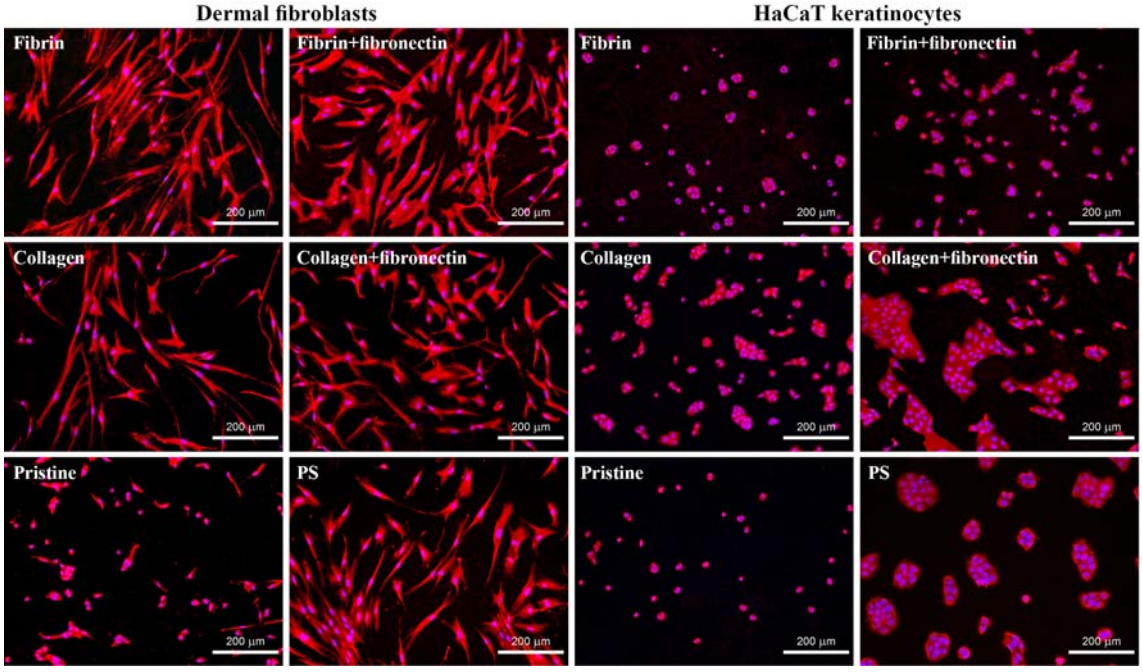

357

358 *Fig. 6: Morphology of human dermal fibroblasts and human HaCaT keratinocytes on day 1*
359 *after seeding on PLGA membranes coated with fibrin, fibrin+fibronectin, collagen or*
360 *collagen+fibronectin, and on non-coated PLGA membranes (Pristine). Polystyrene culture*
361 *dishes (PS) were used as a reference material. Cells stained with Texas Red C_2-Maleimide and*
362 *Hoechst #33258. Olympus IX 51 microscope, obj. 10 x, DP 70 digital camera.*

363 The morphology of the keratinocytes also varied among the different types of
364 samples. On membranes coated with collagen, the cells were well-spread and formed
365 larger cell clusters (islands) than on membranes coated with fibrin or on non-coated

membranes (Fig. 4, 6). The size of the cell cluster spreading area on day 1 was larger on membranes with collagen than on non-coated membranes or on membranes with fibrin. Fibronectin improved the cell attachment on the protein nanocoatings, mainly on the collagen nanocoating, where the largest cell cluster area was observed. The cluster area of keratinocytes on the fibrin nanocoating was only slightly and non-significantly larger than on the non-coated membranes (Fig. 7).

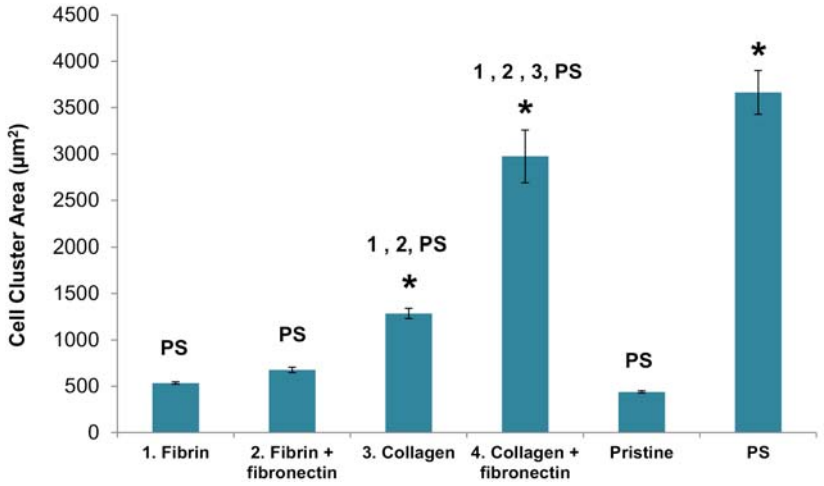

*Fig. 7: Cell cluster spreading area of HaCaT keratinocytes on day 1 after seeding on PLGA membranes in modified states (1. – 4.) or in a non-modified state (Pristine). Polystyrene culture dishes (PS) were used as a reference material. Arithmetic mean ± S.E.M from 283 to 779 measurements. ANOVA, Student-Newman-Keuls method, statistical significance ($p \leq 0.05$): 1, 2, 3, 4, PS in comparison with the experimental group of the same label and * in comparison with the pristine sample.*

3.4 Cell proliferation and viability

The cell proliferation was estimated by measuring the cell mitochondrial activity. In all culture intervals, the mitochondrial activity of dermal fibroblasts was significantly higher on protein-coated membranes (with the exception of the collagen-coated membranes) than on non-coated (pristine) membranes (Fig. 8). On membranes with collagen nanocoating, the cell mitochondrial activity was mostly comparable with the metabolic activity of the cells growing on non-coated membranes (with the exception of PLA membranes on day 7 after cell seeding, where the mitochondrial activity was higher). Fibronectin attached to the collagen nanocoating greatly improved the fibroblast proliferation. The cell mitochondrial activity on samples of this type was significantly higher than on the membranes coated only with collagen. The highest

metabolic activity of the fibroblasts was found on membranes with fibrin nanocoating. Fibronectin attached to the fibrin nanocoating promoted the attachment of fibroblasts, and further increased their mitochondrial activity. This was apparent mainly on day 3 after seeding.

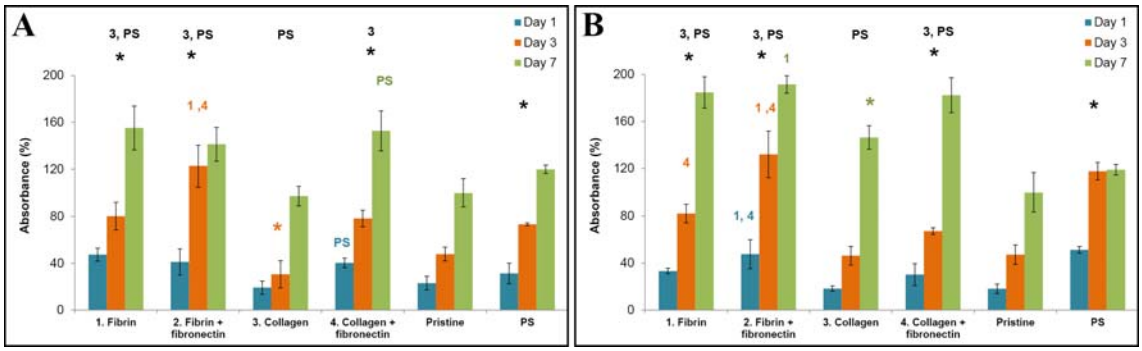

*Fig. 8: Mitochondrial activity in human dermal fibroblasts determined by MTS assay in three time intervals (on days 1, 3, and 7 after cell seeding) on a PLGA membrane (**A**) or on a PLA membrane (**B**) in modified states (1. – 4.) or in a non-modified state (Pristine). Polystyrene culture dishes (PS) were used as a reference material. Arithmetic mean ± SD from 12 measurements made on 3 independent samples for each experimental group and time interval. ANOVA, Student-Newman-Keuls method, statistical significance ($p \leq 0.05$): 1, 2, 3, 4, PS in comparison with the experimental group of the same label and * in comparison with the pristine sample in all three intervals (black label) or in particular intervals (color label).*

In comparison with dermal fibroblasts, HaCaT keratinocytes adhered and proliferated better on membranes with a collagen nanocoating than on membranes with a fibrin nanocoating (Fig. 9). The cell mitochondrial activity was significantly higher on membranes coated with collagen than on non-coated membranes and on membranes coated with fibrin. The cell mitochondrial activity on fibrin was mostly comparable with the activity on non-coated membranes. On fibrin-coated PLGA membranes further modified with fibronectin, the cell mitochondrial activity was even lower than on pristine PLGA membranes (Fig. 9A). In general, however, there were no major differences in cell adhesion, in mitochondrial activity and in proliferation between the two types of polymeric membranes, i.e. PLGA membranes and PLA membranes (Fig. 8, 9).

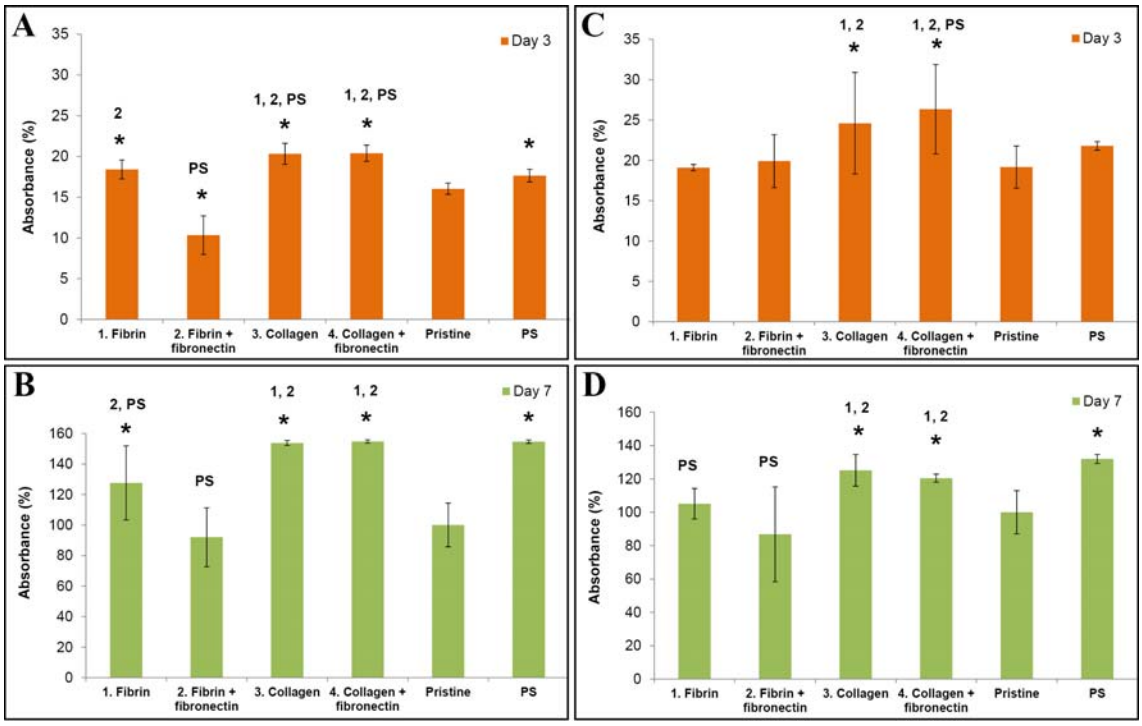

*Fig. 9: Mitochondrial activity in human HaCaT keratinocytes determined by MTS assay in two time intervals (on day 3 and 7 after cell seeding) on PLGA (**A, B**) or PLA membranes (**C, D**) in modified states (1. – 4.) or in a non-modified state (Pristine). Polystyrene culture dishes (PS) were used as a control material. Arithmetic mean ± SD from 12 measurements made on 3 independent samples for each experimental group and time interval. ANOVA, Student-Newman-Keuls method, statistical significance ($p \leq 0.05$): 1, 2, 3, 4, PS in comparison with the experimental group of the same label and * in comparison with the pristine sample.*

The viability of both cell types - dermal fibroblast and HaCaT keratinocytes - was high and reached almost 100% on both coated and non-coated membranes. The lower adhesion and proliferation rate of the cells on non-coated membranes did not affect the cell viability (Fig. 10).

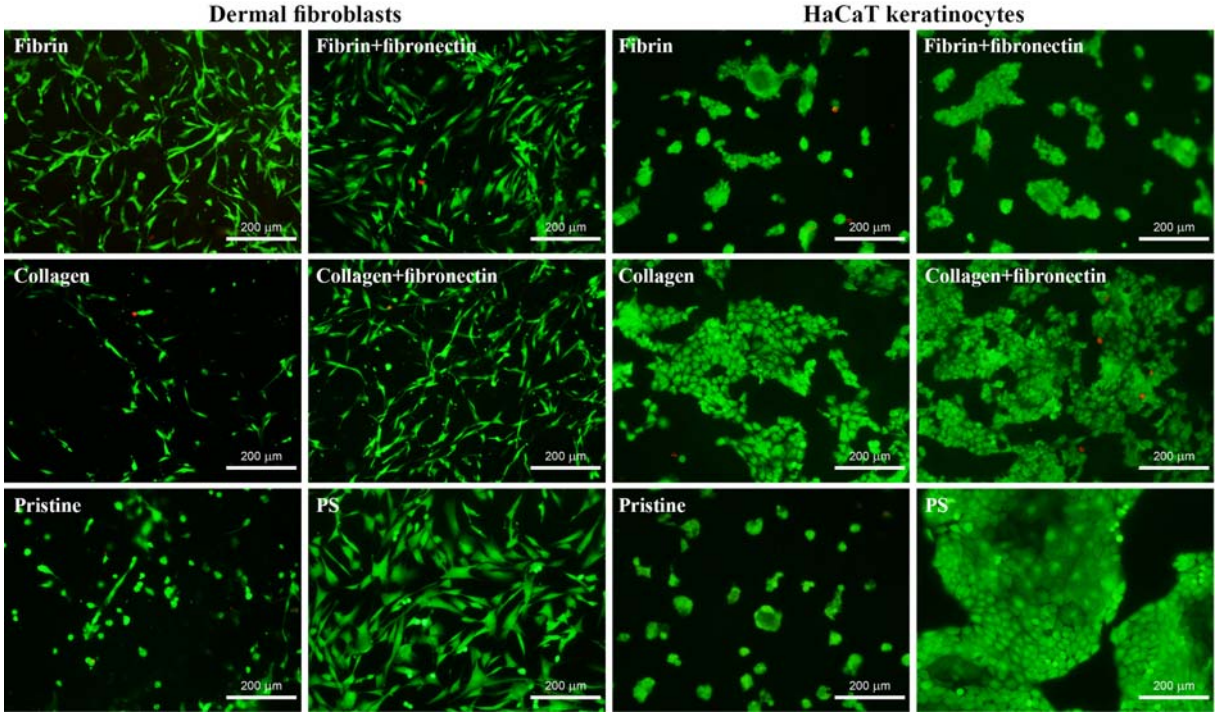

Fig. 10: Viability of human dermal fibroblasts and human HaCaT keratinocytes determined by a Live/Dead kit on day 1 after seeding on PLGA membranes coated with fibrin, fibrin+fibronectin, collagen or collagen+fibronectin, and on non-coated PLGA membranes (Pristine). Polystyrene culture dishes (PS) were used as a reference material. Cells stained with Calcein AM (green live cells) and with EthD-1 (red dead cells). Olympus IX 51 microscope, obj. 10 x, DP 70 digital camera.

4. Discussion

Nanofibrous membranes made from bioresorbable polymers are promising carriers of skin cells for treating acute or chronic wounds. However, the synthetic polymers used for fabricating nanofibrous cell carriers often do not provide sufficient support for cell adhesion, proliferation and deposition of ECM. Desirable cell behavior can be achieved by modifying the polymer carrier physically or chemically. In our previous studies, modification of PLA membranes by plasma treatment enhanced the adhesion and growth of human keratinocytes [8], and fibrin nanocoating on PLA membranes improved the adhesion and proliferation of human fibroblasts, and also collagen synthesis and deposition by these cells as ECM [9] Modifying nanofibrous carriers of skin cells by biomolecules naturally occurring in the skin or during skin regeneration could therefore be promising for the development of desirable skin substitutes. In this study, we have focused on fabricating fibrin, collagen and fibronectin

446 nanocoatings on nanofibrous PLGA and PLA membranes in order to enhance the
447 adhesion, proliferation and ECM synthesis in skin cells.

448 Fibrin deposited on membrane nanofibers greatly improved the adhesion,
449 spreading and proliferation of dermal fibroblasts. In some places on the membranes,
450 moreover, fibrin formed a thin nanofibrous mesh, mimicking ECM and promoting more
451 cell adhesion and spreading than was observed on non-modified membranes. These
452 results were similar to those obtained in our previous work. As we discussed there,
453 fibrin enabled the cell adhesion receptors to bind to its molecule, and further support
454 cell adhesion by attracting cell adhesion-mediating molecules (such as fibronectin or
455 vitronectin) from the serum supplement of the cell culture medium. We showed that
456 fibrin enhanced the development of focal adhesion plaques containing β_1-integrins in
457 dermal fibroblasts [9]. Studies by other authors have also shown similar positive effects
458 of fibrin on the adhesion and growth of fibroblasts [39, 40].

459 However, our results showed that - unlike in the case of fibroblasts - there was not
460 significantly greater proliferation of keratinocytes on fibrin-coated membranes than on
461 non-coated membranes. The explanation for this could be that keratinocytes, unlike
462 fibroblasts, do not naturally come into direct contact with fibrin. During wound healing,
463 fibroblasts migrate into the fibrin clot, start to produce ECM and are the first to
464 contribute to wound healing. Keratinocytes then migrate to the wound, attach to the
465 ECM matrix and form new cell layers of epidermis. Many previous studies have
466 attempted to reveal the role of fibrin in the adhesion and proliferation of keratinocytes,
467 but they have not reached consistent conclusions. Sese et al. reported that keratinocyte
468 proliferation in three-dimensional fibrin constructs was influenced by the thrombin
469 concentration. These authors found that the optimal thrombin concentration in fibrin
470 matrices for stimulating keratinocyte proliferation was about 1 U/ml [41], while the
471 proliferation of fibroblasts was not strongly dependent on the thrombin concentration.
472 Fibroblasts proliferated well within three-dimensional fibrin clots containing 1-167
473 U/mL of thrombin [42]. In our study, we used thrombin in a concentration of 2.5 U/ml
474 to fabricate a fibrin nanocoating. This concentration was optimal for forming the
475 nanocoating on the membrane and for supporting the proliferation of fibroblasts, but it
476 was probably not convenient for the growth of keratinocytes. Gugerell et al. reported
477 that high concentrations (about 820 U/ml) of thrombin activated apoptotic mechanisms
478 in keratinocytes, and also decreased their attachment and spreading on fibrin sealants

[43]. Kubo et al. showed that fibrin and fibrinogen were non-adhesive for keratinocytes, due to a lack in these cells of $\alpha_v\beta_3$ integrin receptors, which are important for binding cells to fibrin molecules [44]. In our study, the HaCaT keratinocytes were able to adhere to fibrin-coated membranes, though they were not so well flattened as on collagen-coated membranes. This may be explained by the relatively long exposure of the fibrin coatings to the adhering keratinocytes, i.e. more than 24 hours, which is sufficient time for these cells to alter or to remove the protein coating in order to enhance their adhesion [44]. In addition, the adhesion and proliferation of keratinocytes on fibrin matrices can be improved by crosslinking them, e.g. by factor XII, and also by adding fibronectin [45]. It cannot be excluded that fibronectin, which is present in the serum supplement of the culture medium, was bound onto our fibrin matrices through their αC domains [20], and was then recognized by the $\alpha_5\beta_1$, $\alpha_v\beta_1$ and $\alpha_v\beta_6$ integrin adhesion receptors present on keratinocytes, including HaCaT [46]. However, the attachment of fibronectin to fibrin coatings from PBS solution in our study did not improve the adhesion and growth of keratinocytes.

Our experiments also suggested that fibrin stimulated fibroblasts to synthetize fibronectin and deposit it as ECM in the cell surroundings. On the fibrin coating, the amount of fibronectin in the cell surroundings increased markedly from day 3 to day 7, and the fibronectin was clearly associated with the cells, i.e. it was localized in the immediate vicinity of the cell membrane. This was particularly apparent on day 7, when fibronectin clearly contoured the cells (Fig. 5). This pattern could be attributed to *de novo* synthesis of fibronectin by the cells, rather than to its spontaneous adsorption or binding to fibrin from the serum of the culture medium. A similar pattern of fibronectin deposition was observed in cardiac fibroblasts cultured on three-dimensional fibrin gels [47]. In our previous study, we showed that fibroblasts were stimulated by a fibrin nanocoating to produce collagen ECM fibers [9]. Studies by other authors have also described a stimulatory effect of fibrin on ECM synthesis (mainly collagen I) by fibroblasts [40, 48].

Collagen deposited on the membranes also enhanced adhesion, spreading and proliferation of the cells, particularly of HaCaT keratinocytes. Collagen is a major component of ECM, and most of the cells bind to its oligopeptide sequence DGEA (Asp-Gly-Glu-Ala) mainly by $\alpha_2\beta_1$ or $\alpha_3\beta_1$ integrin receptors [49, 50]. These receptors are also expressed in HaCaT keratinocytes [51]. The HaCaT keratinocytes in our study

adhered, spread and proliferated faster on collagen-coated membranes than on fibrin-coated or non-coated membranes. After skin injury, the keratinocytes physiologically migrate into the wound and interact through their integrin receptors with ECM molecules, mainly with collagen I nanofibers [11]. It seems to be beneficial to modify nanofibrous scaffolds by collagen or directly to fabricate collagen nanofibrous scaffolds [36, 38]. The native ECM in the dermis consists of collagen nanofibers less than 100 nm in diameter. However, the diameter of collagen fibers in nanofibrous matrices is usually greater than 100 nm (Fu et al. 2014). For this reason, Fu et al. developed composite polycaprolactone-collagen (PCL-Coll) nanofibrous matrices coated with a thin layer of collagen gel, forming a secondary ultrafine network of nanofibers (55 ± 26 nm in diameter), in order to better simulate the natural conditions. This ultrafine collagen fibrous network significantly increases the adhesion and the migration of keratinocytes in comparison with non-modified PCL-Coll composite fibers, which were 331 ± 112 nm in diameter [37]. Thus, the improvement in the adhesion and growth of keratinocytes on our collagen-modified PLA and PLGA nanofibrous membranes can be explained by the formation of a soft collagen gel on the membrane surface rather than to the collagen coating of the individual fibers in the membranes.

In contrast to keratinocytes, the adhesion and proliferation of dermal fibroblasts on collagen-coated membranes was usually similar to the adhesion and proliferation on non-coated membranes. Dermal fibroblasts naturally generate contractile forces that affect the surrounding tissue. During wound healing, the fibroblasts produce strong ECM fibers made of collagen and elastin, which resist the traction forces of the cells. However, on our membranes, the collagen mostly formed a gel that was probably too soft, and was deformed by the traction forces generated by the fibroblasts. The collagen gel was therefore probably not able to provide an appropriate substrate for the attachment and migration of dermal fibroblasts. This was suggested by the fibroblast peeling of the collagen gel observed in our study. Eastwood et al. made a systematic study of the generation of contractile forces by dermal fibroblasts on a collagen gel. They found that most of the forces were induced during attachment and spreading of the cells, and different groups of fibroblasts might vary in their contraction activity [52]. The different behavior of the fibroblasts and the keratinocytes on our collagen-coated membranes was probably due to the different contraction forces generated by these cells on the collagen gel. Agis et al. compared the fibroblast behavior on a collagen gel and

on a collagen porous sponge. They found that a collagen sponge provided better support for cell migration, proliferation and ECM production than a collagen gel [53]. These results suggest that for the fibroblast component of a skin substitute, it would be better to use nanofibrous scaffolds made of pure collagen, or collagen combined with other degradable materials, as mentioned above [36, 38]. These scaffolds did not seem to be ideal for keratinocytes but might be suitable for fibroblasts.

Fibronectin was deposited on a fibrin or collagen nanocoating in order to enhance the attachment and spreading of the cells. Fibronectin is the main adhesive protein of ECM, and is bound by cell integrin adhesion receptors through the RGD amino acid sequence (Arg-Gly-Asp) [54]. Fibronectin attached to collagen-coated membranes improved the adhesion and spreading of HaCaT keratinocytes. The measured cell cluster area, i.e. the size of the keratinocyte islands formed on day 1 after seeding, was larger on fibronectin-collagen-coated membranes than on only collagen-coated membranes. Moreover, fibronectin attached to a collagen and fibrin nanocoating enhanced the proliferation of dermal fibroblasts. This positive effect was more pronounced on collagen-coated membranes, i.e. on a material where the adhesion and the growth of fibroblasts were less stimulated than on fibrin. The enhancement of fibroblast proliferation by fibronectin was probably due to better primary attachment of the cells.

The way in which the cells degraded and reorganized the protein nanocoatings differed between fibroblasts and keratinocytes. The fibroblasts slowly and continuously degraded and reorganized all types of protein nanocoatings during cultivation, whereas the effects of HaCaT keratinocytes were different on fibrin-based nanocoatings and on collagen-based nanocoatings. The morphology of the collagen nanocoating was not significantly changed by the keratinocyte behavior. However, the morphology of the thin fibrous mesh of a fibrin nanocoating was strongly altered by keratinocytes already 24 hours after cell seeding. Interestingly, while fibronectin attached to fibrin was significantly degraded by keratinocytes, fibronectin attached to collagen was not significantly degraded. During the attachment, spreading and migration of keratinocytes, the cells develop traction forces that affect ECM. The thin fibrous fibrin mesh was probably not able to resist these contractile forces, and was pulled down at an early stage, together with the attached fibronectin. However, the collagen coating probably provided a firmer surface for keratinocyte adhesion and migration. In addition,

578 the collagen gel that formed on the surface of the nanofibrous membranes provided a
579 relatively flat growth support, which may be more convenient for the adhesion of
580 keratinocytes, i.e. flat and polygonal epithelial cells. Last but not least, keratinocytes
581 lack $\alpha_v\beta_3$ integrin receptors, which are important for binding to fibrin molecules. They
582 therefore did not use the fibrin molecules as a substrate for their adhesion, migration
583 and growth, and they tried to reorganize or even remove this coating. From
584 physiological wound healing *in vivo*, it is known that keratinocytes slough the fibrin
585 eschar from the newly formed epidermis [44].

586 On the PLA and PLGA membranes, there was no apparent difference in the
587 morphology of the protein nanocoatings and also in the cell behavior on these coatings.
588 The cell behavior was also similar on both types of nanofibrous membranes. Both PLA
589 and PLGA are degradable polyesters widely used in tissue engineering and in other
590 biotechnologies, e.g. for drug delivery. However, certain differences have been reported
591 in the behavior of the two polymers in the biological environment. For example, when
592 prepared in the form of microspheres for drug delivery, PLA had a longer degradation
593 time than PLGA, and the degradation time of PLGA decreased with a decreasing
594 percentage of PLA in this copolymer [55]. Accordingly, the loss of mechanical integrity
595 was faster in PLGA than in PLA [29]. PLA microspheres showed a more porous and
596 more hydrophobic surface than PLGA, which resulted in differences in protein
597 adsorption on these polymers, including fibrinogen. PLA adsorbed slightly more
598 fibronectin, but also more albumin, which is non-adhesive for cells [30]. The adhesion
599 and proliferation of porcine chondrocytes was better on PLGA films (ratio 85:15) than
600 on poly(L- lactide) films [32]. Similarly, rat osteoblasts cultured on PLGA films (ratio
601 75:25) showed increased activity of alkaline phosphatase, i.e. a marker of osteogenic
602 cell differentiation, than the cells on poly(L-lactide) films [31].

603 **5. Conclusion and future perspectives**

604 The protein nanocoatings developed in our study on nanofibrous PLGA and PLA
605 membranes has a major influence on the behavior of skin cells. Fibrin enhanced the
606 adhesion, spreading, proliferation and fibronectin ECM synthesis of human dermal
607 fibroblasts. In contrast to fibroblasts, HaCaT keratinocytes adhered, spread and
608 proliferated faster on collagen-coated membranes than on fibrin-coated or non-coated

membranes. Fibronectin attached to fibrin or to a collagen nanocoating further enhanced cell adhesion and spreading. Moreover, fibronectin increased fibroblast proliferation. No differences were observed in the adhesion and growth of the cells on PLGA and PLA membranes.

Taken together, a degradable nanofibrous membrane with protein nanocoating could be promising for the construction of a bilayered skin substitute. On one side of the membrane, the fibrin-coated nanofibers could support the adhesion, proliferation and ECM synthesis of fibroblasts. With its collagen nanocoating, the opposite side of the membrane could serve as an appropriate carrier for keratinocytes.

Acknowledgement

This study was supported by the Grant Agency of Charles University in Prague (Grant No. 38214), by the Grant Agency of the Czech Republic (Grant No. P108/12/G108), and by the "BIOCEV – Biotechnology and Biomedicine Centre of the Academy of Sciences and Charles University" project (CZ.1.05/1.1.00/02.0109). Mr. Robin Healey (Czech Technical University in Prague) is gratefully acknowledged for his language revision of the manuscript.

6. References

1. Eisenbud D, Huang NF, Luke S, Silberklang M. Skin substitutes and wound healing: current status and challenges Wounds. 2004;16(1): 2-17.

2. McMillan JR, Akiyama M, Tanaka M, Yamamoto S, Goto M, Abe R, et al. Small-diameter porous poly (epsilon-caprolactone) films enhance adhesion and growth of human cultured epidermal keratinocyte and dermal fibroblast cells. Tissue Eng. 2007;13(4): 789-798.

3. Sun L, Stout DA, Webster TJ. The nano-effect: improving the long-term prognosis for musculoskeletal implants. J Long Term Eff Med Implants. 2012;22(3): 195-209.

4. Bacakova L, Filova E, Parizek M, Ruml T, Svorcik V. Modulation of cell adhesion, proliferation and differentiation on materials designed for body implants. Biotechnol Adv. 2011;29(6): 739-767.

638 5. Groeber F, Holeiter M, Hampel M, Hinderer S, Schenke-Layland K. Skin tissue
639 engineering--in vivo and in vitro applications. Adv Drug Deliv Rev. 2011;63(4-5): 352-
640 366.
641 6. Kai D, Liow SS, Loh XJ. Biodegradable polymers for electrospinning: towards
642 biomedical applications. Mater Sci Eng C Mater Biol Appl. 2014;45: 659-670.
643 7. Hoveizi E, Nabiuni M, Parivar K, Rajabi-Zeleti S, Tavakol S. Functionalisation
644 and surface modification of electrospun polylactic acid scaffold for tissue engineering.
645 Cell Biol Int. 2014;38(1): 41-49.
646 8. Bacakova M, Lopot F, Hadraba D, Varga M, Zaloudkova M, Stranska D, et al.
647 Effects of fiber density and plasma modification of nanofibrous membranes on the
648 adhesion and growth of HaCaT keratinocytes. J Biomater Appl. 2015;29(6): 837-853.
649 9. Bacakova M, Musilkova J, Riedel T, Stranska D, Brynda E, Zaloudkova M, et
650 al. The potential applications of fibrin-coated electrospun polylactide nanofibers in skin
651 tissue engineering. Int J Nanomedicine. 2016;11: 771-789.
652 10. Rajangam T, An SS. Fibrinogen and fibrin based micro and nano scaffolds
653 incorporated with drugs, proteins, cells and genes for therapeutic biomedical
654 applications. Int J Nanomedicine. 2013;8: 3641-3662.
655 11. O'Toole EA. Extracellular matrix and keratinocyte migration. Clin Exp
656 Dermatol. 2001;26(6): 525-530.
657 12. Auxenfans C, Fradette J, Lequeux C, Germain L, Kinikoglu B, Bechetoille N, et
658 al. Evolution of three dimensional skin equivalent models reconstructed in vitro by
659 tissue engineering. Eur J Dermatol. 2009;19(2): 107-113.
660 13. Nuutila K, Peura M, Suomela S, Hukkanen M, Siltanen A, Harjula A, et al.
661 Recombinant human collagen III gel for transplantation of autologous skin cells in
662 porcine full-thickness wounds. J Tissue Eng Regen Med. 2013.
663 14. Sarkar SD, Farrugia BL, Dargaville TR, Dhara S. Chitosan-collagen scaffolds
664 with nano/microfibrous architecture for skin tissue engineering. J Biomed Mater Res A.
665 2013;101(12): 3482-3492.
666 15. Peh P, Lim NS, Blocki A, Chee SM, Park HC, Liao S, et al. Simultaneous
667 Delivery of Highly Diverse Bioactive Compounds from Blend Electrospun Fibers for
668 Skin Wound Healing. Bioconjug Chem. 2015;26(7): 1348-1358.

16. Niiyama H, Kuroyanagi Y. Development of novel wound dressing composed of hyaluronic acid and collagen sponge containing epidermal growth factor and vitamin C derivative. J Artif Organs. 2014;17(1): 81-87.
17. Butler CE, Orgill DP. Simultaneous in vivo regeneration of neodermis, epidermis, and basement membrane. Adv Biochem Eng Biotechnol. 2005;94: 23-41.
18. Wang F, Wang M, She Z, Fan K, Xu C, Chu B, et al. Collagen/chitosan based two-compartment and bi-functional dermal scaffolds for skin regeneration. Mater Sci Eng C Mater Biol Appl. 2015;52: 155-162.
19. Mutsaers SE, Bishop JE, McGrouther G, Laurent GJ. Mechanisms of tissue repair: from wound healing to fibrosis. Int J Biochem Cell Biol. 1997;29(1): 5-17.
20. Laurens N, Koolwijk P, de Maat MP. Fibrin structure and wound healing. J Thromb Haemost. 2006;4(5): 932-939.
21. Gorodetsky R, Clark RA, An J, Gailit J, Levdansky L, Vexler A, et al. Fibrin microbeads (FMB) as biodegradable carriers for culturing cells and for accelerating wound healing. J Invest Dermatol. 1999;112(6): 866-872.
22. Fabris G, Trombelli L, Schincaglia GP, Cavallini R, Calura G, del Senno L. Effects of a fibrin-fibronectin sealing system on proliferation and type I collagen synthesis of human PDL fibroblasts in vitro. J Clin Periodontol. 1998;25(1): 11-14.
23. Ahmed TA, Dare EV, Hincke M. Fibrin: a versatile scaffold for tissue engineering applications. Tissue Eng Part B Rev. 2008;14(2): 199-215.
24. Braziulis E, Biedermann T, Hartmann-Fritsch F, Schiestl C, Pontiggia L, Bottcher-Haberzeth S, et al. Skingineering I: engineering porcine dermo-epidermal skin analogues for autologous transplantation in a large animal model. Pediatr Surg Int. 2011;27(3): 241-247.
25. Mazzone L, Pontiggia L, Reichmann E, Ochsenbein-Kolble N, Moehrlen U, Meuli M. Experimental tissue engineering of fetal skin. Pediatr Surg Int. 2014;30(12): 1241-1247.
26. Monteiro IP, Gabriel D, Timko BP, Hashimoto M, Karajanagi S, Tong R, et al. A two-component pre-seeded dermal-epidermal scaffold. Acta Biomater. 2014;10(12): 4928-4938.
27. de la Puente P, Ludena D, Fernandez A, Aranda JL, Varela G, Iglesias J. Autologous fibrin scaffolds cultured dermal fibroblasts and enriched with encapsulated bFGF for tissue engineering. J Biomed Mater Res A. 2011;99(4): 648-654.

28. Sivan U, Jayakumar K, Krishnan LK. Constitution of fibrin-based niche for in vitro differentiation of adipose-derived mesenchymal stem cells to keratinocytes. Biores Open Access. 2014;3(6): 339-347.
29. Kranz H, Ubrich N, Maincent P, Bodmeier R. Physicomechanical properties of biodegradable poly(D,L-lactide) and poly(D,L-lactide-co-glycolide) films in the dry and wet states. Journal of Pharmaceutical Sciences. 2000;89(12): 1558-1566.
30. Luck M, Pistel KF, Li YX, Blunk T, Muller RH, Kissel T. Plasma protein adsorption on biodegradable microspheres consisting of poly(D,L-lactide-co-glycolide), poly(L-lactide) or ABA triblock copolymers containing poly(oxyethylene) - Influence of production method and polymer composition. Journal of Controlled Release. 1998;55(2-3): 107-120.
31. Ishaug SL, Yaszemski MJ, Bizios R, Mikos AG. Osteoblast function on synthetic biodegradable polymers. J Biomed Mater Res. 1994;28(12): 1445-1453.
32. Tsai WB, Chen CH, Chen JF, Chang KY. The effects of types of degradable polymers on porcine chondrocyte adhesion, proliferation and gene expression. Journal of Materials Science-Materials in Medicine. 2006;17(4): 337-343.
33. Riedel T, Brynda E, Dyr JE, Houska M. Controlled preparation of thin fibrin films immobilized at solid surfaces. J Biomed Mater Res A. 2009;88(2): 437-447.
34. Boukamp P, Petrussevska RT, Breitkreutz D, Hornung J, Markham A, Fusenig NE. Normal keratinization in a spontaneously immortalized aneuploid human keratinocyte cell line. J Cell Biol. 1988;106(3): 761-771.
35. Hornig-Do HT, von Kleist-Retzow JC, Lanz K, Wickenhauser C, Kudin AP, Kunz WS, et al. Human epidermal keratinocytes accumulate superoxide due to low activity of Mn-SOD, leading to mitochondrial functional impairment. Journal of Investigative Dermatology. 2007;127(5): 1084-1093.
36. Rho KS, Jeong L, Lee G, Seo BM, Park YJ, Hong SD, et al. Electrospinning of collagen nanofibers: effects on the behavior of normal human keratinocytes and early-stage wound healing. Biomaterials. 2006;27(8): 1452-1461.
37. Fu X, Xu M, Liu J, Qi Y, Li S, Wang H. Regulation of migratory activity of human keratinocytes by topography of multiscale collagen-containing nanofibrous matrices. Biomaterials. 2014;35(5): 1496-1506.

733 38. Mahjour SB, Fu X, Yang X, Fong J, Sefat F, Wang H. Rapid creation of skin
734 substitutes from human skin cells and biomimetic nanofibers for acute full-thickness
735 wound repair. Burns. 2015;41(8): 1764-1774.
736 39. Mazlyzam AL, Aminuddin BS, Fuzina NH, Norhayati MM, Fauziah O, Isa MR,
737 et al. Reconstruction of living bilayer human skin equivalent utilizing human fibrin as a
738 scaffold. Burns. 2007;33(3): 355-363.
739 40. Nair RP, Joseph J, Harikrishnan VS, Krishnan VK, Krishnan L. Contribution of
740 fibroblasts to the mechanical stability of in vitro engineered dermal-like tissue through
741 extracellular matrix deposition. Biores Open Access. 2014;3(5): 217-225.
742 41. Sese N, Cole M, Tawil B. Proliferation of human keratinocytes and cocultured
743 human keratinocytes and fibroblasts in three-dimensional fibrin constructs. Tissue Eng
744 Part A. 2011;17(3-4): 429-437.
745 42. Cox S, Cole M, Tawil B. Behavior of human dermal fibroblasts in three-
746 dimensional fibrin clots: dependence on fibrinogen and thrombin concentration. Tissue
747 Eng. 2004;10(5-6): 942-954.
748 43. Gugerell A, Schossleitner K, Wolbank S, Nurnberger S, Redl H, Gulle H, et al.
749 High thrombin concentrations in fibrin sealants induce apoptosis in human
750 keratinocytes. J Biomed Mater Res A. 2012;100(5): 1239-1247.
751 44. Kubo M, Van de Water L, Plantefaber LC, Mosesson MW, Simon M, Tonnesen
752 MG, et al. Fibrinogen and fibrin are anti-adhesive for keratinocytes: a mechanism for
753 fibrin eschar slough during wound repair. J Invest Dermatol. 2001;117(6): 1369-1381.
754 45. Weiss E, Yamaguchi Y, Falabella A, Crane S, Tokuda Y, Falanga V. Un-cross-
755 linked fibrin substrates inhibit keratinocyte spreading and replication: correction with
756 fibronectin and factor XIII cross-linking. J Cell Physiol. 1998;174(1): 58-65.
757 46. Koivisto L, Larjava K, Hakkinen L, Uitto VJ, Heino J, Larjava H. Different
758 integrins mediate cell spreading, haptotaxis and lateral migration of HaCaT
759 keratinocytes on fibronectin. Cell Adhes Commun. 1999;7(3): 245-257.
760 47. Trombetta-eSilva J, Eadie EP, Zhang Y, Norris RA, Borg TK, Bradshaw AD.
761 The effects of age and the expression of SPARC on extracellular matrix production by
762 cardiac fibroblasts in 3-D cultures. PLoS One. 2013;8(11): e79715.
763 48. Tuan TL, Song A, Chang S, Younai S, Nimni ME. In vitro fibroplasia: matrix
764 contraction, cell growth, and collagen production of fibroblasts cultured in fibrin gels.
765 Exp Cell Res. 1996;223(1): 127-134.

766 49. Marchisio PC, Cancedda R, De Luca M. Structural and functional studies of
767 integrin receptors in cultured human keratinocytes. Cell Differ Dev. 1990;32(3): 355-
768 359.
769 50. Staatz WD, Fok KF, Zutter MM, Adams SP, Rodriguez BA, Santoro SA.
770 Identification of a tetrapeptide recognition sequence for the alpha 2 beta 1 integrin in
771 collagen. J Biol Chem. 1991;266(12): 7363-7367.
772 51. Scharffetter-Kochanek K, Klein CE, Heinen G, Mauch C, Schaefer T,
773 Adelmann-Grill BC, et al. Migration of a human keratinocyte cell line (HACAT) to
774 interstitial collagen type I is mediated by the alpha 2 beta 1-integrin receptor. J Invest
775 Dermatol. 1992;98(1): 3-11.
776 52. Eastwood M, Porter R, Khan U, McGrouther G, Brown R. Quantitative analysis
777 of collagen gel contractile forces generated by dermal fibroblasts and the relationship to
778 cell morphology. J Cell Physiol. 1996;166(1): 33-42.
779 53. Agis H, Collins A, Taut AD, Jin Q, Kruger L, Gorlach C, et al. Cell population
780 kinetics of collagen scaffolds in ex vivo oral wound repair. PLoS One. 2014;9(11):
781 e112680.
782 54. Ruoslahti E, Pierschbacher MD. New perspectives in cell adhesion: RGD and
783 integrins. Science. 1987;238(4826): 491-497.
784 55. Shive MS, Anderson JM. Biodegradation and biocompatibility of PLA and
785 PLGA microspheres. Adv Drug Deliv Rev. 1997;28(1): 5-24.

786